

# **The distinct roles of *Pseudomonas* $\alpha$ -glucan and trehalose in desiccation and osmotic stress tolerances**

**Stuart Daniel Woodcock**

**September 2019**

Thesis submitted to the University of East Anglia for  
the degree of Doctor of Philosophy

John Innes Centre

Norwich, United Kingdom

© This copy of the thesis has been supplied on condition that anyone who consults it is understood to recognise that its copyright rests with the author and that use of any information derived there-from must be in accordance with current UK Copyright Law. In addition, any quotation or extract must include full attribution.

# Abstract

*Pseudomonas aeruginosa* and *Pseudomonas syringae* are significant pathogens of humans and plants, respectively. An important prelude to infection is the ability of the pathogen to survive independently of the host and to withstand environmental stresses. This is achieved through several mechanisms including the biosynthesis of trehalose. Trehalose has previously been implicated in the tolerance of a wide range of abiotic stresses, particularly osmotic shock. Trehalose biosynthetic enzymes in *Pseudomonas* spp. were thought to be encoded by the *treS* or *treY/treZ* operons, deletion of which reduces pathogenicity *in planta*, illustrating the importance of trehalose metabolism during plant infection.

We used a combination of genetics and biochemistry to dissect trehalose metabolism. This work has allowed us to examine the relationship between the biosynthesis of this molecule, and its roles in stress protection. Contrary to previous understanding, we show that the *treS* operon is responsible for the degradation of trehalose in *Pseudomonas* spp. forming the polysaccharide  $\alpha$ -glucan. As expected, we found that trehalose was a key molecule during survival in osmotic conditions. An absence of intracellular trehalose yielded osmotically-sensitive strains, whereas those with increased levels of trehalose were osmotically-resistant. Surprisingly  $\alpha$ -glucan conferred no discernable effect on osmotic sensitivity but was important for survival under desiccating conditions. This phenotype was independent of the level of trehalose, marking a clear distinction between the roles of these two molecules in plant interactions and infection.

Other groups have observed the upregulation of genes responsible for the production of the exopolysaccharide alginate during desiccation stress, in *Pseudomonas* spp. We showed that alginate is also involved in the protection against desiccation stress. Using *Arabidopsis thaliana* as an infection model, we observe attenuation when trehalose,  $\alpha$ -glucan, and alginate biosynthetic pathways are absent, demonstrating importance of water stress during various stages of the *Pseudomonas* life cycle.

# Acknowledgements

Firstly, I would like to thank Jake Malone, Cyril Zipfel, Stephen Bornemann and Richard Little for all their supervision, guidance and support throughout my PhD. I would also like to thank the Malone and Bornemann groups for all their advice, help and training along the way. A special thanks goes to the Molecular Microbiology department for being such a welcoming, warm and fun place to work. Additional thanks are owed to Karl Syson, James Brown, Govind Chandra, Gerhard Saalbach and Sergey Nepogodiev for their expertise and assistance with enzymology, statistical analysis, bioinformatics, mass-spectrometry and NMR. I am extremely grateful to Carmen Chen, Wai Hoe Chin, Despoina Sifouna and Thomas Gate for being amazing students and putting up with my supervision. You guys taught me a lot. A big thanks to my lovely proof-readers Catriona Thompson and Hannah McDonald.

I could not have completed this thesis without the love and support of my friends and family. To my Mom and Dad, I don't know what I would have done without your endless love, encouragement and ability to listen to my continuous ramblings. To my best friend Corinne, thank you for all the coffee, pizza and spontaneous trips around the world. Finally, to Corinne's appendix, you were not helpful.

# Contents

Abstract .....	ii
Acknowledgements .....	iii
Contents .....	iv
List of Figures .....	viii
List of Tables .....	xii
List of Abbreviations .....	xiii
Chapter 1: General Introduction .....	1
1.1 Introduction .....	2
1.1.1 General Introduction to Pseudomonads .....	2
1.1.2 <i>Pseudomonas aeruginosa</i> .....	2
1.1.3 <i>Pseudomonas syringae</i> .....	4
1.1.4 Bacterial Stress .....	6
1.1.5 Water Stress .....	7
1.1.6 Trehalose .....	13
1.1.7 The biosynthesis of bacterial $\alpha$ -glucan .....	15
1.1.8 GlgE pathway .....	16
1.1.9 Predicted trehalose and $\alpha$ -glucan biosynthesis in <i>Pseudomonas</i> spp. ....	18
1.1.10 Function of trehalose and $\alpha$ -glucan in <i>Pseudomonas</i> spp. ....	21
1.2 Thesis Aims .....	23
Chapter 2: General Materials and Methods .....	24
2.1 Media and Methods .....	25
2.2 Genetic Manipulation .....	25
2.2.1 Construction of gene deletion plasmids .....	25
2.2.2 Construction of <i>otsA/otsB</i> expression plasmids .....	26
2.2.3 Construction of <i>PglgA-lacZ</i> fusion reporter plasmids .....	26
2.3 Specialised transformation of <i>Pseudomonas</i> .....	27
2.3.1 Transformation of <i>Pseudomonas</i> spp. using pTS1 and pME6032 based vectors .....	27
2.3.2 Selection of double crossover candidates using pME3087 based vectors .....	27
2.3.3 Transformation of <i>Pseudomonas</i> spp. using pUC18 based vectors .....	28
2.3.4 Storage and access of biological material .....	28
2.4 Metabolite Extraction .....	28

2.5	Nuclear Magnetic Resonance Spectroscopy .....	29
2.6	Iodine Staining .....	29
2.7	Osmotic Stress Assays .....	29
Chapter 3: Reverse genetics and biochemical characterisation of trehalose and $\alpha$ -glucan biosynthesis in <i>Pseudomonas</i> spp.....		30
3.1	Introduction .....	31
3.2	Results.....	33
3.2.1	Reverse genetics and nuclear magnetic resonance spectroscopy can be used to explore changes within the soluble carbohydrate metabolome of <i>Pseudomonas</i> spp. mutants .....	33
3.2.2	PAO1 and <i>Pto</i> produce $\alpha$ -glucan, trehalose and maltose 1-phosphate .....	34
3.2.3	GlgA is a starch synthase that utilises UDP-glucose to produce linear $\alpha$ -glucan.....	35
3.2.4	GlgP recycles $\alpha$ -glucan and produces glucose 1-phosphate from maltooligosaccharides .....	37
3.2.5	TreS/Pep2 utilises trehalose to produce maltose 1-phosphate .....	39
3.2.6	GlgE utilises maltose 1-phosphate to produce linear $\alpha$ -glucan .....	41
3.2.7	Absence of GlgB results in the accumulation of long linear $\alpha$ -glucan .....	43
3.2.8	GlgX functions to debranch $\alpha$ -glucan in <i>Pseudomonas</i> spp.....	45
3.2.9	TreS(2) functions as a second trehalose synthase in <i>Pto</i> .....	46
3.2.10	TreY and TreZ produce trehalose by degrading linear $\alpha$ -glucan producing maltooligosyltrehalose as an intermediate .....	47
3.2.11	MalQ disproportionates $\alpha$ -glucan and is capable of synthesising maltose .....	49
3.2.12	Characterisation of linear $\alpha$ -glucan.....	51
3.3	Discussion.....	54
Chapter 4: Trehalose and $\alpha$ -glucan protect against distinct abiotic stresses in <i>Pseudomonas</i> .....		61
4.1	Introduction .....	62
4.2	Materials and Methods.....	63
4.2.1	Desiccation Tolerance Assay .....	63
4.2.2	Plant Infection Assays .....	64
4.3	Results - Phenotypic characterisation of trehalose and $\alpha$ -glucan biosynthesis in <i>Pseudomonas aeruginosa</i> PAO1.....	65
4.3.1	Disruption of trehalose biosynthesis results in osmotic sensitivity in <i>Pseudomonas aeruginosa</i> PAO1.....	65
4.3.2	Loss of $\alpha$ -glucan but not trehalose results in desiccation sensitivity in PAO1.....	68
4.3.3	<i>In trans</i> expression of <i>Microbacterium koreensis</i> 3J1 <i>otsA/otsB</i> recovers trehalose biosynthesis .....	70
4.3.4	Reintroduction of trehalose biosynthesis rescues osmotic sensitivity .....	73

4.3.5	Reintroduction of trehalose biosynthesis rescues desiccation sensitivity in PAO1 but only when TreS/Pep2 is present .....	75
4.3.6	Maltose and maltose 1-phosphate do not play a role in desiccation stress in <i>Pseudomonas aeruginosa</i> PAO1. ....	76
4.3.7	Alginate plays a role in protecting PAO1 during desiccation stress.....	79
4.4	Phenotypic characterisation of trehalose and $\alpha$ -glucan biosynthesis in <i>Pto</i> .....	82
4.4.1	Operon deletions resulted in abolition of both trehalose and $\alpha$ -glucan biosynthesis in <i>Pto</i> but do not allow the distinction between these two molecules .....	82
4.4.2	Loss of both trehalose and $\alpha$ -glucan in <i>Pto</i> results in osmotic sensitivity .....	84
4.4.3	Loss of both trehalose and $\alpha$ -glucan in <i>Pto</i> results in desiccation sensitivity.....	85
4.4.4	Alginate works in combination with $\alpha$ -glucan to protect against desiccation stress in <i>Pto</i> .....	86
4.4.5	Trehalose, $\alpha$ -glucan and alginate are important during plant infection.....	87
4.5	Discussion.....	91
Chapter 5: Investigating the regulation of trehalose and $\alpha$ -glucan biosynthesis.....		99
5.1	Introduction .....	100
5.1.1	Regulation .....	100
5.1.2	Regulation of trehalose.....	100
5.1.3	Regulation of classical $\alpha$ -glucan biosynthesis .....	101
5.1.4	Regulation of alginate biosynthesis .....	104
5.1.5	Chapter Aims.....	106
5.2	Materials and Methods.....	107
5.2.1	Liquid Metabolite Extraction .....	107
5.2.2	RNA Extraction and Retrotranscription .....	107
5.2.3	qPCR.....	108
5.2.4	Biparental Mating .....	108
5.2.5	Transposon Mutagenesis .....	109
5.2.6	DNA-Affinity Chromatography.....	109
5.3	Results.....	112
5.3.1	Regulation of trehalose and $\alpha$ -glucan biosynthesis occur at the level of transcription in <i>Pto</i> .....	112
5.3.2	Generation of $P_{glgA}$ - <i>lacZ</i> transcriptional fusion vectors.....	114
5.3.3	Transposon mutagenesis .....	115
5.3.4	Identification of potential regulators of trehalose and $\alpha$ -glucan biosynthesis in <i>Pto</i> ...	116
5.3.5	Identification of potential regulators of trehalose and $\alpha$ -glucan biosynthesis in <i>Pseudomonas aeruginosa</i> PAO1. ....	119
5.3.6	Deletion of <i>cmpX</i> resulted in increased trehalose production but sensitivity to osmotic stress. ....	119

5.3.7 Disruption of <i>algB</i> indicates a role as a repressor of trehalose and $\alpha$ -glucan biosynthesis in PAO1.....	122
5.3.8 Disruption of <i>fimS</i> implicates the AlgR/FimS two-component system as an activator of trehalose and $\alpha$ -glucan biosynthesis in PAO1.....	123
5.3.9 Gac/Rsm System .....	124
5.3.10 DNA-affinity chromatography.....	127
5.4 Discussion.....	128
Chapter 6: General Discussion .....	136
6.1 Introduction .....	137
6.2 Does the GlgE pathway exist and function in <i>Pseudomonas</i> spp.? .....	137
6.3 How do trehalose and $\alpha$ -glucan function in <i>Pseudomonas</i> spp.?.....	139
6.4 How are trehalose and $\alpha$ -glucan biosynthesis regulated in <i>Pseudomonas</i> spp.?.....	140
6.5 What is the molecular basis for the function of $\alpha$ -glucan and alginate function in <i>Pseudomonas</i> ? .....	142
6.6 Evolution of the GlgE Pathway.....	143
6.7 Widespread connections .....	146
6.8 Industrial application .....	147
Chapter 7: References.....	149
Appendix .....	a

# List of Figures

Figure 1-1: Overview of <i>Pseudomonas syringae</i> pv. tomato DC3000 infection of plants. ....	5
Figure 1-2: A summary of water activity ( $A_w$ ) in bacteria during desiccation stress over time. ....	9
Figure 1-3: Overview of alginate biosynthesis in <i>Pseudomonas aeruginosa</i> PAO1. ....	12
Figure 1-4: Overview of classical $\alpha$ -glucan and trehalose biosynthesis in bacteria. ....	14
Figure 1-5: Structural schematic of bacterial $\alpha$ -glucan. ....	16
Figure 1-6: Overview of the mycobacterial GlgE pathway. ....	17
Figure 1-7: The genomic organisation of predicted trehalose and $\alpha$ -glucan biosynthesis genes in <i>Pseudomonas aeruginosa</i> PAO1. ....	18
Figure 1-8: The genomic organisation of predicted trehalose and $\alpha$ -glucan biosynthesis genes in <i>Pto</i> . ....	19
Figure 1-9: Predicted pathway of trehalose and $\alpha$ -glucan biosynthesis in <i>Pseudomonas</i> spp. ....	21
Figure 3-1: The predicted reaction catalysed by GlgA. ....	35
Figure 3-2: $^1\text{H-NMR}$ spectroscopy of the soluble metabolome following the deletion of <i>glgA</i> in <i>Pseudomonas</i> spp. ....	36
Figure 3-3: The predicted reaction catalysed by GlgP. ....	37
Figure 3-4: $^1\text{H-NMR}$ spectroscopy of the soluble metabolome following the deletion of <i>glgP</i> in <i>Pseudomonas</i> spp. ....	38
Figure 3-5: The predicted reactions catalysed by TreS/Pep2: the processing of trehalose into maltose and maltose 1-phosphate (M1P). ....	39
Figure 3-6: $^1\text{H-NMR}$ spectroscopy of the soluble metabolome following the deletion of <i>treS/pep2</i> in <i>Pseudomonas</i> spp. ....	40
Figure 3-7: The predicted reaction catalysed by GlgE: the extension of linear $\alpha$ -glucan using maltose 1-phosphate (M1P) as a substrate. ....	41
Figure 3-8: $^1\text{H-NMR}$ spectroscopy of the soluble metabolome following the deletion of <i>glgE</i> in <i>Pseudomonas</i> spp. ....	42
Figure 3-9: The predicted reaction catalysed by GlgB and GlgX. ....	43
Figure 3-10: $^1\text{H-NMR}$ spectroscopy of the soluble metabolome following the deletion of <i>glgB</i> in <i>Pseudomonas</i> spp. ....	44
Figure 3-11: Visualising the production of $\alpha$ -glucan in PAO1 strains using iodine staining. ....	45
Figure 3-12: $^1\text{H-NMR}$ spectroscopy of the soluble metabolome following the deletion of <i>glgX</i> in <i>Pseudomonas</i> spp. ....	46

Figure 3-13: <sup>1</sup> H-NMR spectroscopy of the soluble metabolome following the deletion of <i>treS(2)</i> in <i>Pseudomonas syringae</i> pv. tomato.....	47
Figure 3-14: The predicted reactions catalysed by TreY, TreZ and TreS/Pep2.....	48
Figure 3-15: <sup>1</sup> H-NMR spectroscopy of the soluble metabolome following the deletion of <i>treZ</i> and <i>treY</i> in <i>Pseudomonas</i> spp. ....	49
Figure 3-16: <sup>1</sup> H-NMR spectroscopy of the soluble metabolome following the deletion of <i>malQ</i> in <i>Pseudomonas</i> spp. ....	50
Figure 3-17: Iodine staining of linear $\alpha$ -glucan in <i>Pseudomonas aeruginosa</i> PAO1 strains using iodine vapour. ....	53
Figure 3-18: Current understanding of trehalose and $\alpha$ -glucan biosynthesis in <i>Pseudomonas</i> spp. ....	54
Figure 4-1: Growth of PAO1 and mutant strains in M9 minimal medium $\pm$ 0.85 M NaCl. ...	67
Figure 4-2: Linear mixed modelling analysis of the survival of PAO1, $\Delta$ <i>glgA</i> , $\Delta$ <i>treS/pep2</i> and $\Delta$ <i>glgB</i> strains when incubated at 100% (white bars) and 75% RH (grey bars). ....	69
Figure 4-3: Scheme showing the genetic and biochemical basis following the production of trehalose biosynthetic enzymes OtsA/OtsB in wildtype PAO1 (A), $\Delta$ <i>treS/pep2</i> (B) and $\Delta$ <i>glgA</i> (C). ....	71
Figure 4-4: <sup>1</sup> H-NMR spectroscopy of the soluble metabolome following the over-expression <i>otsA/otsB</i> in PAO1 strains.....	72
Figure 4-5: Growth of PAO1 and mutant strains with or without expression of <i>otsA/otsB</i> in M9 minimal medium $\pm$ 0.85 M NaCl.....	74
Figure 4-6: Linear mixed modelling analysis of the survival of PAO1 and mutant strains expressing <i>otsA/otsB</i> when incubated at 100% (white bars) and 75% RH (grey bars). ....	76
Figure 4-7: Scheme representing the genetic approach used to generate a $\alpha$ -glucan-null mutant capable of synthesising maltose and maltose 1-phosphate (M1P).....	77
Figure 4-8: <sup>1</sup> H-NMR spectroscopy of the soluble metabolome following the deletion of <i>glgA</i> , <i>glgE</i> and the over-expression of <i>otsA/otsB</i> in PAO1. ....	78
Figure 4-9: Linear mixed modelling analysis of the survival of PAO1 and $\Delta$ <i>glgA</i> $\Delta$ <i>glgE</i> :: <i>otsA/otsB</i> strains when incubated at 100% (white bars) and 75% RH (grey bars).....	79
Figure 4-10: Growth of PAO1 and $\Delta$ <i>alg</i> in M9 minimal medium $\pm$ 0.85 M NaCl. ....	80
Figure 4-11: Linear mixed modelling analysis of the survival of PAO1 and $\Delta$ <i>alg</i> when incubated at 100% (white bars) and 75% RH (grey bars). ....	81
Figure 4-12: The genomic organisation of the trehalose and $\alpha$ -glucan biosynthesis genes in <i>Pto</i> . ....	82
Figure 4-13: <sup>1</sup> H-NMR spectroscopy of the soluble metabolome following the deletion of <i>PSPTO_2760-2762</i> , <i>PSPTO_3125-3134</i> and <i>PSPTO_2760-2762 PSPTO_3125-3134</i> ( $\Delta\Delta$ ) in <i>Pto</i> . ....	83
Figure 4-14: Growth of wild-type <i>Pto</i> and $\Delta\Delta$ in M9 minimal medium $\pm$ 0.35 M NaCl. ....	84

Figure 4-15: Linear mixed modelling analysis of the survival of <i>Pto</i> , $\Delta\Delta$ , $\Delta alg$ and $\Delta alg \Delta\Delta$ strains when incubated at 100% (white bars) and 75% RH (grey bars). .....	86
Figure 4-16: <i>A. thaliana</i> (Col-0) infection with <i>Pto</i> , $\Delta\Delta$ and $\Delta alg$ .....	89
Figure 4-17: <i>A. thaliana</i> (Col-0) infection with <i>Pto</i> and $\Delta alg \Delta\Delta$ .....	90
Figure 4-18: The current understanding of water stress protection mechanisms of <i>Pseudomonas</i> spp. ....	97
Figure 5-1: A graphical representation of the Gac/Rsm system in <i>P. aeruginosa</i> .....	104
Figure 5-2: <sup>1</sup> H-NMR spectroscopy shows the effects of growth in liquid culture upon the soluble metabolome of the <i>Pto</i> $\Delta glgB$ strain. ....	112
Figure 5-3: The addition of Lugol's solution to metabolome extracts from <i>Pto</i> $\Delta glgB$ cultured in liquid (L) or on solid medium (S). ....	113
Figure 5-4: Quantitative PCR data showing the absolute quantification of transcripts from <i>Pto</i> cultured using solid or liquid M9 minimal medium relative to the housekeeping gene <i>rpoD</i> .....	114
Figure 5-5: The reporter strain <i>Pto</i> $P_{glgA}$ - <i>lacZ</i> cultured on L medium supplemented with 50 $\mu$ g/mL X-Gal. ....	115
Figure 5-6: <sup>1</sup> H-NMR spectroscopy of the soluble metabolome following transposon insertion within <i>Pto</i> $P_{glgA}$ - <i>lacZ</i> .....	118
Figure 5-7: <sup>1</sup> H-NMR spectroscopy of the soluble metabolome following transposon insertion within <i>cmpX</i> in the PAO1 $P_{glgA}$ - <i>lacZ</i> strain. ....	120
Figure 5-8: Growth of PAO1 and <i>cmpX</i> mutant strains in M9 minimal medium with and without addition of 0.85 M NaCl. ....	121
Figure 5-9: <sup>1</sup> H-NMR spectroscopy of the soluble metabolome following insertion within <i>algB</i> of the PAO1 $P_{glgA}$ - <i>lacZ</i> strain. ....	122
Figure 5-10: Growth of PAO1 $P_{glgA}$ - <i>lacZ</i> and <i>tn::algB</i> in M9 minimal medium with and without addition of 0.85 M NaCl. ....	123
Figure 5-11: <sup>1</sup> H-NMR spectroscopy of the soluble metabolome following transposon insertion within <i>fimS</i> in the PAO1 $P_{glgA}$ - <i>lacZ</i> strain. ....	124
Figure 5-12: Growth of PAO1 $P_{glgA}$ - <i>lacZ</i> and <i>tn::fimS</i> in M9 minimal medium with and without addition of 0.85 M NaCl. ....	124
Figure 5-13: <sup>1</sup> H-NMR spectroscopy of the soluble metabolome following Gac/Rsm system mutations in <i>Pseudomonas aeruginosa</i> strains.....	127
Figure 5-14: The current understanding of the regulatory network governing trehalose and $\alpha$ -glucan in <i>Pseudomonas</i> spp. ....	135
Figure 6-1: Illustration of futile cycling of $\alpha$ -glucan biosynthesis and degradation in <i>Pseudomonas</i> spp. ....	145
Figure i: Heat map representing the statistical significance of desiccation responses between PAO1 strains based on linear mixed modelling.....	k

Figure ii: Heat map representing the statistical significance of desiccation responses between *Pto* strains based on linear mixed modelling. ....|

# List of Tables

Table 3-1: Concentrations of trehalose and M1P produced by PAO1 strains. ....	33
Table 3-2: Concentrations of trehalose and M1P produced by <i>Pto</i> strains.....	34
Table 4-1: Concentrations of trehalose and M1P produced by PAO1 mutant strains with or without expression of <i>otsA/otsB</i> . ....	73
Table 4-2: Concentrations of trehalose and M1P produced by wild-type PAO1 and PAO1 $\Delta glgA \Delta glgE :: otsA/otsB$ strains. ....	77
Table 4-3: Concentrations of trehalose and M1P produced by <i>Pto</i> strains.....	83
Table 5-1: Transposon candidates for potential regulators of trehalose and $\alpha$ -glucan biosynthesis in <i>Pto</i> . ....	116
Table 5-2: Concentrations of trehalose and M1P produced by <i>Pto</i> $P_{glgA}$ - <i>lacZ</i> transposon mutants.....	117
Table 5-3: Transposon candidates for potential regulators of trehalose and $\alpha$ -glucan biosynthesis in PAO1. ....	119
Table 5-4: Concentrations of trehalose and M1P produced by PAO1 $P_{glgA}$ - <i>lacZ</i> transposon mutants.....	120
Table 5-5: Concentrations of trehalose and M1P produced by PAO1-L, $\Delta gacA$ and $\Delta gacS$ strains.....	126
Table 5-6: Concentrations of trehalose and M1P produced by PAO1-N, $\Delta rsmA$ , $\Delta rsmN$ , and $\Delta rsmA \Delta rsmN$ strains. ....	126
Table 5-7: Putative regulators that were identified through specific binding to PAO1 $P_{glgA}$ . ....	128
Table i: Primers used for genetic manipulations .....	
Table ii: Primers used for genetic manipulations .....	
Table iii: Primers used for genetic manipulations .....	
Table iv: Primers used for genetic manipulations .....	
Table v: Primers used for genetic manipulations .....	
Table vi: Primers used for genetic manipulations .....	
Table vii: Primers used for arbitrary PCR and sequencing.....	
Table viii: Primers used for qPCR .....	
Table ix: List of <i>Pto</i> strains used in this study .....	i
Table x: List of PAO1 strains used in this study.....	j

# List of Abbreviations

X-gal	5-bromo-4-chloro-3-indolyl $\beta$ -D-galactopyranoside
Csr	carbon storage regulator
cAMP	cyclic adenosine monophosphate
CRP	cAMP receptor protein
CFU	colony forming units
CF	cystic fibrosis
ddH <sub>2</sub> O	double distilled H <sub>2</sub> O
DPI	days post infection
DP	degree of polymerisation
$\Delta$	deletion of specified gene(s) or operon
EPS	exopolysaccharides
G1P	glucose 1-phosphate
G6P	glucose 6-phosphate
HPr	histidine phosphocarrier protein
LEA	late embryogenesis proteins
M1P	maltose 1-phosphate
MALDI-MS	matrix-assisted laser desorption/ionization mass spectrometry
T <sub>m</sub>	melting temperature
OD <sub>600</sub>	optical density at $\lambda$ 600 nm
PBS	phosphate buffer saline
PTS	phosphoenopyruvate:carbohydrate phosphotransferase system
P-HPr	phosphorylated form of the histidine phosphocarrier protein
pppGpp	guanosine pentaphosphate
ppGpp	guanosine tetraphosphate
<sup>1</sup> H-NMR	proton nuclear magnetic resonance
<i>Psa</i>	<i>Pseudomonas syringae</i> pv. <i>actinidiae</i>
<i>Pto</i>	<i>Pseudomonas syringae</i> pv. <i>tomato</i>
RH	relative humidity
TMSP	trimethylsilyl propanoic acid

v/v	volume of solute/volume of solution
w/v	mass of solute/volume of solution
$A_w$	water activity

# Chapter 1: General Introduction

## 1.1 Introduction

The *Pseudomonas* genus encompasses agriculturally and clinically important pathogens which cause significant socioeconomic cost. In order to successfully infect, they first need to survive in the environment and cope with various stresses. They synthesise molecules to help tolerate stresses, but this is not fully understood. One such molecule is trehalose, which has been shown to provide protection against several abiotic stresses and ultimately play a role in virulence. Our understanding of its metabolism has had to be substantially revised with the recent discovery of a novel  $\alpha$ -glucan biosynthetic pathway. This thesis therefore addresses the role of these two molecules, trehalose and  $\alpha$ -glucan, and their roles in *Pseudomonas* species (spp.) against water stresses.

### 1.1.1 General Introduction to Pseudomonads

*Pseudomonas* is one of the most diverse bacterial genera. These bacteria exhibit extensive metabolic plasticity and are found in a variety of environments, including soil [1, 2], bodies of water [3] and precipitation [4]. Certain species are also associated with the colonisation of animals [5, 6], plants [1], and insects [7]. Moreover, the human pathogen *Pseudomonas aeruginosa* can colonise artificial environments such as hospital equipment [8, 9]. Despite *Pseudomonas* spp. representing both commensal and pathogenic organisms, the two major pathogenic species, *P. aeruginosa* and *Pseudomonas syringae*, have been most extensively researched. As such, these two species form the primary focus of this thesis.

### 1.1.2 *Pseudomonas aeruginosa*

*P. aeruginosa* is a significant pathogen of humans and is one of the most common causes of nosocomial infections [10]. It is an opportunistic pathogen that primarily affects immunocompromised individuals, including patients with immunodeficiencies [11, 12], those with disruption of the skin barrier, such as burns victims [13], and those who have had foreign bodies introduced, such as cannulas or catheters [8]. *P. aeruginosa* is more commonly known as a pneumonial agent causing acute and chronic infection of the lungs, with the former a result of sudden trauma to the lung tissue such as smoke inhalation or other injury [14, 15]. Acute infections are usually resolved relatively quickly by host defences or treatment with antibiotics. However, these infections are difficult to eradicate due to the intrinsic resistance to antibiotics exhibited by *P. aeruginosa*. [16, 17]. Acute infections can become chronic if they are not resolved by the host.

Chronic infections are described as the persistent colonisation or infection of the lung by *P. aeruginosa* where the patient's immune system has responded by the production of anti-pseudomonad antibodies [18]. Chronic *P. aeruginosa* infections occur in 80% of adult cystic fibrosis (CF) patients where morbidity and mortality rates are significantly increased when compared to CF patients who have not been infected with *P. aeruginosa* [18-20].

Following colonisation of the CF lung with *P. aeruginosa*, a phenotypic diversification to a mucoid strain is extremely likely marking the onset of chronic infection [21-23]. The mucoid phenotype is attributed to the over-expression of the exopolysaccharide (EPS) alginate [24]. Alginate production is controlled by the sigma factor AlgU, which itself is normally repressed by the anti-sigma factor MucA and its cognate partner MucB [25]. In mucoid strains, MucA is typically mutated leading to the de-repression of AlgU and the over-production of alginate [26]. Alginate over-expression and the subsequent effect on biofilm production leads to increased antibiotic resistance [24], thereby enhancing the antibiotic tolerance profile of an already highly resistant organism. However, the importance of the biofilm is not limited to chronic infections, as the formation of biofilms has also been observed with acute infection [27].

In order to establish a chronic infection, *P. aeruginosa* must be able to resist and tolerate hostile conditions, including constant stimulation of the host immune system and numerous rounds of antibiotic treatment. In order to cope with a constant barrage of hostility and stress, *P. aeruginosa* has evolved various mechanisms to help it to survive [9]. *P. aeruginosa* can alter its immunogenicity and dampen the inflammatory response by down-regulating or preventing the expression of immunogenic structures, such as flagella and type IV pili [28, 29]. Furthermore, various other virulence factors that stimulate inflammatory responses or have necrotic effects can also be down-regulated or are absent altogether [29]. As well as evading the host immune system, *P. aeruginosa* is intrinsically resistant to most antibiotics. This characteristic is attributable to the low permeability of their outer membrane [30], alongside the expression or upregulation of chromosomally-encoded lactamases and multi-drug efflux systems [17]. Pseudomonads can attain additional genetic resistance through chromosomal mutations and horizontal gene transfer. This can include the acquisition of extended spectrum  $\beta$ -lactamases [31] or the mutation of regulatory elements which can result in the over-expression of efflux pumps [32]. Antibiotic-resistant *P. aeruginosa* infections translates into longer hospital admissions and up to a 500% increase in mortality rates when compared to susceptible strains [33]. As

a consequence of this, *P. aeruginosa* has been classified as a serious threat equal to methicillin-resistant *Staphylococcus aureus* and extensively drug-resistant *Mycobacterium tuberculosis* [34]. This emphasises the economic and health consequences of *P. aeruginosa* infections.

Owing to the difficulty of treating *P. aeruginosa* infections due to the factors discussed above, there has been much emphasis upon the prevention of chronic infection [35]. *P. aeruginosa* is thought to be transmitted by contact with contaminated surfaces [36] and hospital equipment [37]. Contact with health care professionals [36, 38], other patients [39] or healthy relatives [40] can also be sources of contamination. Furthermore, there are reports of transmission between CF patients and pet animals [41, 42]. Soil and agricultural produce also present a significant reservoir of this pathogen [43, 44]. Investigating the underlying mechanisms that *P. aeruginosa* utilises to survive and persist in these various environments may be applicable in preventing transmission and therefore the establishment of infection.

### 1.1.3 *Pseudomonas syringae*

*P. syringae* is one of the most significant pseudomonad plant pathogens. More than 60 varieties (pathovars) have been described based upon the host plant species and the symptoms that are caused [45, 46]. This bacterium can infect over 180 plant species resulting in significant economic costs and loss of yield. Hosts include cereals and other economically relevant plants, including wheat [47], tomato [48] and kiwifruit [49].

One specific pathovar, *P. syringae* pv. *actinidiae* (*Psa*), is the causative agent of bacterial canker in kiwifruit. An epidemic of *Psa* began to infect New Zealand kiwifruit orchards in 2010 and spread to approximately 85% of the New Zealand kiwifruit orchards by 2015 [50]. It was predicted that *Psa* would incur economic costs of up to NZ \$410 million by 2015, however, in 2017 it was reported that actual costs incurred were as high as NZ \$930 million [51]. The agricultural industry uses various methods to control and prevent the infection, including streptomycin and copper sulphate sprays. However, like *P. aeruginosa*, *P. syringae* has also developed resistance to these control mechanisms [52] exacerbating the socio-economic costs associated with infection.

As depicted in Figure 1-1, there are two generally accepted phases of the lifecycle of *P. syringae* during plant infection, these are termed epiphytic and endophytic. *P. syringae* is disseminated through the water cycle or through agricultural activities such as pollination

[53, 54]. The epiphytic phase begins when the bacterium lands on the surface of the plant and forms microcolonies and biofilms. The surface-exposed portion of the plant is also known as the phyllosphere which includes the stem, leaves, flowers and fruit. Below the soil surface, epiphytic habitats are known as the rhizosphere [55, 56]. Following the epiphytic phase, *P. syringae* can migrate and enter the plant tissue through natural openings, such as stomata, or through sites of injury [46, 57]. This marks the start of the endophytic stage of the lifecycle and once in the apoplastic space *P. syringae* will multiply and cause disease. During the course of infection, recognition of bacterial pathogen-associated molecular patterns or effectors can stimulate the plant immune system. This triggered immunity will activate the hypersensitive response, suppress bacterial growth and limit the progression of infection. *P. syringae* responds by utilising its repertoire of effector proteins to suppress the plant immunity and to acquire nutrient access [58-60]. Strategies regarding the entry of the bacterium into the apoplastic space can include the secretion of phytotoxins to interfere with plant hormone signalling and prevent the closing of the stomata [61]. An alternative strategy is to induce the nucleation of ice *via* the ice nucleating protein INA, this causes cellular damage and provides additional entry points into the plant tissue [62].

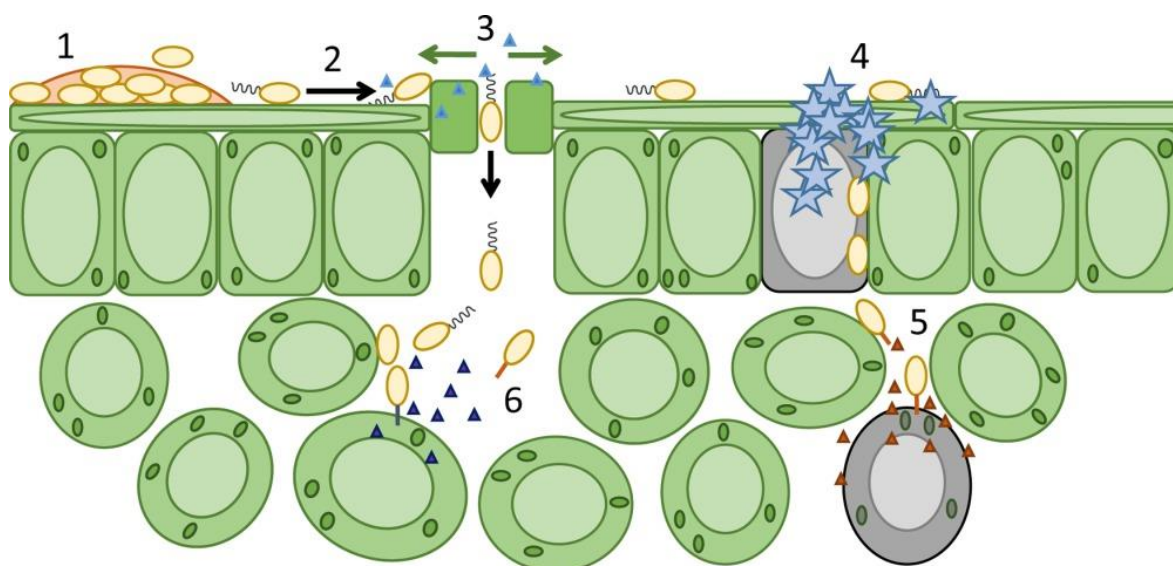


Figure 1-1: Overview of *Pseudomonas syringae* pv. tomato DC3000 infection of plants. Bacteria arrive on the surface of the phyllosphere where there is colony and biofilm formation. (2) Migration across the surface of the plant to natural openings or wounds to gain access to the apoplast. (3) Release of phytotoxins such as coronatine to prevent stomatal closure as represented by light blue triangles. (4) The use of the ice nucleation protein, as represented by blue stars, to wound the plant tissue and create alternative entry points. Grey colouring represents dead or damaged plant cells. Once in the apoplastic space bacteria will secrete various effectors and toxins to access nutrients (5) and to modulate the host (6), this is represented by the orange and dark blue triangles respectively. This figure is reproduced with permission from Pfeilmeier *et al.* (2016) [63].

#### 1.1.4 Bacterial Stress

The bacterial response to stress is important at all stages of the life cycle. Bacteria must survive various abiotic and biotic stresses to survive in their environment or within their host during infection. Abiotic stresses encompass environmental factors such as temperature, pH, ultra-violet radiation, water availability, salinity and nutrient starvation [64-66]. By contrast, biotic stresses are factors born from other living organisms such as microbial competition or host defences [67]. Nutrient availability can be a consequence of either an abiotic or biotic stress, the latter of which can be caused by the competition for resources with other microorganisms [68]. Bacteria withstand these biotic stresses using a variety of mechanisms, such as the production of siderophores to sequester iron [69], through the direct competition with other microorganisms *via* the production of antibiotics [70] or through the deployment of type VI secretion systems [71]. Importantly, an understanding of the mechanisms that bacteria use to respond to and resist environmental abiotic stresses can lead to an alternative strategy to combat bacterial disease. By exploiting these systems, bacterial persistence and environmental transmission could be prevented.

*P. syringae* and *P. aeruginosa* spend significant parts of their life cycle in soils and in association with host organisms. As part of this, these bacteria will be subjected to rapidly changing levels of pH (acid stress), water stress, ultraviolet radiation, temperature and nutrient starvation [55, 56, 72]. For example, the leaf surface is exposed to extreme fluctuations of water availability [73]. Consequently, the ability of *P. syringae* to produce water stress protection molecules has been shown to be important during epiphytic colonisation [74]. Similarly, during colonisation of the cystic fibrosis lung *P. aeruginosa* is exposed to various abiotic stresses, such as water stress, nutrient stress and oxidative stress [75]. *P. aeruginosa* and *P. syringae* must be able to respond to these varying conditions effectively to ensure survival in the environment, a successful life cycle and the ability to cause disease. As an example, oxidative stress is generated by the formation of intracellular reactive oxygen species which damages DNA, proteins and lipids [76]. This damage can interfere with cellular processes and even result in cell death. Bacteria respond to this stress by producing scavenging enzymes, such as superoxide dismutases, catalases and peroxidases to convert the damaging species into harmless by-products [77]. An alternative strategy is the expression of oxidative damage-resistant forms of enzymes [78].

The bacterial response to stress not only governs the protection of the cell against a given stress but can also alter bacterial virulence and resistance to antimicrobial agents [79]. For example, DNA damage, caused by both abiotic and biotic factors, can induce the production of phage-encoded toxins in shiga-toxin producing *Escherichia coli* [80]. Furthermore, the response to osmotic stress can induce the production of the type III secretion system thereby promoting virulence in *Salmonella enterica* serovar Typhimurium [81]. The bacterial response to various stresses can also increase resistance to antimicrobial agents in several ways. This can include the transfer of antimicrobial resistance genes from one cell to another [82], the prevention of cellular division [83], or the production of slow-growing persister cells [84]. This illustrates the importance of understanding the mechanisms that pathogenic bacteria use to survive in rapidly changing environments and how they respond to specific stresses.

#### 1.1.5 Water Stress

The availability of water is generally regarded as one of the most important abiotic factors affecting all domains of life. It is essential for cellular functions and all living organisms. With the current threat of climate change, water stress has become an important factor for agriculture because 64% of the global arable land has been predicted to be affected by water deficit or drought [85]. Microbial tolerance to water stress has become a more active field of research as microbial-plant interactions have been shown to increase the tolerance of plants to abiotic stresses [86] including drought [87, 88]. This is likely due to the ability of select microorganisms to survive under dry conditions and subsequently confer stress-tolerance to the host plant [89].

Water stress manifests itself in at least two distinct phenomena; osmotic and desiccation stress. There are two types of osmotic stress, hypo- and hyperosmotic stress. Hypoosmotic stress is defined by a decrease in the osmotic pressure of the external environment translating to influx of water into the bacterial cell. This causes an increase in the cytosolic volume and can cause cell lysis [90]. Hyperosmotic stress is defined as the loss of water and reduction of cytosolic volume due to an increase in the osmotic pressure of the external environment. When the concentration of external solutes is greater than the concentration of internal cytosolic solutes, water will leave the bacterial cell by osmosis to equalise the osmotic pressure [90]. This decreases the water availability within the bacterium, compromising essential cellular processes. The work discussed within this thesis relates to

hyperosmosis therefore subsequent references to osmotic stress refers to hyperosmotic conditions (unless otherwise stated).

Desiccation stress is defined as the dehydration of the cell and subsequent loss of water. This differs from osmotic stress due to the fact that desiccation stress is independent of solute concentration and the immediate environment to which water is lost [91]. Under osmotic conditions, bacteria are surrounded by an aqueous environment of reduced water activity. Conversely, during desiccation stress, bacteria are exposed to air and water is lost to the atmosphere and cannot be recovered [92]. Desiccation stress is a multi-factorial phenomenon where the removal of water from bacterial cells can cause a variety of deleterious effects. The key stages of desiccation are summarised in Figure 1-2. Desiccation stress consists of three main stages; drying, storage and rewetting [93]. The drying stage can manifest as either fast or slow drying, where the rate of dehydration determines the outcome of bacterial survival. Bacteria exposed to slow desiccating conditions exhibit a higher rate of survival than those that are rapidly dehydrated [94]. As the intracellular water potential decreases, bacteria are exposed to various stresses, including osmotic and oxidative stress, toxicity due to the build-up of intracellular salts and other molecules as well as the disruption of cellular processes due to the denaturing of enzymes and proteins. In contrast to rapid desiccation, slow drying is likely to allow bacteria sufficient time to mount the appropriate responses.

The storage phase begins when the water activity of the cell plateaus. During storage, the number of viable bacteria will reduce over time. Although the exact mechanisms are unknown, this is probably due to accumulative damage governed by oxidative and radiation stresses [93, 95].

The final phase of desiccation is the rewetting or reviving of dehydrated bacteria. This is governed by the reintroduction of water, most likely due to precipitation. Similar to drying, the rate of rehydration dictates bacterial fate [93] in that fast rehydration leads to increased cell death as compared to slow rehydration [96]. This is most likely due to cell lysis because of rapid water influx owing to high intracellular solute concentrations from the drying phase. In contrast to slow rehydration, rapid rehydration is likely to cause cell lysis as the cell does not have sufficient time to respond and modulate the intracellular solute concentration.

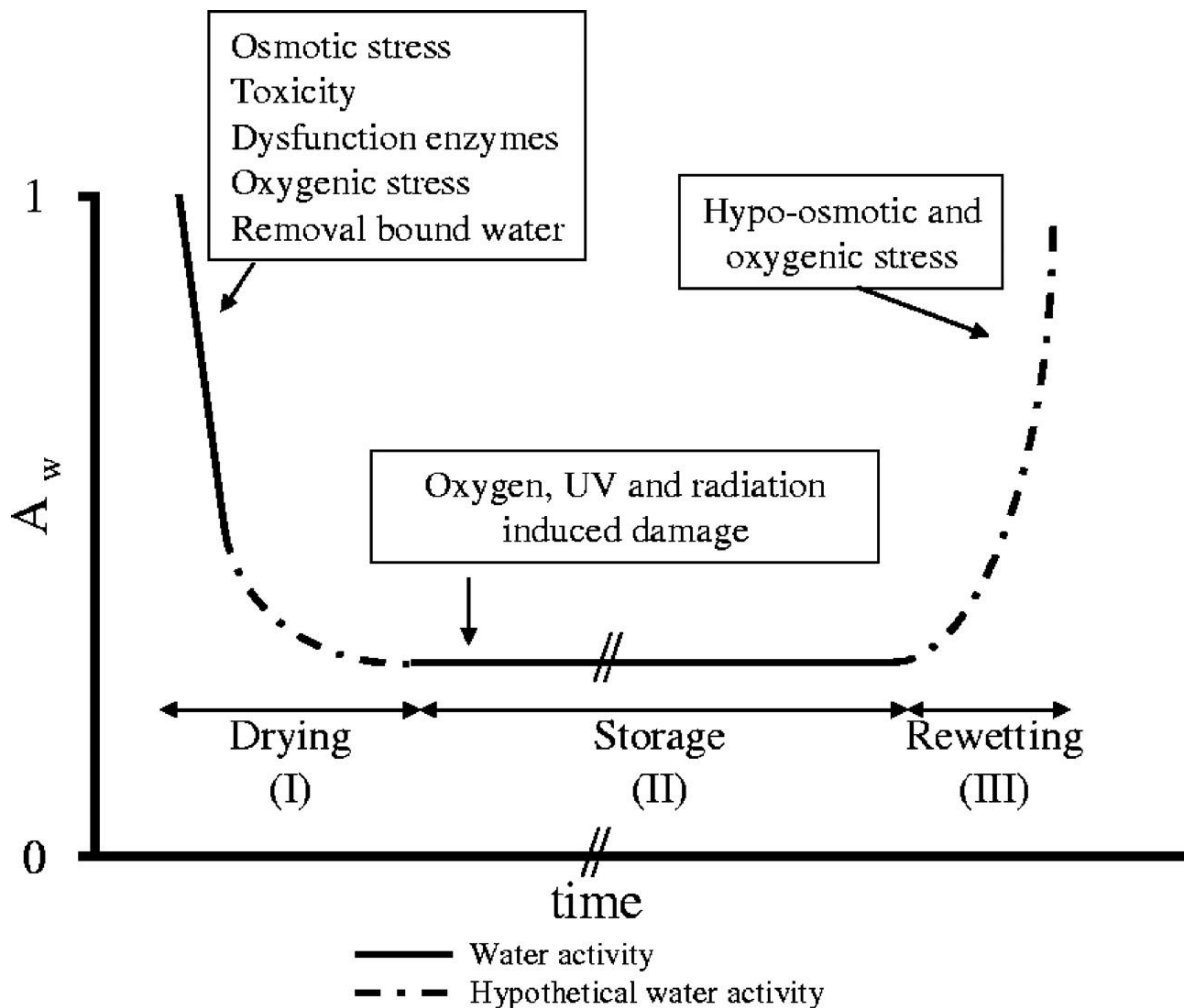


Figure 1-2: A summary of water activity ( $A_w$ ) in bacteria during desiccation stress over time. A depiction of the three stages of desiccation stress, drying, storage and rewetting. The additional stresses encountered during each stage are indicated. This figure is reproduced with permission from Vriezen *et al.* (2007) [93].

Owing to the multi-factorial components of desiccation stress, the mechanisms conferring tolerance to dehydration are less well-understood. Mechanisms that have been found to confer desiccation stress tolerance are also intrinsically linked to the tolerance of osmotic stress. However, there has been some effort towards dissecting individual responses to the two stresses [97].

One strategy to tolerate low water conditions is the modulation of metabolism. This can be *via* the formation of either metabolically-inert bacteria [98] or highly stress-resistant spores. These mechanisms ensure the long-term survival of the bacteria by shutting down virtually all metabolic processes. Certain genera of bacteria undergo sporulation when they encounter unfavourable abiotic stresses, such as nutrient, pH or competition stress. Spores are extremely hardy and resistant to a variety of abiotic stresses including water stress, ultraviolet radiation, heat and even modern disinfectants [99, 100]. Bacteria are thought to accumulate various molecules within the spore to protect against abiotic stresses. For

example, *Streptomyces* spp. spores have been shown to accumulate the compatible solute trehalose. Increased concentrations of which have been shown to correlate with the stress resistance of the spore [101]. However, sporulation as a method of resisting water stress is not widespread among bacteria because relatively few genera contain representatives that are capable of producing spores [102].

A more widespread method of resisting water stress is the biosynthesis of protective molecules. For example, bacterial desiccation stress resistance can be conferred by the expression of desiccation-specific proteins. The expression of hydrophilins, such as the late embryogenesis abundant (LEA) proteins, have been reported to protect against desiccation stress in bacteria [103]. It has been shown that the addition of bacterial LEA proteins to purified enzymes preserve enzymatic function during desiccating conditions [104]. In addition to desiccation stress, LEA proteins have also been shown to improve osmotic tolerance in human cell lines [105]. However, it is thought that the molecular mechanism of protection conferred by LEA proteins differs to that of compatible solutes such as trehalose [104].

#### 1.1.5.1 Compatible Solutes

One of the most common mechanisms to protect against water stress in bacteria is the accumulation of compatible solutes. These include betaine derivatives, sugars, amino acids and inorganic ions [90]. Investigation into the responses of *P. aeruginosa* PAO1 and *P. syringae* pv. tomato DC3000 (*Pto*) to osmotic stress revealed the accumulation of the compatible solutes glutamate, trehalose and *N*-acetylglutaminylglutamine amide [74, 106, 107]. Compatible solutes protect the cell against osmotic stress by minimising water loss. They have also been shown to play roles in stabilising proteins [108, 109] and membranes [110] thereby preserving cellular functions during conditions of low water availability. These stabilisation functions have also implicated compatible solutes in the protection against other stresses, such as desiccation [111] and temperature stress [112, 113]. For example, glycine betaine was found to protect *Bacillus subtilis* during low temperatures [114] whereas trehalose has been implicated in the protection against desiccation stress in both bacteria and yeast [113, 115].

Compatible solutes accumulate within bacteria *via* active uptake from the environment or through *de novo* synthesis. An example of this is the biosynthesis of the compatible solute glycine betaine in *E. coli* which requires the uptake of choline through the choline-specific

transporter BetT. Choline is then metabolised into glycine betaine through the action of the BetA and BetB enzymes [116]. In contrast, compatible solute glutamate can be taken up from the environment [117] or synthesised *de novo* [118] in response to osmotic stress.

#### 1.1.5.2 Biofilms and alginate production

Biofilms are structured communities of bacteria which can adhere to each other or a range of biological or inert surfaces. The biofilm itself is formed from mainly water and bacteria, but also contains polysaccharides, nucleic acids, lipids, and proteins. These extracellular factors are collectively known as the extracellular polymeric substance matrix [119]. The biofilm provides a variety of functions, including protection against abiotic and biotic stresses. For example, the microenvironment of the biofilm can affect the behaviour of the bacteria. When in this sessile, nutrient and oxygen-limiting environment, *P. aeruginosa* can adopt a different gene expression profile [120, 121]. This results in slow growth and upregulation of stress responses under the control of the alternative sigma factor S [122]. Furthermore, the biofilm matrix can provide steric hinderance to antibacterial molecules entering the biofilm, preventing or delaying bacterial uptake of these molecules and subsequent killing [123].

The EPS produced by *P. aeruginosa* PAO1 mainly consists of three polysaccharides: alginate, pel and psl [124]. *P. syringae* has been shown to produce alginate, cellulose, levans and psl as components of their biofilm [125, 126]. Although their exact functions are unknown, each polysaccharide plays its own role in the formation of the biofilm [124].

In addition to other abiotic stresses [127], biofilms have been implicated in protecting against water stress. *Pseudomonas* spp. respond to desiccating conditions by increasing the amount of EPS produced within the biofilm [128]. This suggests that EPS and therefore biofilms play a role in keeping cells hydrated. Subsequently, further work has specifically implicated the EPS component alginate in the protection of *Pseudomonas* spp. against water stress [129-131]. Moreover, the biosynthesis of alginate has been shown to be a key adaptation of *P. aeruginosa* within the CF lungs [29] and that alginate biosynthesis is important for *P. syringae* when colonising the plant host [132]. Both of these environments are thought to be exposed to osmotic stress and desiccation [73].

The bacterial production of alginate is restricted to two genera, *Pseudomonas* and *Azotobacter* [133], but is highly conserved within *Pseudomonas* spp. Alginate is formed of  $\beta$ -1,4-linked L-guluronic and D-mannuronic acids. The first step in the biosynthesis of

alginate is the production of a linear polymer of D-mannuronic acid (Figure 1-3). The enzymes responsible for this are encoded by *algA*, *algC*, *algD* and *alg8*. The polymannurate is then secreted into the periplasmic space where AlgG converts D-mannuronic acid residues to L-guluronic acid and the combined actions of AlgI, AlgJ, AlgK and AlgX O-acetylate the mannuronic acid residues [134, 135]. Mature alginate is then secreted through the AlgE pore. Individual deletion of the *algK*, *algX*, *algG* or *algD* genes results in the abolition of alginate production [134, 136].

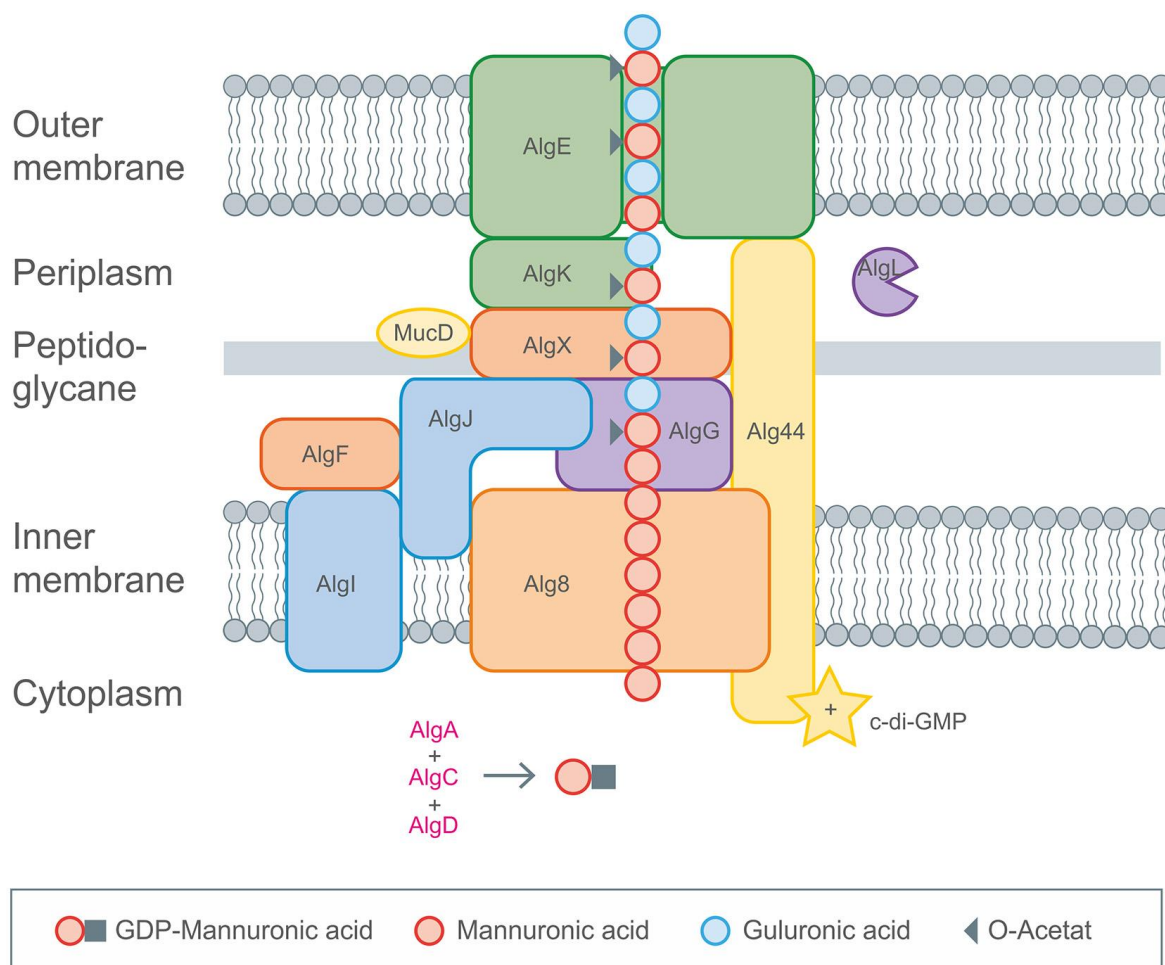


Figure 1-3: Overview of alginate biosynthesis in *Pseudomonas aeruginosa* PAO1. Guanosine diphosphate-mannuronic acid is formed through the enzymatic functions of AlgA, AlgC and AlgD. This is then polymerised by Alg8. Polymannurate traverses the inner and outer membranes *via* the complex of Alg8 Alg44, AlgX, AlgK, AlgG, AlgL and AlgE. The mannuronic acid residues are O-acetylated by AlgI, AlgJ and AlgK or epimerised into L-guluronic acid via AlgG. The mature alginate is then secreted out of the cell via the AlgE pore. This figure is reproduced with permission from Schmid and Rehm (2015) [135].

The decoration of alginate by O-acetylation not only protects alginate against degradation by alginate lyase (AlgL) [137], but the degree of acetylation determines the water-holding capacity of the polysaccharide where an increase in O-acetylation results in a higher degree of water-holding capacity [138].

Alginate has been shown to be important in desiccating conditions in *Pseudomonas putida* as disruption of the *algD* biosynthesis gene leads to increased cell death at low humidity [130]. This suggested that alginate maintains a hydrated environment to enhance survival of *P. putida* during desiccating conditions. The authors claimed that disruption of alginate biosynthesis in *P. aeruginosa* and *P. syringae* also conferred sensitivity to desiccation stress. However, this was performed using a high molecular weight solute to stimulate stress rather than subjecting the strains to lower relative humidity (RH). Although this could be interpreted as osmotic stress rather than a true desiccation stress, disruption of alginate biosynthesis did not confer sensitivity to osmotic conditions induced by NaCl.

#### 1.1.6 Trehalose

Trehalose is a ubiquitous disaccharide found in virtually all organisms [139]. First studied enzymatically in 1953 [140], this compatible solute has since been found to play a variety of roles including protection against abiotic stresses, carbon storage, and even as a virulence factor [141]. Trehalose has also found use in the food and pharmaceutical industry [142, 143] creating interest in producing large amounts of trehalose using biological systems [144, 145].

The biosynthesis of trehalose has been implicated in the tolerance of many biotic and abiotic stresses in a range of organisms [146-148], most notably of osmotic stress [112, 149]. Trehalose has also been implicated in protecting against desiccation stress. Positive correlations have been found between the intracellular concentration of trehalose and the level of desiccation resistance in bacteria [150, 151]. Additionally, the introduction and expression of trehalose biosynthesis genes from the high-trehalose producing and markedly desiccation-resistant organism *Microbacterium korensis* 3J1 conferred increased desiccation-protection upon the desiccation-sensitive *P. putida* KT2440 [151].

Bacterial mutants lacking trehalose biosynthetic genes have also been found to be attenuated during infection models [152, 153] making the biosynthesis of trehalose an attractive topic of research. Our understanding of bacterial trehalose biosynthesis has been informed by investigating the mechanisms in various bacteria. There are three widespread trehalose metabolic pathways in bacteria: OtsA/OtsB, TreY/TreZ and TreS (Figure 1-4) [147, 154].

The most prominent route of trehalose biosynthesis in bacteria is *via* the OtsA/OtsB pathway [154]. The OtsA/OtsB pathway produces trehalose using the trehalose 6-phosphate synthase OtsA and the trehalose 6-phosphatase OtsB. OtsA produces trehalose 6-phosphate from glucose 6-phosphate and UDP-glucose [155]. Trehalose 6-phosphate is then dephosphorylated by OtsB, forming trehalose.

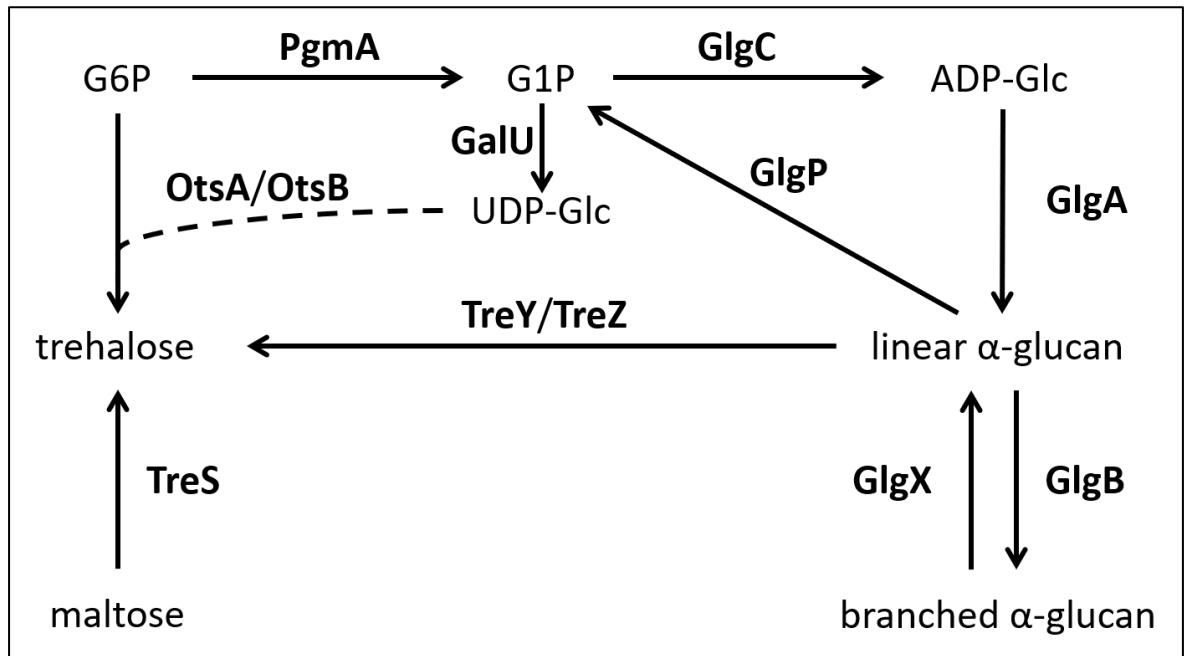


Figure 1-4: Overview of classical  $\alpha$ -glucan and trehalose biosynthesis in bacteria.(G6P; Glucose 6-phosphate, G1P; Glucose 1-phosphate, UDP-Glc; UDP-glucose, M1P; maltose 1-phosphate)

The TreS pathway utilises a single enzyme, the trehalose synthase TreS, to produce trehalose through the isomerisation of maltose [156]. However, as explained below, this is not the physiological role of this enzyme in all organisms [157]. The TreY/TreZ pathway utilises  $\alpha$ -glucans, such as bacterial glycogen produced by the classical GlgC-GlgA glycogen biosynthetic pathway, to synthesise trehalose [147, 158]. The maltooligosyl trehalose synthase TreY facilitates the conversion of the terminal reducing-end  $\alpha$ -1,4 bond of the  $\alpha$ -glucan molecule into an  $\alpha$ -1,1 glycosidic bond forming maltooligosyl trehalose. Trehalose is then liberated from maltooligosyl trehalose by the hydrolase action of TreZ.

Bacteria contain varying combinations of all three trehalose biosynthetic pathways or, in some cases, multiple copies of the same pathway or components thereof [159]. For

example, the only route to synthesise trehalose in *E. coli* is through the OtsA/OtsB pathway because it lacks gene homologues for the other trehalose biosynthetic pathways.

### 1.1.7 The biosynthesis of bacterial $\alpha$ -glucan

$\alpha$ -Glucan (also referred to as bacterial glycogen) is a large polysaccharide reported to have a relative molecular mass of up to  $1 \times 10^8$ . It is formed of thousands of glucose monomers linked via  $\alpha$ -1,4 glycosidic links with branch points formed from  $\alpha$ -1,6 linkages [160]. Each  $\alpha$ -glucan molecule consists of three different types of chain (Figure 1-5) [161]. The C chain is the chain possessing the sole free-reducing end, B chains bare  $\alpha$ -1,6 branches whereas the A chains do not.  $\alpha$ -Glucan is most commonly used as a carbon store which accumulates during the exponential phase of bacterial growth and can be recycled during unfavourable conditions. First studied in *E. coli* [162], the GlgC-GlgA pathway generates a linear  $\alpha$ -glucan *via* the action of the nucleotide diphosphoglucose pyrophosphorylase GlgC and glycogen synthase GlgA (Figure 1-4). GlgC catalyses the synthesis of ADP-glucose from glucose 1-phosphate (G1P), generated by the phosphoglucomutase PgmA [163, 164]. The activated glucose molecule is subsequently utilised by GlgA to extend an  $\alpha$ -1,4 linear  $\alpha$ -glucan chain [165, 166]. The linear  $\alpha$ -glucan is then branched by the branching enzyme GlgB. This involves the transfer of a non-reducing end oligomer to the 6-position of a residue within a linear chain to form a  $\alpha$ -1,6 branch point [167, 168]. Degradative enzymes GlgX and GlgP break down  $\alpha$ -glucan by debranching [169] and removing glucose units from the non-reducing end of the  $\alpha$ -glucan, respectively, [170] feeding into primary metabolism (Figure 1-4).

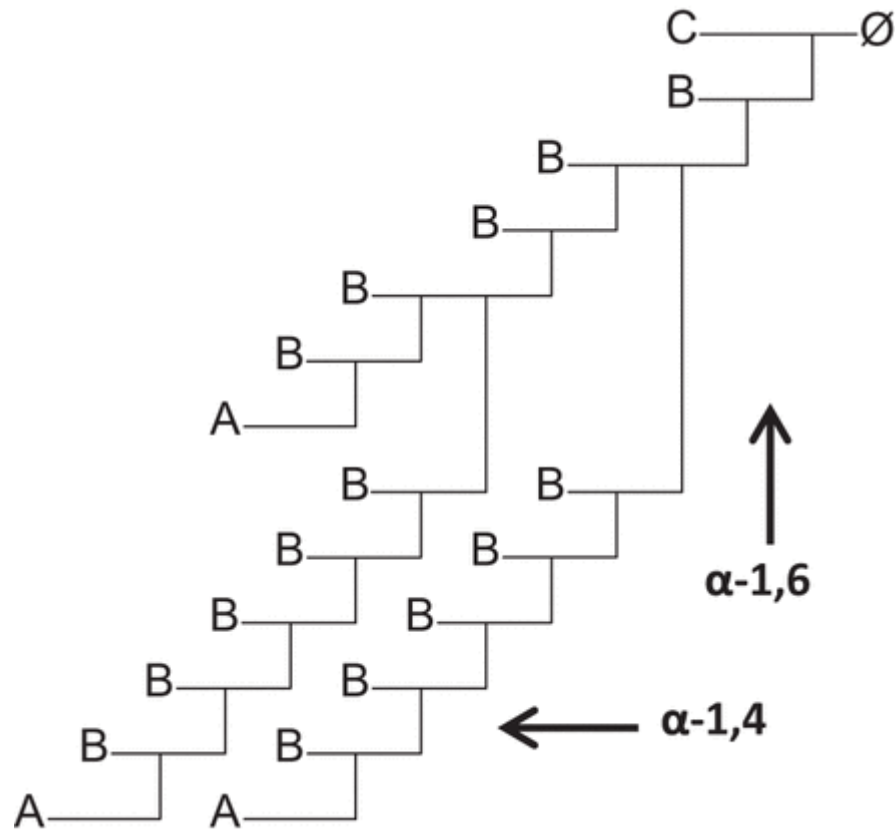


Figure 1-5: Structural schematic of bacterial  $\alpha$ -glucan.  $\alpha$ -Glucan consists of a primary C chain possessing the sole reducing end ( $\emptyset$ ). B chains are those that possess  $\alpha$ -1,6-branches whereas A chains possess no branches. This figure is reproduced with permission from Syson *et al.* (2016) [161].

### 1.1.8 GlgE pathway

The classical GlgC-GlgA pathway was once thought to be the only widespread bacterial method of synthesising  $\alpha$ -glucans with the genes responsible originally found to be present within 34% of sequenced bacterial genomes, although this was later refined to 20% [171, 172]. Furthermore, trehalose and  $\alpha$ -glucan were only linked through the classical GlgC-GlgA pathway and the subsequent degradation of  $\alpha$ -glucan by TreY/TreZ producing trehalose (Figure 1-4).

In 2010, Kalscheuer *et al.* identified a novel mechanism of synthesising  $\alpha$ -glucan in *Mycobacterium* spp.; this was the so-called GlgE pathway [153] (Figure 1-6). This four-step pathway, utilising trehalose to produce  $\alpha$ -glucan, consists of TreS, Pep2, GlgE and GlgB. This represents an additional link between trehalose and  $\alpha$ -glucan biosynthesis [153].

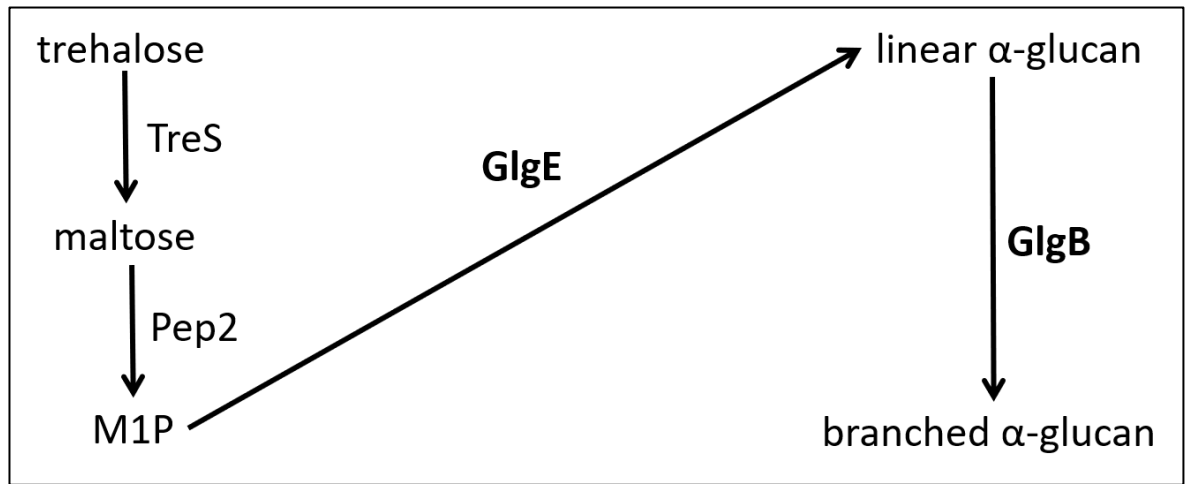


Figure 1-6: Overview of the mycobacterial GlgE pathway. Trehalose is isomerised into maltose by the trehalose synthase (TreS), maltose is then phosphorylated into maltose 1-phosphate by the maltokinase Pep2. M1P is then polymerised into linear  $\alpha$ -glucan by GlgE and branched by GlgB.

The first step of this pathway is the conversion of trehalose into maltose by TreS. As discussed above, TreS can catalyse the isomerisation of maltose into trehalose as one of the three main routes to trehalose biosynthesis [147]. Although the production of trehalose by TreS is energetically favourable, it was shown that in *Mycobacterium* spp. the overall flux favours the isomerisation of trehalose into maltose due to the presence of the GlgE pathway [157]. This is driven largely by the adenosine triphosphate (ATP)-dependent activity of the maltokinase Pep2 [173]. Maltose is phosphorylated by Pep2 into maltose 1-phosphate (M1P) [157, 174]. The maltosyltransferase GlgE enzyme then transfers the maltosyl moiety of M1P forming  $\alpha$ -1,4 linkages with the non-reducing ends of  $\alpha$ -glucan chains [175].

Mycobacterial  $\alpha$ -glucan is found both intra- and extra-cellularly in the cytosol and capsule, respectively. It was shown that purified capsular  $\alpha$ -glucan mediated interaction with the complement 3 receptor of mammalian macrophages [176] and that reduced levels of capsular  $\alpha$ -glucan led to reduced pathogenicity in murine infection models [177]. Taken together, this suggests that mycobacterial  $\alpha$ -glucan is an important disease determining factor.

The genes encoding the GlgE pathway are predicted to exist in 14% of sequenced bacterial genomes including those of *Pseudomonas* spp. [171, 178, 179]. Given that the *Pseudomonas* genus encompasses bacteria from a wide variety of environments and host-ranges, including both human and plant pathogens, it seems unlikely that the function of the predicted GlgE pathway and  $\alpha$ -glucan in *Pseudomonas* spp. would relate to disease in

mammals and plants. **This prompts the question: Is the GlgE pathway functional and what is its purpose in *Pseudomonas* spp.?**

#### 1.1.9 Predicted trehalose and $\alpha$ -glucan biosynthesis in *Pseudomonas* spp.

Given the intrinsic links between trehalose and  $\alpha$ -glucan biosynthesis in bacteria and to gain insight into the biology of  $\alpha$ -glucan, both systems must be studied. Trehalose and  $\alpha$ -glucan biosynthesis has been relatively understudied in *Pseudomonas* spp. with trehalose biosynthetic operons only being identified recently [74]. Comparative genomics has predicted that *Pseudomonas* spp. possess the gene homologues for the classical trehalose biosynthesis pathways, TreS and TreY/TreZ, but lack gene homologues of *otsA* and *otsB* [74]. Previous work assumed that both the TreS and TreY/TreZ pathways were both associated with the production of trehalose, however, they did not account for the presence of the GlgE pathway and its impact upon subsequent interpretations.

In *P. aeruginosa* PAO1 and *Pto*, the predicted trehalose biosynthetic genes are found within two main clusters, the *treS* and *treY/treZ* operons (Figures 1-7 and 1-8) [74, 180]. The predicted gene homologues of the GlgE pathway and classical  $\alpha$ -glucan biosynthesis are clustered within the *treS* and *treY/treZ* operons, respectively [171].

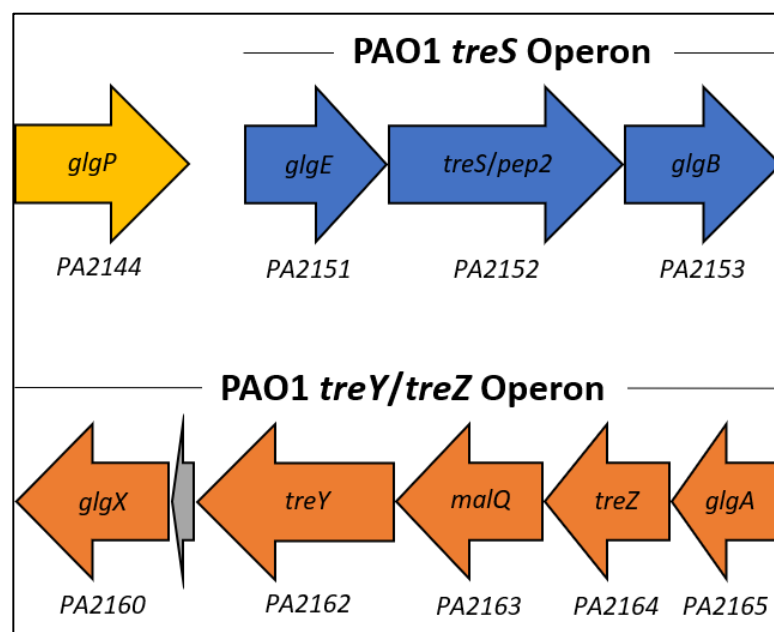


Figure 1-7: The genomic organisation of predicted trehalose and  $\alpha$ -glucan biosynthesis genes in *Pseudomonas aeruginosa* PAO1.

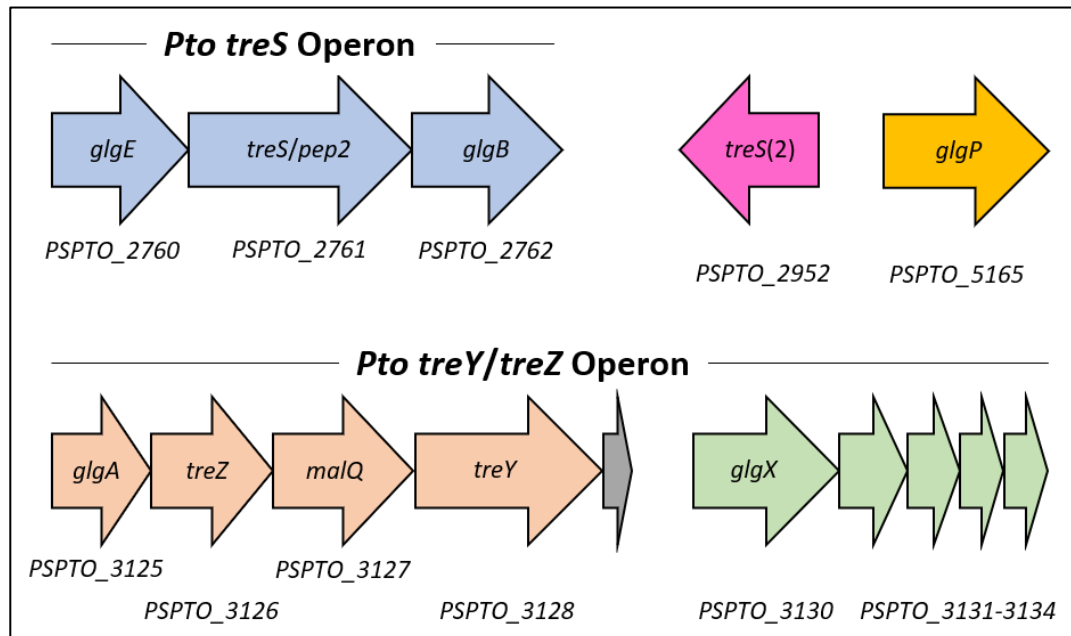


Figure 1-8: The genomic organisation of predicted trehalose and  $\alpha$ -glucan biosynthesis genes in *Pto*.

The so-called *treS* operon consists of predicted gene homologues encoding GlgE, (designated PA2151 in PAO1 and PSPTO\_2760 in *Pto*), TreS (PA2152, PSPTO\_2761) and GlgB (PA2153, PSPTO\_2762). In both the PAO1 and *Pto* genome the gene annotated as *treS* is fused to the predicted *pep2* encoding maltokinase and is henceforth referred to as *treS/pep2*.

The *treY/treZ* operon consists of the genes encoding predicted homologues of GlgA (PA2165, PSPTO\_3125), TreZ (PA2164, PSPTO\_3126), the glucanotransferase MalQ (PA2163, PSPTO\_3127) [74], TreY (PA2162, PSPTO\_3128) and GlgX (PA2160, PSPTO\_3130).

*Pto glgX* is predicted to form its own operon (PSPTO\_3130 – PSPTO\_3134) with four accessory genes whose functions are unknown (Figure 1-7, Figure 1-8) [181]. PA2161 and PSPTO\_3129 encode a small predicted open reading frame designated by the grey arrow in Figures 1-7 and 1-8 in both genomes, however these are not studied in this thesis. The gene encoding the recycling enzyme GlgP (PA2144, PSPTO\_5165) is orphaned in both species and found elsewhere in the genome. *Pto* is also predicted to possess a second homologue of TreS (PSPTO\_2952). This gene is not predicted to encode the Pep2 domain.

Although homologues of the phosphomutase PgmA are present, neither the PAO1 or *Pto* genomes harbour gene homologues predicted to encode GlgC. This suggests that these organisms lack the ability to produce ADP-glucose. However, gene homologues of the UDP-glucose pyrophosphorylase GalU are present. When *galU* from *E. coli* was expressed in *Corynebacterium glutamicum*, the concentrations of  $\alpha$ -glucan and trehalose increased

[182]. This suggests that there was increased flux through trehalose biosynthetic pathways. The authors suggest that UDP-glucose could be utilised in  $\alpha$ -glucan biosynthesis. Indeed, subsequent work has shown that GlgA from *M. tuberculosis* can utilise UDP-glucose as a donor when G1P was used as a substrate [183]. Therefore, we anticipate that GalU provides the phosphosugar donor for  $\alpha$ -glucan in *Pseudomonas* spp.

The clustering of the genes within the *treY/treZ* operon does indeed suggest that the function of this operon is to produce trehalose from GlgA-synthesised  $\alpha$ -glucan as previously published [74, 180]. The *treS* operon was originally thought to be involved in the biosynthesis of trehalose. However, the fusion of the *treS* gene with the maltokinase *pep2* and the genomic clustering of all four homologues of the GlgE pathway (*glgE*, *treS/pep2* and *glgB*) suggest that the *treS* operon is actually involved with the conversion of trehalose into  $\alpha$ -glucan rather than synthesising trehalose as previously thought.

By combining previous bioinformatic analysis of trehalose biosynthesis in *Pseudomonas* spp. [74, 180] with that of the GlgE pathway in *Mycobacterium* spp., I propose a model of trehalose and  $\alpha$ -glucan biosynthesis (Figure 1-9). One limitation of my model is that it does not account for the functions of MalQ or the presence of the second TreS homologue in *Pto*. This is addressed experimentally in Chapter 3.

My model predicts that the presence of both GlgA and GlgE results in two mechanisms of synthesising  $\alpha$ -glucan. It is currently unclear as to why *Pseudomonas* spp. has evolved two distinct biosynthetic pathways of  $\alpha$ -glucan biosynthesis and therefore prompts the following question: are there differences between these two pools of  $\alpha$ -glucan?

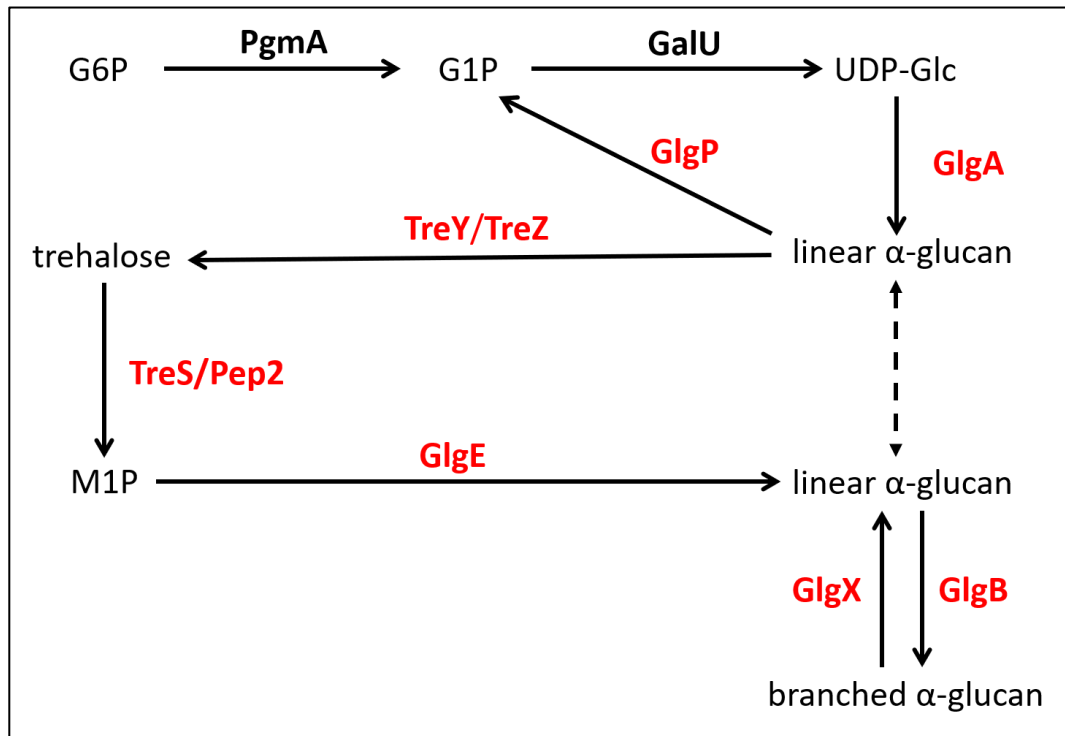


Figure 1-9: Predicted pathway of trehalose and  $\alpha$ -glucan biosynthesis in *Pseudomonas* spp. Red indicates the enzymatic reactions studied within this thesis (G6P; Glucose 6-phosphate, G1P; Glucose 1-phosphate, UDP-Glc; UDP-glucose, M1P; maltose 1-phosphate).

#### 1.1.10 Function of trehalose and $\alpha$ -glucan in *Pseudomonas* spp.

As described above, the function of trehalose has been well-studied in other bacteria. Indeed, trehalose has been implicated in the protection against hyperosmotic stress in *Pseudomonas* spp. Metabolomic analysis shows the accumulation of trehalose and other compatible solutes during osmotic conditions [106, 107]. Furthermore, the genes representing the *treS* and *treY/treZ* operons are upregulated in both PAO1 and *Pto* under hyperosmotic conditions [107, 184]. Furthermore, deletion of the *treY/treZ* and *treS* operons in *Pto*, resulted in the abolition of trehalose production and the generation of osmotically-sensitive strains [74]. This was not the case in *P. aeruginosa* PA14 where deletion of the trehalose biosynthesis operons abolished trehalose production albeit without an effect on osmotolerance [180].

Trehalose has also been implicated in the protection of *Pseudomonas* spp. against desiccation stress. The expression of the trehalose biosynthetic genes *otsA* and *otsB* from *Microbacterium koreensis* 3J1 conferred increased desiccation resistance to *P. putida* [151]. This suggests that trehalose can also protect *Pseudomonas* spp. against desiccating

conditions. However, given the presence of the GlgE pathway, this phenotype may have been indirectly related to trehalose.

Trehalose has previously been shown to be an important factor for plant infection. Transcriptomic profiling of *P. syringae* pv. *syringae* revealed that the genes representing the *treS* and *treY/treZ* operons were upregulated during both epiphytic and apoplactic lifestyles when compared to laboratory grown cells [132]. Furthermore, deletion of the *treS* and *treY/treZ* operons in both *Pto* and PA14 results in attenuation during infection of tomato plants or *Arabidopsis thaliana*, respectively [74, 180]. In the case of *Pto*, attenuation was exacerbated by reduced RH [74]. These studies implicate trehalose as an important virulence factor for survival in the phyllosphere and during apoplactic growth. Although important for plant infection, loss of the *treS* and *treY/treZ* operons did not attenuate PA14 during infection of insect or murine models [180]. Although trehalose was implicated, the impact of the potential abolition of  $\alpha$ -glucan biosynthesis was not considered.

The above studies have implicated trehalose as a stress protectant and as a virulence factor in *Pseudomonas* spp. However, the interpretation of these results did not consider the intrinsic genetic and functional linkage of trehalose and  $\alpha$ -glucan biosynthesis afforded by the GlgE pathway. For example, during osmotic conditions, genes responsible for trehalose and  $\alpha$ -glucan biosynthesis are both upregulated [184], and deletion of both trehalose and  $\alpha$ -glucan biosynthetic operons results in osmotically-sensitive strains in *Pto* [74]. **The question therefore arises: does  $\alpha$ -glucan play a role in protecting *Pseudomonas* spp. against osmotic stress?**

The increase in intracellular trehalose in *P. putida* via the expression of *otsA* and *otsB* was correlated with increased desiccation tolerance [151]. However, based on my predicted model (Figure 1-9) increased concentrations of trehalose could also have resulted in the increased biosynthesis of  $\alpha$ -glucan. Furthermore, attenuation during infection of tomato plants with *Pto* lacking both trehalose and  $\alpha$ -glucan biosynthetic genes is exacerbated by decreased RH. **This raises the question: does  $\alpha$ -glucan play a role during desiccation stress?**

Similarly, transcriptomic data show the upregulation of both trehalose and  $\alpha$ -glucan biosynthesis genes during the epiphytic and apoplactic lifestyle [132]. Furthermore, the strains used for plant infection contained whole operon deletions or large deletions of the surrounding loci. Little consideration was given to the effects of these deletions on  $\alpha$ -glucan

biosynthesis [74, 180, 181]. Conclusions drawn from the disruption of what was thought to be solely trehalose biosynthesis should therefore be revisited and the function of  $\alpha$ -glucan during *Pseudomonas* infection should be investigated. **This therefore leads to the following question: does  $\alpha$ -glucan play a role during the epiphytic or apoplastic lifestyle or during infection?**

## 1.2 Thesis Aims

Based on recent findings in *Mycobacterium* and *Pseudomonas*, it has become apparent that the biosynthesis of trehalose in *Pseudomonas* spp. is poorly understood. This is evident by the co-occurrence of trehalose biosynthetic genes with predicted homologues of the GlgE pathway genes. Previous work characterising the functions of trehalose in *Pseudomonas* spp. did not consider the presence of  $\alpha$ -glucan biosynthesis and how this impacts on the interpretation of subsequent data.

As described in this thesis, I probed the existence of the GlgE pathway and therefore  $\alpha$ -glucan biosynthesis in the human and plant pathogens *P. aeruginosa* PAO1 and *Pto*. I functionally characterised the roles of trehalose and  $\alpha$ -glucan in stress-tolerance individually by decoupling their biosynthesis. I then examined the contribution of these sugars during the bacterial infection of plants. Finally, I probed the regulation of trehalose and  $\alpha$ -glucan biosynthesis.

# Chapter 2: General Materials and Methods

## 2.1 Media and Methods

For routine experiments *Pseudomonas aeruginosa* PAO1 and *Escherichia coli* DH5 $\alpha$  strains were cultured in lysogeny broth (10 g/L tryptone, 5 g/L yeast extract, 10 g/L NaCl) at 37 °C. *Pseudomonas syringae* pv. *tomato* DC3000 strains were grown in L medium (10 g/L tryptone, 5 g/L yeast extract, 5 g/L NaCl, 1 g/L glucose anhydrous) at 28 °C [185]. The selection of transformants was facilitated by supplementing the appropriate media with tetracycline at concentrations of 12.5  $\mu$ g/mL (100  $\mu$ g/mL for *P. aeruginosa*) or 25  $\mu$ g/mL of gentamycin. For NMR spectroscopy and stress tolerance assays, M9 minimal medium was used (20 mM NH<sub>4</sub>Cl, 12 mM Na<sub>2</sub>HPO<sub>4</sub>, 22 mM KH<sub>2</sub>PO<sub>4</sub>, 8.6 mM NaCl, 1 mM MgSO<sub>4</sub>, 1 mM CaCl<sub>2</sub>, and 0.4% glucose, 0.4% casamino acids, 50  $\mu$ M FeCl<sub>3</sub>) [185]. Where appropriate liquid media were shaken or solidified with 1.5% Bacto agar (Difco, Surrey, UK).

## 2.2 Genetic Manipulation

Cloning was accomplished using standard molecular biology techniques, described below [186]. Polymerase chain reaction (PCR) products and plasmid digestion derivatives were purified using the Nucleospin<sup>®</sup> Gel and PCR Clean-up kit (Macherey-Nagel). Plasmids were extracted from *E. coli* DH5 $\alpha$  strains using the Nucleospin<sup>®</sup> Plasmid DNA Purification commercial kit (Macherey-Nagel). DNA digestions were performed using the appropriate restriction endonucleases (New England Biolabs). T4 DNA ligase (New England Biolabs) was used in the construction of all vectors in this study.

Unless otherwise stated, all PCR reactions were facilitated using Q5<sup>®</sup> High-Fidelity DNA polymerase (New England Biolabs). PCR protocols were conducted as per the manufacturers' guidance. Primary denaturation was performed for 30 seconds at 98 °C. Following this, 30 cycles of denaturation (98 °C, 10 seconds), annealing (varying temperatures, 30 seconds) and extension (72 °C, 30 seconds) was performed. Following this a final extension was performed at 72 °C for 120 seconds. The melting temperature (T<sub>m</sub>) of each primer was determined using the NEB T<sub>m</sub> Calculator (<http://tmcalculator.neb.com>). The annealing temperature for a given reaction was calculated as T<sub>m<sub>b</sub></sub> – 2 °C. Where T<sub>m<sub>b</sub></sub> represents the lowest T<sub>m</sub> of the primer pair. All primers and melting temperatures are listed in the appendix.

### 2.2.1 Construction of gene deletion plasmids

Primers were designed manually, and incorporate *Bam*HI or *Hind*III external restriction sites and an *Xba*I internal restriction site. Primers 7-12 and 61-66 were designed by Dr Jacob. G.

Malone and incorporate *BamHI*, *EcoRI* or *KpnI* external restriction sites and *XbaI* internal sites. Gene deletions were achieved by amplifying the upstream and downstream regions flanking the desired gene from the PAO1 and *Pto* genomes. For example the PCR reaction to amplify the upstream region of *PA2151* was performed using primers 1 and 2 (Appendix). This annealing temperature for this reaction was 70 °C.

The deletion of the *Pto treY/treZ* operon was facilitated by amplifying the upstream and downstream regions of *PSPTO\_3125* and *PSPTO\_3134* respectively using primers 117, 74 and 120, 121 (table A1). This generated approximately 1 Kb regions flanking the *treY/treZ* operon. The deletion of the *Pto treS* operon was facilitated by amplifying the upstream and downstream regions of *PSPTO\_2760* and *PSPTO\_2762* using primers 55, 56 and 69, 70 respectively.

The appropriate purified PCR fragments were digested with the appropriate restriction enzymes, this reaction was purified, and the PCR fragments were ligated using the internal *XbaI* sites and incorporated into pTS1 utilising the unique *BamHI* and *HindIII* restriction sites. pTS1 is a derivative of the suicide vector pME3087 containing a tetracycline resistance gene and a counter selection *sacB* gene marker [187]. Knockout vectors for *PA2152* and *PSPTO\_2761* were constructed from pME3087 utilising *BamHI* and *EcoRI* or *KpnI* restriction sites. This was performed by Jacob Malone.

### 2.2.2 Construction of *otsA/otsB* expression plasmids

To introduce *otsA/otsB* into the *Tn7* site of the *Pseudomonas* genomes, The *otsA/otsB* gene was amplified from the *Microbacterium koreensis* 3J1 genome [188] (Manzanera 2017, Gift) using primers 124 and 125 [151]. The resulting PCR product was cloned into the multiple cloning site of pME6032 [189]. Primers *Ptac\_F* (Primer 126) and *Ptac\_R* (Primer 127) were then used to amplify *otsA/otsB* in addition to the *tac* promoter and terminator of pME6032. This product was then cloned into the pUC18-mini-*Tn7T*-Gm vector [190].

### 2.2.3 Construction of *PglgA-lacZ* fusion reporter plasmids

Reporter strains PAO1 and *Pto P<sub>glgA</sub>-lacZ* were generated by introducing  $\beta$ -galactosidase gene fusion constructs under the control of the appropriate gene promoter. To ensure all proximal promoter elements would be included, I designated the upstream 500 bp relative to the predicted start codon of *glgA* in each strain as *P<sub>glgA</sub>*. This is because the promoter elements of both PAO1 and *Pto glgA* genes had not been previously investigated. In both

cases, this included 19 bp of the predicted coding sequence of *glgA* to ensure the in-frame translation of LacZ. The PAO1 *glgA* promoter was amplified using primers 19, 115, whereas the *Pto glgA* promoter was amplified using primers 73 and 116. The  $P_{glgA}$  fragments were then individually incorporated into the multiple cloning site of pUC18-mini-Tn7T-Gm-*lacZ10* [191] utilising the *Bam*HI and *Hind*III restriction sites, forming pUC18-mini-Tn7T-Gm-PAO1- $P_{glgA}$ -*lacZ* and pUC18-mini-Tn7T-Gm-*Pto-PglgA-lacZ*. The respective construct was transformed into the appropriate wild-type strain and integrated into the *att*Tn7 genomic site as described in Section 2.3.3.

## 2.3 Specialised transformation of *Pseudomonas*

### 2.3.1 Transformation of *Pseudomonas* spp. using pTS1 and pME6032 based vectors

*P. syringae* and *P. aeruginosa* were transformed with the appropriate pTS1 based deletion vector by adapting a previously described method [192]. This involved the preparation of electrocompetent cells by washes with 300 mM sucrose solution and their electroporation (2500 volts) with approximately 300 ng of the respective construct. Single crossover integration of the plasmid into the chromosome was selected for by the presence of tetracycline. Allele replacement was facilitated through growth to stationary phase and selected for by supplementing appropriate agar with 10% w/v sucrose. Gene deletion in tetracycline-sensitive, sucrose-resistant candidates was confirmed using PCR. To test for gene deletions, we used the respective test primers (tables A1) and a GoTaq® (Promega) based reaction. For example, primers 5 and 6 were used to test for deletion of *PA2151*. Primary denaturation was performed for 300 seconds at 95 °C. Following this, 30 cycles of denaturation (95 °C, 60 seconds), annealing (54 °C, 30 seconds) and extension (72 °C, 60 seconds) was performed. Following this a final extension was performed at 72 °C for 300 seconds.

### 2.3.2 Selection of double crossover candidates using pME3087 based vectors

As pME3087-based vectors  $\Delta$ *PA2152* and  $\Delta$ *PSPTO\_2761* lack the *sacB* counter selection gene, we used tetracycline enrichment to select for double crossover candidates. Tetracycline resistant single crossover strains were grown overnight in 50 mL of the appropriate medium, this culture was then diluted 100-fold in 3 mL of fresh medium and incubated for 2 hours, allowing cells to enter logarithmic growth. A sub-inhibitory concentration of tetracycline (5 µg/mL) was then added and cultures were incubated

further for 1 hour. Following this, the cultures were pelleted, and the supernatant was removed. The pellet was then subsequently resuspended with 5 mL of the appropriate media supplemented with tetracycline (5 µg/mL), phosphomycin (2 mg/mL) and piperacillin (2 mg/mL) to kill tetracycline resistant cells. Cultures were incubated for an additional 5 hours.

Following this final incubation, cells were pelleted and resuspended in 3 mL of fresh medium. Samples were then serially diluted and plated onto appropriate agar and incubated. Tetracycline-sensitive candidates, which had survived antibiotic treatment, were then screened for the appropriate gene deletion using PCR. To test for gene deletions, we used the respective test primers and a GoTaq<sup>®</sup> (Promega) based reaction. Tetracycline enrichment was performed by Jacob Malone.

### 2.3.3 Transformation of *Pseudomonas* spp. using pUC18 based vectors

pUC18 based vectors and the helper plasmid pTNS2 were combined in a 1:1 ratio to a final concentration of 100 ng [193]. This was then mixed with 100 µL of electrocompetent cells with subsequent electroporation. Integration of the plasmid into the *att::Tn7* chromosomal insertion site was selected for using gentamycin.

### 2.3.4 Storage and access of biological material

Once generated, strains were cultured in 6 mL of the appropriate liquid media and incubated overnight. Following this, 925 µL of overnight culture was added to 75 µL of dimethylsulfoxide and strains were stored at – 80 °C until required. When necessary strains were accessed by plating cryo-material onto appropriate solid medium and streaking for single colonies.

## 2.4 Metabolite Extraction

Liquid cultures of bacteria were diluted to an optical density at λ 600 nm (OD<sub>600</sub>) of 0.5 using PBS. This was plated onto mixed cellulose ester filter discs (Merck Millipore) placed on the surface of solidified M9 minimal medium. Once growth was sufficient (approximately 16 hours for *P. aeruginosa*, 48 hours for *P. syringae*) cells were harvested from the discs and resuspended in 5 mL of double-distilled H<sub>2</sub>O (ddH<sub>2</sub>O). Water was removed from the samples using vacuum drying for 16 hours. Following this, the sample dry weight was determined. Dry cells were resuspended in ddH<sub>2</sub>O and boiled at 95 °C for 20 minutes. Boiled cells were then centrifuged (10,000 x g, 10 minutes) and the resulting

supernatant was subject to additional boiling and centrifugation. The supernatant, now containing the total soluble metabolite content of the cells was vacuum dried for 16 hours. The resulting dried pellet was resuspended in 1200  $\mu\text{L}$  deuterium oxide ( $\text{D}_2\text{O}$ ).

## 2.5 Nuclear Magnetic Resonance Spectroscopy

Metabolite samples were subjected to NMR spectroscopy. Spectra were recorded with the Bruker AVANCE III 400 spectrometer, at room temperature using 400 megahertz for proton spectra with water suppression. Metabolite chemical shifts were recorded as parts per million (ppm) compared to the standard, 0.5 mM trimethylsilyl propanoic acid (TMSP; 0.00 ppm). Spectra were analysed using Topspin 3.0 (Bruker) and the concentrations of metabolites were established through the manual integration of peaks relative to TMSP. The area under the TMSP peak at 0.00 ppm was integrated and calibrated to a concentration of 4.5 mM  $\text{H}^+$ . The concentration of  $\text{H}^+$  of each metabolite of interest was then calculated relative to the reference peak divided by the number of protons responsible for the given resonance. For example, the  $\alpha$ -1,1 peak (5.2 ppm) corresponding to trehalose results from two identical protons. The metabolite mass was calculated as a product of the concentration, molecular weight and volume of sample (1.2 mL). The percentage of cell dry weight was then calculated by dividing the metabolite mass by the cell dry weight as determined in Section 2.4. Metabolite resonances were assigned based on previously established spectra [194].

## 2.6 Iodine Staining

The production of  $\alpha$ -glucan in bacterial colonies was visualised using iodine crystals (Sigma-aldrich). Crystals were placed in the lid of upside-down petri-dishes. Strains were stained for up to 2 minutes. The presence of  $\alpha$ -glucan within metabolite extracts was visualised by the addition of approximately 15% (v/v) Lugol's solution (Sigma-Aldrich).

## 2.7 Osmotic Stress Assays

The growth kinetics of each bacterial strain were measured using a 96-well microplate spectrometer (BioTek Instruments). *P. aeruginosa* cultures were diluted to  $\text{OD}_{600}$  of 0.01 and 5  $\mu\text{L}$  of this was used to inoculate 150  $\mu\text{L}$  of M9 minimal medium. *P. syringae* was diluted to an  $\text{OD}_{600}$  of 0.1 in M9 minimal medium and 150  $\mu\text{L}$  of this was used in each well. To examine osmotic stress conditions, media were supplemented with 0.35 M or 0.85 M NaCl for *Pto* and PAO1 respectively. Growth was monitored by measuring the  $\text{OD}_{600}$  every hour until stationary phase had been attained.

Chapter 3: Reverse genetics  
and biochemical  
characterisation of trehalose  
and  $\alpha$ -glucan biosynthesis in  
*Pseudomonas* spp.

### 3.1 Introduction

Trehalose is a ubiquitous disaccharide found to play a variety of roles in bacteria including protection against abiotic stresses, carbon storage, and even as a virulence factor [141]. As described in Section 1.1.6, there are three main mechanisms of synthesising trehalose in bacteria: the OtsA/OtsB, TreY/TreZ and TreS pathways. These trehalose biosynthetic pathways have been characterised in a wide range of bacteria [147, 154], however, trehalose biosynthesis in *Pseudomonas* spp. has been relatively understudied.

The biosynthetic operons for trehalose biosynthesis in *Pto* and *P. aeruginosa* PA14 were identified in 2010 and 2013, respectively [74, 180]. *Pseudomonas* spp. are predicted to possess gene homologues of *treS*, *treY* and *treZ*, clustered within the *treS* and *treY/treZ* operons, respectively (Figure 1-7, Figure 1-8). Some species, such as *Pto*, are predicted to possess an additional *treS* homologue. There are reports of *otsB* homologues found in certain *P. aeruginosa* species, however, this is not representative of the genus [181, 195].

In 2010, a novel mechanism of synthesising  $\alpha$ -glucan from trehalose was identified in *Mycobacterium* spp.; the so-called GlgE pathway. This four-step pathway, utilising trehalose to produce  $\alpha$ -glucan, consists of TreS, Pep2, GlgE and GlgB [153]. Although originally thought to synthesise trehalose, it was shown that TreS catalyses the degradation of trehalose in *M. smegmatis*, and that flux through TreS is from trehalose into maltose [157], driven by the ATP-dependent activity of Pep2 [173]. Maltose is then rapidly phosphorylated by Pep2 into M1P [157, 174]. After this, GlgE transfers the maltosyl moiety of M1P forming  $\alpha$ -1,4 linkages with the non-reducing ends of linear  $\alpha$ -glucan chains [175].

*Pseudomonas* spp. are predicted to possess homologues of the GlgE pathway genes and they are clustered within the *treS* and *treY/treZ* operons [171, 178, 179]. The genomic clustering of the genes within the *treY/treZ* operon (*glgA*, *treZ*, *malQ*, *treY* and *glgX*) does indeed suggest that the function of this operon in *Pseudomonas* spp. is to produce trehalose from GlgA-synthesised  $\alpha$ -glucan as previously published [74, 180]. The genetic organisation of the *treS* operon, however, may indicate something different. This operon is predicted to contain all four homologues of the GlgE pathway (*glgE*, *treS/pep2* and *glgB*). Furthermore, the *treS* gene homologue is predicted to be fused with the maltokinase *pep2*. Taken together, this suggests that the *treS* operon is actually involved with the degradation of trehalose into  $\alpha$ -glucan in *Pseudomonas* spp. rather than synthesising trehalose as

previously thought [74, 180]. This led to the proposition of a new biosynthetic model of trehalose and  $\alpha$ -glucan biosynthesis in *Pseudomonas* spp. (Figure 1-9).

Freeman *et al.* shows that following deletion of the *treS* or *treY/treZ* operons in *Pto*, trehalose biosynthesis is abolished [74]. This results in an osmotically-sensitive strain which is attenuated during tomato plant infection. Similarly, Djonović *et al.* reports that transposon insertions within the *glgA* and *treZ* genes in PA14, as well as deletion of the *treS* and/or *treY/treZ* operon, also results in the loss of trehalose production [180]. Although this did not result in an osmotically-sensitive strain, pathogenicity during plant infection was reduced. However, the authors did not consider the predicted presence of the GlgE pathway and therefore potential  $\alpha$ -glucan biosynthesis and how this impacts the subsequent interpretations. **This prompts the question: is the GlgE pathway functional and does *Pseudomonas* spp. produce  $\alpha$ -glucan?**

Given the intrinsic link between trehalose and  $\alpha$ -glucan biosynthesis, both of these systems must be studied. This chapter aims to systematically elucidate the mechanisms that *Pseudomonas* spp. use to synthesise trehalose and  $\alpha$ -glucan. Our hypothesis-driven approach used our biosynthetic model to predict the likely function of each gene product within the pathway (Figure 1-9). In order to test these hypotheses and experimentally characterise trehalose and  $\alpha$ -glucan biosynthesis in *Pseudomonas* spp., I generated strains possessing individual deletions of genes predicted to encode the key enzymes in both *P. aeruginosa* PAO1 and *Pto*. Proton nuclear magnetic resonance ( $^1\text{H-NMR}$ ) spectroscopy was then used to probe the effect of each deletion on the soluble metabolome and thereby infer protein function. This was then used to refine our model. Where required, other biochemical methods such as enzymology and iodine staining were used to robustly test the hypotheses.

Our model also suggested that the presence of both GlgA and GlgE may result in two mechanisms of synthesising linear  $\alpha$ -glucan. It was unclear whether these pools of linear  $\alpha$ -glucan are structurally unique or if they were interchangeable and can be used as substrates for other enzymes than those indicated by the model. This chapter also attempted to elucidate differences in chain length of GlgA- and GlgE- derived linear  $\alpha$ -glucan using iodine staining.

## 3.2 Results

3.2.1 Reverse genetics and nuclear magnetic resonance spectroscopy can be used to explore changes within the soluble carbohydrate metabolome of *Pseudomonas* spp. mutants

The genes encoding each of the predicted trehalose or  $\alpha$ -glucan biosynthesis proteins were deleted individually and in-frame in PAO1 and *Pto*. Additionally, several gene deletions were combined to create strains lacking two or more genes predicted to relate to trehalose or  $\alpha$ -glucan biosynthesis. To assess protein function, the effect of each gene deletion on the soluble metabolome was measured using  $^1\text{H-NMR}$  spectroscopy. The soluble metabolites for each mutant strain were extracted and their relative concentrations were determined and compared to the wild-type strain. The relative concentrations of trehalose and M1P produced by PAO1 and *Pto* mutant strains are summarised in Table 3-1 and Table 3-2, respectively. In most cases, glucose, maltose and  $\alpha$ -glucan concentrations cannot be resolved because their  $\alpha$ -anomeric signals overlap, and other distinguishing signals are hidden by other resonances. For example, the doublet corresponding to the  $\alpha$ -1,4 linkage of maltose can be obscured by the broad  $\alpha$ -glucan peak at 5.41 ppm, therefore, the presence or absence of glucose, maltose and  $\alpha$ -glucan will be noted as appropriate without quantification. The interpretation of results from individual strains and follow-on experiments are described in the following sections.

Table 3-1: Concentrations of trehalose and M1P produced by PAO1 strains. Metabolites are presented as percentages of cellular dry weight  $\pm$  standard error ( $n \geq 2$ ). – indicates no measurable metabolite, \* indicates significant differences as compared to the wild-type PAO1 as determined by a student's t-test ( $p \leq 0.05$ ). Presence or absence of  $\alpha$ -glucan as indicated by + or – respectively, ++ indicates increased  $\alpha$ -glucan production, <sup>a</sup> indicates linear  $\alpha$ -glucan only.

Strain	Trehalose (%)	M1P (%)	Presence of $\alpha$ -glucan
PAO1	0.13 $\pm$ 0.03	0.30 $\pm$ 0.03	+
PAO1 $\Delta$ glgE	0.12 $\pm$ 0.05	2.35 $\pm$ 0.43*	++
PAO1 $\Delta$ treS/pep2	0.89 $\pm$ 0.25*	-	-
PAO1 $\Delta$ glgB	0.74 $\pm$ 0.08*	0.78 $\pm$ 0.04*	++ <sup>a</sup>
PAO1 $\Delta$ glgA	-	-	-
PAO1 $\Delta$ treZ	-	0.25 $\pm$ 0.06	++
PAO1 $\Delta$ malQ	0.32 $\pm$ 0.04*	0.22 $\pm$ 0.03	++
PAO1 $\Delta$ treY	-	0.45 $\pm$ 0.13	+
PAO1 $\Delta$ glgX	-	0.03 $\pm$ 0.03*	-
PAO1 $\Delta$ glgP	0.24 $\pm$ 0.01*	0.29 $\pm$ 0.09	+

Table 3-2: Concentrations of trehalose and M1P produced by *Pto* strains. Metabolites are presented as percentages of cellular dry weight  $\pm$  standard error ( $n \geq 2$ ). – indicates no measurable metabolite, \* indicates significant differences as compared to the wild-type *Pto* as determined by a student's t-test ( $p \leq 0.05$ ). Presence or absence of  $\alpha$ -glucan as indicated by + or – respectively, <sup>a</sup> indicates linear  $\alpha$ -glucan only.

Strain	Trehalose (%)	M1P (%)	Presence of $\alpha$ -glucan
Wild-type <i>Pto</i>	1.33 $\pm$ 0.14	0.43 $\pm$ 0.15	-
<i>Pto</i> $\Delta$ glgE	1.24 $\pm$ 0.2	3.11 $\pm$ 0.45*	+
<i>Pto</i> $\Delta$ treS/pep2	0.57 $\pm$ 0.13*	-	-
<i>Pto</i> $\Delta$ glgB	1.34 $\pm$ 0.07	0.65 $\pm$ 0.31	+ <sup>a</sup>
<i>Pto</i> $\Delta$ glgA	0.1 $\pm$ 0.01*	0.16 $\pm$ 0.04	+
<i>Pto</i> $\Delta$ treZ	-	0.17 $\pm$ 0.02	+
<i>Pto</i> $\Delta$ malQ	1.03 $\pm$ 0.25	0.13 $\pm$ 0.09	+
<i>Pto</i> $\Delta$ treY	-	0.12 $\pm$ 0.05	+
<i>Pto</i> $\Delta$ glgX	0.01 $\pm$ 0.0*	0.09 $\pm$ 0.03*	+
<i>Pto</i> $\Delta$ glgP	2.04 $\pm$ 0.13*	0.23 $\pm$ 0.04	+
<i>Pto</i> $\Delta$ treS(2)	2.34 $\pm$ 0.15*	0.11 $\pm$ 0.02	-

### 3.2.2 PAO1 and *Pto* produce $\alpha$ -glucan, trehalose and maltose 1-phosphate

Wild-type PAO1 and *Pto* accumulated trehalose and maltose 1-phosphate (M1P) when cultured on M9 medium. PAO1 metabolomic extracts yielded concentrations of trehalose and M1P of 0.13  $\pm$  0.03% and 0.30  $\pm$  0.03% of the cellular dry weight, respectively. *Pto* produced higher amounts of trehalose than PAO1, with concentrations of trehalose and M1P corresponding to 1.1  $\pm$  0.25% and 0.38  $\pm$  0.12% of the cellular dry weight, respectively. PAO1 also accumulated low levels of glucose and/or maltose.

*Pseudomonas* spp. are not widely reported to accumulate  $\alpha$ -glucan [74]. Indeed  $\alpha$ -glucan was reportedly undetectable in both PA14 and *Pto* [74, 180]. However, broad peaks corresponding to  $\alpha$ -1,4 linkages were detected at 5.41 ppm in PAO1, indicating the accumulation of  $\alpha$ -glucan. Similar peaks were not convincingly present within the metabolome of wild-type *Pto*. However,  $\alpha$ -glucan was subsequently isolated from *Pto*, via chloroform/ethanol extraction and this was shown to be similar to  $\alpha$ -glucan extracted from *Mycobacterium* spp. (Karl Syson, personal communication) [196]. This suggests that PAO1 and *Pto* both produce  $\alpha$ -glucan and that the methods reported previously were not sensitive enough to detect the production of this polymer in *Pseudomonas* spp.

### 3.2.3 GlgA is a starch synthase that utilises UDP-glucose to produce linear $\alpha$ -glucan

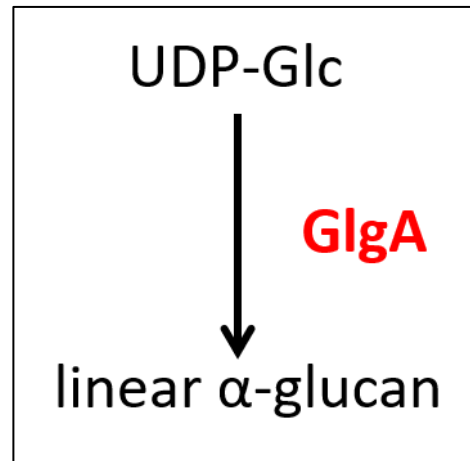


Figure 3-1: The predicted reaction catalysed by GlgA: the extension of linear  $\alpha$ -glucan using UDP-glucose as a substrate.

GlgA is annotated as a starch synthase [181] and based on our model (Figure 1-9) is the first committed enzyme in the pathway of trehalose and  $\alpha$ -glucan biosynthesis. It is predicted to extend linear  $\alpha$ -glucan using UDP-glucose and existing maltooligosaccharides as substrates (Figure 3-1). Because of this, I hypothesise that a *glgA* deletion ( $\Delta$ *glgA*) would result in the accumulation of UDP-glucose and the absence of linear  $\alpha$ -glucan and all downstream metabolites. To investigate the function of GlgA and thereby test this hypothesis, *glgA* was deleted in PAO1 and *Pto* and the soluble metabolome was extracted and analysed using  $^1\text{H-NMR}$  spectroscopy. Although UDP-glucose was not present at detectable levels, all downstream metabolites were absent within the metabolome of the PAO1  $\Delta$ *glgA* strain (Figure 3-2). In contrast to this, trehalose, M1P and  $\alpha$ -glucan were present in the metabolome of *Pto*  $\Delta$ *glgA*, suggesting there are alternative routes into trehalose and  $\alpha$ -glucan biosynthesis in this strain.

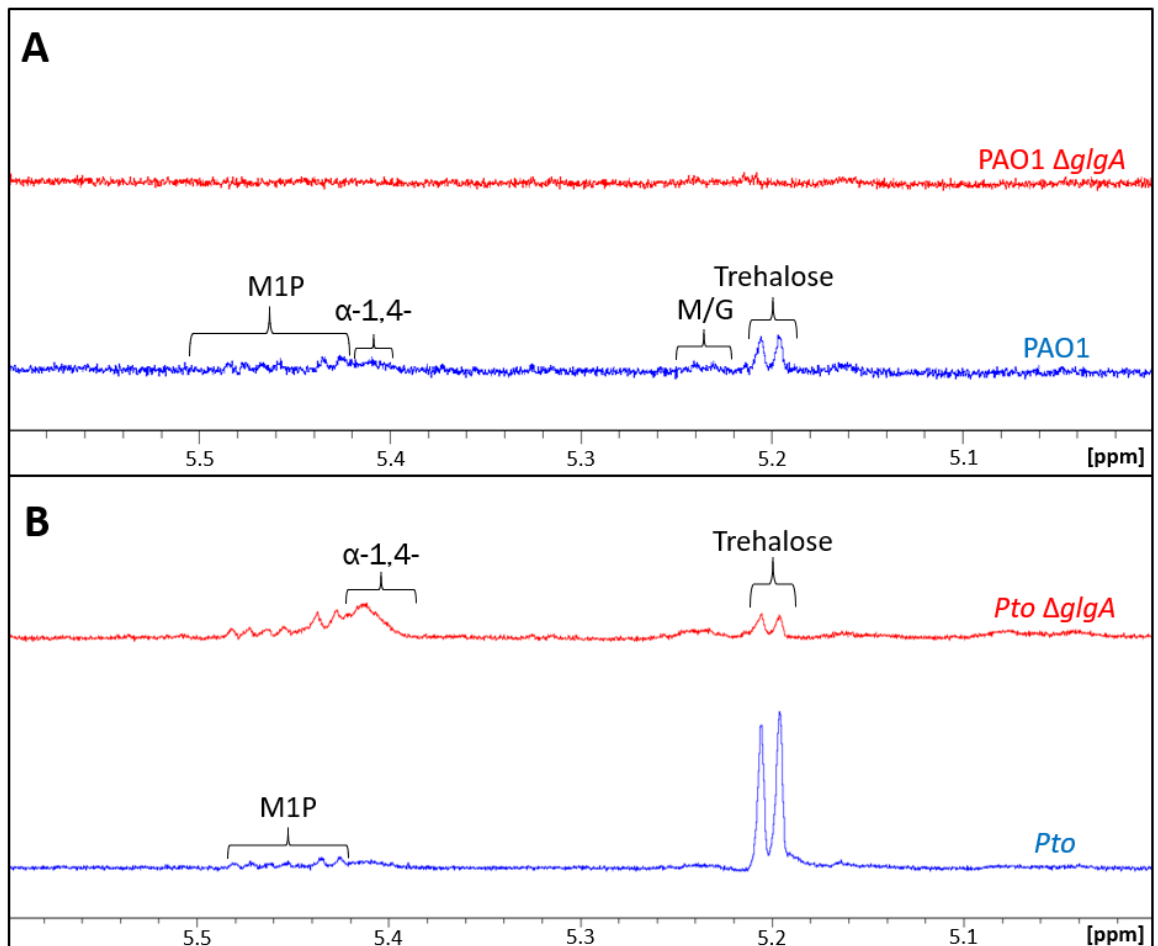


Figure 3-2: <sup>1</sup>H-NMR spectroscopy of the soluble metabolome following the deletion of *glgA* in *Pseudomonas* spp. Metabolomes were extracted from wild-type PAO1 (blue) and  $\Delta glgA$  (red) (A) and wild-type *Pto* (blue) and  $\Delta glgA$  (red) (B) cultured on M9 minimal medium. Peak assignments are as indicated based on previously established spectra. (M/G; maltose and/or glucose, M1P; maltose 1-phosphate,  $\alpha$ -1,4-;  $\alpha$ -glucan internal linkages). Resonances corresponding to metabolites of interest were absent following deletion of *glgA* in PAO1. Following deletion of *glgA* in *Pto* resonances corresponding to trehalose decreased, whereas those assigned to  $\alpha$ -glucan increased.

Because UDP-glucose was not detected upon deletion of *glgA* in PAO1, Karl Syson investigated the activity of GlgA *in vitro*. To investigate the substrate specificity and activity of GlgA, recombinant PAO1 GlgA protein was purified and provided with either ADP- or UDP-glucose as donor substrates. According to <sup>1</sup>H-NMR spectroscopy, GlgA produced linear  $\alpha$ -glucan from either substrate, without an acceptor maltooligosaccharide, with a preference for UDP-glucose (Karl Syson, unpublished data). A basic local alignment search tool revealed that *Pseudomonas* spp. lack ADP-glucose pyrophosphorylase homologues required to produce ADP-glucose, therefore UDP-glucose is the likely substrate of GlgA to produce linear  $\alpha$ -glucan.

Due to time constraints, the activity of *Pto* GlgA was not investigated *in vitro*. *Pto* GlgA shares 60.55% protein sequence percentage identity with PAO1 GlgA and is therefore thought to function the same.

3.2.4 GlgP recycles  $\alpha$ -glucan and produces glucose 1-phosphate from maltooligosaccharides

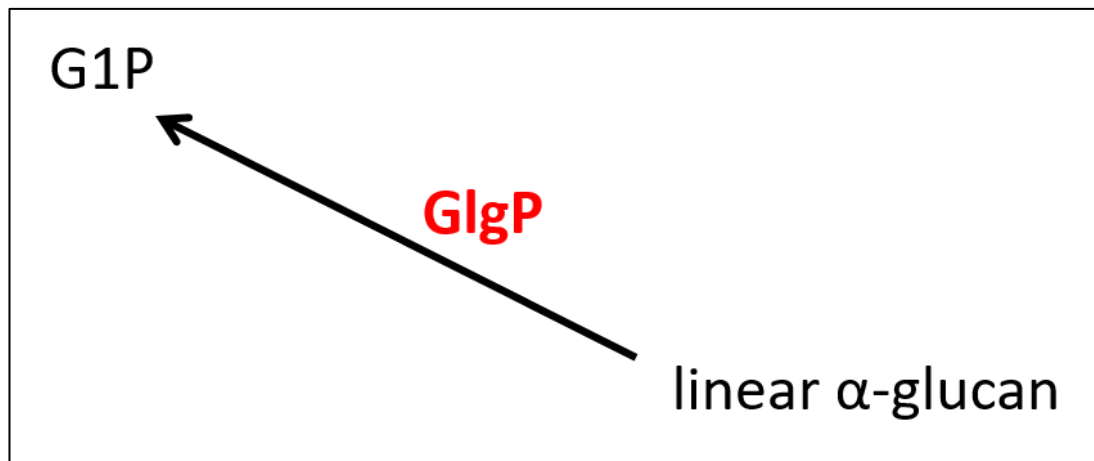


Figure 3-3: The predicted reaction catalysed by GlgP: the recycling of linear  $\alpha$ -glucan into glucose 1-phosphate (G1P).

Our predicted pathway suggests that the glycogen phosphorylase GlgP degrades the non-reducing ends of either linear or branched  $\alpha$ -glucan into G1P (Figure 3-3). This implies that the deletion of *glgP* ( $\Delta glgP$ ) should result in a decrease in the intracellular concentration of G1P and an increase in the concentration of linear  $\alpha$ -glucan and possibly other intermediate metabolites. However, as G1P is not accumulated to detectable levels in wild-type strains, we would not expect to be able to determine changes in this metabolite.

The *glgP* genes were deleted in both PAO1 and *Pto* and the soluble metabolomes were extracted and analysed. Following *glgP* deletion, the intracellular concentration of trehalose significantly increased by approximately 2-fold in both species, whereas M1P concentrations were not altered (Figure 3-4). The concentration of linear  $\alpha$ -glucan also appeared to increase as the corresponding peaks appeared larger when compared to the respective wild-type strain (5.41 ppm).

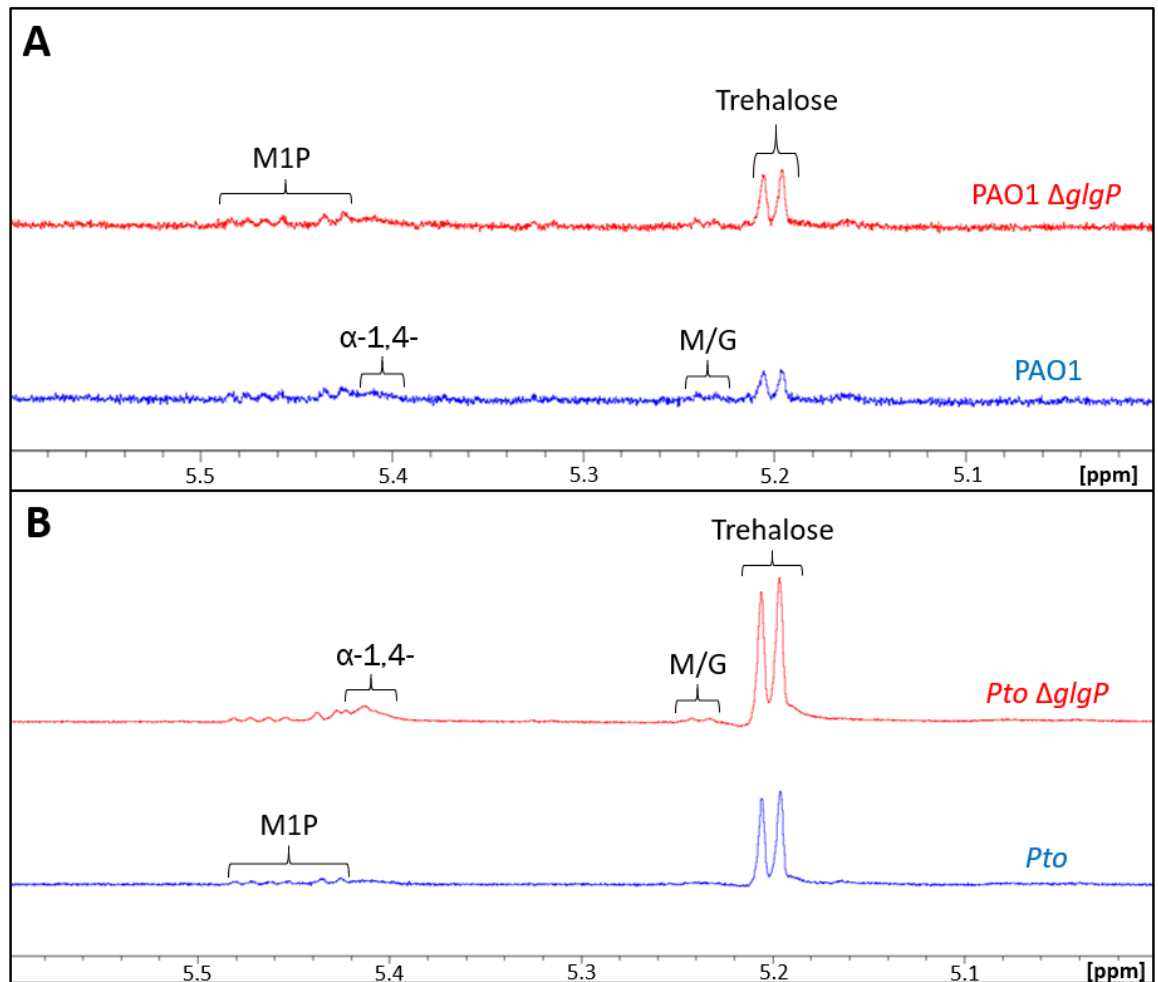


Figure 3-4: <sup>1</sup>H-NMR spectroscopy of the soluble metabolome following the deletion of *glgP* in *Pseudomonas* spp. Metabolomes were extracted from wild-type PAO1 (blue) and  $\Delta$ *glgP* (red) (A) and wild-type *Pto* (blue) and  $\Delta$ *glgP* (red) (B) cultured on M9 minimal medium. Peak assignments are as indicated based on previously established spectra. (M/G; maltose and/or glucose, M1P; maltose 1-phosphate,  $\alpha$ -1,4-;  $\alpha$ -glucan internal linkages). Resonances corresponding to trehalose and  $\alpha$ -glucan increased following deletion of *glgP* in both PAO1 and *Pto*.

As G1P was undetectable in *Pseudomonas* spp. metabolome extracts under the conditions tested, the product and substrate specificity of GlgP was investigated *in vitro*. Both *Pto* and PAO1 GlgP protein homologues were shown by <sup>1</sup>H-NMR spectroscopy to produce G1P when provided rabbit liver glycogen and phosphate as substrates (Karl Syson, unpublished data not shown).

Taken together, GlgP is a glycogen phosphorylase, absence of which leads to increased accumulation of the GlgE pathway metabolites, trehalose and  $\alpha$ -glucan, *in vivo*. GlgP also would be expected to produce G1P from maltooligosaccharides and use a branched substrate *in vitro*.

### 3.2.5 TreS/Pep2 utilises trehalose to produce maltose 1-phosphate

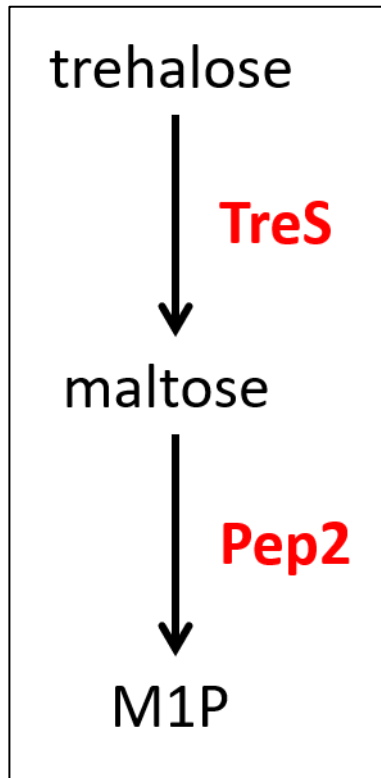


Figure 3-5: The predicted reactions catalysed by TreS/Pep2: the processing of trehalose into maltose and maltose 1-phosphate (M1P).

The fusion protein TreS/Pep2 is predicted to convert trehalose into maltose *via* the TreS domain and maltose into M1P *via* the Pep2 domain (Figure 3-5), therefore, deletion of *treS/pep2* ( $\Delta treS/pep2$ ) should result in an increase in the levels of trehalose and the absence of M1P and other downstream metabolites. Deletion of *treS/pep2* in PAO1 and subsequent analysis of the metabolome revealed an approximate 7-fold accumulation of trehalose when compared to wild-type PAO1. Peaks corresponding to M1P and  $\alpha$ -glucan were absent (Figure 3-6). This indicates that TreS/Pep2 does metabolise trehalose into M1P in PAO1.

In contrast, the levels of trehalose were reduced by approximately 50% in *Pto* following the deletion of *treS/pep2*. Peaks corresponding to M1P and  $\alpha$ -glucan were also absent (Figure 3-6). Although downstream metabolites are absent, the decrease in the levels of trehalose contradicts our predicted model. However, *Pto* possesses a second *treS* homologue, which is investigated later (Section 3.2.9).

The function of TreS/Pep2 was further investigated *in vitro*. Both PAO1 and *Pto* TreS/Pep2 recombinant fusion proteins exhibited trehalase and maltokinase activity. For example, maltose was produced when TreS/Pep2 was incubated with trehalose.

Furthermore, ATP activity was detected with either trehalose or maltose as substrates (Karl Syson, unpublished data).

Taken together, this shows that TreS/Pep2 does indeed function by metabolising trehalose into M1P as predicted. This shows flux through the TreS domain is from trehalose into maltose similar to the case in *M. smegmatis* [157].

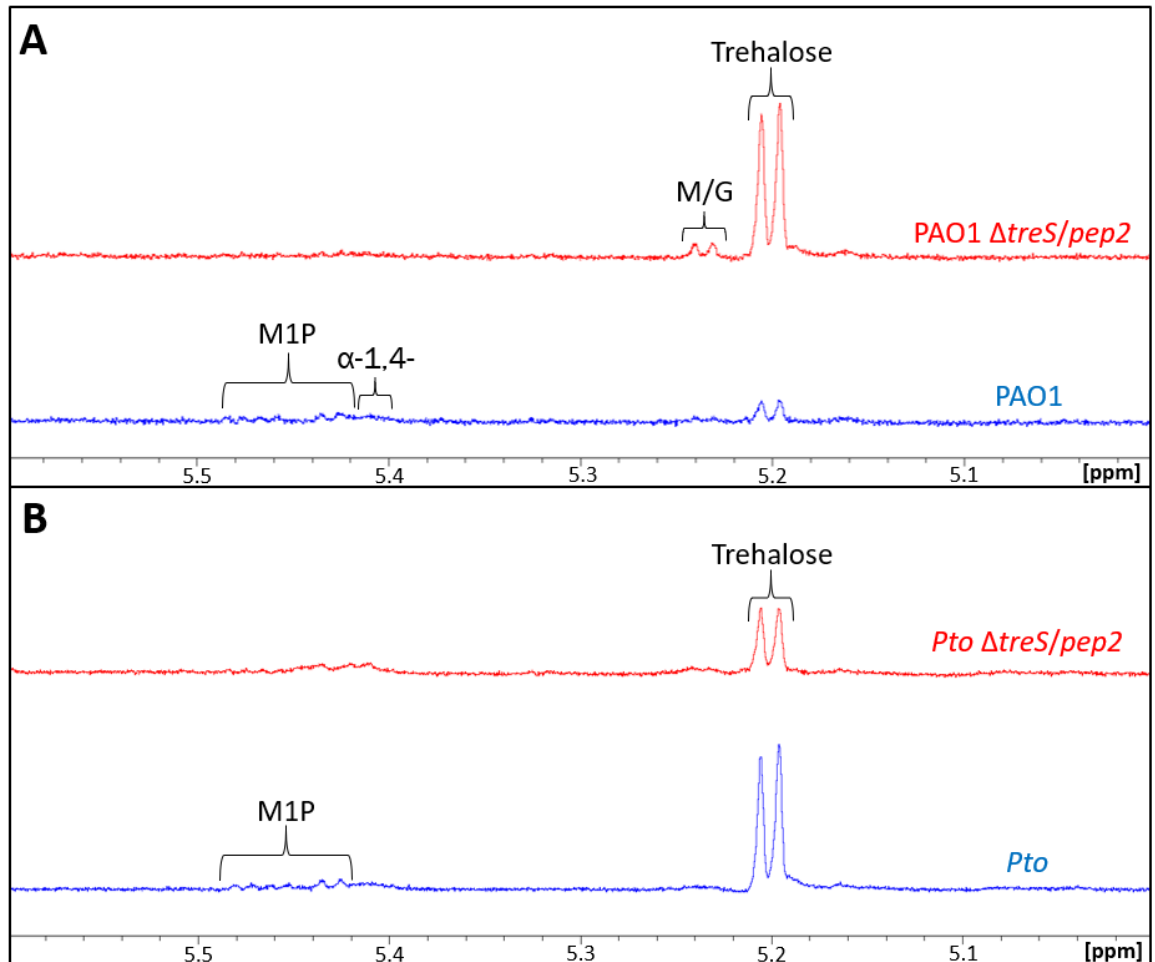


Figure 3-6: <sup>1</sup>H-NMR spectroscopy of the soluble metabolome following the deletion of *treS/pep2* in *Pseudomonas* spp. Metabolomes were extracted from wild-type PAO1 (blue) and  $\Delta treS/pep2$  (red) (A) and wild-type *Pto* (blue) and  $\Delta treS/pep2$  (red) (B) cultured on M9 minimal medium. Peak assignments are as indicated based on previously established spectra. (M/G; maltose and/or glucose, M1P; maltose 1-phosphate,  $\alpha$ -1,4-;  $\alpha$ -glucan internal linkages). Resonances corresponding to trehalose and maltose/glucose increased following deletion of *treS/pep2* in PAO1, whereas those corresponding to M1P decreased. Following deletion of *treS/pep2* in *Pto* resonances corresponding to trehalose and M1P decreased.

### 3.2.6 GlgE utilises maltose 1-phosphate to produce linear $\alpha$ -glucan



Figure 3-7: The predicted reaction catalysed by GlgE: the extension of linear  $\alpha$ -glucan using maltose 1-phosphate (M1P) as a substrate.

The predicted maltosyltransferase GlgE is thought to extend linear  $\alpha$ -glucan using M1P as a substrate (Figure 3-7), therefore, deletion of *glgE* should result in an increase in M1P and a build-up of up-stream metabolites such as trehalose and GlgA-derived  $\alpha$ -glucan. Following deletion of *glgE*, M1P levels accumulated to approximately 2.3 and 3.1% of the cell dry weight of PAO1 and *Pto*, respectively (Figure 3-8). Trehalose was detected at near-wild-type levels, while broad peaks corresponding to  $\alpha$ -1,4-linkages of  $\alpha$ -glucan appeared to have increased compared to the wild-type strains. Maltose and/or glucose was also detected in the spectra of PAO1  $\Delta$ *glgE*. Together, this suggests that GlgE utilises M1P and  $\alpha$ -glucan as substrates.

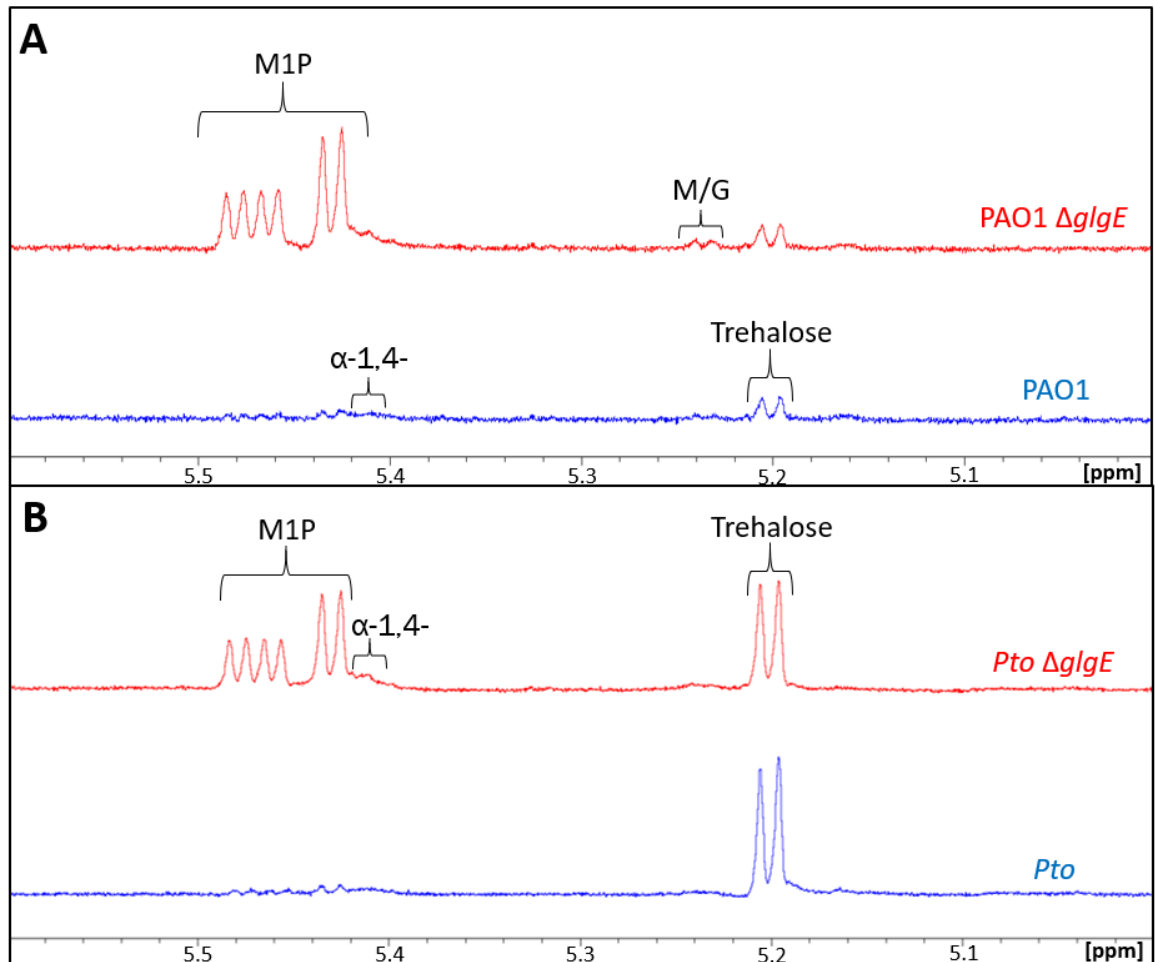


Figure 3-8: <sup>1</sup>H-NMR spectroscopy of the soluble metabolome following the deletion of *glgE* in *Pseudomonas* spp. Metabolomes were extracted from wild-type PAO1 (blue) and  $\Delta$ glgE (red) (A) and wild-type *Pto* (blue) and  $\Delta$ glgE (red) (B) cultured on M9 minimal medium. Peak assignments are as indicated based on previously established spectra. (M/G; maltose and/or glucose, M1P; maltose 1-phosphate,  $\alpha$ -1,4-;  $\alpha$ -glucan internal linkages). Resonances corresponding to M1P and  $\alpha$ -glucan increased following deletion of *glgE* in PAO1 and *Pto*.

To show that GlgE was capable of synthesising  $\alpha$ -glucan, PAO1 and *Pto* GlgE recombinant proteins were purified and their activities were characterised *in vitro*. Enzyme kinetics confirmed that both PAO1 and *Pto* GlgE proteins utilised both M1P and maltooligosaccharides as substrates and produced inorganic phosphate as a measurable bi-product (Karl Syson, unpublished data). Taken together, the *in vitro* and *in vivo* data suggest that GlgE is a maltosyltransferase utilising M1P to extend  $\alpha$ -glucan chains.

### 3.2.7 Absence of GlgB results in the accumulation of long linear $\alpha$ -glucan

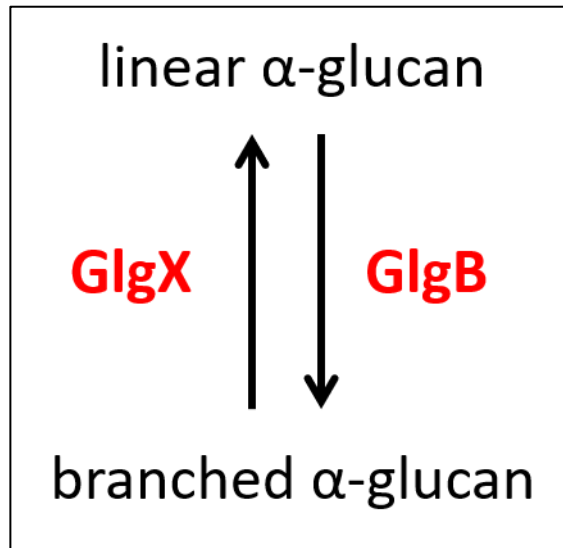


Figure 3-9: The predicted reaction catalysed by GlgB and GlgX: the branching of linear  $\alpha$ -glucan into branched  $\alpha$ -glucan *via* GlgB and the debranching of branched  $\alpha$ -glucan into linear  $\alpha$ -glucan by GlgX.

The branching enzyme GlgB is predicted to act upon linear  $\alpha$ -glucan to produce branched  $\alpha$ -glucan (Figure 3-9), therefore, deletion of *glgB* should result in an increase in longer linear  $\alpha$ -glucan chains and the absence of branched  $\alpha$ -glucan. The deletion of the gene encoding the predicted branching enzyme in PAO1 (PAO1  $\Delta$ *glgB*) led to increased concentrations of upstream metabolites: trehalose, maltose and/or glucose and M1P (Figure 3-10). The levels of trehalose and M1P were increased by approximately 6-fold and 2.5-fold respectively when compared to wild-type PAO1. The absence of GlgB also resulted in an increase in the broad signal associated with  $\alpha$ -1,4 linear glucan. The metabolome of *Pto*  $\Delta$ *glgB* showed an increase in linear  $\alpha$ -glucan, but no significant changes were observed in the concentrations of trehalose or M1P when compared to wild-type *Pto* (Figure 3-10).

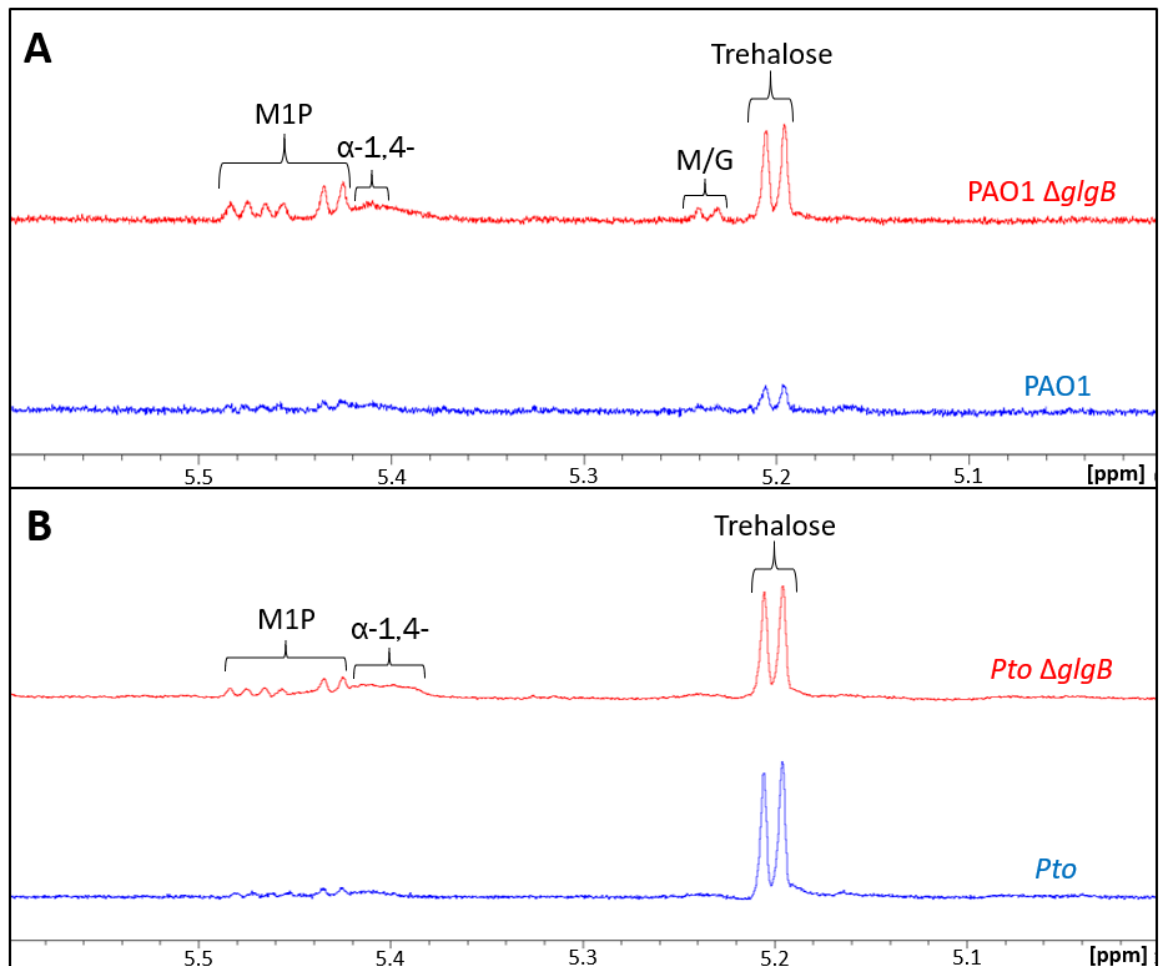


Figure 3-10:  $^1\text{H-NMR}$  spectroscopy of the soluble metabolome following the deletion of *glgB* in *Pseudomonas* spp. Metabolomes were extracted from wild-type PAO1 (blue) and  $\Delta\text{glgB}$  (red) (A) and wild-type *Pto* (blue) and  $\Delta\text{glgB}$  (red) (B) cultured on M9 minimal medium. Peak assignments are as indicated based on previously established spectra. (M/G; maltose and/or glucose, M1P; maltose 1-phosphate,  $\alpha$ -1,4-;  $\alpha$ -glucan internal linkages). Resonances corresponding to trehalose, M1P and  $\alpha$ -glucan increased following deletion of *glgB* in PAO1. Resonances corresponding to  $\alpha$ -glucan increased following deletion of *glgB* in *Pto*. Trehalose and M1P concentrations did not appear to change.

Although  $^1\text{H-NMR}$  spectroscopy showed an increase in the concentration of  $\alpha$ -1,4 linkages in the metabolome of  $\Delta\text{glgB}$ , it cannot directly indicate the average linear  $\alpha$ -glucan chain length. Matrix-assisted laser desorption/ionization mass spectrometry (MALDI-MS) was initially used to investigate the length of linear  $\alpha$ -glucan in  $\Delta\text{glgB}$  strains. However, the metabolomic extracts were too crude to identify relevant carbohydrate peaks.

As an alternative, iodine staining was used as a semi-quantitative method to investigate the length of  $\alpha$ -glucan [197]. When wild-type PAO1 was exposed to iodine vapour there was no obvious staining. In contrast, when PAO1  $\Delta\text{glgB}$  was exposed to iodine vapour, the cellular material stained a dark brown colour suggesting the increased presence of long linear  $\alpha$ -glucan (Figure 3-11). Similar staining was also observed when Lugol's solution was added to the metabolite extracts, where the absence of GlgB ( $\Delta\text{glgB}$  strain) resulted in

purple staining of the extracts (Figure 3-11). This may suggest that there was an accumulation of linear  $\alpha$ -glucan with an estimated DP between 33 – 38 [197].

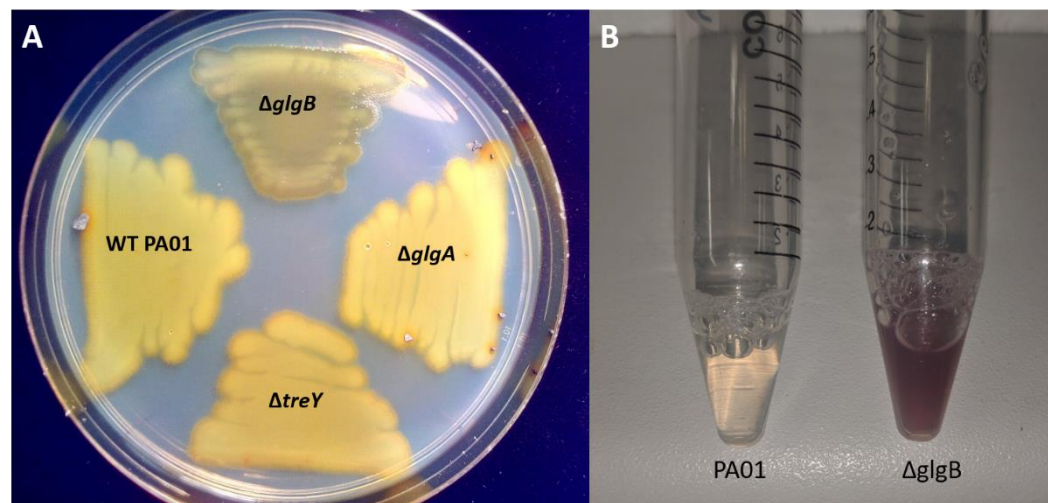


Figure 3-11: Visualising the production of  $\alpha$ -glucan in PAO1 strains using iodine staining. (A) Iodine staining of *Pseudomonas aeruginosa* PAO1 strains cellular material using iodine vapour. Wild-type PAO1,  $\Delta glgA$  and  $\Delta treY$  do not exhibit iodine staining, whereas  $\Delta glgB$  cellular material stain brown upon exposure to iodine vapour. (B) Staining of PAO1 and  $\Delta glgB$  soluble metabolome extractions using Lugol's solution. The metabolome extracted from PAO1  $\Delta glgB$  stains purple upon addition of Lugol's solution.

To test if GlgB could produce branched  $\alpha$ -glucan, the activity of GlgB was investigated *in vitro*. Maltohexaose and M1P was incubated with both recombinant GlgE and GlgB from PAO1 and *Pto*. Subsequently, MALDI-MS and transmission electron microscopy showed that together GlgE and GlgB formed branched  $\alpha$ -glucan (Karl Syson, unpublished data).

Together, these results show that GlgB is a branching enzyme that introduces branches into linear  $\alpha$ -glucan. The absence of this enzyme can result in a build-up of up-stream metabolites and the accumulation of long linear  $\alpha$ -glucan in PAO1.

### 3.2.8 GlgX functions to debranch $\alpha$ -glucan in *Pseudomonas* spp.

The glycogen debranching enzyme GlgX is predicted to remove  $\alpha$ -1,6 branches from  $\alpha$ -glucan (Figure 3-9), therefore, there should be an accumulation of branched  $\alpha$ -glucan following deletion of *glgX*. Metabolomic extracts from *Pto* strains lacking the predicted glycogen debranching enzyme GlgX ( $\Delta glgX$ ) yielded peaks corresponding to both trehalose and M1P (Figure 3-12). However, the concentration of these metabolites was significantly lower than compared to the wild-type *Pto*. Although peaks associated with  $\alpha$ -1,6 linkages were below the detection limit, the concentration of  $\alpha$ -1,4 glycosidic bonds of  $\alpha$ -glucan was increased. This contradicts my model because an increase in  $\alpha$ -glucan was not observed. This suggests that the degradation and recycling of branched  $\alpha$ -glucan is required for the

presence of trehalose and M1P in *Pto*. No relevant metabolite signals were detected in the corresponding PAO1 strain (Figure 3-12).

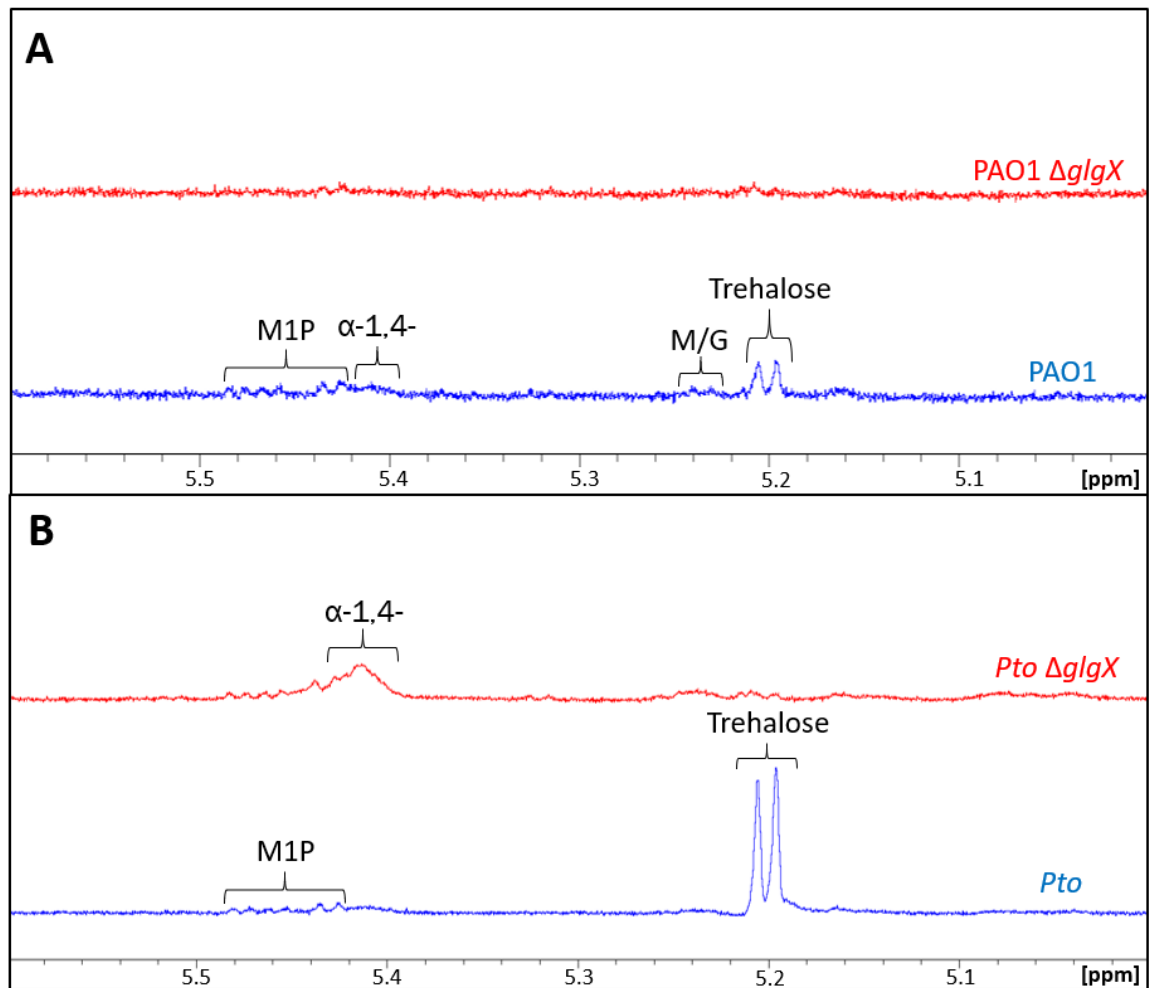


Figure 3-12: <sup>1</sup>H-NMR spectroscopy of the soluble metabolome following the deletion of *glgX* in *Pseudomonas* spp. Metabolomes were extracted from wild-type PAO1 (blue) and  $\Delta glgX$  (red) (A) and wild-type *Pto* (blue) and  $\Delta glgX$  (red) (B) cultured on M9 minimal medium. Peak assignments are as indicated based on previously established spectra. (M/G; maltose and/or glucose, M1P; maltose 1-phosphate,  $\alpha$ -1,4-;  $\alpha$ -glucan internal linkages). Resonances corresponding to metabolites of interest were absent following deletion of *glgX* in PAO1. Following deletion of *glgX* in *Pto* resonances corresponding to trehalose were absent, whereas those assigned to  $\alpha$ -glucan increased.

To determine whether GlgX possessed debranching activity, GlgX from PAO1 and *Pto* was incubated with rabbit liver glycogen. MALDI-MS showed that a carbohydrate profile was produced following incubation of rabbit liver glycogen with GlgX consistent with debranching activity (Karl Syson, personal communication).

### 3.2.9 TreS(2) functions as a second trehalose synthase in *Pto*

Unlike PAO1, bioinformatic analysis predicts that the *Pto* genome contains a second homologue of TreS designated TreS(2). Assuming TreS(2) exhibits the same isomerisation activity as the TreS domain of TreS/Pep2 (Figure 3-5), deletion of *treS(2)* should result in

altered levels of intracellular trehalose when compared to wild-type *Pto*. Deletion of *treS(2)* in *Pto* resulted in an approximate 2-fold increase in the levels of intracellular trehalose, whereas M1P levels were not significantly different when compared to the wild-type *Pto* strain (Figure 3-13). This suggests that this TreS homologue is responsible for the degradation of trehalose, presumably into maltose.

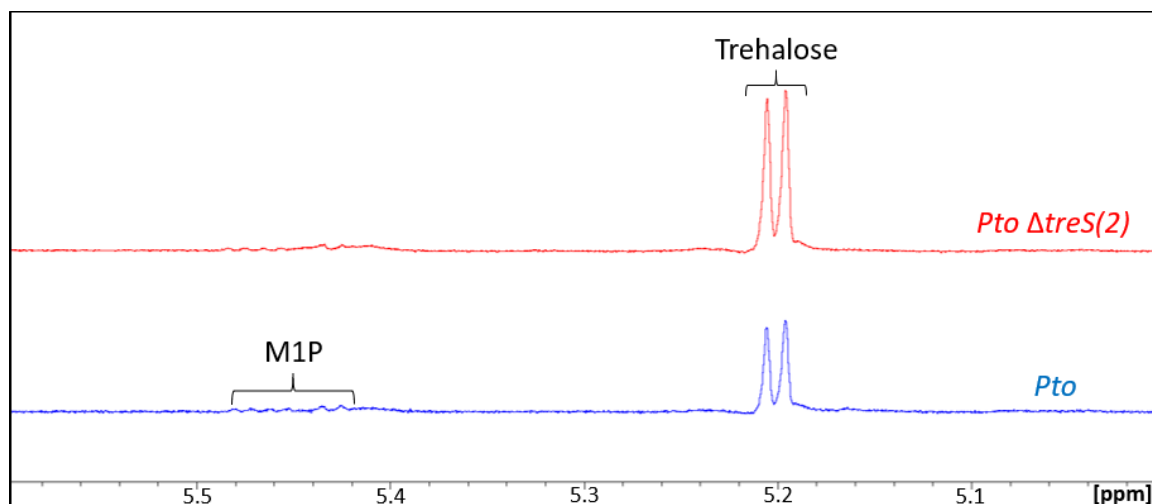


Figure 3-13:  $^1\text{H}$ -NMR spectroscopy of the soluble metabolome following the deletion of *treS(2)* in *Pseudomonas syringae* pv. tomato. Metabolomes were extracted from wild-type *Pto* (blue) and  $\Delta\text{treS}(2)$  (red) cultured on M9 minimal medium. Peak assignments are as indicated based on previously established spectra. (M1P; maltose 1-phosphate). Resonances corresponding to trehalose were increased following deletion of *treS(2)* in *Pto*. The concentration of M1P did not appear to change.

To show that TreS(2) can utilise both trehalose and maltose as substrates, recombinant TreS(2) was purified and incubated with either disaccharide.  $^1\text{H}$ -NMR spectroscopy showed that TreS(2) can utilise both trehalose to synthesise maltose and maltose to synthesise trehalose *in vitro* (Karl Syson, personal communication). These results together show that *Pto* possesses two functional TreS homologues, the second of which (TreS(2)) likely functions to metabolise trehalose into maltose for entry into the GlgE pathway.

### 3.2.10 TreY and TreZ produce trehalose by degrading linear $\alpha$ -glucan producing maltooligosyltrehalose as an intermediate

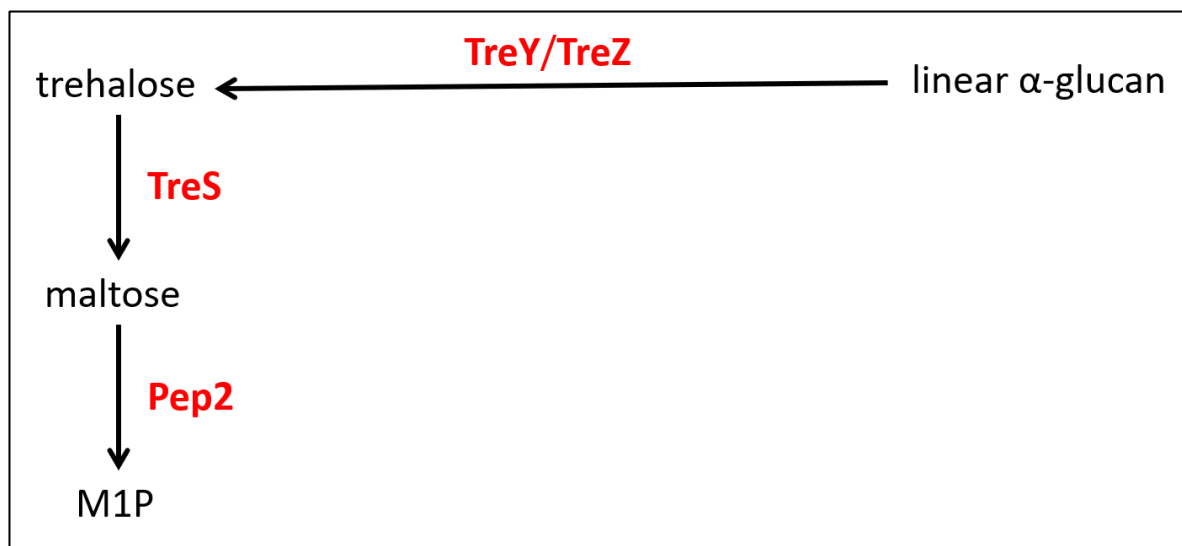


Figure 3-14: The predicted reactions catalysed by TreY, TreZ and TreS/Pep2: the degradation of linear  $\alpha$ -glucan into trehalose and the subsequent processing of trehalose into maltose and maltose 1-phosphate (M1P) by TreS/Pep2.

The maltooligosyl trehalose synthase TreY and the maltooligosyl trehalose trehalohydrolase TreZ are predicted to degrade the reducing end of linear  $\alpha$ -glucan into trehalose (Figure 3-14). First, TreY is predicted to facilitate the conversion of the terminal  $\alpha$ -1,4 bond of  $\alpha$ -glucan into an  $\alpha$ -1, $\alpha$ -1-glycosidic bond forming maltooligosyl trehalose. Trehalose is then predicted to be liberated from maltooligosyltrehalose by the hydrolase action of TreZ. Based on this prediction, I hypothesise that the deletion of either *treY* or *treZ* would result in the abolition of trehalose production and in an increase of  $\alpha$ -glucan levels. Furthermore, deletion of *treZ* should lead to an accumulation of maltooligosyl trehalose due to the isomerisation activity of TreY.

Deletion of *treY* and *treZ* resulted in the loss of trehalose production in both PAO1 and *Pto*. This can be seen in Figure 3-15 which also shows that levels of  $\alpha$ -glucan appeared to increase in both  $\Delta treY$  and  $\Delta treZ$  for both species (this was more evident in  $\Delta treZ$  strains). Deletion of *treZ* also resulted in the formation of a broad species at 5.2 ppm corresponding to the terminal  $\alpha$ -1,1 linkage of maltooligosyl trehalose. This supports the hypothesis that in *Pseudomonas* spp. TreY and TreZ work in concert to produce trehalose through the degradation of  $\alpha$ -glucan, producing maltooligosyl trehalose as an intermediate metabolite.

Surprisingly, peaks corresponding to M1P were present in the metabolomes of both  $\Delta treY$  and  $\Delta treZ$  for PAO1 and *Pto*. This was not expected as my model predicts that the only route to M1P biosynthesis in *Pseudomonas* spp. is dependent on trehalose production and therefore TreY and TreZ. This shows that an alternative route exists to maltose and M1P biosynthesis in *Pseudomonas* spp.

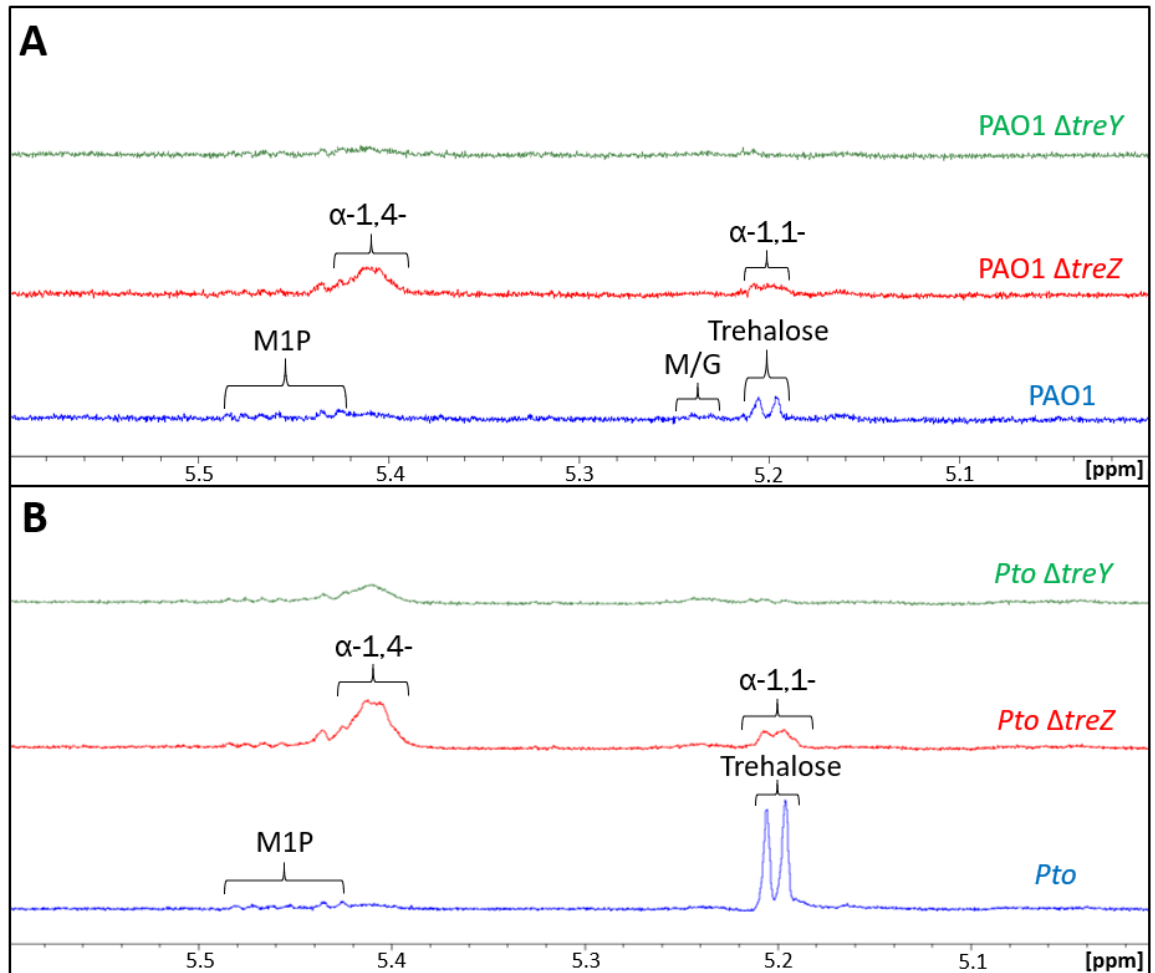


Figure 3-15:  $^1\text{H-NMR}$  spectroscopy of the soluble metabolome following the deletion of *treZ* and *treY* in *Pseudomonas* spp. Metabolomes were extracted from wild-type PAO1 (blue),  $\Delta\text{treZ}$  (red) and  $\Delta\text{treY}$  (green) (A) and wild-type *Pto* (blue) and  $\Delta\text{treZ}$  (red) and  $\Delta\text{treY}$  (green) (B) cultured on M9 minimal medium. Peak assignments are as indicated based on previously established spectra. (M/G; maltose and/or glucose, M1P; maltose 1-phosphate,  $\alpha$ -1,4-;  $\alpha$ -glucan internal linkages  $\alpha$ -1,1-; terminal linkage of maltooligosyl trehalose). Resonances corresponding to trehalose were absent, whilst those corresponding to  $\alpha$ -glucan increased following deletion of *treZ* or *treY* in PAO1 and *Pto*. Furthermore, peaks corresponding to the terminal linkage of maltooligosyl trehalose were present within the metabolomes extracted from  $\Delta\text{treZ}$  strains. M1P was present following deletion of *treZ* or *treY* in PAO1 and *Pto*.

### 3.2.11 MalQ disproportionates $\alpha$ -glucan and is capable of synthesising maltose

To identify the source of M1P found within the  $\Delta\text{treY}$  and  $\Delta\text{treZ}$  metabolomes, it was hypothesised that the predicted  $\alpha$ -glucanotransferase *malQ* [181] may utilise  $\alpha$ -glucan to produce maltose that would be converted to M1P by the Pep2 kinase domain. *malQ* is clustered between *treZ* and *treY* within the PAO1 and *Pto* genomes and the function of MalQ had yet to be tested.

To address the function of MalQ and the potential to synthesise maltose, a strain deficient in MalQ was generated in both *Pto* and PAO1. As compared to the wild-type strain, the PAO1  $\Delta\text{malQ}$  metabolome showed increased concentrations of trehalose (Figure 3-16).

Levels of  $\alpha$ -glucan were increased in both the PAO1 and *Pto*  $\Delta malQ$  strains. These results indicate that MalQ could use  $\alpha$ -glucan as a substrate, because the deletion of *malQ* resulted in an increase in the concentration of  $\alpha$ -glucan in both species. This increase in  $\alpha$ -glucan may result in an increased substrate concentration for TreY and TreZ resulting in the increase in trehalose as observed in PAO1  $\Delta malQ$ .

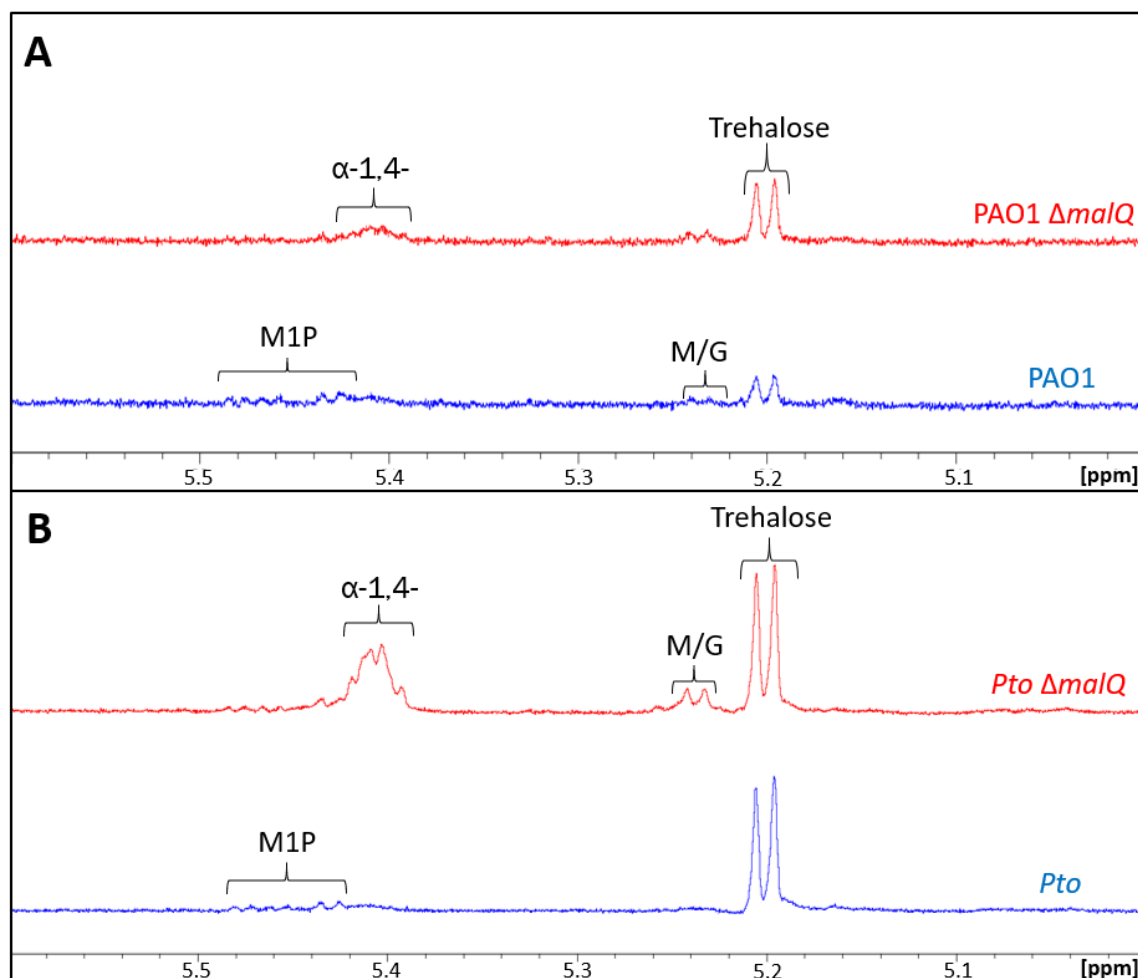


Figure 3-16: <sup>1</sup>H-NMR spectroscopy of the soluble metabolome following the deletion of *malQ* in *Pseudomonas* spp. Metabolomes were extracted from wild-type PAO1 (blue) and  $\Delta malQ$  (red) (A) and wild-type *Pto* (blue) and  $\Delta malQ$  (red) (B) cultured on M9 minimal medium. Peak assignments are as indicated based on previously established spectra. (M/G; maltose and/or glucose, M1P; maltose 1-phosphate,  $\alpha$ -1,4-;  $\alpha$ -glucan internal linkages). Resonances corresponding to trehalose increased following deletion of *glgB* in PAO1. Resonances corresponding to  $\alpha$ -glucan increased following deletion of *glgB* in PAO1 and *Pto*.

As my genetic data indicated that MalQ acts upon  $\alpha$ -glucan *in vivo* we then sought to identify the product of this activity. To address this, recombinant PAO1 MalQ was purified and provided with maltohexose as a substrate. Products of this reaction were identified and analysed using matrix-assisted laser desorption/ionization mass spectrometry. When maltohexose (DP6) was provided as a substrate, MalQ was shown to produce maltooligosaccharides of varying lengths ranging from DP4 to over DP22. Maltooligosaccharides of length DP3 or less were undetectable because these overlap with

the MALDI matrix signals. This disproportionation activity was also seen when MalQ was provided with maltose (DP2) whereupon it produced maltooligosaccharides of up to DP10. (Karl Syson, unpublished data). Although we had shown that MalQ could use maltose as a substrate, due to the limitations of this methodology we were not able to demonstrate the production of maltose by MalQ. However, since enzyme-catalysed reactions are reversible, MalQ should be capable of producing maltose from maltooligosaccharides.

We then reasoned that if MalQ was capable of producing maltose, it could be acted upon by the kinase domain of TreS/Pep2 producing M1P that would be readily detectable by <sup>1</sup>H-NMR spectroscopy. To test this, PAO1 recombinant MalQ and TreS/Pep2 were purified and provided with maltohexaose and ATP. The products were analysed using <sup>1</sup>H-NMR spectroscopy. After 1 hour, we observed the presence of M1P, thus confirming that MalQ can produce maltose (experimental design by Stuart Woodcock and Karl Syson, with the experiment conducted by Karl Syson, unpublished data).

### 3.2.12 Characterisation of linear $\alpha$ -glucan

At this stage, one of the limitations of the predicted pathway was that there was no distinction between the linear  $\alpha$ -glucans produced by either GlgA or GlgE. It was unclear whether these pools of linear  $\alpha$ -glucan were structurally unique or if they were interchangeable. To investigate the difference in length between the GlgA-derived linear  $\alpha$ -glucan and the GlgE-derived linear  $\alpha$ -glucan, strains were generated in PAO1 to distinguish between these two sources.

A PAO1 strain lacking GlgB accumulates only linear  $\alpha$ -glucan as described above (Section 3.2.7). However, this may represent a pool of both GlgA- and GlgE-dependent linear  $\alpha$ -glucan. To generate solely GlgA-dependent linear  $\alpha$ -glucan, a *treS* operon deletion strain deficient in GlgE, TreS/Pep2 and GlgB (*PA2151-2153*) was generated. To test for the accumulation of GlgA-dependent linear  $\alpha$ -glucan, the metabolome was extracted and analysed using <sup>1</sup>H-NMR. This strain showed a stark increase in the levels of both GlgA-derived linear  $\alpha$ -glucan and trehalose (data not shown), however, peaks associated with  $\alpha$ -glucan were absent upon subsequent biological repetitions. This could be a result of technical error or compensatory mutations to prevent the accumulation of linear  $\alpha$ -glucan. Furthermore, this strain did not exhibit staining when exposed to iodine vapour (Figure 3-17).

I reasoned that GlgA-dependent  $\alpha$ -glucan could be degraded by TreY and TreZ and MalQ based on previously described *in vitro* and *in vivo* data (Sections 3.2.10 and 3.2.11, respectively). Deletion of *malQ* or *treY* in addition to  $\Delta glgE \Delta treS/pep2 \Delta glgB$  should result in a strain producing solely GlgA-dependent linear  $\alpha$ -glucan.

Iodine vapour staining of cellular material was used to test if deletion of *malQ* in addition to  $\Delta glgE \Delta treS/pep2 \Delta glgB$  resulted in the accumulation of GlgA-derived  $\alpha$ -glucan. When exposed to iodine vapour,  $\Delta malQ \Delta glgE \Delta treS/pep2 \Delta glgB$  did not produce staining (Figure 3-17). This suggests that GlgA-dependent  $\alpha$ -glucan was not present in sufficient quantities or length.

Iodine vapour staining of cellular material was used to test if deletion of *treY* in addition to  $\Delta glgE \Delta treS/pep2 \Delta glgB$  resulted in the accumulation of GlgA-derived  $\alpha$ -glucan in PAO1. When exposed to iodine vapour,  $\Delta treY \Delta glgE \Delta treS/pep2 \Delta glgB$  stained blue-purple (Figure 3-17). This suggested that this strain accumulated GlgA-dependent  $\alpha$ -glucan and that this could be estimated to be over DP 40, longer than that estimated to be accumulated by  $\Delta glgB$  [197]. This suggested that GlgA possessed the potential to synthesise long linear  $\alpha$ -glucan, however, this is likely not physiological as this is likely to be rapidly degraded by TreY and TreZ into trehalose. However, as MalQ and GlgP are still present within this strain, this still may not represent true GlgA-dependent  $\alpha$ -glucan because  $\alpha$ -glucan disproportionation and recycling cannot be ruled out.

Taken together, this suggests that GlgA was capable of synthesising long linear  $\alpha$ -glucan as indicated by iodine staining. However, this is rapidly degraded by TreY and TreZ and possibly used as a substrate by MalQ. I was unable to generate a strain producing solely GlgE-dependent  $\alpha$ -glucan and therefore was not able to determine the relative length. Further experiments are required to robustly determine the lengths of both GlgA- and GlgE-dependent  $\alpha$ -glucan.

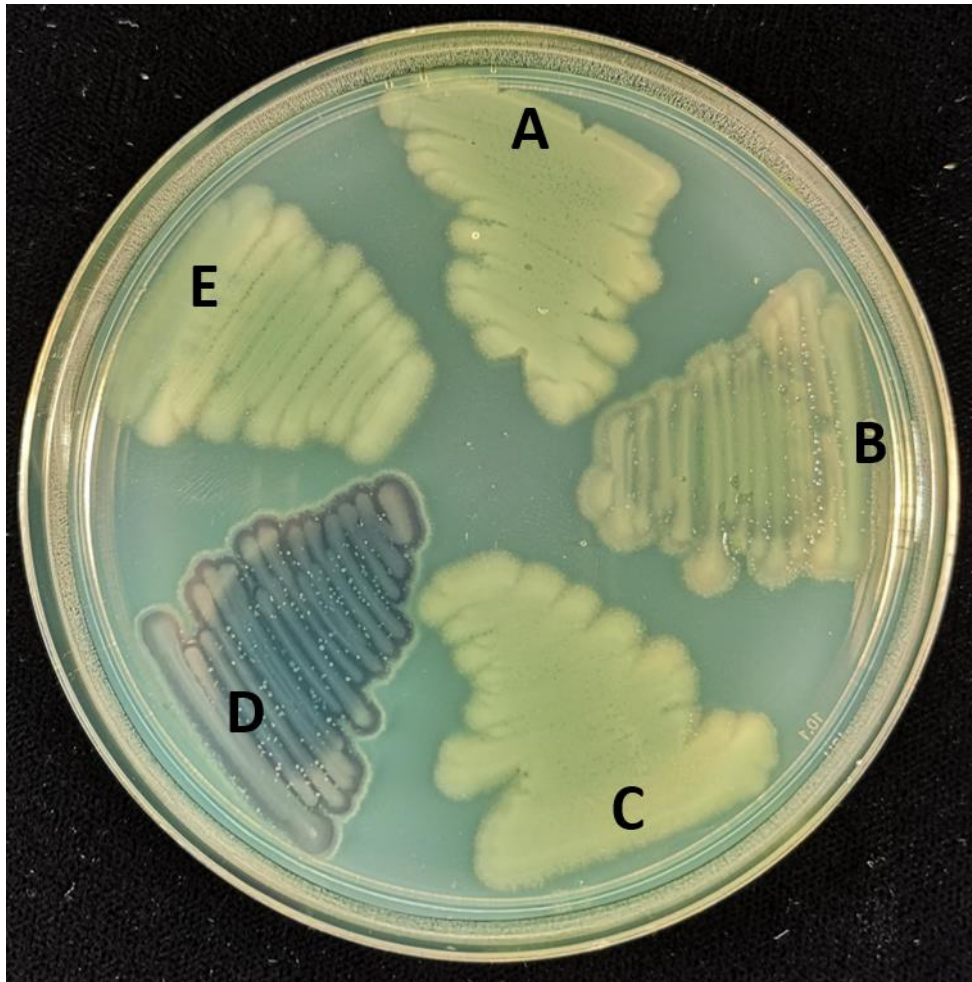


Figure 3-17: Iodine staining of linear  $\alpha$ -glucan in *Pseudomonas aeruginosa* PAO1 strains using iodine vapour. Wild-type PAO1 (A),  $\Delta glgB$  (B),  $\Delta PA2151-2153$  (C),  $\Delta treY \Delta PA2151-2153$  (D) and  $\Delta malQ \Delta PA2151-2153$  (E).  $\Delta glgB$  and  $\Delta treY \Delta PA2151-2153$  exhibit differential staining when exposed to iodine vapour.

### 3.3 Discussion

Trehalose biosynthesis in *Pseudomonas* spp. has up to now been relatively understudied. The recent discovery of the GlgE pathway, a novel pathway for the biosynthesis of  $\alpha$ -glucan in *Mycobacterium* spp., has changed our understanding of trehalose biosynthesis. Although previously thought to catalyse the biosynthesis of trehalose, flux through TreS is from trehalose to maltose and through the rest of the GlgE pathway to produce  $\alpha$ -glucan in *Mycobacterium* spp. [157]. *Pseudomonas* spp. are predicted to possess gene homologues of the GlgE pathway. The existence of the GlgE pathway implies the function of TreS is to convert trehalose into maltose in *Pseudomonas* spp. This contrasts with what was previously thought and has implications for the interpretation of past data concerning the function of trehalose.

A combination of reverse genetics and analytical biochemistry was used to investigate the functions of the gene products predicted to be involved in trehalose and  $\alpha$ -glucan biosynthesis in *Pseudomonas* spp. To the best of my knowledge this is the first report characterising the genetic and biochemical basis of trehalose and  $\alpha$ -glucan biosynthesis in an organism possessing both the GlgA and GlgE pathway.

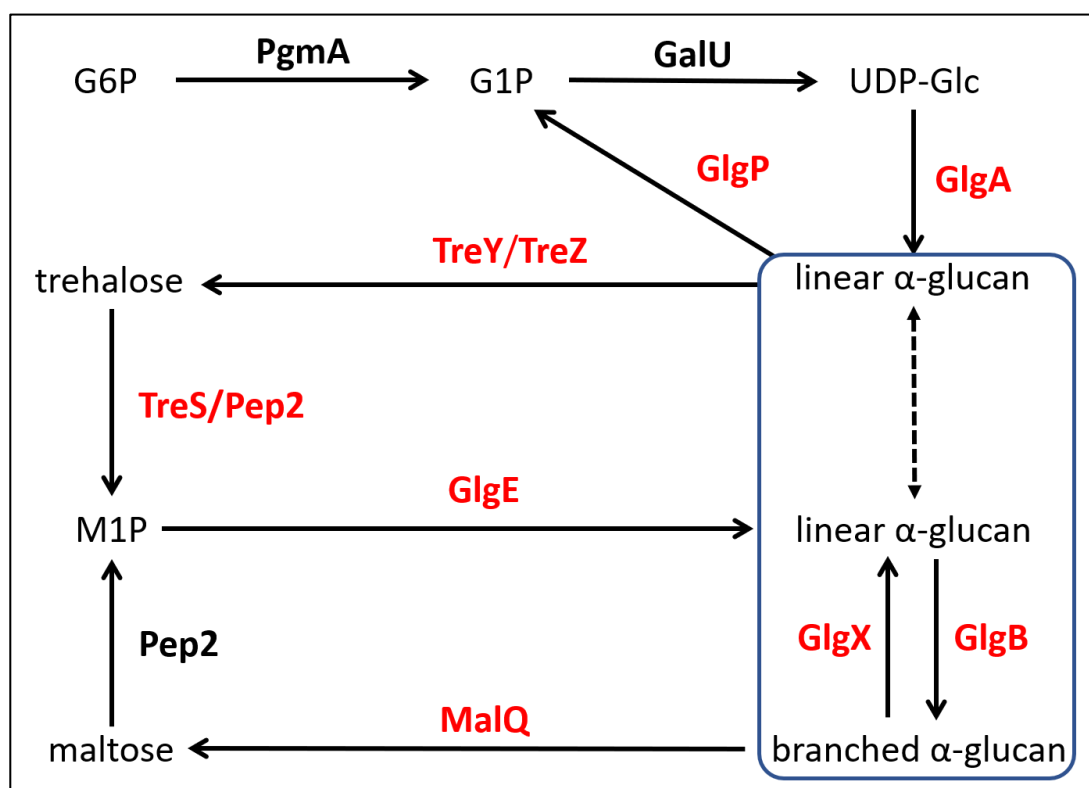


Figure 3-18: Current understanding of trehalose and  $\alpha$ -glucan biosynthesis in *Pseudomonas* spp. Dashed lines indicate interchangeable substrate utilisation from the combined pool of  $\alpha$ -glucan species, represented by the blue box. Disproportionation activity of MalQ is not shown for simplicity. (G6P; Glucose 6-phosphate, G1P; Glucose 1-phosphate, UDP-Glc; UDP-glucose, M1P; maltose 1-phosphate).

In this chapter, I demonstrated that the function of most gene products involved with trehalose and  $\alpha$ -glucan biosynthesis were as predicted (Figure 1-9). In consideration of the data generated within this chapter, I have amended my model to reflect our current understanding of trehalose and  $\alpha$ -glucan biosynthesis in *Pseudomonas* (Figure 3-18).

We have demonstrated that GlgA catalyses the first committed step in this pathway, the polymerisation of UDP-glucose into linear  $\alpha$ -glucan. Interestingly, the preferred substrate UDP-glucose was not accumulated by PAO1 following the deletion of *glgA*. UDP-glucose is not unique to trehalose and  $\alpha$ -glucan biosynthesis and is required for many other cellular processes therefore it can be reasoned that UDP-glucose does not accumulate to detectable levels because it is utilised rapidly [198]. An alternative explanation is that the build-up of UDP-glucose is prevented because it may be toxic to the cell. The build-up of phosphosugars trehalose 6-phosphate or M1P has direct or indirect toxic effects in *M. tuberculosis* [199] therefore similar toxicity may occur with a build-up of UDP-glucose in *Pseudomonas* spp. *In vitro* data showed that PAO1 GlgA can produce linear  $\alpha$ -glucan from UDP-glucose as a donor. The lack of requirement for an added acceptor substrate suggests some UDP-glucose is hydrolysed to give glucose which then acts as the initial acceptor.

Surprisingly, M1P, trehalose and  $\alpha$ -glucan were present in the metabolome of *Pto* following deletion of *glgA*, albeit at reduced concentrations. Although I could not identify a second *Pto glgA* homologue, this suggests that other methods of entry into trehalose and  $\alpha$ -glucan biosynthesis exist within this strain. Further work should be conducted to identify gene products with  $\alpha$ -glucan biosynthetic activity. Alternatively, the presence of these metabolites could be a result of polar effects arising from deletion of *glgA*. This could be due to inaccuracies in the prediction of the *Pto glgA* open reading frame. This should be ruled out by complementation of GlgA in the *Pto*  $\Delta$ *glgA* strain.

The second step of trehalose and  $\alpha$ -glucan biosynthesis in *Pseudomonas* spp. is the degradation of  $\alpha$ -glucan into trehalose by TreY and TreZ. TreY catalyses the conversion of the terminal  $\alpha$ -1,4 bond of  $\alpha$ -glucan into an  $\alpha$ -1, $\alpha$ -1 glycosidic bond forming maltooligosyl trehalose as detected by  $^1\text{H-NMR}$  spectroscopy. TreZ then hydrolyses maltooligosyl trehalose liberating trehalose. Unexpectedly, M1P was present in strains lacking functional TreY and TreZ (Figure 3-15) suggesting an alternative mechanism for the biosynthesis of maltose in *Pseudomonas* spp.

Following this, we probed the function of proximal gene products for maltose biosynthesis activity. We determined that MalQ possessed disproportionation activity and could

metabolise  $\alpha$ -glucan producing a range of chain lengths. It was then established that MalQ could produce maltose which would then be converted into M1P by Pep2. Along with TreS/Pep2, this is the first report of *de novo* maltose biosynthesis in *Pseudomonas* spp. This also suggests a mechanism of GlgE-dependent  $\alpha$ -glucan biosynthesis which is independent of the biosynthesis of trehalose. This therefore could circumvent the production of trehalose in favour of  $\alpha$ -glucan during circumstances which are inappropriate for trehalose biosynthesis.

The first enzymatic step of the GlgE pathway is the conversion of trehalose into M1P by the TreS/Pep2 fusion protein. As *pep2* and other homologues of the GlgE pathway were present, it was predicted that flux through TreS would be in favour of synthesising maltose [157] and therefore TreS/Pep2 was responsible for the degradation of trehalose rather than the biosynthesis of trehalose as previously thought [74, 180]. Metabolomic data from PAO1  $\Delta treS/pep2$  was consistent with TreS/Pep2 utilising trehalose as a substrate.

In contrast to PAO1, deletion of *treS/pep2* in *Pto* resulted in a decrease in intracellular trehalose, inconsistent with the hypothesis that TreS/Pep2 isomerises trehalose into maltose and subsequently M1P. Nevertheless, the activity of TreS/Pep2 was confirmed using *in vitro* techniques. The decrease in trehalose concentration following deletion of *treS/pep2* could be rationalised due to the fact that high levels of trehalose has been hypothesised to be toxic [139]. There no published reports of this in bacteria, with the exception of trehalose 6-phosphate toxicity in *M. tuberculosis* [199]. *Pto* may respond to increased trehalose levels by compensatory mutations or through regulatory processes. An alternative approach to investigate the function of TreS/Pep2 *in vivo* is the overexpression of *treS/pep2* in *Pto*. My model would suggest that increased expression of *treS/pep2* would result in the reduction of trehalose concentrations, consistent with flux flowing from trehalose to maltose. This would thereby prevent pleotropic effects induced by trehalose accumulation.

Studies on the *M. tuberculosis* TreS and Pep2 proteins shows that they form a non-covalent complex *in vitro* [200]. The formation of this complex strikingly increases the kinase activity of Pep2 and subtly increases the activity of TreS. Furthermore, *treS* and *pep2* are fused in 30% of bacterial genomes predicted to possess *glgE* homologues, including *Pseudomonas* spp. (Govind Chandra, personal communication) [171]. The fusion of these two genes could

be a method of regulation within these bacteria to increase activity of the TreS/Pep2 protein.

Interestingly, deletion of the second *Pto treS* homologue (*treS(2)*) resulted in an approximate 2-fold increase in the concentration of intracellular trehalose, consistent with my model. This suggests redundancy within the *Pto* GlgE pathway. This could reflect the environmental lifestyle of *Pto* where increased trehalose degradation by TreS(2) would be required to adapt to rapidly changing environmental osmolarities. Furthermore, it was noted by Chandra *et al.* that the GlgE pathway was possessed largely by plant-associated bacteria [171].

The second step of the GlgE pathway is the polymerisation of M1P into linear  $\alpha$ -glucan. GlgE utilises M1P as a substrate to extend a  $\alpha$ -glucan chain. Deletion of *glgE* in either PAO1 or *Pto* resulted in a stark increase in the levels of M1P, as expected. M1P accumulation has been shown to be toxic in *Mycobacterium* spp. [153] where deletion of GlgE was lethal in *M. tuberculosis* and conditionally lethal in *M. smegmatis* depending on the presence of trehalose. GlgE-deficient strains were viable in *Pseudomonas* spp. and any detrimental effects following the accumulation of this phosphosugar were not apparent. This suggests that *Pseudomonas* spp. are resistant to the direct or indirect effects of M1P and/or that lethality is unique to *Mycobacterium* spp. To further investigate this, the transcriptomic response of  $\Delta$ *glgE* strains would be examined to identify the existence of any M1P-induced stress responses. Finally, GlgB introduces  $\alpha$ -1,6 branch points to the linear chain forming branched  $\alpha$ -glucan, the final product of the GlgE pathway.

$\alpha$ -Glucan is recycled by the phosphorylase GlgP and the debranching enzyme GlgX. GlgP degrades  $\alpha$ -glucan chains producing G1P and GlgX removes the  $\alpha$ -1,6 branch point, producing linear  $\alpha$ -glucan chains. In other bacteria GlgP degrades  $\alpha$ -glucan chains leaving four glucose units from the  $\alpha$ -1,6 branch point [170], providing a suitable substrate for GlgX suggesting that GlgP and GlgX are both required for  $\alpha$ -glucan degradation in *Pseudomonas* spp. I have also demonstrated that the recycling of  $\alpha$ -glucan is required to produce trehalose and M1P where loss of GlgX and therefore the ability to debranch  $\alpha$ -glucan results in a reduction of these metabolites.

Unexpectedly, PAO1  $\Delta$ *glgX* did not yield any relevant metabolites, although the absence of trehalose and M1P supports my model,  $\alpha$ -glucan levels were also undetectable. This is difficult to rationalise but could be a result of regulatory or compensatory mechanisms. For

example, the accumulation of unrecyclable  $\alpha$ -glucan represents a significant energy store which becomes largely inaccessible to the bacterium leading to nutrient stress and could result in the prevention of  $\alpha$ -glucan biosynthesis in PAO1.

The presence of both GlgA and GlgE results in two alternative mechanisms of synthesising linear  $\alpha$ -glucan. It is currently unclear as to why *Pseudomonas* spp. have evolved two distinct biosynthetic pathways of  $\alpha$ -glucan biosynthesis. The most tangible explanation is that there are differences in length between the GlgA- and GlgE-synthesised  $\alpha$ -glucan making them distinct molecules. Efforts to characterise the chain length of GlgA- and GlgE-dependent  $\alpha$ -glucan *in vivo* were based on the generation of PAO1 strains accumulating either pool of linear  $\alpha$ -glucan. The first limitation of this was due to the inability to produce a strain accumulating solely GlgE-dependent  $\alpha$ -glucan. This was due to the dependency of GlgE on the rest of the pathway and the inability to prevent the production of GlgA-dependent  $\alpha$ -glucan. Nevertheless, based on my model, PAO1  $\Delta glgB$  was the best representative of the accumulation of GlgE-dependent  $\alpha$ -glucan. An absence of GlgB led to the production of linear  $\alpha$ -glucan, which could be estimated to be between DP 33 – 38 [197], however, this was not conclusive as this can reflect a combination of both GlgA- and GlgE-dependent linear  $\alpha$ -glucan.

Due to the presence of multiple enzymes such as GlgE, TreY, MalQ, and GlgP which utilise  $\alpha$ -glucan as a substrate, a PAO1 strain accumulating solely GlgA-dependent linear  $\alpha$ -glucan was not possible. Although other  $\alpha$ -glucan modifying activities cannot be ruled out, the GlgA-dependent linear  $\alpha$ -glucan chain may exceed 40 glucose units. However, this is unlikely to be physiologically-relevant as GlgA-dependent linear  $\alpha$ -glucan seems to be rapidly degraded by TreY.

In order to conclusively characterise the chain lengths of GlgA- and GlgE-dependent  $\alpha$ -glucan *in vivo*, the sole effects of GlgA and GlgE must be studied. To study the length of GlgA-dependent linear  $\alpha$ -glucan, a strain should be generated that would only possess the *glgA* gene and lack every other gene product of the GlgE pathway. This strain would only produce GlgA-dependent linear  $\alpha$ -glucan and lack any other enzymes which utilise  $\alpha$ -glucan as a substrate thereby resulting in an accurate representation.

To study the length of GlgE-dependent linear  $\alpha$ -glucan, a strain should be generated that would only possess *treS/pep2* and *glgE*. This strain would therefore only produce GlgE-dependent linear  $\alpha$ -glucan when provided with extracellular trehalose and would lack any other enzymes which utilise  $\alpha$ -glucan as a substrate thereby resulting in an accurate

representation. Although iodine staining provides an indication of linear  $\alpha$ -glucan chain length, this method is semi-quantitative. MALDI-MS can be used as a quantitative method to analyse chain length, however, metabolome extracts have proven inappropriate for this instrumentation. Therefore, in order to utilise MALDI-MS, chloroform/ethanol extractions should be used to produce pure samples of  $\alpha$ -glucan.

It is still unclear as to why *Pseudomonas* spp. possess two distinct biosynthetic pathways of  $\alpha$ -glucan biosynthesis and prompts the following questions: are GlgA- and GlgE-dependent  $\alpha$ -glucan interchangeable? For example, genomic and experimental data suggests that TreY utilises GlgA-dependent  $\alpha$ -glucan to produce trehalose. Can TreY utilise GlgE-dependent  $\alpha$ -glucan as a substrate? Can GlgB utilise both GlgA- and GlgE-dependent  $\alpha$ -glucan forming branched  $\alpha$ -glucan? Can branched  $\alpha$ -glucan be extended by both GlgA and GlgE? These questions should be answered using *in vitro* techniques.

Prior to this work, understanding of trehalose biosynthesis in *Pseudomonas* spp. was limited. Both TreY/TreZ and TreS pathways were thought to contribute to trehalose biosynthesis. The only biosynthetic link between  $\alpha$ -glucan and trehalose was thought to occur through a requirement of  $\alpha$ -glucan as a substrate for the TreY/TreZ pathway.

In agreement with prior studies, I have demonstrated that all genes (except *malQ*) within the *treY/treZ* operon are involved in the production of trehalose. In contrast, I have shown that the *treS* operon is not involved in the biosynthesis of trehalose as previously thought, instead it is involved with the conversion of trehalose into maltose and the subsequent production of  $\alpha$ -glucan.

The identification of the GlgE pathway, a novel mechanism of  $\alpha$ -glucan biosynthesis in *Pseudomonas* spp., has wide reaching implications for the interpretation of previous data investigating trehalose biosynthesis and its function in *Pseudomonas* spp. and other bacteria possessing the GlgE pathway. For example, the deletion of both *treS* or *treY/treZ* operons in *Pto* resulted in the abolition of trehalose production and the generation of an osmotically-sensitive strain [74]. Furthermore, deletion of both *treS* or *treY/treZ* operons resulted in compromised tomato infections, a phenomenon which was exacerbated by lower RH. These results were interpreted as a result of the loss of trehalose, implicating trehalose as an osmotic protectant and a virulence factor.

Similarly, deletion of the *treY/treZ* operon in PA14 resulted in the abolition of trehalose production [180], while deletion of the *treS* operon resulted in decreased levels of

intracellular trehalose. Although osmotic sensitivity was not affected, deletion of either operon resulted in attenuated virulence during infection of *Arabidopsis thaliana* plants, again implicating trehalose as a virulence factor.

Furthermore, the highly trehalose-accumulating bacterium *M. koreensis* 3J1 is markedly tolerant to desiccation stress [151]. This led to the positive-correlation of intracellular trehalose concentrations and desiccation tolerance. Furthermore, the *M. koreensis* 3J1 trehalose biosynthetic genes *otsA/otsB* expressed in *P. putida* results in an increase in trehalose production and subsequent desiccation tolerance. Both *M. koreensis* 3J1 and *P. putida* both are predicted to possess homologues of the GlgE pathway and therefore should be genetically capable of producing  $\alpha$ -glucan. Following the proposal of my model (figure 3-18), an increase in trehalose may result in flux through the GlgE pathway and therefore an increase in  $\alpha$ -glucan.

Considering our new understanding of the *treS* operon and the GlgE pathway in *Pseudomonas* spp. previous reports investigating the role of trehalose must be re-interpreted. For example, the biosynthesis of GlgE-dependent  $\alpha$ -glucan is dependent on trehalose, therefore, the modulation of intracellular trehalose concentrations also impacts the biosynthesis of  $\alpha$ -glucan. Subsequently,  $\alpha$ -glucan may be at least in part responsible for the phenotypes attributed to trehalose. The following questions then arise: does  $\alpha$ -glucan function as an osmotic stress protectant? Does  $\alpha$ -glucan play a role during desiccation stress? And does  $\alpha$ -glucan play a role during plant infection?

The exploitation of the mutant strains and metabolomic data generated within this chapter will allow future investigation into the individual functions of trehalose and  $\alpha$ -glucan in *Pseudomonas* spp.

Chapter 4: Trehalose and  $\alpha$ -  
glucan protect against distinct  
abiotic stresses in  
*Pseudomonas*

## 4.1 Introduction

Trehalose functions as a protectant against a variety of stresses in bacteria. However, in *Mycobacterium* and *Pseudomonas* spp. trehalose is used as a substrate by the novel GlgE pathway to produce  $\alpha$ -glucan (Chapter 3) [153, 157]. The role of classical  $\alpha$ -glucan in bacteria has been extensively studied and usually functions as a form of carbon and energy storage [162]. However, the function of the GlgE pathway and therefore GlgE-dependent  $\alpha$ -glucan has only been investigated in *M. tuberculosis*. Mycobacterial GlgE-dependent  $\alpha$ -glucan is exported to the capsule where it interacts with the human immune system and modulates phagocytosis during infection [176, 177].

As *Pseudomonas aeruginosa* and *Pto* are significant pathogens of humans and plants, respectively, it is unlikely that *Pseudomonas* GlgE-dependent  $\alpha$ -glucan functions to solely modulate the human immune system. Since I have established the genetic and biosynthetic link between trehalose and  $\alpha$ -glucan through the GlgE pathway in *Pseudomonas* spp., we can gain clues as to the function of  $\alpha$ -glucan from previous studies investigating the roles of trehalose.

Such studies have implicated trehalose as a stress protectant, important for both osmotic and desiccation stress in *Pseudomonas* spp. Trehalose has also been shown to be important for plant infection, implicating this sugar as a virulence factor in *Pseudomonas* spp. On the contrary, the interpretation of these studies did not consider the intrinsic genetic and functional linkage of trehalose and  $\alpha$ -glucan biosynthesis afforded by the GlgE pathway as shown in Chapter 3. For example, during osmotic stress, genes responsible for trehalose and  $\alpha$ -glucan biosynthesis are both upregulated [184], and deletion of both trehalose and  $\alpha$ -glucan biosynthetic operons results in osmotically-sensitive strains in *Pto* [74]. However, equivalent mutations in PA14 do not result in osmotically-sensitive strains convoluting the role of trehalose in *Pseudomonas* spp.

Desiccation resistance can be conferred to *P. putida* by increasing intracellular concentrations of trehalose. *In trans* expression of *M. koreensis* 3J1 *otsA* and *otsB* in *P. putida* increases trehalose production which subsequently correlates with increased desiccation tolerance [151]. However, increasing the levels of trehalose could result in higher flux through the GlgE pathway resulting in the increased biosynthesis of  $\alpha$ -glucan (Figure 3-18). Furthermore, infection of tomato plants with *Pto* lacking both trehalose and  $\alpha$ -glucan biosynthetic genes are exacerbated by decreased RH. Similarly,  $\alpha$ -glucan may play

a role during plant colonisation and infection. For example, transcriptomic data show the upregulation of both trehalose and  $\alpha$ -glucan biosynthesis genes in *Pto* during the epiphytic and apoplasmic lifestyle [132]. Furthermore, strains used to implicate trehalose as a virulence factor during plant infection were also deficient in  $\alpha$ -glucan [74, 180, 181].

This chapter aims to investigate the roles of both trehalose and  $\alpha$ -glucan in *Pseudomonas* spp. With a combination of gene deletions (generated in Chapter 3), and the introduction of non-native *M. koreensis* 3J1 *otsA/otsB*, I decoupled the biosynthesis of trehalose and  $\alpha$ -glucan thereby enabling the elucidation of the individual roles of both trehalose and  $\alpha$ -glucan. This chapter will aim to answer the following questions:

- **Do trehalose and  $\alpha$ -glucan play a role in protecting *Pseudomonas* spp. against osmotic stress?**
- **Does  $\alpha$ -glucan play a role during desiccation stress?**
- **Does  $\alpha$ -glucan play a role during the epiphytic or apoplasmic lifestyle or during infection?**

To answer these questions biosynthetic mutant strains of *Pseudomonas aeruginosa* PAO1 and *Pto* were exposed to osmotic and desiccation stresses, respectively. Osmotic stress was conferred by the addition of NaCl to growth media and osmotic sensitivity was determined by the subsequent effects on growth. Finally, desiccation sensitivity was determined by measuring bacterial survival following incubation at high and low levels of RH.

In addition to this, several studies have also implicated the EPS molecule alginate in the protection against water stress in *P. putida*. In this chapter I have investigated whether alginate also functions in a similar capacity in PAO1 and *Pto*, and if there is interplay with trehalose or  $\alpha$ -glucan.

Furthermore, as shown by Chapter 3, *Pseudomonas* spp. are capable of producing  $\alpha$ -glucan by two different pathways (GalU-GlgA and GlgE). Where appropriate, I have attempted to distinguish between these two pools of  $\alpha$ -glucan.

## 4.2 Materials and Methods

### 4.2.1 Desiccation Tolerance Assay

Liquid cultures of bacteria grown in M9 minimal media were diluted to an OD<sub>600</sub> of 0.1 using PBS and 10  $\mu$ L was spotted onto nine 15-mm grade 1 Whatman filter discs per strain (GE Healthcare Life Sciences). After drying for a minute at room temperature these filter discs

were placed onto solidified M9 minimal media and incubated at either 28 °C or 37 °C for four hours. Following incubation, time zero samples were determined by resuspending three filter discs per strain in 3 mL of PBS. Colony forming units (CFU) were determined following serial dilutions. The remaining filter discs were subjected to desiccation in tightly sealed bell chambers containing either water (100% RH) or a saturated NaCl solution (75% RH [201]) for two hours. Three technical replicates per strain were included for both conditions. Bacteria were then recovered from the filter discs in 3 mL of PBS and following serial dilutions, the CFU were then determined. Each experiment was repeated at least twice.

Data transformed by logarithms to base 10 on CFU were analysed using Genstat by linear mixed modelling using restricted maximum likelihood. The random effect was date of experiment and Condition \* Strain were fixed effects, where \* is the crossing operator; Condition includes T<sub>0</sub>, 100% RH and 75% RH. The three technical replicate samples with the same Condition and Strain tested on the same Date provided the residual error term. The statistical significance of Condition, Strain and their interaction was determined by F-tests of Wald statistics. The response of a strain to lower humidity was calculated as the difference between its predicted mean log<sub>10</sub>(CFU) at 100% RH and at 75% RH. The standard error of the difference (SED) between the response of a mutant strain and that of the wild-type strain was calculated from the appropriate standard errors (SE) with the formula:  $SED = (SE[100\%, \text{Mutant}]^2 + SE[75\%, \text{Mutant}]^2 + SE[100\%, \text{wild-type}]^2 + SE[75\%, \text{wild-type}]^2)^{0.5}$ . The significance of the response difference was tested using the normal distribution with a variance of SED<sup>2</sup>.

Linear mixed modelling was chosen to account for variation in between technical and biological replications, including environmental and biological factors, allowing comparison between all strains tested. Statistical analysis was designed by James Brown. Statistical significance between the desiccation response of all PAO1 strains is summarised in the appendix Figure i, whereas the significance between all *Pto* strains is summarised in appendix Figure ii.

#### 4.2.2 Plant Infection Assays

For *Pto* infection assays, *Arabidopsis thaliana* (Col-0) was used. These plants were grown at 22 °C, 80% RH, under a 10-hour light period for 5-6 weeks. *Pto* strains were grown in M9 minimal medium overnight and diluted with 10 mM MgCl<sub>2</sub> to OD<sub>600</sub> 0.1 for spray infection and 0.0002 for infiltration infection. Before spray infection, cultures were amended with

0.04% of the surfactant Silwet-77 (De Sangosse). Plants were then sprayed until saturation. For infiltration, cultures were injected into the underside of the leaf using a 1 mL blunt end syringe until there was complete coverage of the leaf. For the duration of infection plants were covered with a clear lid and watered where specified. To determine bacterial load, two leaf discs of diameter 0.77 cm were taken from each plant and homogenised in 10 mM MgCl<sub>2</sub>, using 3 mm glass beads (Millipore) and the Spex® Geno/Grinder. CFU counts were calculated by serially diluting the homogenised sample and plating onto L medium supplemented with rifampicin (50 µg/mL) and nystatin (25 µg/mL). Rifampicin was used to select for the *Pto* strains and nystatin to select against fungal contaminants.

### 4.3 Results - Phenotypic characterisation of trehalose and $\alpha$ -glucan biosynthesis in *Pseudomonas aeruginosa* PAO1.

#### 4.3.1 Disruption of trehalose biosynthesis results in osmotic sensitivity in *Pseudomonas aeruginosa* PAO1

Since trehalose has been implicated in the survival of osmotic stress in *Pseudomonas* spp., loss of trehalose biosynthesis should result in an osmotically-sensitive strain. These experiments should also determine if  $\alpha$ -glucan plays a role during osmotic conditions. To investigate the roles of trehalose and  $\alpha$ -glucan during osmotic stress, PAO1 strains were cultured in the presence and absence of NaCl. Growth kinetics were determined using optical density at 600 nm. Osmotic stress was induced by the supplementation of 0.85 M NaCl to M9 minimal medium. There was no difference in the growth characteristics of any PAO1 strain when grown under non-stressed conditions (Figure 4-1). When incubated with NaCl, PAO1 exhibited a severely delayed lag-phase, but higher maximal density as compared to non-stressed growth (Figure 4-1). The trehalose and  $\alpha$ -glucan null mutant PAO1  $\Delta glgA$  (trehalose<sup>-</sup>/ $\alpha$ -glucan<sup>-</sup>) showed an increased lag phase when compared to the wild-type strain during osmotic stress, whereas the increased trehalose-producing, GlgE-dependent  $\alpha$ -glucan deficient strain PAO1  $\Delta treS/pep2$  (trehalose<sup>++</sup>/GlgE-dependent  $\alpha$ -glucan<sup>-</sup>) yielded a wild-type-like growth profile. Additionally, the trehalose-null but  $\alpha$ -glucan-producing strains PAO1  $\Delta treY$  and  $\Delta treZ$  (trehalose<sup>-</sup>/ $\alpha$ -glucan<sup>+</sup>) showed attenuation during osmotic growth. Interestingly, the  $\Delta glgB$  and  $\Delta glgX$  strains lacking the  $\alpha$ -glucan branching and debranching enzymes were also attenuated during osmotic conditions, even though basal levels of trehalose were increased in the PAO1  $\Delta glgB$  strain (3.2.7). This suggests that efficient branching and debranching of  $\alpha$ -glucan is needed for an optimal response to osmotic stress. Loss of GlgE, MalQ and GlgP had little effect on PAO1 growth

during osmotic stress. These results support the hypothesis that trehalose protects PAO1 against osmotic stress. Although the presence of  $\alpha$ -glucan alone does not confer osmotic protection, efficient branching and debranching of  $\alpha$ -glucan may be required for the optimal response to osmotic stress.

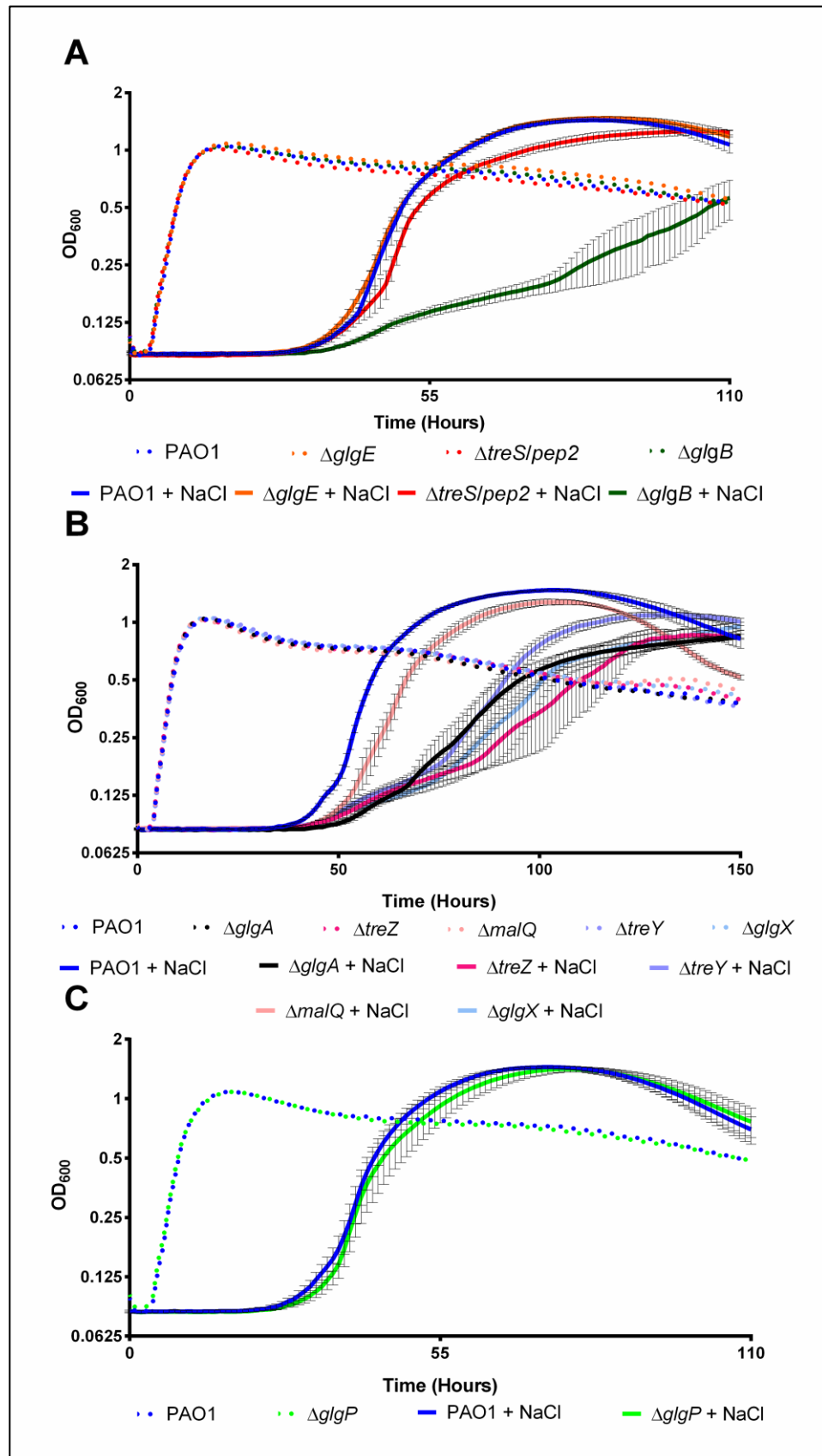


Figure 4-1: Growth of PAO1 and mutant strains in M9 minimal medium  $\pm$  0.85 M NaCl. (A) PAO1 *treS* operon mutants:  $\Delta$ *glgE*,  $\Delta$ *treS/pep2* and  $\Delta$ *glgB*. (B) PAO1 *treY/treZ* operon mutants:  $\Delta$ *glgA*,  $\Delta$ *treZ*,  $\Delta$ *malQ*,  $\Delta$ *treY* and  $\Delta$ *glgX*. (C) PAO1 and  $\Delta$ *glgP*. Values represent the mean OD<sub>600</sub>  $\pm$  SEM of five technical replicates. Results are representative of at least three independent experiments. Error bars are not shown for growth under non-stressed conditions for reasons of legibility. Trehalose deficient strains ( $\Delta$ *treZ*,  $\Delta$ *treY* and  $\Delta$ *glgA*) and glucan (de)branching mutants ( $\Delta$ *glgB* and  $\Delta$ *glgX*) are attenuated during osmotic conditions.

#### 4.3.2 Loss of $\alpha$ -glucan but not trehalose results in desiccation sensitivity in PAO1

To investigate the roles that trehalose and  $\alpha$ -glucan play during desiccation stress, PAO1 strains were inoculated onto paper filter discs and incubated at 100% and 75% RH. CFU was determined after incubation at each RH. The resulting data were analysed using linear mixed modelling and represented as predicted means of  $\log_{10}(\text{CFU/mL})$ . The response of a strain to lower humidity was calculated as the difference between its predicted mean  $\log_{10}(\text{CFU/mL})$  at 100% and at 75% RH. An increased response of a mutant strain as compared to the wild-type to lower RH translates to a more desiccation-sensitive strain.

As shown earlier (3.2.3), PAO1  $\Delta glgA$  lacks the ability to synthesise either trehalose or  $\alpha$ -glucan. PAO1  $\Delta treS/pep2$  accumulates increased levels of trehalose but lacks the genetic capacity to convert trehalose into GlgE-dependent  $\alpha$ -glucan. Although retaining the genetic potential to produce GlgA-dependent  $\alpha$ -glucan, this was not present within the metabolome when analysed using  $^1\text{H-NMR}$  spectroscopy, nevertheless, the presence of GlgA-dependent  $\alpha$ -glucan cannot be ruled out. PAO1  $\Delta glgB$  accumulates both trehalose and linear  $\alpha$ -glucan more than wild-type PAO1.

Incubation of PAO1 and all derived strains at 100% RH resulted in the recovery of predicted means of approximately 7.5 – 7.9  $\log_{10}(\text{CFU/mL})$ . Incubation at 75% RH resulted in approximately 10-fold reduction in the recovery of viable wild-type PAO1 to a predicted mean of  $\log_{10}(\text{CFU/mL}) = 6.5$  (Figure 4-2). This translated to in a desiccation response of approximately 1.1  $\log_{10}(\text{CFU/mL})$ , to which all mutant strains were compared.

Incubation of the  $\alpha$ -glucan and trehalose null mutant PAO1  $\Delta glgA$  at 75% RH resulted in enhanced cell death corresponding to a 1000-fold reduction in cell recovery to 4.8  $\log_{10}(\text{CFU/mL})$  equating to a desiccation response of approximately 2.6  $\log_{10}(\text{CFU/mL})$ . Surprisingly, the trehalose-producing, GlgE-dependent  $\alpha$ -glucan-null mutant PAO1  $\Delta treS/pep2$  showed similar desiccation sensitivity to the  $\Delta glgA$  strain, with recovery at 75% RH equating to a predicted mean of 4.4  $\log_{10}(\text{CFU/mL})$  resulting in a desiccation response of approximately 3.1  $\log_{10}(\text{CFU/mL})$ . In both cases the desiccation response of PAO1  $\Delta glgA$  and PAO1  $\Delta treS/pep2$  was highly significant ( $p \leq 0.0001$ ) when compared to that of the wild-type PAO1. Incubation of PAO1  $\Delta glgB$  at 75% RH resulted in very little attenuation compared to recovery at 100% RH. This corresponded to a desiccation response of

approximately 0.3 log<sub>10</sub>(CFU/mL). This lack of cell death was significant ( $p \leq 0.05$ ) when compared to wild-type PAO1.

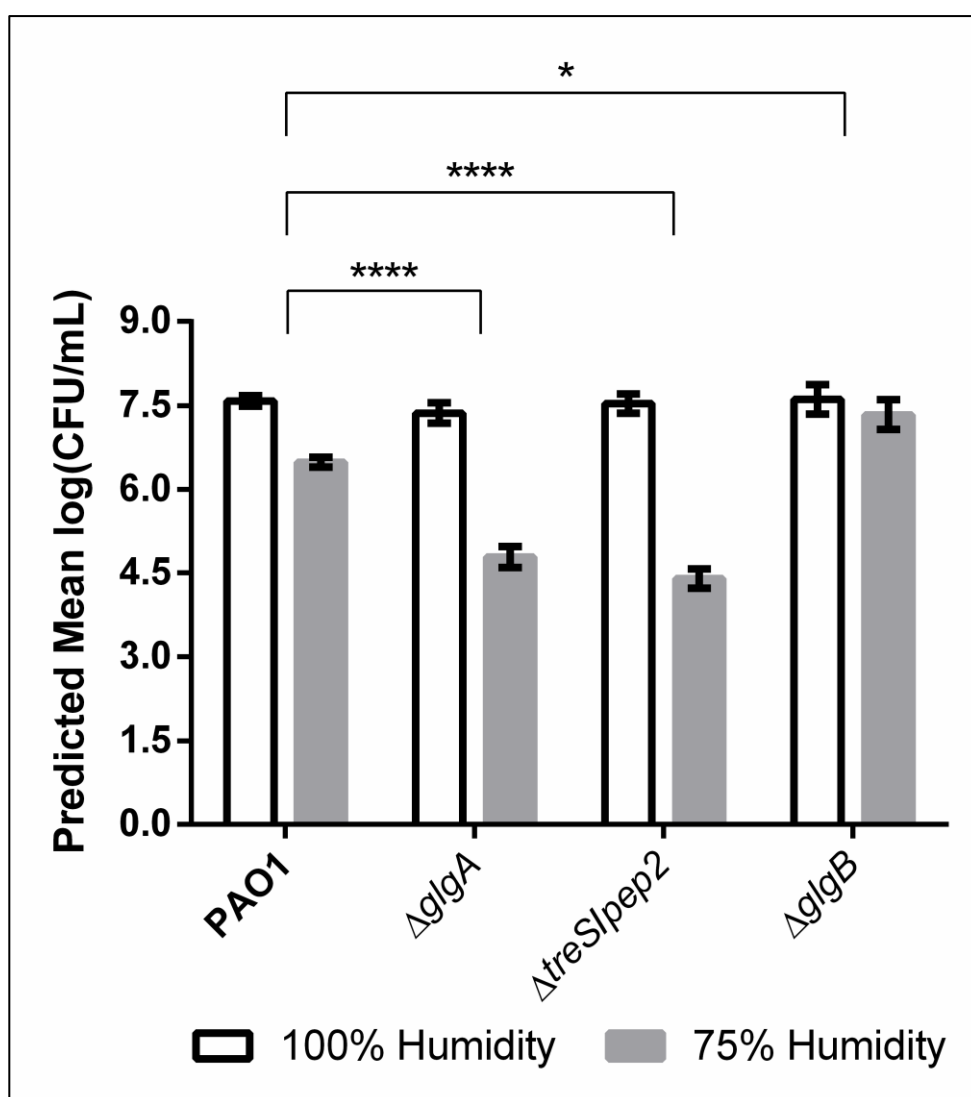


Figure 4-2: Linear mixed modelling analysis of the survival of PAO1,  $\Delta glgA$ ,  $\Delta treS/pep2$  and  $\Delta glgB$  strains when incubated at 100% (white bars) and 75% RH (grey bars). Bacterial recovery is presented as the predicted mean of log<sub>10</sub>(CFU/mL). Results are representative of at least three independent experiments. PAO1 strains lacking *glgA* and *treS/pep2* were significantly attenuated during incubation at 75% RH compared to wild-type PAO1. Conversely the desiccation resistance of  $\Delta glgB$  was increased. \*\*\*\* indicates  $p \leq 0.0001$ , \* indicates  $p \leq 0.05$ .

Taken together, these results show that the absence of both trehalose and  $\alpha$ -glucan results in desiccation sensitivity. This phenotype is not rescued by the production of trehalose even when trehalose is overproduced as occurs in the  $\Delta treS/pep2$  strain. Furthermore, the absence of GlgB, resulting in the accumulation of both trehalose and linear  $\alpha$ -glucan in the PAO1  $\Delta glgB$  strain, increased desiccation stress protection. This implicates GlgE-dependent  $\alpha$ -glucan in the protection against desiccation stress, irrespective of the state of branching, a function which was independent of trehalose.

### 4.3.3 *In trans* expression of *Microbacterium koreensis* 3J1 *otsA/otsB* recovers trehalose biosynthesis

In contrast to previous reports, the presence of trehalose within PAO1  $\Delta treS/pep2$  did not protect against desiccation stress [151]. However, the levels of intracellular trehalose produced by  $\Delta treS/pep2$  may not have been sufficient to confer desiccation-resistance. *M. koreensis* 3J1 is a bacterium that produces high levels of intracellular trehalose and is markedly resistant to desiccation stress [151]. The introduction and over-expression of the non-native *M. koreensis* 3J1 *otsA* and *otsB* trehalose biosynthetic genes results in an increase in trehalose production and confers desiccation resistance in *P. putida* [151, 188].

To investigate whether further enhanced levels of trehalose conferred desiccation stress resistance, the *M. koreensis* *otsA otsB* (*otsA/otsB*) genes were introduced and overexpressed in our PAO1 mutant strains. *M. koreensis* 3J1 genomic DNA was kindly gifted by Professor Maximino Manzanera, University of Granada, Spain. The *otsA/otsB* gene fragment was placed under the constitutive control of a  $P_{tac}$  promoter. This cassette was integrated into a neutral genomic location of wild-type PAO1, PAO1  $\Delta glgA$  and PAO1  $\Delta treS/pep2$ , generating derivatised strains constitutively expressing the *M. koreensis* 3J1 *otsA/otsB* genes. To ensure the effective production of functional *M. koreensis* 3J1 OtsA/OtsB, the effect of over-expression of *otsA/otsB* upon the soluble metabolome was investigated. OtsA/OtsB should catalyse the production of trehalose by using G6P and presumably UDP-glucose as substrates in PAO1 thereby increasing the intracellular levels of trehalose and subsequent flux through the GlgE pathway (Figure 4-3).

The production of OtsA/OtsB in  $\Delta glgA$  should result in the recovery of trehalose biosynthesis as it is predicted to bypass the *glgA* deletion and therefore the dependency on TreY- and TreZ-catalysed trehalose biosynthesis. As TreS/Pep2, GlgE and GlgB are still present within this strain, intracellular trehalose could be converted into GlgE-dependent  $\alpha$ -glucan (Figure 4-3).

The expression of *otsA/otsB* in  $\Delta treS/pep2$  should result in enhanced production of trehalose. As this strain lacks functional TreS/Pep2, the metabolism of trehalose into  $\alpha$ -glucan through the GlgE pathway is not expected. There is still the possibility that  $\Delta treS/pep2 :: otsA/otsB$  may produce GlgA-dependent  $\alpha$ -glucan, however, as OtsA/OtsB and GlgA compete for UDP-glucose as a shared substrate, this pool of  $\alpha$ -glucan is expected to be diminished or absent (Figure 4-3).

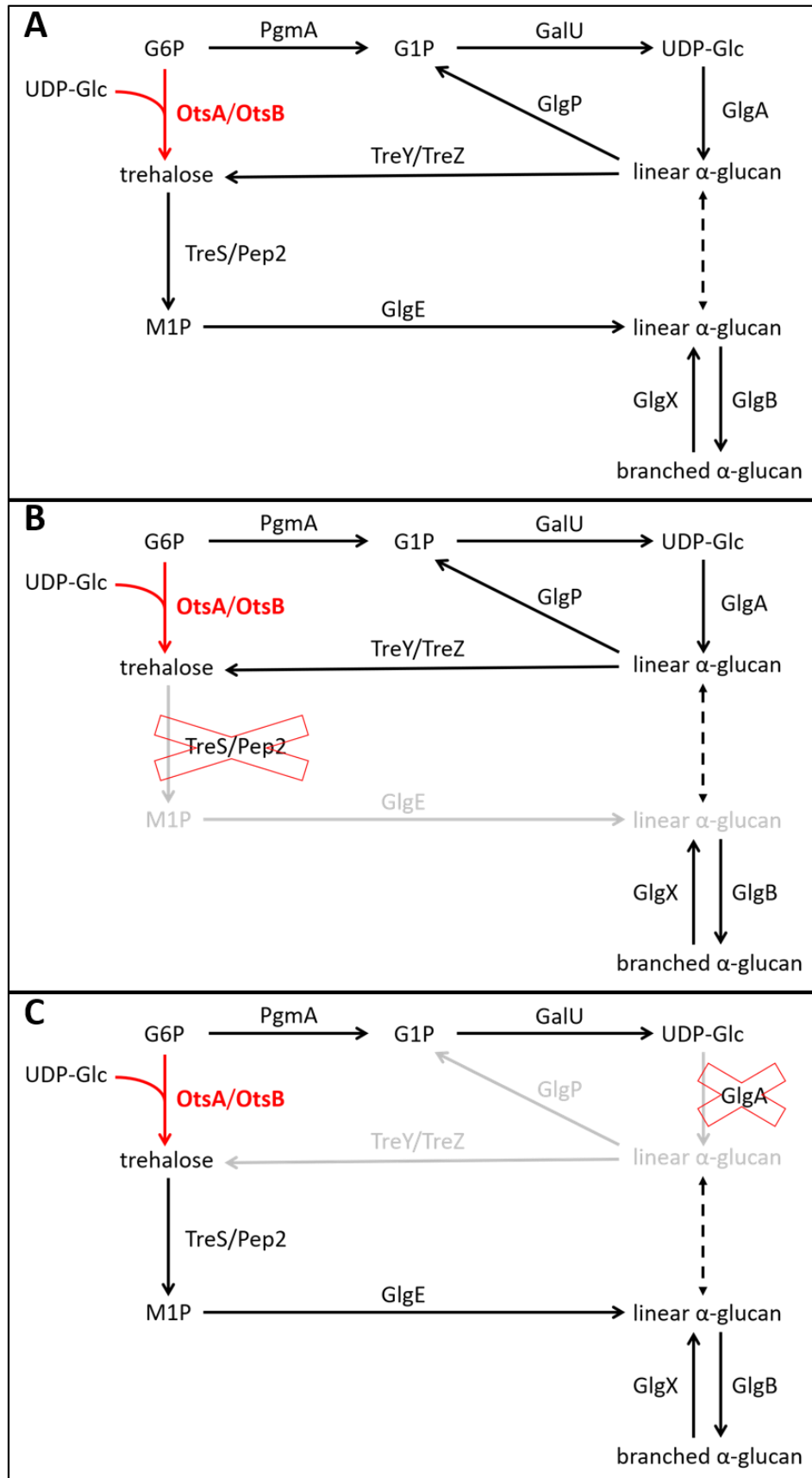


Figure 4-3: Scheme showing the genetic and biochemical basis following the production of trehalose biosynthetic enzymes OtsA/OtsB in wildtype PAO1 (A),  $\Delta treS/pep2$  (B) and  $\Delta glgA$  (C). Red crosses represent gene deletions. Grey arrows, enzymes and metabolites indicates parts of the pathway not expected to be active. (G6P; Glucose 6-phosphate, G1P; Glucose 1-phosphate, UDP-Glc; UDP-glucose, M1P; maltose 1-phosphate).

The soluble metabolomes of PAO1 :: *otsA/otsB*, PAO1  $\Delta$ *glgA* :: *otsA/otsB* and PAO1  $\Delta$ *treS/pep2* :: *otsA/otsB* were extracted and subject to  $^1\text{H-NMR}$  spectroscopy as described previously (Sections 2.4-2.5). Expression of *otsA/otsB* in PAO1 resulted in a non-significant increase in trehalose accumulation and a significant reduction in M1P levels when compared to the parental PAO1 strain (Table 4-1, Figure 4-4). The expression of *otsA/otsB* in PAO1  $\Delta$ *glgA* restored the biosynthesis of trehalose, M1P and  $\alpha$ -glucan. Expression of *otsA/otsB* in PAO1  $\Delta$ *treS/pep2* resulted in a non-significant increase in the levels of trehalose as compared to the parental  $\Delta$ *treS/pep2*. M1P and  $\alpha$ -glucan were still undetectable. Although intracellular trehalose concentrations did not significantly differ from the parental strains following the expression of *otsA/otsB* in wild-type PAO1 and  $\Delta$ *treS/pep2*, the recovery of trehalose and M1P biosynthesis in  $\Delta$ *glgA* :: *otsA/otsB* suggests that OtsA/OtsB is functional in PAO1.

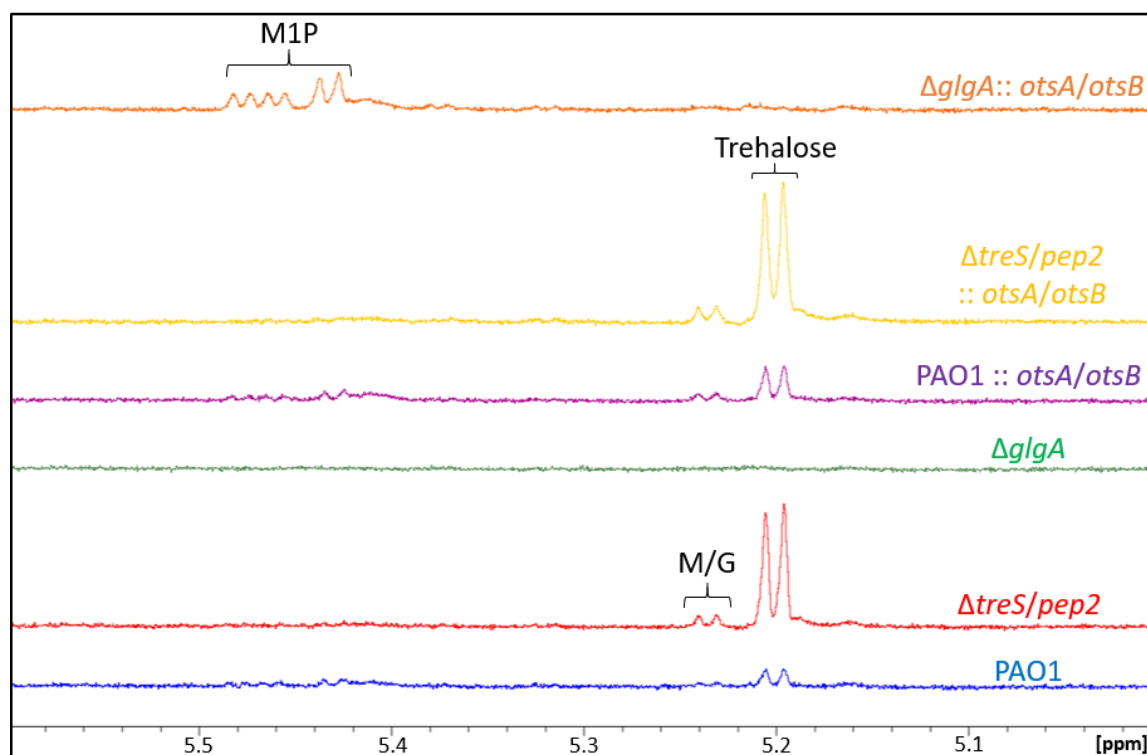


Figure 4-4:  $^1\text{H-NMR}$  spectroscopy of the soluble metabolome following the over-expression *otsA/otsB* in PAO1 strains. Metabolomes were extracted from wild-type PAO1 (blue),  $\Delta$ *treS/pep2* (red),  $\Delta$ *glgA* (green), PAO1 :: *otsA/otsB* (purple),  $\Delta$ *treS/pep2* :: *otsA/otsB* (yellow) and  $\Delta$ *glgA* :: *otsA/otsB* (orange) cultured on M9 minimal medium. Peak assignments are as indicated based on previously established spectra (M/G; maltose and/or glucose, M1P; maltose 1-phosphate). M1P concentration decreased following over-expression of *otsA/otsB* in PAO1. The expression of *otsA/otsB* did not affect the concentration of trehalose within the soluble metabolome of PAO1 or  $\Delta$ *treS/pep2*. Although trehalose was not present, over-expression of *otsA/otsB* in  $\Delta$ *glgA* resulted in the production of M1P.

Table 4-1: Concentrations of trehalose and M1P produced by PAO1 mutant strains with or without expression of *otsA/otsB*. Metabolites are presented as percentages of cellular dry weight  $\pm$  standard error ( $n \geq 2$ ). – indicates no measurable metabolite, \* indicates significant differences compared to the parental strain as determined by a student's t-test. Parental strain data are replicated from table 3-1.

Strain	Trehalose (%)	M1P (%)
<b>PAO1</b>	0.13 $\pm$ 0.03	0.30 $\pm$ 0.03
<b><i>ΔtreS/pep2</i></b>	0.89 $\pm$ 0.25	-
<b><i>ΔglgA</i></b>	-	-
<b>PAO1 :: <i>otsA/otsB</i></b>	0.17 $\pm$ 0.06	0.17 $\pm$ 0.02*
<b><i>ΔtreS/pep2</i> :: <i>otsA/otsB</i></b>	0.91 $\pm$ 0.13	-
<b><i>ΔglgA</i> :: <i>otsA/otsB</i></b>	0.06 $\pm$ 0.03	0.48 $\pm$ 0.06*

#### 4.3.4 Reintroduction of trehalose biosynthesis rescues osmotic sensitivity

Although the over-expression of *otsA/otsB* did not result in a significant increase in trehalose production under non-stressed conditions, OtsA/OtsB production may result in increased tolerance to osmotic stress. Because of this, the effect of *in trans* expression of *otsA/otsB* was investigated during growth with osmotic stress. PAO1, PAO1 *ΔtreS/pep2*, PAO1 *ΔglgA* and the respective derivatives expressing *otsA/otsB* were cultured in the presence and absence of NaCl in 96-well microplates as described earlier (Section 2.7). Growth kinetics were determined using optical density at 600 nm.

As expected, the expression of *otsA/otsB* did not affect growth during non-stressed conditions when compared to the parental strains (Figure 4-5). All strains producing OtsA/OtsB were equally enhanced in their ability to resist osmotic stress irrespective of the original background, with shorter lag phases when compared to their respective parental strain. Although PAO1 :: *otsA/otsB* and *ΔglgA* :: *otsA/otsB* exhibited increased tolerance to osmotic stress, these strains had the genetic capacity to produce  $\alpha$ -glucan. As a result of this, increased tolerance to osmotic stress could not be solely attributed to the enhanced production of trehalose *via* OtsA/OtsB. Conversely, *ΔtreS/pep2* :: *otsA/otsB* lacked the genetic capacity to produce GlgE-dependent  $\alpha$ -glucan from trehalose. Furthermore, there is no evidence of the accumulation of GlgA-dependent  $\alpha$ -glucan as this was undetectable via  $^1\text{H-NMR}$ . Moreover,  $\alpha$ -glucan is unlikely to be produced through the metabolism of trehalose by TreY/TreZ in the reverse direction due to the presence of high concentrations of water.

Taken together, this suggests that the over-expression of *otsA/otsB* during osmotic conditions results in enhanced trehalose production, thereby increasing the resistance of

PAO1 strains to osmotic stress and rescuing the osmotically-sensitive phenotype of PAO1  $\Delta glgA$ . This further supports the hypothesis that trehalose, not  $\alpha$ -glucan, protects against osmotic stress in *Pseudomonas* spp.

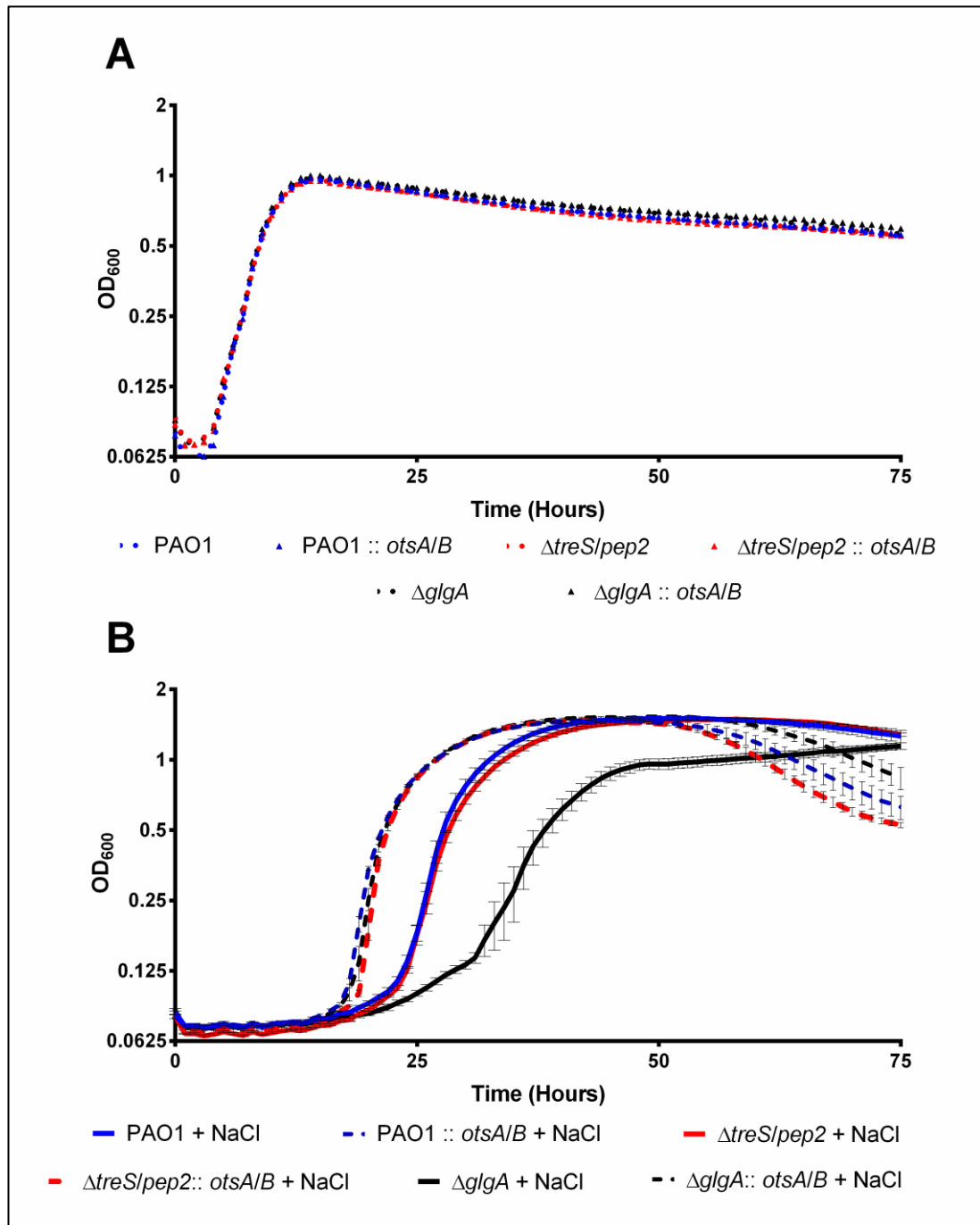


Figure 4-5: Growth of PAO1 and mutant strains with or without expression of *otsA/otsB* in M9 minimal medium  $\pm$  0.85 M NaCl. (A) Growth of PAO1 strains in the absence of NaCl. (B) Growth of PAO1 strains in the presence of NaCl. Values represent the mean OD600 of five replicates. Results are representative of at least three independent experiments. Error bars are not shown for growth under non-stressed conditions for reasons of legibility. Expression of *otsA/otsB* enhanced growth of all strains under osmotic conditions irrespective of original genetic background.

#### 4.3.5 Reintroduction of trehalose biosynthesis rescues desiccation sensitivity in PAO1 but only when TreS/Pep2 is present

The expression of *otsA/otsB* increases the desiccation stress tolerance in *P. putida* thereby implicating trehalose in the protection during desiccating conditions. To investigate the role of enhanced trehalose production during desiccation stress, the previously sensitive parental strains, PAO1  $\Delta$ *glgA* and PAO1  $\Delta$ *treS/pep2*, now expressing *otsA/otsB* were subjected to desiccating conditions. This was performed as described in section 4.2.1.

The expression of *otsA/otsB* rescued the desiccation sensitivity exhibited by the PAO1  $\Delta$ *glgA* strain (Appendix Figure i). This resulted in a desiccation response of 0.9  $\log_{10}$ (CFU/mL) similar to that of wild-type PAO1 (Figure 4-6). In contrast, PAO1  $\Delta$ *treS/pep2* :: *otsA/otsB* exhibited a desiccation response of approximately 4  $\log_{10}$ (CFU/mL) ( $p \leq 0.001$ ) translating to significant desiccation sensitivity when compared to the wild-type PAO1 (Figure 4-6), despite over-expression of the trehalose biosynthetic enzymes.

Taken together, the expression of *otsA/otsB* and therefore enhanced biosynthesis of trehalose resulted in increased resistance to osmotic stress in PAO1 strains. Expression of *otsA/otsB* also rescued desiccation sensitivity, however, this phenomenon depended on the presence of functional TreS/Pep2. This suggests that trehalose is not directly responsible for desiccation resistance in *Pseudomonas* spp. Conversely, the ability of trehalose to rescue desiccation sensitivity in PAO1 strains is dependent on the presence of TreS/Pep2. This implicates that the function of the GlgE pathway and thereby  $\alpha$ -glucan is to protect *Pseudomonas* spp. against desiccation stress.

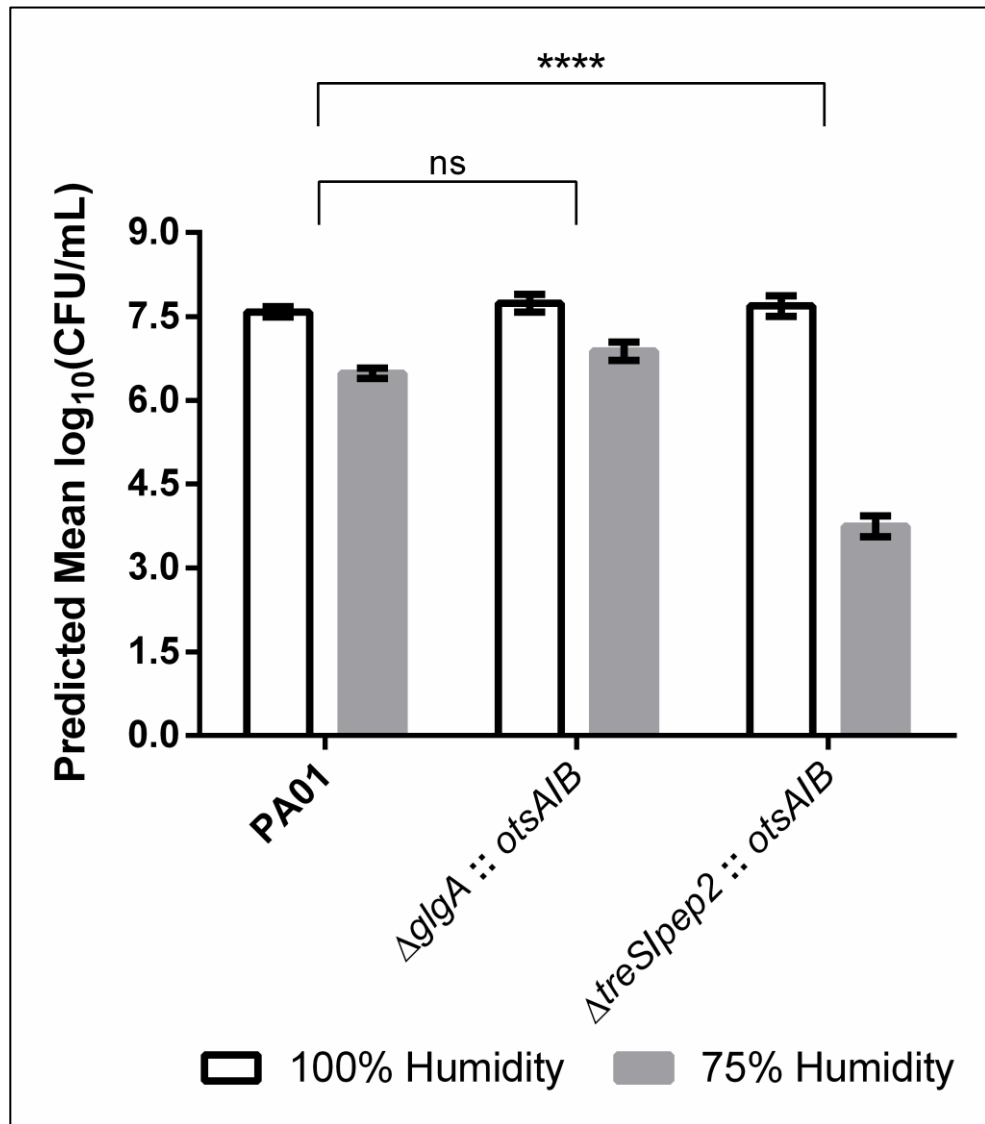


Figure 4-6: Linear mixed modelling analysis of the survival of PAO1 and mutant strains expressing *otsA/otsB* when incubated at 100% (white bars) and 75% RH (grey bars). Bacterial recovery is presented as the predicted mean of log<sub>10</sub>(CFU/mL). Results are representative of at least three independent experiments. Expression of *otsA/otsB* resulted in the rescuing of the desiccation sensitive mutant  $\Delta glgA$ . Conversely  $\Delta treS/pep2 :: otsA/otsB$  was significantly attenuated during incubation at 75% RH compared to wild-type PAO1. \*\*\*\* indicates  $p \leq 0.0001$ , ns indicates non-significant.

#### 4.3.6 Maltose and maltose 1-phosphate do not play a role in desiccation stress in *Pseudomonas aeruginosa* PAO1.

Although  $\alpha$ -glucan is the most likely candidate to protect against desiccation stress, it is possible that the GlgE pathway intermediate metabolites, maltose and M1P, may contribute to desiccation resistance. For example, maltose protects yeast against desiccation stress [115].

To address the roles of maltose and M1P in desiccation stress, a strain able to produce maltose and M1P but deficient in  $\alpha$ -glucan biosynthesis was engineered. First, a strain lacking both  $\alpha$ -glucan biosynthesis enzymes GlgA and GlgE was generated in PAO1 (PAO1

*ΔglgA ΔglgE*). The production of trehalose, maltose and M1P was then facilitated by the over-expression of *otsA/otsB* as described earlier (Section 4.3.3). This is illustrated in Figure 4-7. The soluble metabolome of PAO1 *ΔglgA ΔglgE :: otsA/otsB* was extracted and analysed using <sup>1</sup>H-NMR spectroscopy to confirm the production of the expected metabolites.

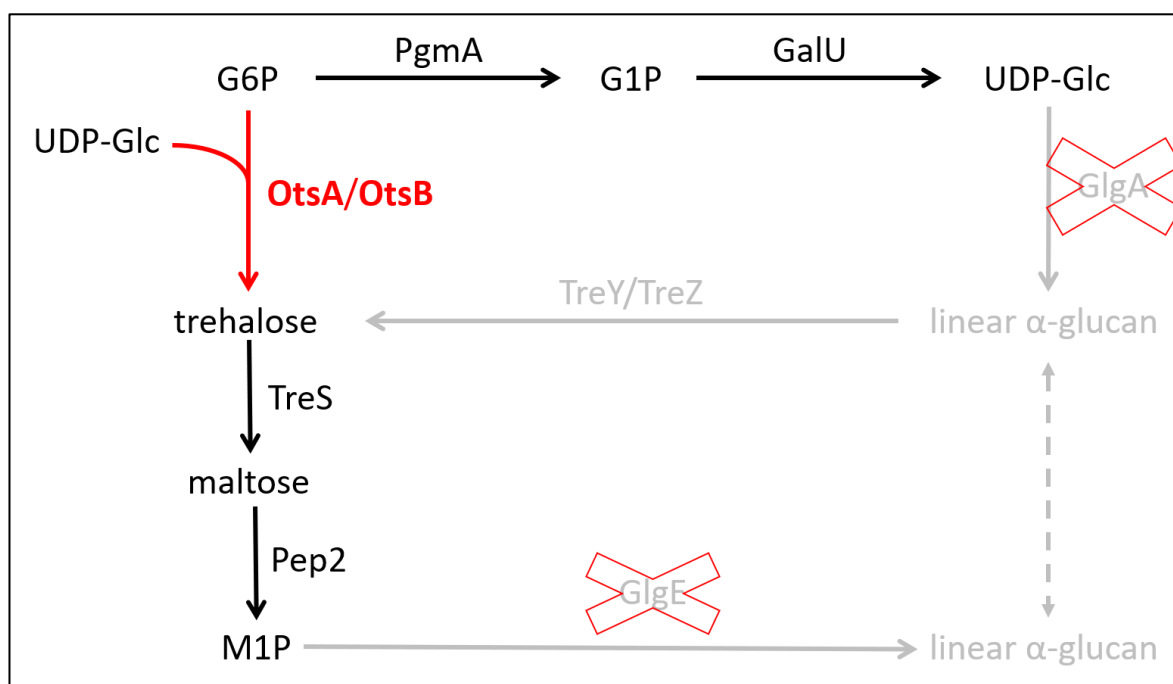


Figure 4-7: Scheme representing the genetic approach used to generate a  $\alpha$ -glucan-null mutant capable of synthesising maltose and maltose 1-phosphate (M1P). To produce a strain unable to synthesise  $\alpha$ -glucan, genes encoding the GlgA and GlgE enzymes were deleted. The ability to synthesise maltose and M1P was facilitated by the introduction of the trehalose biosynthesis enzymes OtsA/OtsB (red) from *M. koreensis* 3J1. Maltose and M1P intermediates are represented in this pathway by separating the individual domain functions of the TreS/Pep2 fusion protein. (G6P; Glucose 6-phosphate, G1P; Glucose 1-phosphate, UDP-Glc; UDP-glucose).

Table 4-2: Concentrations of trehalose and M1P produced by wild-type PAO1 and PAO1 *ΔglgA ΔglgE :: otsA/otsB* strains. Metabolites are presented as percentages of cellular dry weight  $\pm$  standard error ( $n \geq 2$ ). – indicates no measurable metabolite, \* indicates significant differences as compared to the wild-type PAO1 as determined by a student's t-test ( $p \leq 0.05$ ). Presence or absence of  $\alpha$ -glucan as indicated by + or – respectively. Parental PAO1 strain data is replicated from table 3-1.

Strain	Trehalose (%)	M1P (%)	Presence of $\alpha$ -glucan
PAO1	0.13 $\pm$ 0.03	0.30 $\pm$ 0.03	+
PAO1 <i>ΔglgA ΔglgE :: otsA/otsB</i>	0.07 $\pm$ 0.02	0.66 $\pm$ 0.11 *	-

As expected, PAO1 *ΔglgA ΔglgE :: otsA/otsB* yielded a significant increase in M1P to 0.66  $\pm$  0.11%, ( $p \leq 0.05$ ) of the cell dry weight, whereas trehalose levels (0.07  $\pm$  0.02%) were not significantly different to that wild-type PAO1 (Table 4-2). Moreover, peaks associated with maltose and  $\alpha$ -glucan were undetectable (Figure 4-8). Low levels of trehalose and the

absence of maltose likely represents the relationship between trehalose, maltose and M1P, where the equilibrium favours the biosynthesis of M1P driven by the ATP-dependent activity of Pep2 [157]. Moreover, trehalose is unlikely to be metabolised by the reverse reaction of TreY and TreZ due to high concentrations of water.

Although maltose was not identified by  $^1\text{H-NMR}$  spectroscopy, the accumulation of M1P indicated that PAO1  $\Delta\text{glgA } \Delta\text{glgE} :: \text{otsA/otsB}$  was capable of producing maltose. This showed that a strain able to produce maltose and M1P but deficient in  $\alpha$ -glucan biosynthesis was successfully engineered.

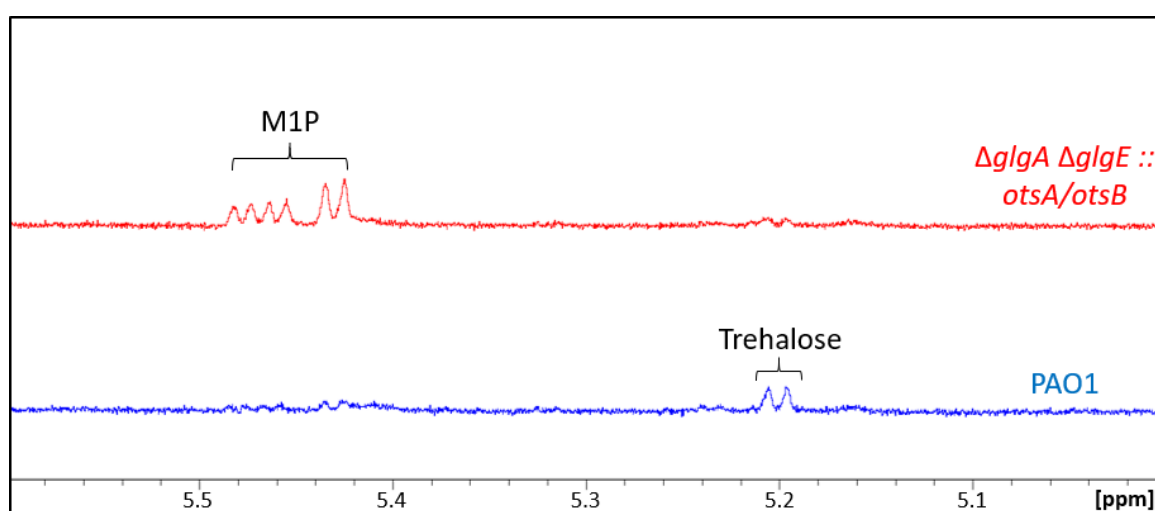


Figure 4-8:  $^1\text{H-NMR}$  spectroscopy of the soluble metabolome following the deletion of *glgA*, *glgE* and the over-expression of *otsA/otsB* in PAO1. Metabolomes were extracted from wild-type PAO1 (blue) and  $\Delta\text{glgA } \Delta\text{glgE} :: \text{otsA/otsB}$  (red) cultured on M9 minimal medium. Peak assignments are as indicated based on previously established spectra. (M1P; maltose 1-phosphate). Resonances corresponding to M1P were increased in the metabolome of  $\Delta\text{glgA } \Delta\text{glgE} :: \text{otsA/otsB}$  as compared to wild-type PAO1. Whereas, the production of  $\alpha$ -glucan was not detected.

To investigate the roles of maltose and M1P during desiccating conditions, the survival of PAO1  $\Delta\text{glgA } \Delta\text{glgE} :: \text{otsA/otsB}$  at decreased RH was determined. When subjected to desiccation stress, PAO1  $\Delta\text{glgA } \Delta\text{glgE} :: \text{otsA/otsB}$  yielded sensitivity similar to that of strains lacking TreS/Pep2 resulting in a desiccation response of  $3.2 \log_{10}(\text{CFU/mL})$  ( $p \leq 0.001$ ) (Figure 4-9). This indicated that the M1P does not play a role in desiccation stress resistance in PAO1. Although maltose was not detected, this strain possessed the genetic and metabolic capacity to produce this metabolite under desiccation stress. Nevertheless, this did not protect against desiccation stress.

Although the levels of trehalose in this experiment were reduced, it shows that desiccation resistance is not dependent on the production of M1P or the capacity of the cell to produce maltose. Combined with the data from previous desiccation experiments this shows that that desiccation sensitivity is due to the absence of GlgE-dependent  $\alpha$ -glucan.

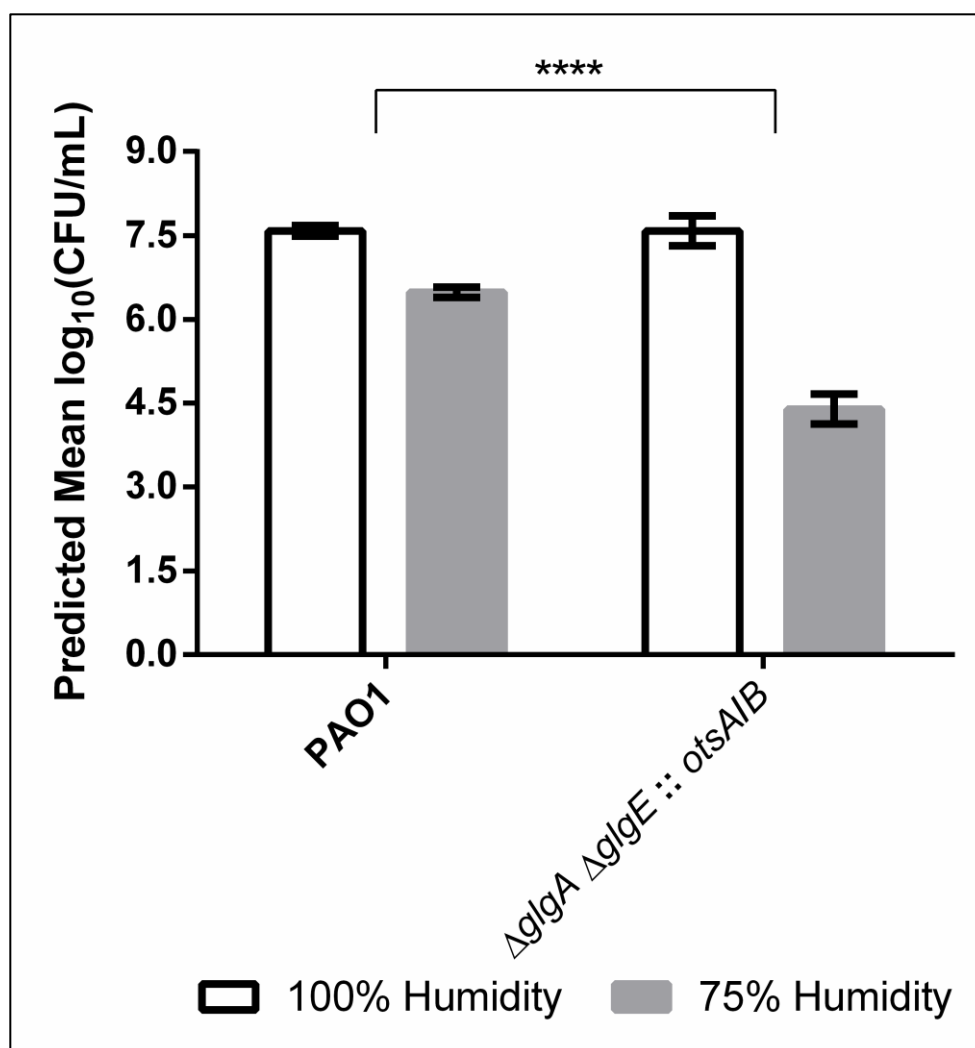


Figure 4-9: Linear mixed modelling analysis of the survival of PAO1 and  $\Delta glgA \Delta glgE :: otsA/otsB$  strains when incubated at 100% (white bars) and 75% RH (grey bars). Bacterial recovery is presented as the predicted mean of  $\log_{10}(\text{CFU/mL})$ . Results are representative of at least three independent experiments.  $\Delta glgA \Delta glgE :: otsA/otsB$  was significantly attenuated during incubation at 75% RH compared to wild-type PAO1. \*\*\*\* indicates  $p \leq 0.0001$ .

#### 4.3.7 Alginate plays a role in protecting PAO1 during desiccation stress

The alginate biosynthesis genes have been implicated in the transcriptomic response to water stress and loss of alginate production impacts survival during low RH in *P. putida* [130, 202]. Because of this, the role of alginate as an osmotic and desiccation stress protectant was considered in PAO1. To this end, an alginate null mutant in PAO1 was generated by the deletion of the genes encoding the biosynthesis proteins AlgG and AlgX

(PAO1  $\Delta alg$ ) [203, 204]. The construction of the deletion vector was performed by Sebastian Pfeilmeier.

To assess the effect of alginate production during growth with osmotic stress, PAO1 and PAO1  $\Delta alg$  were cultured in the presence and absence of NaCl (Figure 4-10). Loss of alginate did not affect growth in either stressed or non-stressed conditions. This suggests that the production of alginate does not play a role in tolerating osmotic stress.

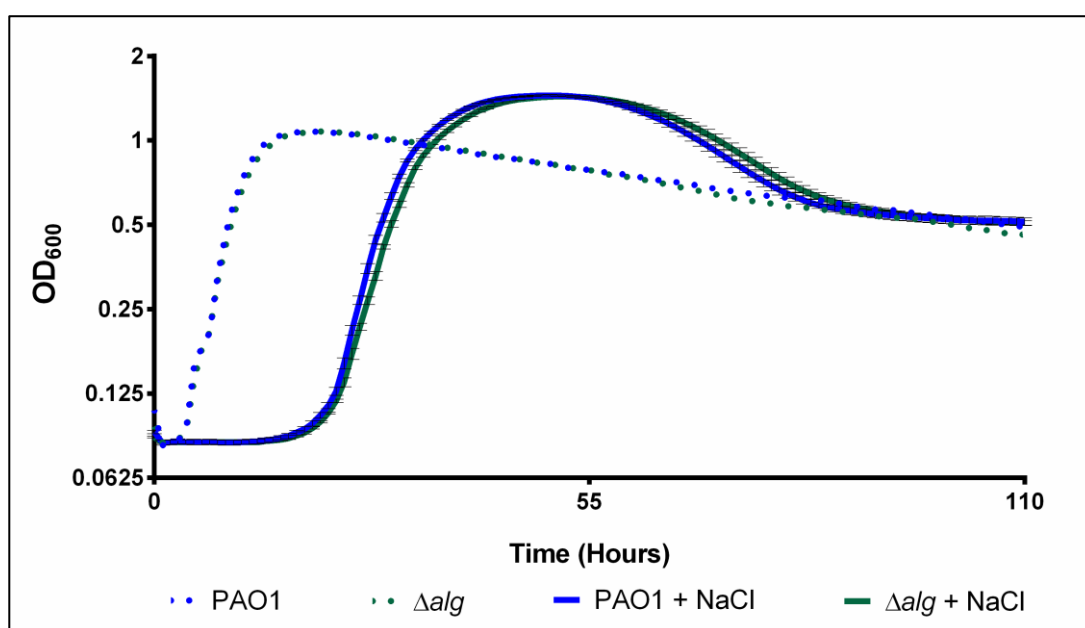


Figure 4-10: Growth of PAO1 and  $\Delta alg$  in M9 minimal medium  $\pm$  0.85 M NaCl. Values represent the mean OD<sub>600</sub>  $\pm$  SEM of five technical replicates. Error bars are not shown for growth under non-stressed conditions for reasons of legibility. The alginate deficient strain was not attenuated during osmotic conditions as compared to wild-type PAO1.

To investigate the role of alginate as a desiccation stress protectant, the viability of PAO1  $\Delta alg$  following exposure to desiccating conditions was determined (Figure 4-11). When subjected to desiccation stress, PAO1  $\Delta alg$  yielded a statistically significant desiccation response of 3  $\log_{10}$ (CFU/mL) ( $p \leq 0.001$ ) compared to that of the wild-type PAO1 strain (Figure 4-11). Taken together, this suggests that the production of alginate is important in the resistance of desiccation stress but not osmotic stress in *P. aeruginosa* PAO1.

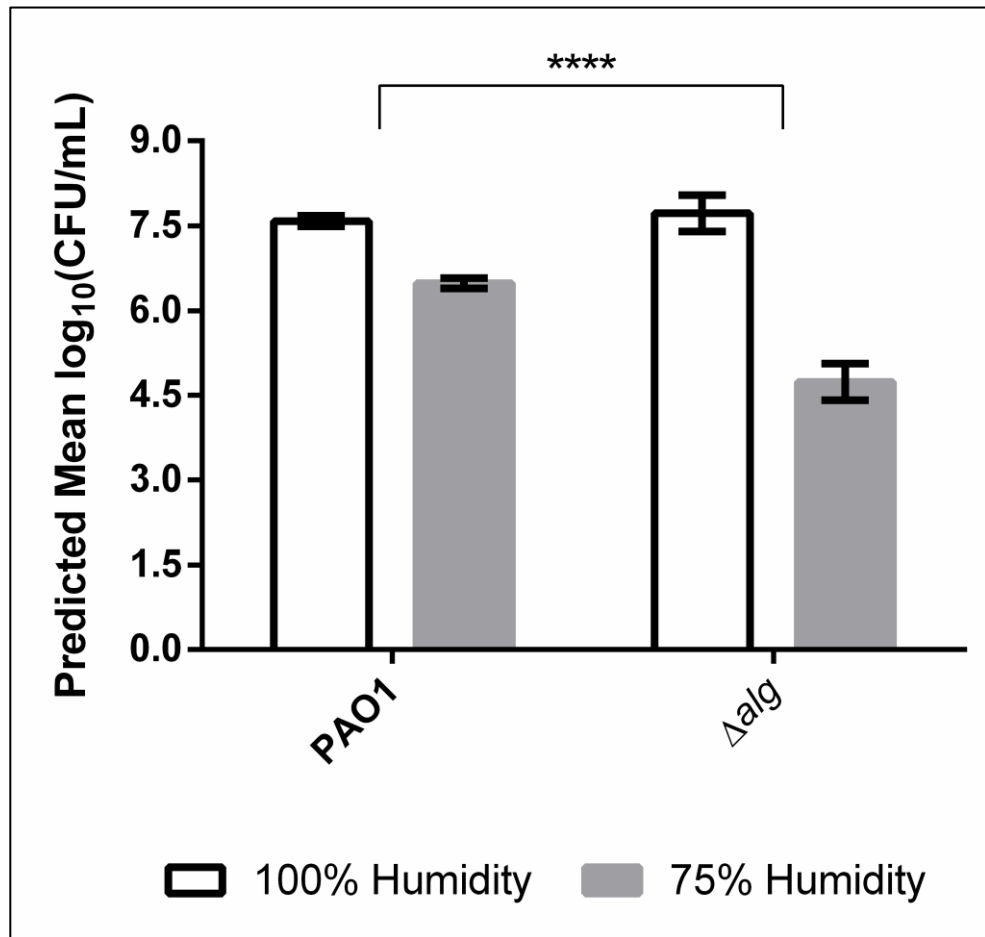


Figure 4-11: Linear mixed modelling analysis of the survival of PAO1 and  $\Delta alg$  when incubated at 100% (white bars) and 75% RH (grey bars). Bacterial recovery is presented as the predicted mean of  $\log_{10}(\text{CFU/mL})$ . Results are representative of at least three independent experiments.  $\Delta alg$  was significantly attenuated during incubation at 75% RH compared to wild-type PAO1. \*\*\*\* indicates  $p \leq 0.0001$ .

## 4.4 Phenotypic characterisation of trehalose and $\alpha$ -glucan biosynthesis in *Pto*.

4.4.1 Operon deletions resulted in abolition of both trehalose and  $\alpha$ -glucan biosynthesis in *Pto* but do not allow the distinction between these two molecules

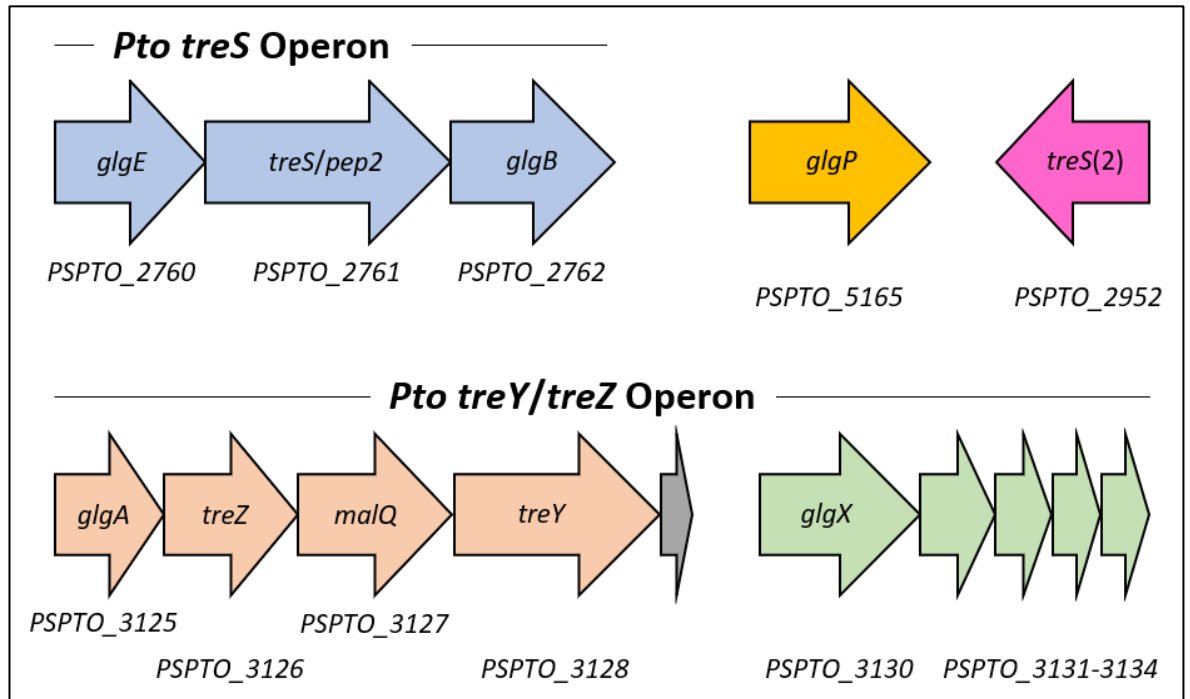


Figure 4-12: The genomic organisation of the trehalose and  $\alpha$ -glucan biosynthesis genes in *Pto*.

Since the genetic and biochemical characterisation of the predicted *Pto* trehalose and  $\alpha$ -glucan biosynthesis pathways resulted in ambiguity, I changed strategies and opted for deletion of both the *treS* (PSPTO\_2760 – PSPTO\_2762) and *treY/treZ* (PSPTO\_3125 – PSPTO\_3134) operons to ensure loss of trehalose and  $\alpha$ -glucan (Figure 4-12). This resulted in the generation of *Pto*  $\Delta$ PSPTO\_2760-2762 and *Pto*  $\Delta$ PSPTO\_3125-3134, respectively. The operon deletions were also combined to generate *Pto*  $\Delta$ PSPTO\_2760-2762  $\Delta$ PSPTO\_3125-3134, abbreviated as *Pto*  $\Delta\Delta$ .

To show that trehalose and  $\alpha$ -glucan biosynthesis had indeed been abolished, the soluble metabolomes of these strains were extracted and analysed using  $^1\text{H-NMR}$  spectroscopy. Analysis of the soluble metabolome of *Pto*  $\Delta$ PSPTO\_2760-2762,  $\Delta$ PSPTO\_3125-3134 and  $\Delta\Delta$  revealed the absence of all relevant metabolites, except for  $\Delta$ PSPTO\_2760-2762 which yielded low levels of trehalose ( $0.04 \pm 0.006\%$  dry cell weight) (Table 4-3, Figure 4-13).

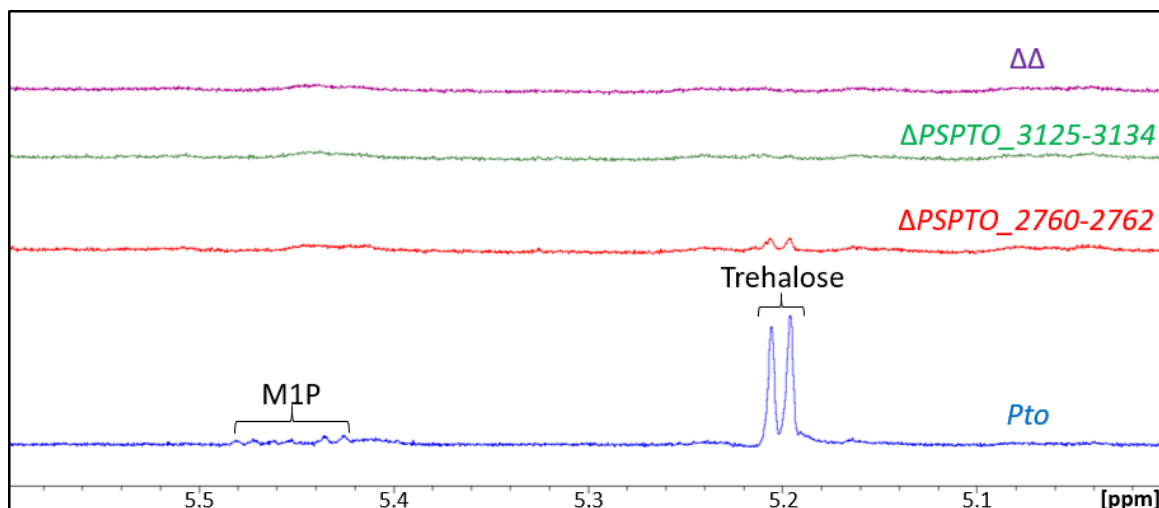


Figure 4-13:  $^1\text{H}$ -NMR spectroscopy of the soluble metabolome following the deletion of *PSPTO\_2760-2762*, *PSPTO\_3125-3134* and *PSPTO\_2760-2762 PSPTO\_3125-3134* ( $\Delta\Delta$ ) in *Pto*. Metabolomes were extracted from wild-type *Pto* (blue),  $\Delta PSPTO_2760-2762$  (red),  $\Delta PSPTO_3125-3134$  (green) and  $\Delta\Delta$  (purple) cultured on M9 minimal medium. Peak assignments are as indicated based on previously established spectra. (M1P; maltose 1-phosphate). Resonances corresponding to metabolites of interest were absent in the metabolomes of  $\Delta PSPTO_3125-3134$  and  $\Delta\Delta$ . Decreased levels of trehalose was detected in the metabolome of  $\Delta PSPTO_2760-2762$ .

Table 4-3: Concentrations of trehalose and M1P produced by *Pto* strains. Metabolites are presented as percentages of cellular dry weight  $\pm$  standard error ( $n \geq 2$ ). – indicates no measurable metabolite, \* indicates significant differences as compared to the wild-type *Pto* as determined by a student's t-test ( $p \leq 0.05$ ). Presence or absence of  $\alpha$ -glucan as indicated by + or – respectively. Parental *Pto* strain data is replicated from table 3-1.

Strain	Trehalose (%)	M1P (%)	Presence of $\alpha$ -glucan
<i>Pto</i>	$0.13 \pm 0.03$	$0.30 \pm 0.03$	+
<i>Pto</i> $\Delta PSPTO_2760-2762$	$0.04 \pm 0.01$	-	-
<i>Pto</i> $\Delta PSPTO_3125-3134$	-	-	-
<i>Pto</i> $\Delta\Delta$	-	-	-

Although trehalose was produced by the  $\Delta PSPTO_2760-2762$  strain, this was at lower concentrations than expected based on our predicted pathway, consistent with previous work [74, 180] (Section 3.2.5). Moreover, as the intracellular concentration of both trehalose and  $\alpha$ -glucan were depleted in these mutant strains as compared to the wild-type *Pto*, subsequent stress sensitivity phenotypes could not be attributed to either the loss of trehalose or  $\alpha$ -glucan individually.

To decouple the biosynthesis of trehalose and  $\alpha$ -glucan, and therefore distinguish their individual roles in *Pto*, I attempted to increase the intracellular concentration of trehalose within the *Pto* operon deletion strains by introducing *M. koreensis* 3J1 *otsA/otsB* as described with PAO1 earlier (Section 4.3.3). However, the introduction of *otsA/otsB*

resulted in the majority of transformants not being viable. Where colonies did appear, they exhibited morphological irregularities. This suggested that the production of these proteins or an increase in intracellular trehalose concentration was toxic. Consequently, I did not continue with this strategy. Although the individual roles of trehalose and  $\alpha$ -glucan could not be elucidated reliably in *Pto*, the phenotypic analysis was continued with *Pto*  $\Delta\Delta$  to investigate the effect of the loss of both trehalose and  $\alpha$ -glucan during water stress and to draw comparisons to the system in PAO1.

#### 4.4.2 Loss of both trehalose and $\alpha$ -glucan in *Pto* results in osmotic sensitivity

To investigate the roles of trehalose and  $\alpha$ -glucan in *Pto* during osmotic stress, wild-type *Pto* and  $\Delta\Delta$  were cultured in the presence and absence of NaCl. Wild-type *Pto* showed attenuated growth with a longer lag-phase under osmotic stress when compared to non-stressed growth (Figure 4-14) *Pto*  $\Delta\Delta$  yielded a similar growth profile to wild-type *Pto* under non-stressed growth but exhibit increased osmotic sensitivity when compared to the wild-type when NaCl was present. Due to the variable behaviour of these bacteria under osmotic stress, these datasets were difficult to reproduce.

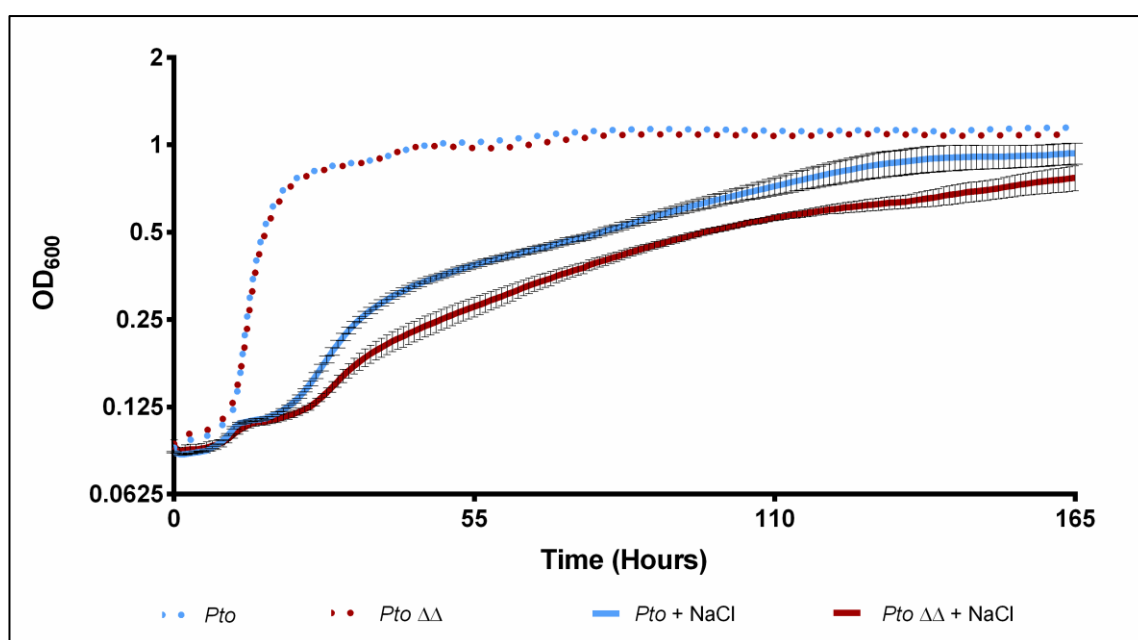


Figure 4-14: Growth of wild-type *Pto* and  $\Delta\Delta$  in M9 minimal medium  $\pm$  0.35 M NaCl. Values represent the mean OD<sub>600</sub> of five replicates. Error bars are not shown for growth under non-stressed conditions for reasons of legibility.  $\Delta\Delta$  exhibited osmotic sensitivity compared to wild-type *Pto*.

#### 4.4.3 Loss of both trehalose and $\alpha$ -glucan in *Pto* results in desiccation sensitivity

To investigate the roles of trehalose and  $\alpha$ -glucan in *Pto* during desiccation stress, wild-type *Pto* and  $\Delta\Delta$  were examined under conditions of different RH as described above (Section 4.2.1). Following incubation at 100% RH, recovery of wild-type *Pto* yielded a predicted mean of approximately 5.8  $\log_{10}$ (CFU/mL) (Figure 4-15). Recovery after incubation at 75% RH resulted in a predicted mean of 5.05  $\log_{10}$ (CFU/mL) equating to a desiccation response of approximately 0.74  $\log_{10}$ (CFU/mL). When subjected to either 100% or 75% RH, the trehalose and  $\alpha$ -glucan null mutant  $\Delta\Delta$  resulted in recovery of a predicted mean of 5.9 and 4.4  $\log_{10}$ (CFU/mL), respectively. This equated to a desiccation response of approximately 1.5  $\log_{10}$ (CFU/mL). Although this response was less severe than initially expected based on equivalent data in PAO1, this was significantly different ( $p \leq 0.05$ ) when compared to that of the wild-type *Pto* strain.

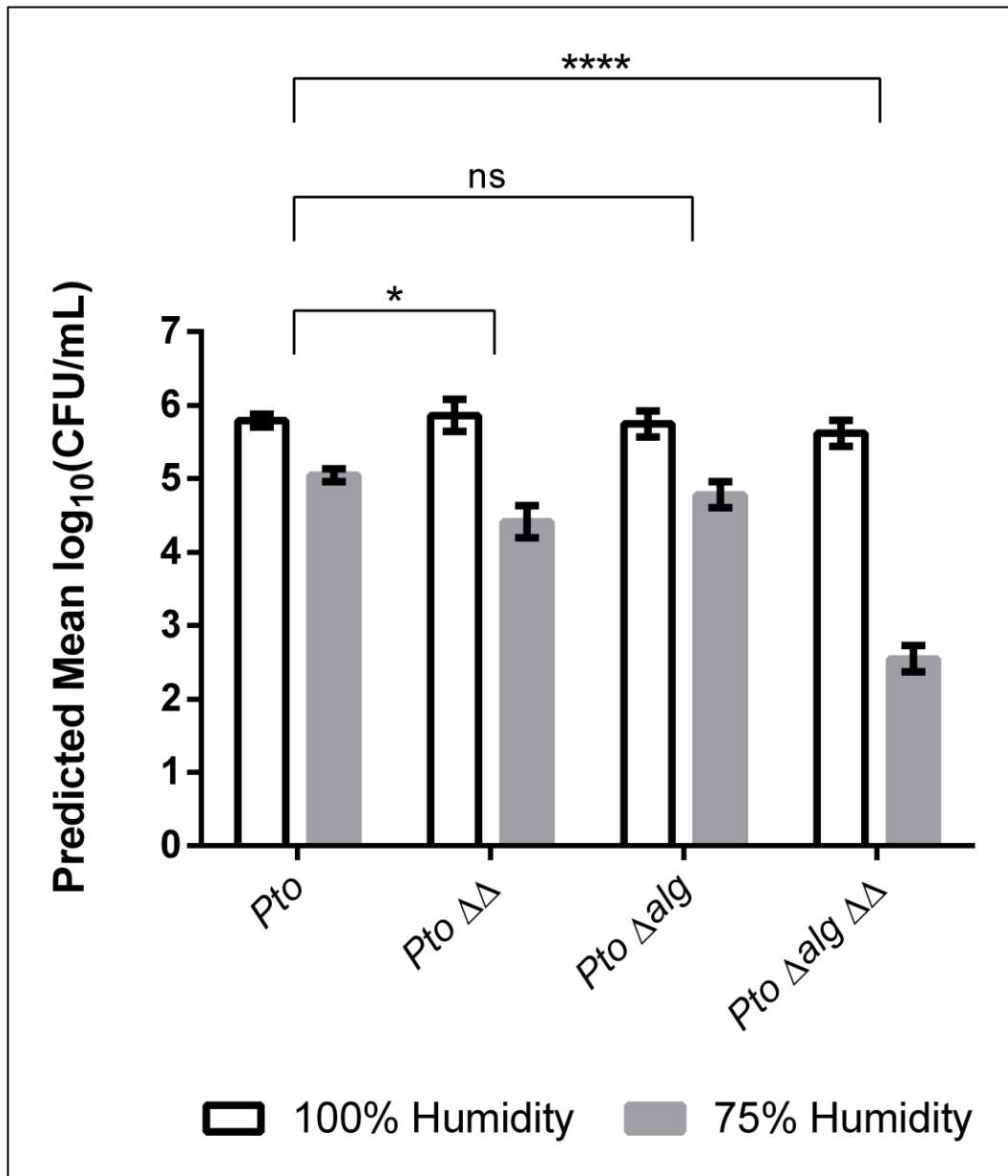


Figure 4-15: Linear mixed modelling analysis of the survival of *Pto*, ΔΔ, Δalg and Δalg ΔΔ strains when incubated at 100% (white bars) and 75% RH (grey bars). Bacterial recovery is presented as the predicted mean of log<sub>10</sub>(CFU/mL). Results are representative of at least three independent experiments. ΔΔ exhibited desiccation sensitivity when compared to wild-type *Pto*, whereas the desiccation response of Δalg was not significantly different. Δalg ΔΔ was exhibited enhanced attenuation during incubation at 75% RH compared to wild-type *Pto* and ΔΔ. \*\*\*\* indicates  $p \leq 0.0001$ , \* indicates  $p \leq 0.05$ , ns indicates non-significant.

#### 4.4.4 Alginate works in combination with α-glucan to protect against desiccation stress in *Pto*

Since alginate played a role during the response to desiccation stress in PAO1 (4.3.7), I also investigated the role of alginate production during desiccation stress in *Pto*. To this end, a previously generated *Pto* strain harbouring a deletion of both *algG* and *algX* (Δalg) was exposed to desiccating conditions as described earlier (Section 4.2.1). The deletion

construct *pΔalg* was constructed and the strain *Pto Δalg* was generated by Sebastian Pfeilmeier.

When subjected to desiccation conditions, *Pto Δalg* yielded a desiccation response of 0.96  $\log_{10}$ (CFU/mL) (Figure 4-15). This was not significantly different to the response of wild-type *Pto* when the data was analysed using linear mixed modelling. Regardless of significance, the desiccation response of *Pto ΔΔ* and *Δalg* were unexpectedly low when compared to the desiccation response of the corresponding PAO1 strains. As a result, I considered that  $\alpha$ -glucan and alginate may exhibit functional redundancy in *Pto* strains and that combining deletions for trehalose,  $\alpha$ -glucan and alginate biosynthesis, may result in desiccation susceptibility similar to that observed in the PAO1 strains.

To investigate this, the *algG* and *algX* genes were deleted to abolish alginate production in the *Pto ΔΔ* strain, generating *Δalg ΔΔ*. This was performed using the *pΔalg* deletion vector constructed by Sebastian Pfeilmeier. Exposure of *Δalg ΔΔ* to desiccating conditions resulted in a desiccation response of 3.1  $\log_{10}$ (CFU/mL), ( $p \leq 0.0001$ ).

The contribution of trehalose to desiccation stress in *Pto* cannot be excluded experimentally. However, based on equivalent data in PAO1, these results suggest that *Pto* utilises both alginate and  $\alpha$ -glucan to resist desiccation stress. Furthermore, this suggests that the polysaccharides are functionally redundant as the loss of both systems is not simply additive.

#### 4.4.5 Trehalose, $\alpha$ -glucan and alginate are important during plant infection

Although I have shown that alginate and  $\alpha$ -glucan are important for desiccation survival *in vitro*, the impact of this *in planta* has not been investigated. Since alginate and  $\alpha$ -glucan biosynthesis mutants have been shown to exhibit sensitivity to desiccation stress, it would follow that the growth of these strains would be attenuated during the epiphytic lifestyle on the surface of the leaf as they are exposed to osmotic and desiccating conditions [73]. To investigate the role of trehalose,  $\alpha$ -glucan and alginate during plant infection, wild-type *Pto*,  $\Delta\Delta$ , *Δalg* and *Δalg ΔΔ* strains were used to infect the model organism *Arabidopsis thaliana* (Col-0).

To investigate the impact of loss of trehalose and  $\alpha$ -glucan biosynthesis during plant infection, *Pto* and  $\Delta\Delta$  were sprayed onto the surface of 6-week-old *A. thaliana* leaves. The course of infection was monitored by determining the bacterial load by sampling the leaves

0, 2, and 3-days post infection (DPI). For the duration of the infection the plants were not watered. Over the course of 3 days wild-type *Pto* showed marked proliferation from the initial inoculum at day 0 indicating successful infection (Figure 4-16). Intracellular trehalose and  $\alpha$ -glucan did not appear to be important for pathogenesis because there was no significant difference in the bacterial load of  $\Delta\Delta$  compared to the wild-type strain for the duration of the experiment. Similarly, the production of alginate did not appear to play a role in plant infection. There was no significant difference of the bacterial load of the  $\Delta alg$  strain compared to wild-type *Pto* during infection. This suggests the loss of either system individually is not important for plant infection.

When *Pto* lacked the ability to biosynthesise trehalose,  $\alpha$ -glucan and alginate together, there was an insignificant decrease in cell recovery during spray infection at 2 DPI. At 3 DPI there was a statistically significant difference ( $p \leq 0.05$ ) between the recovery of  $\Delta alg \Delta\Delta$  and the wild-type strain (Figure 4-17). When *Pto* and  $\Delta alg \Delta\Delta$  were infiltrated directly through the stomata into the apoplast, there was no difference in bacterial recovery up to 3 DPI. This suggests that exposure on the leaf surface is required for the attenuation of infection. Similarly, if the plants were watered regularly, thereby increasing the local RH, the attenuation of  $\Delta alg \Delta\Delta$  during spray infection was also rescued.

Taken together, this suggests that alginate, trehalose and  $\alpha$ -glucan are important for survival on the surface of the leaf. *Pto*  $\Delta alg \Delta\Delta$  exhibits attenuation when exposed to low RH on the surface of the leaf, a stress which is not present during higher RH or within the apoplast. Although the contribution of trehalose during infection cannot be excluded, equivalent data in PAO1 suggests that alginate and  $\alpha$ -glucan protect *Pto* during low RH.

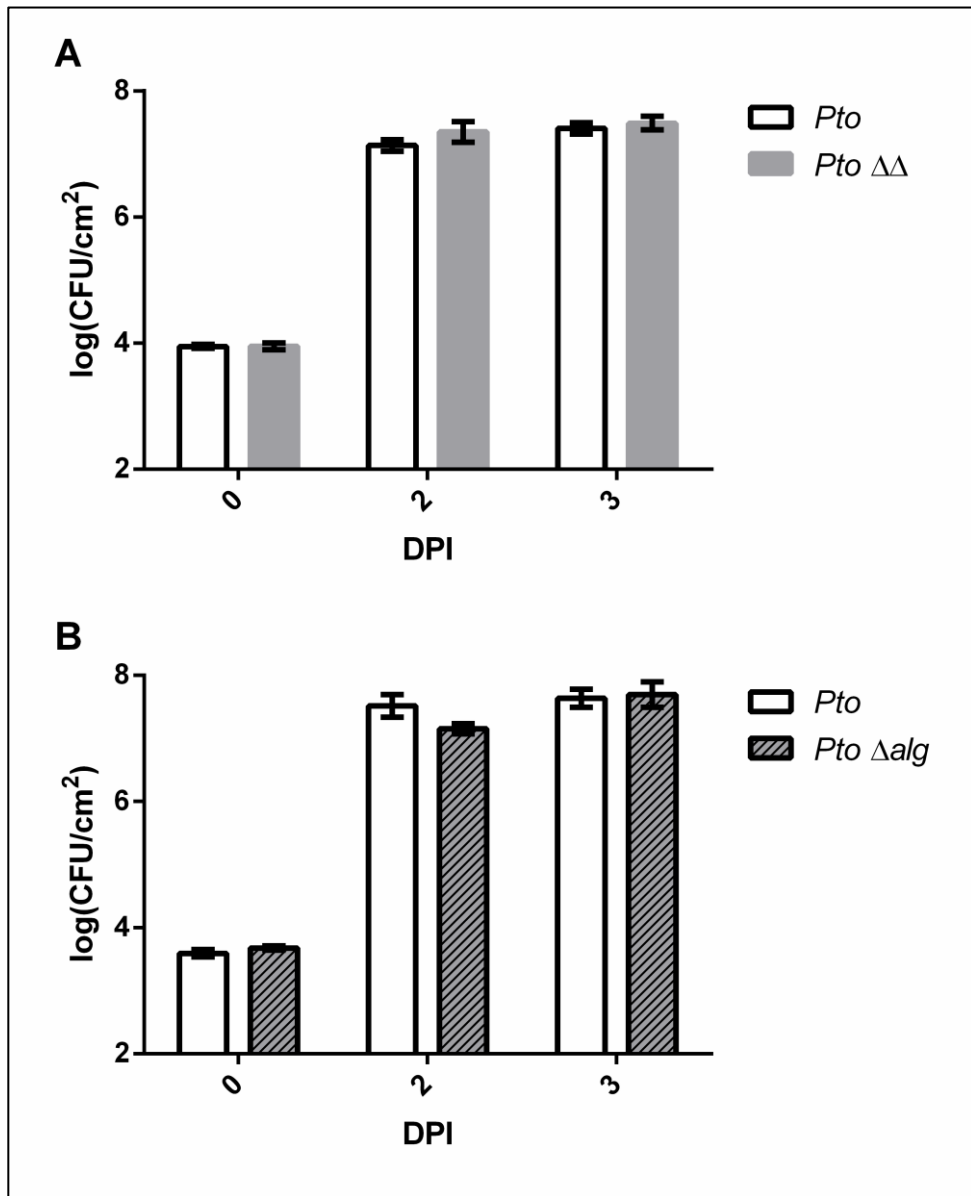


Figure 4-16: *A. thaliana* (Col-0) infection with *Pto*,  $\Delta\Delta$  and  $\Delta alg$ . **(A)** Spray infection with wild-type *Pto* or  $\Delta\Delta$ . **(B)** Spray infection with wild-type *Pto* or  $\Delta alg$ . Spray infection assays were conducted over 3 days and bacterial growth was determined by leaf disc sampling after 0-, 2- and 3-days post infection (DPI). Values represent the mean  $\log_{10}(\text{CFU}/\text{cm}^2)$  of 6 replicates  $\pm$  standard error of the mean. Significance was based on a two-tailed Mann-Whitney test. Results are representative of two independent experiments. No significant differences were observed between the infection profile of either mutant and wild-type *Pto*.

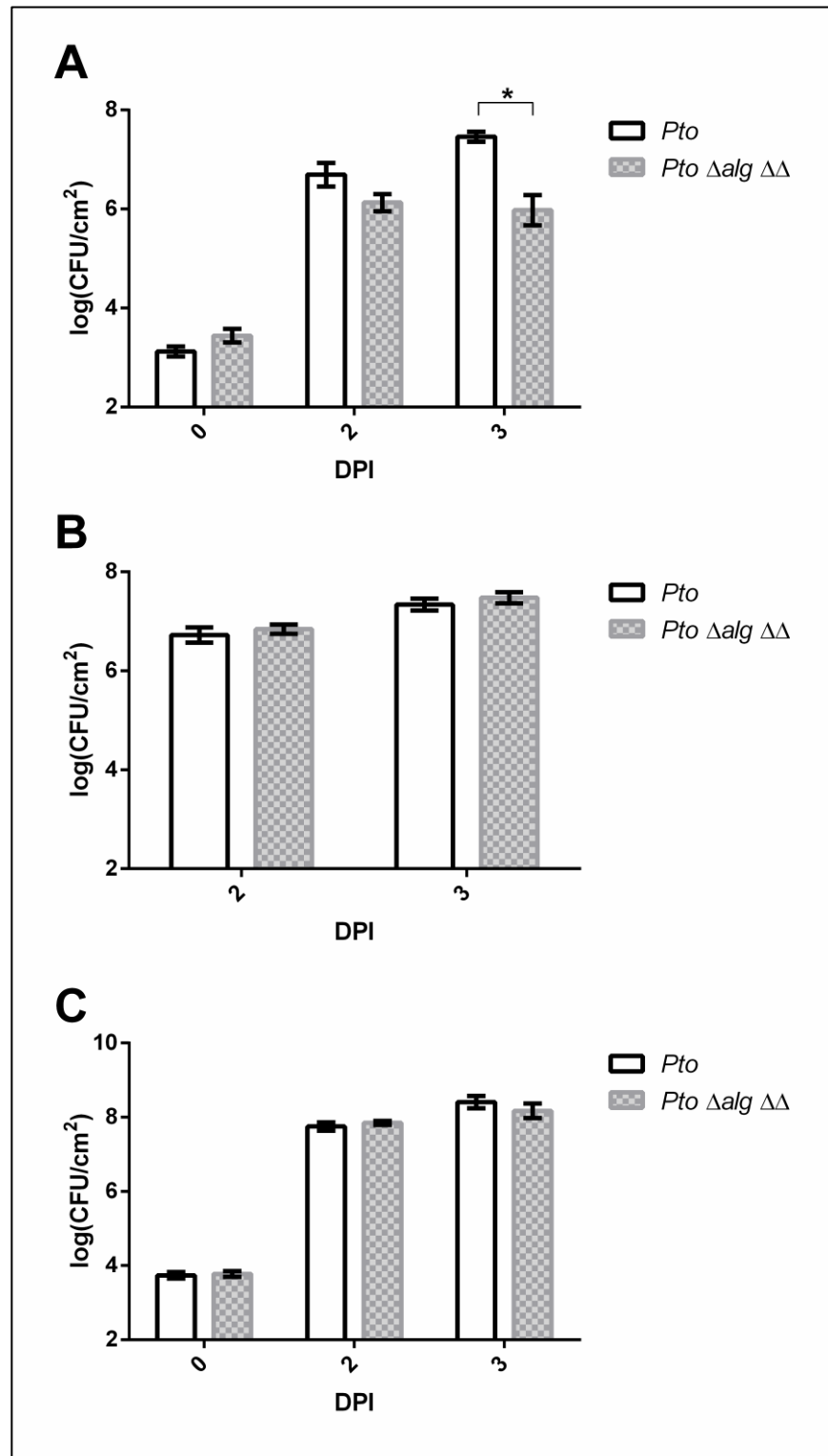


Figure 4-17: *A. thaliana* (Col-0) infection with *Pto* and  $\Delta alg \Delta\Delta$ . **(A)** Spray infection with wild-type *Pto* or  $\Delta alg \Delta\Delta$ . **(B)** Infiltration infection with wild-type *Pto* or  $\Delta alg \Delta\Delta$ . **(C)** Spray infection with wild-type *Pto* or  $\Delta alg \Delta\Delta$  where the plants were frequently watered. Spray infection assays are conducted over 3 days where bacterial growth is numerated by leaf disc sampling after 0-, 2- and 3-days post infection (DPI). Infiltration infection assays were conducted over 3 days where bacterial growth was determined by leaf disc sampling after 2- and 3-DPI. Values represent the mean  $\log_{10}(\text{CFU}/\text{cm}^2)$  of 4-6 replicates  $\pm$  standard error of the mean. Significance (\*  $p \leq 0.05$ ) was based on a two-tailed Mann-Whitney U-test. Results are representative of two independent experiments. Significant attenuation of  $\Delta alg \Delta\Delta$  spray infection was observed compared to wild-type *Pto* at 3 DPI. This was not observed during infiltration infection or spray infection where plants were frequently watered.

## 4.5 Discussion

Prior to this work, many publications had implicated trehalose in the survival of bacteria during water stress, namely osmotic and desiccating conditions [74, 107, 202, 205, 206]. Recent advances in our understanding of the biosynthesis of trehalose in bacteria and the discovery of the GlgE pathway has enabled the discovery of the intrinsic genetic and biosynthetic link between  $\alpha$ -glucan and trehalose to be made in *Pseudomonas* spp. Conclusions drawn from the disruption of what was thought to be trehalose biosynthesis were therefore revisited and the function of trehalose and  $\alpha$ -glucan were investigated.  $\alpha$ -glucan was always considered to be a carbon storage molecule providing energy to the cell when required [207]. However, work in *Mycobacterium* spp. has shown that  $\alpha$ -glucan produced in this species is exported to the capsule where it can interact with the human immune system and modulate virulence [208]. The fact that only a small subset of *Pseudomonas* spp. are human pathogens means that the function of *Pseudomonas*  $\alpha$ -glucan is unlikely to be related solely, if at all, to the human immune system and must therefore be investigated.

Deletion of what was thought to be the trehalose biosynthetic gene operons in *Pseudomonas aeruginosa* PA14 resulted in the generation of strains attenuated during *A. thaliana* infections [180], however these strains were not susceptible to osmotic stress. Similarly, disruption of what was thought to be trehalose biosynthesis in *Pto* resulted in osmotic sensitivity and strains which were attenuated during plant infection [74]. This is a phenotype which was exacerbated by lower RH.

Furthermore, Vílchez *et al.* showed that trehalose concentrations were correlated with bacterial desiccation resistance [151]. For example, *M. koreensis* 3J1 produces high concentrations of trehalose and exhibits high desiccation resistance. Moreover, the *in trans* expression of *M. koreensis* 3J1 *otsA/otsB* resulted in an increase of trehalose production and desiccation resistance in *P. putida*.

The discovery and characterisation of the GlgE pathway in *Pseudomonas* spp. established the ability of these bacteria to metabolise trehalose into  $\alpha$ -glucan, therefore modulation of the intracellular levels of trehalose, through gene deletion or gene introduction, may also affect the levels of  $\alpha$ -glucan. Phenotypes associated with *Pseudomonas* trehalose biosynthesis must be reinterpreted considering recent findings. As a result, the role of  $\alpha$ -

glucan and the interplay with the function of trehalose during water stress were elucidated in *Pseudomonas* spp.

To investigate the role of trehalose and  $\alpha$ -glucan in *Pseudomonas* spp. under osmotic and desiccating conditions, I exploited trehalose and  $\alpha$ -glucan biosynthesis mutant strains and exposed individual strains to specific stress conditions. The combination of phenotypic characterisation and the metabolomic characterisation of each of these mutant strains enabled the assignment of individual functions to either  $\alpha$ -glucan or trehalose.

To characterise the roles of  $\alpha$ -glucan and trehalose during osmotic stress, PAO1 mutant strains were cultured in media in the presence of NaCl. All strains lacking the ability to synthesise trehalose were osmotically-sensitive suggesting that trehalose protects against osmotic conditions. This was irrespective of the concentration of  $\alpha$ -glucan because the  $\alpha$ -glucan accumulating  $\Delta treY$  and  $\Delta treZ$  strains yielded osmotic sensitivity. These strains presumably produce a mixture of both GlgA- and GlgE-dependent  $\alpha$ -glucan due to MalQ-dependent maltose biosynthesis (Section 3.2.11). This suggests that  $\alpha$ -glucan plays no discernible role during growth in osmotic conditions.

PAO1 mutants lacking the branching and debranching enzymes GlgB and GlgX were also osmotically-sensitive. This is surprising because the levels of trehalose in PAO1  $\Delta glgB$  exceed that of the wild-type strain under non-stressed conditions, however, this may not be true during hyper-osmotic conditions. This suggests that  $\alpha$ -glucan is required as a substrate to ensure optimal rates of trehalose production in response to osmotic stress. Perturbation of the ability of PAO1 to branch or debranch  $\alpha$ -glucan could result in pools of inaccessible  $\alpha$ -glucan. This could be due to linear  $\alpha$ -glucan becoming too long and insoluble in the  $\Delta glgB$  strain or due to the inability of PAO1 to fully metabolise  $\alpha$ -glucan after each branch point to produce trehalose in the  $\Delta glgX$  strain. The accumulation of long insoluble  $\alpha$ -glucan may interfere with the function of trehalose yielding an osmotically-sensitive strain. Alternatively, GlgB and GlgX could be indirectly essential for the structural integrity or function of other trehalose biosynthesis enzymes. These results suggest that  $\alpha$ -glucan is not directly required for osmotic tolerance, but effective recycling of  $\alpha$ -glucan, presumably into trehalose, is required. To further characterise this, PAO1,  $\Delta glgB$  and  $\Delta glgX$  should be exposed to osmotic conditions, the soluble metabolomes extracted and the intracellular levels of osmotically induced trehalose analysed and compared using  $^1\text{H-NMR}$  spectroscopy. The protein-protein interactions between the enzymes of trehalose and  $\alpha$ -

glucan and the subsequent impact on function should also be examined. To experimentally validate the hypothesis that  $\alpha$ -glucan recycling was required for osmotic tolerance, intracellular trehalose accumulation should be determined following exposure of  $\Delta glgB$  and  $\Delta glgX$  osmotic stress and compared to that of wild-type PAO1.

When subjected to 100% or 75% RH, it was clear that the loss of GlgE-dependent  $\alpha$ -glucan biosynthesis resulted in desiccation sensitive strains, irrespective of the ability to synthesise trehalose. When the levels of intracellular GlgA- and GlgE-dependent linear  $\alpha$ -glucan are increased in the  $\Delta glgB$  strain desiccation resistance was also increased. This suggested that  $\alpha$ -glucan protected PAO1 against desiccation stress, irrespective of the state of branching. Although I was able to show that GlgA- and GlgE-dependent  $\alpha$ -glucan do not play a role during osmotic stress, I was unable to test the role of GlgA-dependent  $\alpha$ -glucan during desiccation stress. In order to investigate this, mutant strains accumulating solely GlgA-dependent  $\alpha$ -glucan should be generated and their desiccation sensitivity determined.

Other groups have reported that the levels of intracellular trehalose in bacteria directly correlate to desiccation resistance [150, 151]. As I speculated above, although the basal levels of metabolite production were measured under non-stressed conditions, this may not be representative of the metabolome under hyperosmotic and desiccation stress. Because of this, I hypothesised that the levels of trehalose could be insufficient to confer resistance to desiccation. Previous work had shown that the introduction of the biosynthetic proteins OtsA/OtsB from the high trehalose-producing and markedly desiccation-resistant organism *M. koreensis* 3J1 had increased desiccation resistance in *P. putida*. Following this, I introduced *otsA/otsB* into PAO1 mutant strains to investigate the effect of increasing the production of trehalose on the soluble metabolome and under water stress.

Expression of *otsA/otsB* recovered M1P biosynthesis in the PAO1  $\Delta glgA$  mutant, demonstrating the production of functional OtsA/OtsB. However, trehalose concentrations did not significantly increase in any of the strains tested. Nevertheless, the production of OtsA/OtsB by PAO1 strains conferred increased resistance to osmotic stress, consistent with the osmoprotectant function of trehalose. This could indicate that although the OtsA/OtsB proteins are functional, trehalose does not accumulate during non-stressed conditions either due to flux through TreS/Pep2 into M1P or *via* alternative trehalose

degradation mechanisms, such as the PAO1 periplasmic trehalase (TreA). These results also suggest that GlgE-dependent  $\alpha$ -glucan does not play a role under osmotic stress.  $\Delta treS/pep2 :: otsA/otsB$  is genetically incapable of producing GlgE-dependent  $\alpha$ -glucan because of the loss of TreS/Pep2, but still retains osmotic resistance similar to that of PAO1  $:: otsA/otsB$ . Although, metabolomic analysis suggested that  $\Delta treS/pep2 :: otsA/otsB$  did not accumulate  $\alpha$ -glucan, this strain still retains the genetic ability to produce GlgA-dependent  $\alpha$ -glucan. However, because PAO1  $\Delta treY$  and  $\Delta treZ$  strains are genetically capable of the biosynthesis of both GlgA- and GlgE-dependent  $\alpha$ -glucan and still yield an osmotically-sensitive phenotype, I conclude that  $\alpha$ -glucan does not play a direct role during osmotic stress in PAO1.

As the expression of *otsA/otsB* rescued the desiccation sensitivity of  $\Delta glgA$  but did not recover the phenotype of  $\Delta treS/pep2$ , I am confident that if trehalose protected against desiccation stress, the levels of intracellular trehalose would have been sufficient to confer protection in the  $\Delta treS/pep2 :: otsA/otsB$  strain. This suggested that TreS/Pep2 and therefore the production of GlgE-dependent  $\alpha$ -glucan was essential for desiccation resistance. Even though the presence and concentration of intracellular trehalose did not directly contribute to desiccation resistance, the levels of bacterial trehalose may still be an indirect measure of desiccation tolerance in organisms possessing the GlgE pathway due to the intrinsic coupling between the biosynthesis of trehalose and  $\alpha$ -glucan.

Although GlgE-dependent  $\alpha$ -glucan is the likely candidate for desiccation protection, I could not rule out the products of TreS/Pep2, maltose and M1P, contributing to desiccation resistance. It has been previously reported that the provision of maltose to *Saccharomyces cerevisiae* resulted in enhanced desiccation resistance [115]. The generation of a PAO1 strain deficient in  $\alpha$ -glucan but still capable of producing maltose and M1P required the generation of a strain lacking both enzymes capable of synthesising  $\alpha$ -glucan, GlgA and GlgE. The expression of *otsA/otsB* then reintroduced the genetic capacity for trehalose, maltose and M1P biosynthesis. The PAO1  $\Delta glgA \Delta glgE :: otsA/otsB$  strain exhibited desiccation sensitivity when exposed to 75% RH suggesting that the genetic capability to produce maltose and the accumulation of M1P were not responsible for protecting the cell from desiccation. This also further supports the hypothesis that desiccation resistance requires GlgE-dependent  $\alpha$ -glucan biosynthesis and that resistance is not solely dependent on the presence of the TreS/Pep2 protein.

The elucidation of the roles of  $\alpha$ -glucan and trehalose in *Pto* was hindered by the inability to generate strains decoupling their individual biosynthesis. This was due to several factors including the decrease in the levels of trehalose following a *treS/pep2* or *treS* operon deletion. Because levels of trehalose decreased and  $\alpha$ -glucan was absent, I could not confidently assign the resulting phenotypes to either of these molecules individually. An additional factor was that attempts to increase intracellular trehalose in these strains using the expression of *M. koreensis* 3J1 *otsA/otsB* were not successful. *In lieu* of this, I continued investigating the impact of the loss of both trehalose and  $\alpha$ -glucan biosynthesis in *Pto*. In agreement with the phenotypic analysis in PAO1, the *Pto*  $\Delta\Delta$  strain was both osmotic- and desiccation-sensitive compared to wild-type *Pto*. However, the desiccation response of this strain was lower than expected when compared to the equivalent PAO1 strains. This suggested there was some additional mechanism to resist desiccation stress in *Pto*.

In agreement with my findings, Gulez *et al.* reported that trehalose and  $\alpha$ -glucan biosynthesis gene homologues were upregulated during water stress in *Pseudomonas putida* KT2440 [202]. Additionally, transcripts corresponding to the biosynthesis of the polysaccharide and biofilm component alginate were also upregulated. Furthermore, alginate has also been implicated in the desiccation survival of *P. putida* mt-2 [130]. Because of this the involvement of alginate during water stress was also investigated. Alginate was also shown to be involved in the resistance of desiccation stress in PAO1. The disruption of alginate biosynthesis in *Pto* did not result in a desiccation sensitive strain when the data was analysed using linear mixed modelling. However, when alginate, trehalose and  $\alpha$ -glucan biosynthesis mutations were combined, the desiccation response of this strain was greater than the sum of the responses following loss of each individual biosynthesis pathway. This suggested that there was functional redundancy between  $\alpha$ -glucan and alginate in *Pto* and that both of these sugars function to protect against desiccation stress.

The importance of trehalose,  $\alpha$ -glucan and alginate were tested *in planta* where mutant *Pto* strains were spray infected onto the surface of *A. thaliana*. Loss of either trehalose and  $\alpha$ -glucan or alginate alone was not enough to confer any defect during the course of infection. Freeman *et al.* showed through spray competition assays that a strain identical to *Pto*  $\Delta\Delta$  was attenuated compared to the wild-type strain [74]. Although the data reported by Freeman *et al.* is not consistent with the results presented in this chapter, this

may be explained by the fact that my experiments were performed in the absence of competition and therefore may not yield subtle differences in the ability to infect.

The loss of trehalose,  $\alpha$ -glucan and alginate biosynthesis together resulted in a reduced infection phenotype. This phenotype was only present when the plants were kept under dry conditions for the duration of the infection. When the plants were frequently watered, thereby raising the local RH, any significant attenuation was abolished. Infectious attenuation was also reliant on epiphytic survival on the surface of the leaf because bypassing this stage by infiltrating the  $\Delta alg \Delta \Delta$  strain through the stomata into the apoplast resulted in a wild-type like infection. This strongly implies that alginate and  $\alpha$ -glucan are required by *Pto* to resist desiccation stress on the surface of a leaf thus enabling successful plant infection.

Although I can assume that the RH was increased when the plants were watered, this was not quantified. To further validate this, plant infections should be performed in dedicated environments with controlled humidity to show that infection is proportional to RH using methodology described by Xin *et al.* [209]. Nevertheless, the *in planta* experiments show that the loss of both alginate and  $\alpha$ -glucan is required for significant attenuation reflecting the functional redundancy observed in *in vitro* desiccation experiments. The functions of the hypothetical proteins PSPTO\_3129, PSPTO\_3131 and PSPTO\_3132, the predicted methyltransferase PSPTO\_3133 and the predicted glucosyltransferase have yet to be experimentally tested [181] and although unlikely a role during desiccation stress or growth *in planta* cannot be ruled out.

Although *in planta* experiments were not performed with *P. aeruginosa*, Djonovic *et al.* showed through infiltration infection assays with *A. thaliana* that a *P. aeruginosa* PA14 strain lacking both *treS* and *treY/treZ* operons was attenuated during plant growth [180]. The fact that this attenuation was observed during infiltration into the apoplast contradicts the results in this chapter, suggesting that attenuation is a result of exposure to low RH on the leaf surface. however, the watering regime of these plants is not stated and the humidity in the apoplast may have been relatively low.

The results presented in this chapter have shown that although trehalose and  $\alpha$ -glucan are biosynthetically linked, they play distinct roles in the protection of *Pseudomonas* spp. during water stress. Through this work I have been able to apply methodology to confidently decouple the responses to the distinct water stresses, osmotic and desiccation

stress. I have shown that trehalose protects *Pseudomonas* spp. against osmotic stress, most likely due to its role as a compatible solute and its ability to counteract the external solute concentration and to preserve membranes and proteins from damage [139]. However, trehalose does not directly protect against desiccation stress. This role can be attributed to the polysaccharide  $\alpha$ -glucan because although the presence of trehalose can correlate with the protection of the cell against desiccation stress, this is only true when the cell retains the ability to process trehalose into  $\alpha$ -glucan *via* the GlgE pathway.

The exact mechanism of desiccation protection by  $\alpha$ -glucan is currently unknown. Although this work decoupled the biosynthesis of trehalose and  $\alpha$ -glucan to study their individual functions, the ability to interchange between both these molecules is likely to be required for full adaptability to rapidly changing environments. This work also implicates the external polysaccharide alginate as a desiccation stress protectant, functioning in a similar manner to the internal  $\alpha$ -glucan protection mechanism protecting the cell from desiccation stress from either side of the plasma membrane. This is likely due to the capacity of alginate to hold water [130], form a hydrogel and keep the cell hydrated by retaining localised pools of water. I have shown that these systems are important for environmental survival as well as during plant infection as summarised in Figure 4-18.

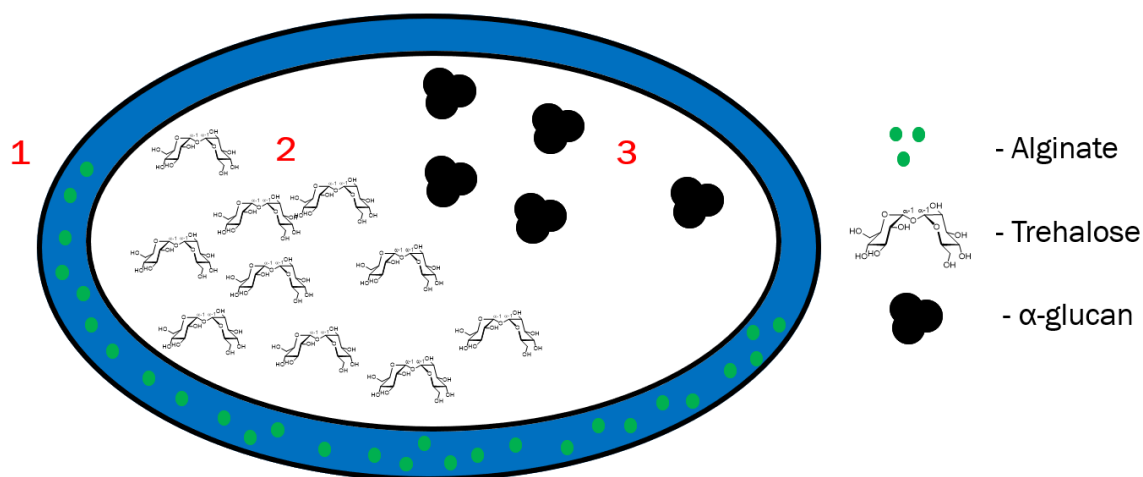


Figure 4-18: The current understanding of water stress protection mechanisms of *Pseudomonas* spp. **(1)** The export of alginate to the biofilm, where it is thought to form an aqueous-rich layer. **(2)** During osmotic stress the cell responds by biosynthesising trehalose. **(3)** During desiccation stress the cell responds by producing  $\alpha$ -glucan to protect against cell death.

The importance of these systems during human infection has yet to be understood. It was previously reported that trehalose and  $\alpha$ -glucan biosynthetic mutants were not attenuated in growth during metazoan, insect and mice infections [180]. However, desiccation stress is not likely to be a factor during the course of metazoan and insect infections.

Furthermore, the infection of mice with the trehalose and  $\alpha$ -glucan biosynthetic mutant was conducted by oropharyngeal colonisation introduced through drinking water [180]. This therefore is not likely to reflect the water stress experienced within the CF lung.

This is a particularly interesting area of research as the over-production of alginate is known to play an important role during infection of the lung in cystic fibrosis patients [29]. In addition to this, it has been found that the trehalose and  $\alpha$ -glucan biosynthesis genes are highly co-expressed with the alginate biosynthesis genes in transcriptomic data of clinically-isolated strains of *P. aeruginosa* (Susanne Haeussler, personal communication). This suggests that trehalose and  $\alpha$ -glucan may contribute to *P. aeruginosa* survival during CF lung infection. This represents an exciting branch of future research. For example, the trehalose and  $\alpha$ -glucan content in mucoid clinical strains of *P. aeruginosa* could be determined and the roles that these polysaccharides play during a cystic fibrosis lung model.

# Chapter 5: Investigating the regulation of trehalose and $\alpha$ -glucan biosynthesis

## 5.1 Introduction

### 5.1.1 Regulation

The ability to co-ordinate cellular processes is essential for successful bacterial lifestyles. *Pseudomonas* spp. exhibit substantial genomic plasticity and can modulate and optimise cellular processes in response to environmental signals. Therefore, it is not surprising that *Pseudomonas* spp. are found in virtually every environment and can survive extreme stresses [210]. This plasticity is largely attributed to extensive regulatory complexity [211]. *Pseudomonas aeruginosa* PAO1 possesses one of the largest bacterial regulatory networks, with regulatory genes making up 12% of the genome [212].

The work described so far in this thesis involved biochemically and phenotypically characterising trehalose and  $\alpha$ -glucan biosynthesis in *Pseudomonas* spp. Additional work has also begun to characterise the role of  $\alpha$ -glucan in the protection against environmental stress and its physiological relevance. To further our understanding of the physiological role of  $\alpha$ -glucan, we next sought to understand the factors that govern its synthesis. To achieve this, the regulatory network controlling trehalose and  $\alpha$ -glucan biosynthesis in *Pseudomonas* spp. were studied. In this chapter I discuss our current understanding of the regulation of trehalose and  $\alpha$ -glucan in bacteria. In chapter 4, I show a functional link between alginate and  $\alpha$ -glucan, where both polysaccharides function to protect against desiccation stress in *Pseudomonas* spp., therefore I also briefly discuss the relevant mechanisms in the regulation of alginate biosynthesis.

### 5.1.2 Regulation of trehalose

The regulation of trehalose biosynthesis in bacteria is complex and surprisingly understudied. Trehalose production is induced by a variety of environmental conditions, including low temperature [213], salt [107], ethanol [214] and during the stationary phase of bacterial growth [215]. Genes related to trehalose biosynthesis have been shown to be under the control of several sigma factors. The *otsA* and *otsB* genes have been shown to be regulated by the stress response sigma factor RpoS in *E. coli* [215]. Furthermore, deletion of *rpoS* in *P. fluorescens* Pf-5 results in osmotically-sensitive strains [216]. The alternative sigma factor RpoN has also been implicated in the regulation of trehalose biosynthesis in bacteria. Deletion of *rpoN* leads to upregulation of *otsA* and *otsB* in *E. coli* [217]. Conversely, *rpoN* mutations in *P. aeruginosa* results in the downregulation of genes involved in trehalose and  $\alpha$ -glucan biosynthesis [218]. Recently Harty *et al.* showed that

the production of trehalose in response to NaCl or ethanol was dependent on the sigma factor AlgU (RpoE) [214]. These authors also showed that the accumulation of trehalose in response to either NaCl or ethanol was also in-part dependent on the stringent response and quorum sensing.

Bacteria use the stringent response to respond to nutrient-limiting conditions, producing an alarmone called guanosine pentaphosphate (pppGpp) or tetraphosphate (ppGpp). In *E. coli* and *Pseudomonas* spp., pppGpp is produced by RelA and SpoT [102, 219]. pppGpp is then degraded into ppGpp by GppA in *E. coli* [220] and presumably by its homologue, Ppx in *Pseudomonas* spp. [181]. SpoT exhibits bifunctional activity and can degrade ppGpp into guanosine diphosphate and pyrophosphate [219, 221]. (p)ppGpp binds to RNA polymerase and facilitates the expression of genes involved with nutrient starvation [222]. Following exposure to ethanol or NaCl, the expression of the trehalose biosynthesis gene *treZ* was significantly decreased in a *P. aeruginosa* *relA* or *spoT* mutant. Furthermore, these mutants also produced less trehalose than the wild-type when exposed to either NaCl or ethanol [214].

### 5.1.3 Regulation of classical $\alpha$ -glucan biosynthesis

In contrast to trehalose biosynthesis, the regulation of classical  $\alpha$ -glucan biosynthesis has been well studied in *E. coli*. I discuss some of the mechanisms of regulation below.

Control of the production of  $\alpha$ -glucan is mainly achieved through allosteric regulation of the biosynthetic enzymes. Products of carbon metabolism have been shown to activate or inhibit these enzymes. For example, when carbon is not limiting, there are high levels of glycolysis and therefore increased amounts of fructose-1,6-bisphosphate [223]. This sugar activates the ADP-glucose pyrophosphorylase GlgC in *E. coli* leading to increased levels of ADP-glucose and therefore  $\alpha$ -glucan biosynthesis. Conversely, when carbon is limiting, the phosphosugar adenosine monophosphate accumulates [224], and this inhibits the enzymatic activity of GlgC, reducing the biosynthesis of ADP-glucose and therefore inhibiting the production of  $\alpha$ -glucan [225, 226].

The recycling enzyme glycogen phosphorylase (GlgP) is also a target of allosteric regulation by the histidine phosphocarrier protein HPr [227], a component of the phosphoenolpyruvate:carbohydrate phosphotransferase system (PTS) [228]. GlgP binds to both HPr and the phosphorylated form of HPr (P-HPr), with higher affinity for the latter. Binding of HPr induces the dimerization and tetramerization of GlgP which increases its

phosphorylase activity, whereas, binding of the P-HPr does not show a stimulatory effect. It is thought that under carbohydrate rich conditions, the phosphorylation state of the PTS components and HPr is induced, which results in high affinity binding of GlgP to P-HPr, preventing  $\alpha$ -glucan degradation. Under low energy conditions, the PTS components will be dephosphorylated and HPr will bind to GlgP and stimulate  $\alpha$ -glucan degradation [229].

Another method of regulating  $\alpha$ -glucan biosynthesis is through modulating the available pool of the precursor substrate ADP-glucose. In *E. coli* ADP-glucose is degraded by the ADP-glucose pyrophosphatase AspP, therefore the activity of AspP directly regulates the levels of  $\alpha$ -glucan production [230]. The activity of AspP is in turn activated by allosteric regulation. The sugar glucose-1,6-bisphosphate and nucleoside molecules both enhance AspP activity *in vitro* [231].

There is some evidence to suggest that  $\alpha$ -glucan biosynthesis in *E. coli* is under the control of the global regulators cyclic AMP (cAMP) and the cAMP receptor protein (CRP). cAMP- or CRP-deficient mutants of *E. coli* were shown to be impaired in their ability to produce  $\alpha$ -glucan [232]. However, as transcriptomic analysis fails to show  $\alpha$ -glucan biosynthesis genes as part of the CRP regulon [233], it is thought that CRP/cAMP regulation of  $\alpha$ -glucan biosynthesis in *E. coli* may be indirect. This could be due to the upregulation of intermediate regulatory elements such as the PTS components [234].

Like trehalose biosynthesis in *Pseudomonas* spp. the stringent response has also been implicated in the regulation of  $\alpha$ -glucan in *E. coli*. Stimulation of the stringent response through amino acid starvation resulted in the accumulation of  $\alpha$ -glucan [235]. Moreover, deletion of *relA* results in strains deficient in their ability to produce  $\alpha$ -glucan [236], whereas overexpression of the genes encoding the degradative enzymes *pggA* and *spoT* results in a reduction in  $\alpha$ -glucan production in *E. coli* K-12 [237].

In *E. coli*  $\alpha$ -glucan biosynthesis is controlled by the carbon storage regulator (Csr) system. The Csr system controls the regulation of genes involved in a range of processes, notably central carbon metabolism [238]. The Csr effector is the small RNA binding protein CsrA, which binds to mRNA transcripts and prevents translation. This is usually a form of negative regulation but examples of positive regulation by CsrA have also been reported [239]. CsrA has been shown to bind to the transcript of *glgC*, preventing expression and therefore the biosynthesis of  $\alpha$ -glucan [240].

Homologues of CsrA are found within the *Pseudomonas* genera. *P. aeruginosa* possesses two CsrA homologues, repressor of secondary metabolism A (RsmA) and RsmN [241], whereas *P. syringae* possesses 5 RsmA homologues, one of which (*PSPTO\_3566*) may be a homolog of RsmE [181, 242].

In *P. aeruginosa* and *P. syringae*, the Rsm proteins are regulated by the GacA-GacS two-component system, which I briefly summarise here (Figure 5-1). The Gac/Rsm system is responsible for the regulation of a variety of processes, including biofilm formation, motility, virulence and the stress response [243, 244]. This system is also implicated in the transition from acute to chronic infection during *P. aeruginosa* cystic fibrosis lung infection [244]. The histidine kinase GacS responds to as-yet unknown environmental signals by autophosphorylation and subsequent phosphorylation of the response regulator GacA [245]. GacA will then induce the expression of the small regulatory RNAs, RsmY and RsmZ [246]. RsmY and RsmZ bind to and sequester the Rsm regulatory proteins, preventing Rsm protein dependent regulation [247]. Similar to CsrA, the Rsm proteins will recognise and bind to the transcript of target genes and usually prevent translation [248-251], but can also have positive regulatory activity, for example, protecting RsmY and RsmZ RNA from degradation [250]. Rsm proteins promote the expression of virulence factors such as the type III secretion system and motility [252, 253], whereas activation of GacS and GacA promotes biofilm production and type VI secretion [252, 254].

In *P. aeruginosa* the Gac/Rsm system is also regulated by the accessory sensor kinase proteins, PA1611 [255], RetS, LadS [256, 257] and CmpX [255, 258]. RetS binds to GacS thereby preventing the phosphorelay to activate GacA, reducing the levels of RsmY and RsmZ and therefore promoting RsmA and RsmN regulation [245, 256]. PA1611 also regulates the Gac/Rsm system through direct interaction with RetS [255]. PA1611 binding to RetS results in the increased expression of RsmY and RsmZ and therefore prevents RsmA and RsmN dependent regulation. This interaction presumably prevents RetS from binding to GacS. LadS promotes the expression of RsmY and RsmZ by phosphorylating GacS which subsequently activates GacA [257]. CmpX regulates the levels of PA1611, whereby deletion of *cmpX* in *P. aeruginosa* results in elevated levels of PA1611 [255] and increased levels of RsmY [258]. However, the mechanism of this regulation is unknown.

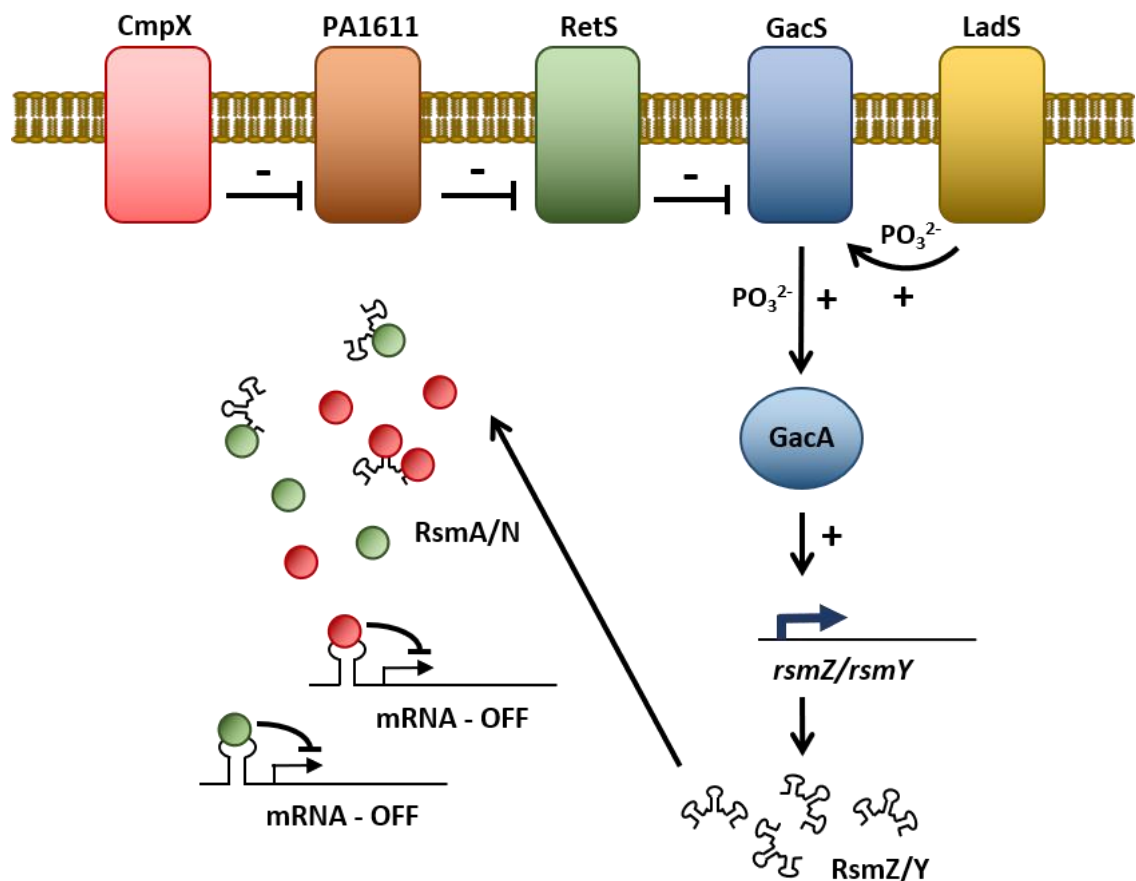


Figure 5-1: A graphical representation of the Gac/Rsm system in *P. aeruginosa*. GacS modulates the activity of GacA through phosphorylation. Subsequently, GacA activates the expression of the small non-coding RNAs RsmY and RsmZ. These RNA molecules sequester the regulation proteins RsmA and RsmN, modulating post-transcriptional regulation. GacS is regulated by the sensor kinases CmpX, PA1611, RetS and LadS. This figure is reproduced and modified with permission from Grenga *et al.* (2017) [259].

#### 5.1.3.3 Regulation of GlgE dependent $\alpha$ -glucan biosynthesis

Although the regulation of classical  $\alpha$ -glucan biosynthesis has been well studied, the regulation of GlgE-dependent  $\alpha$ -glucan biosynthesis is relatively unknown. To the best of my knowledge there is only one published report concerning the regulation of the GlgE pathway. The GlgE enzyme in *Mycobacterium* and *Streptomyces* spp. is modifiable by phosphate groups at several positions. Phosphorylation of GlgE by the PknB kinase leads to a reduction in GlgE enzymatic activity [260].

#### 5.1.4 Regulation of alginate biosynthesis

The first elucidated mechanism of alginate regulation in *Pseudomonas* spp. was through the sigma factor AlgU, driving the transcription of *algD*, the first gene of the alginate biosynthesis operon [261-263]. AlgU is regulated by the anti-sigma factor MucA and its cognate partner MucB, which sequesters AlgU to the inner membrane, preventing the activation of transcription [25]. Upon encountering environmental signals that favour the

production of alginate, MucA is proteolytically degraded, liberating AlgU and allowing the activation of alginate biosynthesis [264]. AlgU also induces the expression of other regulatory proteins including the response regulators AlgB and AlgR [265].

The two-component system AlgB and KinB plays a role in the regulation of alginate biosynthesis in *P. aeruginosa*. Mutation of the *algB* gene in mucoid strains results in a marked reduction in alginate production [266]. Furthermore, it was shown that AlgB directly regulates the expression of *algD*, as it binds specifically to the *algD* promoter *in vitro* [267]. However, AlgB activity seems to be independent of its cognate sensor kinase KinB [267] because alginate production is unaffected by *kinB* deletion in a mucoid strain of *P. aeruginosa* [268]. Conversely, other reports show that a *kinB* deletion in a PAO1 *mucA* mutant results in an increase of alginate production. Moreover, *kinB* deletion mutants yield increased MucA degradation, subsequently inducing alginate production. This suggested that KinB is an antagonist of alginate production [269].

The two-component system AlgR and FimS plays a role in regulating alginate production. Deletion of *algR* in a mucoid strain of *P. aeruginosa* results in alginate deficiency with significantly reduced levels of *algD* transcription [265]. AlgR also binds to the *algD* promoter *in vitro* therefore directly regulating alginate production [270]. Interestingly, similar to AlgB, AlgR activity is independent of phosphorylation and therefore independent of its cognate sensor kinase FimS [268].

The response regulator CbrB and the cognate signal kinase CbrA form the CbrA/CbrB two-component system. This system regulates carbon metabolism, biofilm formation and stress tolerance in *P. putida* [271, 272]. Upon activation by CbrA, CbrB induces the transcription of RpoN-dependent genes, such as the small regulatory RNA *crcZ* [273]. CbrA/CbrB mediated regulation is achieved through modulation of the Crc protein [274].

Crc is a key regulator of carbon catabolite repression, involved in the optimisation of bacterial metabolism based on the available nutrients by repressing specific carbon metabolism pathways. Crc is also involved in the modulation of virulence in *P. aeruginosa* [275, 276]. For example, Crc activity is highest when *P. putida* is cultured in rich complex medium, conversely Crc activity is low when the bacteria are cultured using a poor carbon source [277]. Crc functions as an RNA-binding protein, binding to the transcripts encoding metabolic proteins and preventing translation [278]. The small regulatory RNA *crcZ*

antagonises Crc by sequestration preventing it from binding to transcripts, thereby preventing the repressive activity of Crc.

The CbrA/CbrB system also plays a role in the production of alginate. Transposon insertion within the *cbrB* response regulator results in a reduction in alginate production in *P. fluorescens* [279]. Further analysis using chromatin immunoprecipitation sequencing, revealed the genome-wide binding sites of CbrB in *P. putida*, which includes the *algD* promoter [280].

The Gac/Rsm system is implicated in the regulation of alginate in both *Azotobacter* and *Pseudomonas spp* [281, 282]. *muca* is an RNA target of both RsmA and RsmN in *P. aeruginosa*. Additional experiments showed that deletion of both Rsm proteins results in alginate overproduction, whereas overexpression of RsmN results in reduced levels of alginate. This shows that the Rsm proteins were negative regulators of alginate production [282].

### 5.1.5 Chapter Aims

As very little is known about the regulation of trehalose or  $\alpha$ -glucan biosynthesis in *Pseudomonas spp.*, this chapter aims to identify potential regulators in both *P. aeruginosa* PAO1 and *Pto*.

To identify global regulators of trehalose and  $\alpha$ -glucan biosynthesis, I first generated reporter strains in both PAO1 and *Pto* that express the *E. coli* LacZ  $\beta$ -galactosidase protein under the control of the *glgA* promoter, the first committed gene in the trehalose and  $\alpha$ -glucan biosynthesis pathway. These reporter strains indicate the level of *glgA* regulation by producing a blue pigment when incubated with 5-bromo-4-chloro-3-indolyl  $\beta$ -D-galactopyranoside (X-Gal). I then employed random transposon mutagenesis to identify mutants exhibiting changes in LacZ activity. Changes in LacZ activity suggest that the regulation of *glgA* has been altered. The candidate regulator was then identified in each case using arbitrary PCR and Sanger sequencing.

In order to identify direct regulators of trehalose and  $\alpha$ -glucan biosynthesis, I also utilised DNA-affinity chromatography to identify DNA binding proteins specific to *glgA* regulation. A biotinylated form of the PAO1 *glgA* promoter was used as bait to isolate regulation candidates which were then identified using mass spectrometry.

## 5.2 Materials and Methods

### 5.2.1 Liquid Metabolite Extraction

*Pto ΔglgB* strains were cultured in 50 mL of M9 medium and incubated overnight at 28 °C. The resulting cells were pelleted (4,000 × g, 8 minutes) and the residual medium was discarded. Cell pellets were then resuspended in 5 mL of distilled H<sub>2</sub>O (dH<sub>2</sub>O). The sample dry weight was determined after removing water through drying under vacuum. Dry samples were then resuspended in 5 mL of dH<sub>2</sub>O and boiled at 95 °C for 1 hour. Cellular debris was removed through centrifugation (10,000 × g, 10 minutes) and the resulting supernatant was subject to additional boiling and centrifugation. The water was removed from the resulting soluble metabolite extract by drying under vacuum. The dried extract was resuspended in 1200 μL deuterium oxide (D<sub>2</sub>O).

### 5.2.2 RNA Extraction and Retrotranscription

RNA extraction was performed using the Qiagen RNeasy Mini kit, with a modified protocol. Wild-type *Pto* was cultured in 50 mL of M9 minimal medium or on mixed cellulose ester filter discs on M9 minimal agar as described earlier. RNA was protected in liquid cultures by the addition of 30 mL RNA protect (Qiagen) or the resuspension of cells from solid media in 5 mL of RNA protect. Samples were pelleted and resuspended with 200 μL of 10 mM Tris-Cl pH 8.0. RLT buffer was supplemented with β-mercaptoethanol and cooled to 4 °C, before 700 μL was then added to the lysing matrix (Starlab / Thistle Scientific Ltd). The resuspended pellet was then added to the matrix. Samples were then lysed, using two 30 second pulses with the Bio-Rad Ribolyser at a speed setting of 6.5. Samples were kept incubated at 4 °C between pulses. Samples are then centrifuged at 11,000 × g at 4 °C for three minutes. The sample supernatants were added to 450 μL of ethanol and this was added to the RNeasy spin column and centrifuged at 11,000 × G for 30 seconds at room temperature. RW1 buffer (350 μL) was then added to the column and this was centrifuged. Contaminating DNA was degraded by adding 80 μL of DNase I incubation mix directly to the column and this was incubated at room temperature for 20 minutes. RW1 (350 μL) was added to the column and this was centrifuged. RPE buffer (500 μL) was then added and centrifuged. The column was dried by a further centrifugation for 2 minutes. RNA was collected by the addition of 60 μL of RNase-free water and centrifugation for one minute.

Retrotranscription was performed using the SuperScript II Reverse Transcriptase (Invitrogen). RNA was diluted to 100 ng in a final volume of 13 μl RNase-free water. To this,

1  $\mu$ L of a 1/10 dilution of random primers (Invitrogen) and 1  $\mu$ L of 10 mM dNTPs were added. This was mixed and heated to 65 °C for 5 minutes. Samples were then incubated on ice and 4  $\mu$ L of 5X FirstStrand buffer and 2  $\mu$ L of 0.1 M dithiothreitol was added. This was mixed and incubated at 25 °C for 2 minutes. Samples were then incubated on ice and 1  $\mu$ L of Superscript II Reverse Transcriptase was added. The transcriptase was not added to the controls. RNA was then retrotranscribed through the following cycle; 25 °C for 10 minutes, 42 °C for 50 minutes and 72 °C for 15 minutes.

### 5.2.3 qPCR

qPCR was performed using the SensiFast SYBR No Rox Kit (Bioline). Forward and reverse primers were designed using <http://bioinfo.ut.ee/primer3/> (and the following parameters: fragment size 95-105, primers size min18 opt20 max22, temperature min60 opt62 max64) [283]. The two primers were mixed to a final concentration of 10  $\mu$ M each in a final volume of 100  $\mu$ L. *Pto* genomic DNA was serially diluted to give concentrations of 10, 1 and 0.1 ng/ $\mu$ L. Using a qPCR 96 well plate (4titude Ltd), each reaction contained 10  $\mu$ L SensiFast SYBR, 1  $\mu$ L of the primer mix, 8  $\mu$ L of dH<sub>2</sub>O and either 3.5  $\mu$ L of the individual cDNA or dH<sub>2</sub>O. Controls were conducted for each primer pair including serially diluted genomic controls, non-retrotranscribed controls and a water control. This was then performed and analysed using Bio Rad CFX Manager. The following protocol was used: 180 seconds at 95 °C, then, 50 cycles of 95 °C, 5 seconds, 62 °C, 10 seconds and 72 °C, 7 seconds. Melting curves were then generated starting at 65 °C increasing by 0.5 °C until a final temperature of 95 °C. Absolute quantification of mRNA was calculated and normalised relative to the housekeeping gene *rpoD* as a reference [284].

### 5.2.4 Biparental Mating

*Pto*-*P<sub>glgA</sub>-lacZ* and *E. coli* S17-1 :: pALMAR3 was cultured overnight in 50 mL of media supplemented with gentamycin and tetracycline respectively. Cultures were pelleted and washed to remove the antibiotics. This step was repeated three times, pellets were resuspended in a final volume of 1.5 mL. *Pto*-*P<sub>glgA</sub>-lacZ* and *E. coli* S17-1 :: pALMAR3 were mixed in a 7:3 ratio to a final volume of 1 mL. This mixture was then pelleted, resuspended in 50  $\mu$ L of L medium and spotted onto a cellulose ester filter discs (Merck Millipore) placed on the surface of L agar. Plates were then incubated at 28 °C for 3 hours. Cells were recovered by vortexing with 2 mL of phosphate buffered saline (PBS), *Pto*-*P<sub>glgA</sub>-lacZ* ::

pALMAR3 conjugants were selected for by plating onto L agar containing gentamycin, tetracycline and X-Gal.

### 5.2.5 Transposon Mutagenesis

Reporter strains PAO1 and *Pto P<sub>glgA</sub>-lacZ* were transformed using the mariner plasmid pALMAR3. This was either performed by electroporation (Section 2.3.1) or by biparental mating with *E. coli* S17-1 (5.2.4). Transposon insertions yielding changes in LacZ activity were selected for on solid media supplemented with tetracycline and 50 µg/mL X-Gal. Gentamycin was also used where appropriate to select against the S17-1 donor. Candidates were re-streaked and the location of the transposon was determined by arbitrary PCR [285]. The first semi-random reaction was performed using *Taq* polymerase (New England Biolabs) using Arb-PCR and Arb1b (primers 130 and 131). Primary denaturation was performed for 180 seconds at 95 °C. Following this, 30 cycles of denaturation (95 °C, 15 seconds), annealing (38 °C, 30 seconds) and extension (72 °C, 90 seconds) were performed, and a final extension was performed at 72 °C for 180 seconds.

A second reaction to amplify the first semi-random PCR product was performed using 5 µL of product as a template. Arb1 and Almar3-seq (primers 132 and 133) were used to amplify the semi-random PCR product. Primary denaturation was performed for 180 seconds at 95 °C. Following this, 30 cycles of denaturation (95 °C, 15 seconds), annealing (56 °C, 30 seconds) and extension (72 °C, 90 seconds) was performed. A final extension was performed at 72 °C for 180 seconds.

The resulting PCR product was subject to the BigDye Terminator v3.1 cycle sequencing kit (Invitrogen). PCR product (4 µL) was added to 2.5 µL of dH<sub>2</sub>O, 1.5 µL of BigDye Terminator buffer, 1 µL of Almar3-Seq and 1 µL of BigDye Terminator reaction mix. The sequencing reaction was then performed using a thermocycler. Primary denaturation was performed for 60 seconds at 96 °C. Following this, 25 cycles of denaturation (96 °C, 10 seconds), annealing (50 °C, 5 seconds) and extension (60 °C, 240 seconds) were performed. The sequence sample was then sent to Eurofins genomics using their 'Ready2Load' service. Candidate genes were identified and annotated using the Pseudomonas Genome Project database [181].

### 5.2.6 DNA-Affinity Chromatography

This method has been adapted from Jutras *et al.* (2012) [286]. The promoter region of PAO1 *glgA* was amplified using a Q5 polymerase-based reaction with primers 128 and 129

yielding a 497 bp 5'-biotinylated fragment. A 500 bp 5'-biotinylated region of non-promoter DNA was also amplified as a control.

PAO1 cultures were grown overnight in 50 mL of M9 minimal medium  $\pm$  0.85 M NaCl. Cultures were washed three times with either water or 0.85 M NaCl, respectively, and freeze-thawed using liquid nitrogen. The pellets were resuspended in 1 mL of BS/THES buffer. BS/THES buffer was made by combining BS buffer (10 mM HEPES, 5 mM CaCl<sub>2</sub>, 50 mM KCl, 12% Glycerol), THES buffer (50 mM TRIS-Cl pH 7.5, 10 mM EDTA, 20% Sucrose (w/v), 140 mM NaCl, 0.7% Protease Inhibitor Cocktail company) and water in a 4.43: 2: 3.57 ratio.

The resuspended pellets were then sonicated at 40% amplitude for 10 seconds and kept at 4 °C. This was repeated five times with one-minute intervals. Samples were then centrifuged at 11,000  $\times$  g for 20 minutes at 4 °C. Dynabeads® (Thermo Fisher Scientific) were prepared by adding 200  $\mu$ L of Dynabeads® solution to a microtube for each sample. These were separated from solution using a 12-tube magnet (Qiagen). The beads were then washed with 500  $\mu$ L of B/W buffer (10 mM TRIS-Cl pH 7.5, 1 mM EDTA, 2 M NaCl). This step was repeated three times with a final resuspension of 190  $\mu$ L. Approximately 40  $\mu$ g of biotinylated probe (200  $\mu$ L of  $\sim$ 200 ng/ $\mu$ L) was added to the Dynabeads® suspension and incubated with end-over-end agitation at room temperature for 20 minutes. Following incubation, the probe-bead complex was washed with TE buffer three times (10 mM TRIS-Cl pH 8.0, 1 mM EDTA pH 8.0). The probe-bead solution was then washed twice with BS/THES buffer and once with BS/THES buffer supplemented with 10  $\mu$ g/mL of poly(deoxyinosinic-deoxycytidylic) acid (Thermo Fisher Scientific). To the probe-bead complex 200  $\mu$ L of BS/THES and 600  $\mu$ L of cell lysate were added. This was then incubated with end-over-end agitation at room temperature for 30 minutes. Bead-probe-protein complexes were then washed with BS/THES five times. To the bead-probe-protein complex, 120  $\mu$ L of NaCl elution buffer (25 mM TRIS-Cl, 1 M NaCl, pH 7.5) was added, the resulting supernatant was then concentrated and desalted using a ZipTip with 0.6  $\mu$ L resin (Merck). The desalted eluate was then resolved on a 10% acrylamide resolving gel, excised and this was subjected to mass spectrometry (Orbitrap) analysis to detect bound proteins. Gel slices were prepared according to standard procedures adapted from Shevchenko et al. [287]. Briefly, the slices were de-stained with ethanol, washed with 50 mM TEAB buffer pH 8.0 (Sigma), incubated with 10 mM DTT for 30 min at 65 °C followed by incubation with 30 mM iodoacetamide (IAA) at room temperature (both in 50 mM TEAB). After washing

and dehydration with acetonitrile, the gels were soaked with 50 mM TEAB containing 10 ng/μl Sequencing Grade Trypsin (Promega) and incubated at 50 °C for 8 h. Peptides were extracted, and aliquots were analysed by nanoLC-MS/MS on an Orbitrap Fusion™ Tribrid™ Mass Spectrometer coupled to an UltiMate® 3000 RSLCnano LC system (Thermo Scientific, Hemel Hempstead, UK). The samples were loaded and trapped using a pre-column which was then switched in-line to the analytical column for separation. Peptides were separated on a nanoEase M/Z column (HSS C18 T3, 100 Å, 1.8 μm; Waters, Wilmslow, UK) using a gradient of acetonitrile at a flow rate of 0.25 μl min<sup>-1</sup> with the following steps of solvents A (water, 0.1% formic acid) and B (80% acetonitrile, 0.1% formic acid): 0-4 min 3% B (trap only); 4-15 min increase B to 13%; 15-77 min increase B to 38%; 77-92 min increase B to 55%; followed by a ramp to 99% B and re-equilibration to 3% B.

Data dependent analysis was performed using parallel CID and HCD fragmentation with the following parameters: positive ion mode, orbitrap MS resolution = 120k, mass range (quadrupole) = 300-1800 m/z, MS2 top20 in ion trap, threshold 1.9e4, isolation window 1.6 Da, charge states 2-5, AGC target 1.9e4, max inject time 35 ms, dynamic exclusion 1 count, 15 s exclusion, exclusion mass window ±5 ppm. MS scans were saved in profile mode while MS2 scans were saved in centroid mode.

Recalibrated peaklists were generated with MaxQuant 1.6.3.4 [288] using the *Pseudomonas aeruginosa* protein sequence database downloaded from Uniprot (uniprot.org; 20161212; 5,563 sequences). The final database search was performed with the merged HCD and CID peaklists from MaxQuant using in-house Mascot Server 2.4.1 (Matrixscience, London, UK). The search was performed on the *P. aeruginosa* protein sequence database and the MaxQuant contaminants database. For the search a precursor tolerance of 6 ppm and a fragment tolerance of 0.6 Da was used. The enzyme was set to trypsin/P with a maximum of 2 allowed missed cleavages. Oxidation (M) and deamidation (N/Q) were set as standard variable modifications and carbamido-methylation (CAM) of cysteine as fixed modification. The Mascot search results were imported into Scaffold 4.4.1.1 ([www.proteomsoftware.com](http://www.proteomsoftware.com)) using identification probabilities of 99% for proteins and 95% for peptides. DNA-affinity chromatography was performed in collaboration with Richard Little. Peptide digestion, mass spectrometry and peptide analysis were performed by Gerhard Saalbach and Carlo de-Oliveira-Martins.

## 5.3 Results

### 5.3.1 Regulation of trehalose and $\alpha$ -glucan biosynthesis occur at the level of transcription in *Pto*

Since I have shown that  $\alpha$ -glucan plays a role in the protection against desiccation in *Pseudomonas* spp. (Chapter 4), I hypothesised that this molecule was most likely to be important during epiphytic growth or surface survival. To investigate this, I examined the effect of different growth conditions on the biosynthesis of trehalose and  $\alpha$ -glucan in *Pto*.

First, the effect of growth in liquid medium on the soluble metabolome of the *Pto*  $\Delta$ *glgB* strain was examined.  $^1\text{H-NMR}$  spectroscopy showed that when *Pto*  $\Delta$ *glgB* was cultured in liquid media there were no detectable peaks for trehalose, M1P or  $\alpha$ -glucan (Figure 5-2). This was also reflected using iodine staining. When Lugol's solution was added to metabolome extracts from *Pto*  $\Delta$ *glgB* grown on solid media, there was purple staining indicating the presence of linear  $\alpha$ -glucan (Figure 5-3). There was no staining of the metabolome from *Pto*  $\Delta$ *glgB* when cultured using liquid media. This suggested that biosynthesis of trehalose and  $\alpha$ -glucan was regulated, and that the system was either activated on solid medium or repressed in liquid medium.

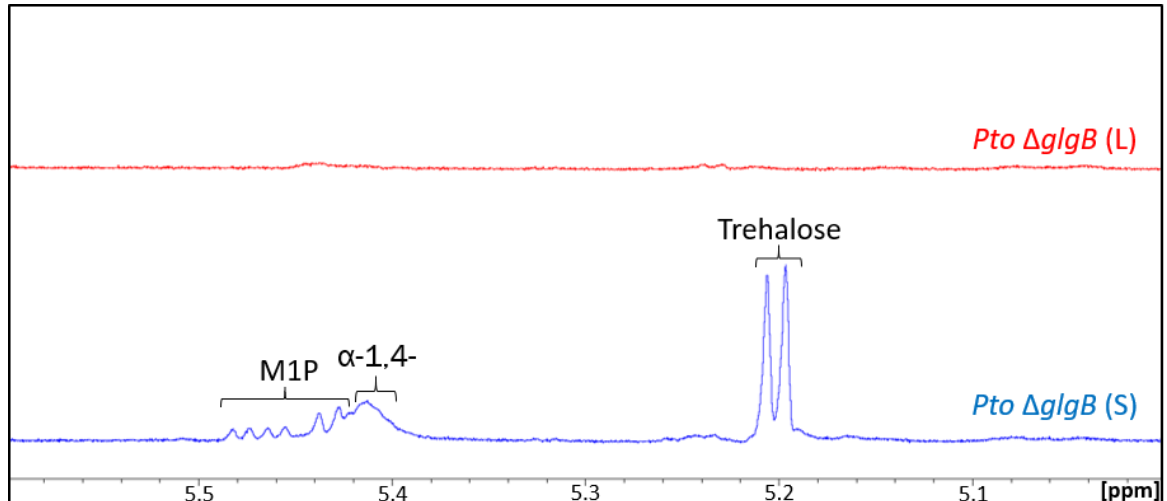


Figure 5-2:  $^1\text{H-NMR}$  spectroscopy shows the effects of growth in liquid culture upon the soluble metabolome of the *Pto*  $\Delta$ *glgB* strain. This illustrates the presence and abundance of trehalose, maltose 1-phosphate (M1P) and  $\alpha$ -glucan when the metabolomes are extracted from cells cultured on solid media (S) or liquid media (L). Peak assignments are as indicated. ( $\alpha$ -1,4-;  $\alpha$ -glucan internal linkages).

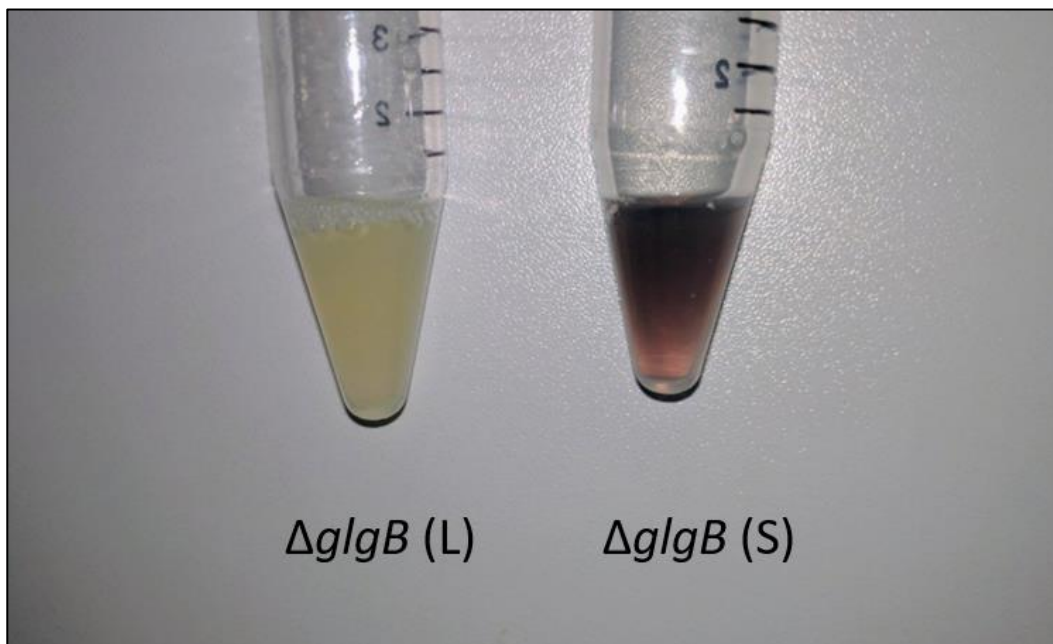


Figure 5-3: The addition of Lugol's solution to metabolome extracts from *Pto*  $\Delta$ *glgB* cultured in liquid (L) or on solid medium (S).

Quantitative PCR (qPCR) was used to investigate the level of regulation controlling trehalose and  $\alpha$ -glucan biosynthesis. If regulation was at the level of transcription, I would expect to see differential levels of mRNA transcripts from trehalose and  $\alpha$ -glucan biosynthesis genes for *Pto* grown on solid or liquid media.

Total RNA was isolated from *Pto* cultured either on solid or in liquid M9 minimal medium. RNA was reverse transcribed into cDNA and this was subject to qPCR using primers specific for the *glgA* gene. The absolute quantification of mRNA was normalised using the housekeeping gene *rpoD* and compared to two other housekeeping genes, *secA* and *gyrA*, as additional controls [284]. The levels of mRNA corresponding to *rpoD*, *secA* and *gyrA* did not change significantly when isolated from wild-type *Pto* cultured on either media (Figure 5-4). However, the levels of *glgA* mRNA significantly decreased ( $p \leq 0.0001$ ) when isolated from *Pto* grown in liquid compared to that of solid M9 minimal media. This suggests that this solid/liquid regulation of trehalose and  $\alpha$ -glucan biosynthesis occurs at the level of transcription.

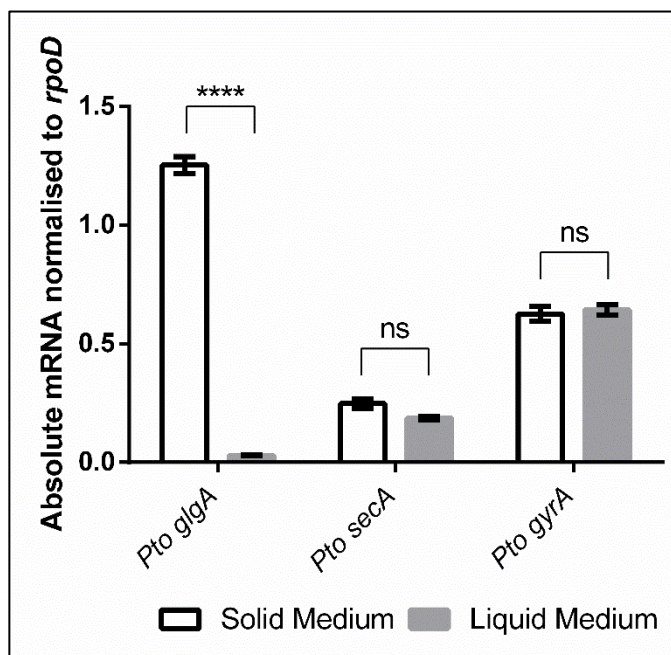


Figure 5-4: Quantitative PCR data showing the absolute quantification of transcripts from *Pto* cultured using solid or liquid M9 minimal medium relative to the housekeeping gene *rpoD*. Statistical significance was derived from a student's t-test. ns indicates non-significant and \*\*\*\* indicates  $p \leq 0.0001$ .

### 5.3.2 Generation of $P_{glgA}$ -*lacZ* transcriptional fusion vectors

To investigate the transcriptional regulation of trehalose and  $\alpha$ -glucan biosynthesis I opted to use a promoter-fusion assay. As a representative of trehalose and  $\alpha$ -glucan biosynthesis I elected to study the regulation of the first committed enzymatic step in this biosynthesis: GlgA. The promoter of *glgA* is also predicted to control the expression of the remaining genes in the *treY/treZ* operon, with *glgA* being the first gene in this operon [181].

$P_{glgA}$  was amplified from PAO1 and *Pto* genomic DNA and were individually incorporated into the multiple cloning site of pUC18-mini-Tn7T-Gm-*lacZ10* [191], forming pUC18-mini-Tn7T-Gm-PAO1- $P_{glgA}$ -*lacZ* and pUC18-mini-Tn7T-Gm-*Pto*- $P_{glgA}$ -*lacZ*. The respective construct was transformed into the appropriate wild-type strain and integrated into the *attTn7* genomic site as described in 2.3.3. To ensure the effective expression of *lacZ* by  $P_{glgA}$ , the resulting reporter strains PAO1  $P_{glgA}$ -*lacZ* and *Pto*  $P_{glgA}$ -*lacZ* were cultured in the presence of X-Gal. This resulted in the formation of blue colonies, indicative of successful control of LacZ by the *glgA* promoter (Figure 5-5).

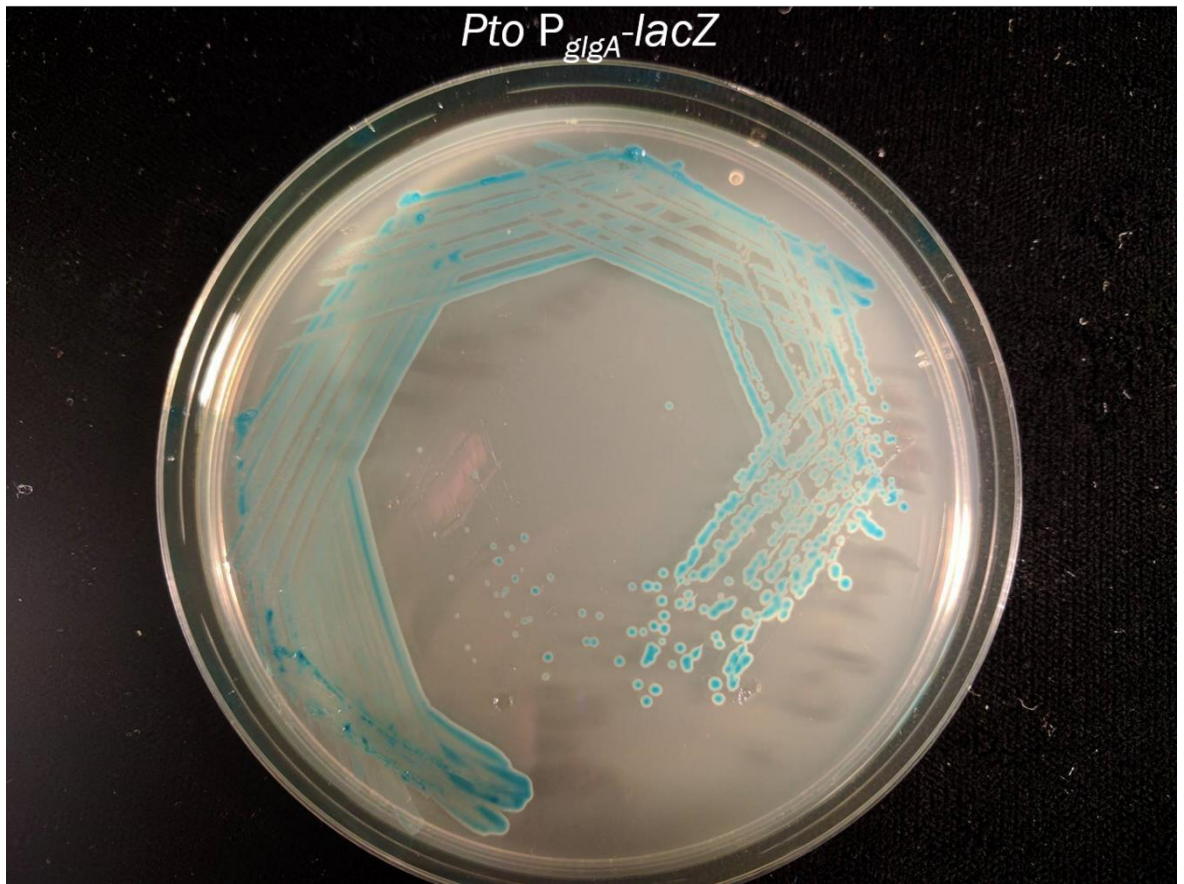


Figure 5-5: The reporter strain *Pto P<sub>glgA</sub>-lacZ* cultured on L medium supplemented with 50 µg/mL X-Gal. The blue colony pigment results from *lacZ* expression under the control of *P<sub>glgA</sub>*.

### 5.3.3 Transposon mutagenesis

Two parallel transposon mutagenesis screens were conducted to identify potential regulators of trehalose and  $\alpha$ -glucan biosynthesis. The transposon pALMAR3 was used to generate random mutant libraries, which were screened to identify colonies with altered LacZ activity based on colony appearance. The reporter strain PAO1 *P<sub>glgA</sub>-lacZ* was transformed with pALMAR3 *via* electroporation whilst the plasmid was introduced into *Pto P<sub>glgA</sub>-lacZ* *via* electroporation or conjugation using *E. coli* S17-1 as a donor. Colonies which yielded differential levels of blue pigment were selected and the location of the transposon was identified using arbitrary PCR and sequencing in each case. Lighter blue colonies resulted from a decrease in LacZ activity and therefore possess transposons inserted within genes predicted to encode activators of trehalose and  $\alpha$ -glucan biosynthesis. Conversely, darker blue colonies resulted from an increase in LacZ activity and therefore would possess transposons inserted within genes predicted to encode repressors. The transposon mutagenesis screen in PAO1 was partially conducted by Despoina Sifouna. Under my supervision, she transformed the PAO1 *P<sub>glgA</sub>-lacZ* reporter strain with pALMAR3, performed

the arbitrary PCR, BigDye® sequencing reaction, and mapped the targets of transposon insertions to the appropriate strain genome.

#### 5.3.4 Identification of potential regulators of trehalose and $\alpha$ -glucan biosynthesis in *Pto*

The transposon screen of *Pto*  $P_{glgA}$ -*lacZ* consisted of over 20,000 colonies from 18 separate transformation/conjugation events resulting in the sequencing of 46 transposon mutants. As expected, there were several mutants with transposons found within the  $P_{glgA}$ -*lacZ* cassette resulting in dark blue or white colonies, driving or abolishing LacZ expression. There were six candidates which harboured transposon insertions within genes predicted to be involved in regulation or which were implicated in stress tolerance [181]. These candidate genes are summarised in Table 5-1.

Although unlikely to regulate GlgA directly, transposon insertions in metabolic or transport genes involved with stress tolerance resulted in reduced LacZ expression (light blue colony phenotypes) suggesting that trehalose and  $\alpha$ -glucan biosynthesis were down-regulated. For example, transposon insertions within the TauC taurine ABC transporter, ArgJ, the predicted glutamate N-acetyltransferase/amino acid acetyltransferase and SyrB syringafactin synthetase resulted in less LacZ activity and therefore down-regulation of *glgA*.

Table 5-1: Transposon candidates for potential regulators of trehalose and  $\alpha$ -glucan biosynthesis in *Pto*.

Gene Hit	Gene Product	Colony Phenotype
<b><i>PSPTO_0966</i></b>	CbrB	Light Blue
<b><i>PSPTO_4796</i></b>	LadS	Light Blue
<b><i>PSPTO_1866</i></b>	TetR family transcriptional regulator	Light Blue
<b><i>PSPTO_5321</i></b>	TauC Taurine ABC Transporter	Light Blue
<b><i>PSPTO_2830</i></b>	SyrB Syringafactin Synthetase	Light Blue
<b><i>PSPTO_4399</i></b>	ArgJ glutamate N-acetyltransferase/amino acid acetyltransferase	White Colony

Three of the six gene candidates were predicted to be involved with bacterial regulation [181]. This included the response regulation CbrB, the histidine kinase LadS and a predicted TetR family transcriptional regulator. Unexpectedly, most target candidates were only hit once. To ensure these gene candidates were *bona fide* regulators of trehalose and  $\alpha$ -glucan

biosynthesis, the effects of each transposon insertion on the soluble metabolome were investigated.

The first mutant candidate harboured a transposon insertion within the gene encoding CbrB (*PSPTO\_0966*). This yielded a light blue colony phenotype when incubated with X-Gal suggesting decreased activity of LacZ. This therefore would suggest that CbrB is an activator of GlgA expression in *Pto* so disruption of the *cbrB* gene would result in reduced levels of trehalose and  $\alpha$ -glucan. To further validate this, the soluble metabolome of *tn::cbrB* was extracted and analysed using  $^1\text{H-NMR}$  spectroscopy as described in 2.4-2.5. The levels of trehalose and maltose 1-phosphate (M1P) were compared to that of the *Pto P<sub>glgA-lacZ</sub>* reporter strain.

The soluble metabolome of *Pto P<sub>glgA-lacZ</sub>* showed no significant difference, as determined by a student's t-test, in the levels of trehalose and M1P when compared to the wild-type *Pto* strain. The metabolome of *tn::cbrB* yielded a decrease in the levels of both trehalose and M1P (Table 5-2, Figure 5-6). Although this indicates that CbrB is a regulator of *glgA* and hence trehalose and  $\alpha$ -glucan biosynthesis in *Pto*, no statistical significance could be derived from this as there was only one biological repeat.

Table 5-2: Concentrations of trehalose and M1P produced by *Pto P<sub>glgA-lacZ</sub>* transposon mutants. Metabolites are presented as percentages of cellular dry weight  $\pm$  standard error ( $n \geq 2$ ). <sup>a</sup> indicates  $n = 1$ , <sup>b</sup> indicates  $p = 0.06$ , \* indicates significant differences ( $p \leq 0.05$ ) as compared to the parental strain as determined by a student's t-test.

Strain	Trehalose (%)	M1P (%)
<b><i>Pto P<sub>glgA-lacZ</sub></i></b>	1.68 $\pm$ 0.19	0.20 $\pm$ 0.03
<b><i>tn::cbrB</i></b> <sup>a</sup>	0.41	0.11
<b><i>tn::ladS</i></b>	0.31 $\pm$ 0.07 *	0.05 $\pm$ 0.02 *
<b><i>tn::PSPTO_1866</i></b>	0.82 $\pm$ 0.21 <sup>b</sup>	0.26 $\pm$ 0.04

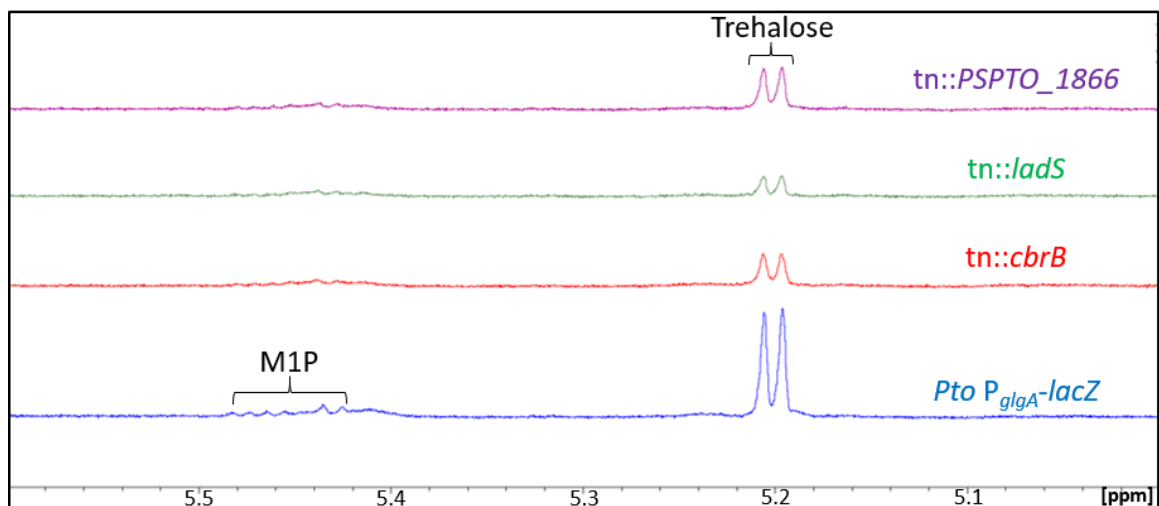


Figure 5-6:  $^1\text{H}$ -NMR spectroscopy of the soluble metabolome following transposon insertion within *Pto P<sub>glgA</sub>-lacZ*. Metabolomes were extracted from *Pto P<sub>glgA</sub>-lacZ* (blue), *tn::cbrB* (red), *tn::ladS* (green) and *tn::PSPTO\_1866* (purple) cultured on M9 minimal medium. Peak assignments are as indicated based on previously established spectra. (M1P; maltose 1-phosphate). Resonances corresponding to trehalose and M1P appeared to decrease in the metabolomes of *tn::cbrB* and *tn::ladS* as compared to the parental *Pto P<sub>glgA</sub>-lacZ*.

The second regulation mutant candidate harboured a transposon insertion within the gene encoding *LadS* (*PSPTO\_4796*). This gene target was identified twice during the transposon screen. However, this arose from the same transformation event and could be a result of clonal replication. Nevertheless, transposon insertion within this gene resulted in a light blue colony phenotype indicating decreased *LacZ* activity, the down-regulation of *glgA* and therefore reduced trehalose and  $\alpha$ -glucan biosynthesis in *Pto*. Analysis of the soluble metabolome from *tn::ladS* revealed significant decreases in both the levels of trehalose and M1P when compared to the wild-type reporter strain (Table 5-2, Figure 5-6) indicating that *LadS* is an activator of trehalose and  $\alpha$ -glucan biosynthesis.

The third regulation mutant candidate harboured a transposon insertion within the gene encoding a hypothetical TetR family transcriptional regulator (*PSPTO\_1866*). Transposon insertion within this gene resulted in a light blue colony phenotype (Table 5-2) indicating decreased *LacZ* activity therefore *PSPTO\_1866* plays a role in the activation of trehalose and  $\alpha$ -glucan biosynthesis in *Pto*. Analysis of the soluble metabolome reveals no difference in the levels of M1P when compared to *Pto P<sub>glgA</sub>-lacZ*. Levels of trehalose may have decreased, but this was not statistically significant ( $p = 0.06$ ) (Table 5-2, Figure 5-6), therefore, this candidate was not investigated further.

### 5.3.5 Identification of potential regulators of trehalose and $\alpha$ -glucan biosynthesis in *Pseudomonas aeruginosa* PAO1.

Potential regulators of trehalose and  $\alpha$ -glucan biosynthesis in PAO1 were identified through a second transposon mutagenesis screen. We transformed the reporter strain PAO1  $P_{glgA}$ -*lacZ* with the pALMAR3 mariner plasmid and screened for changes in LacZ activity, and thus changes in the regulation of GlgA. We screened approximately 10,000 mutant colonies, 52 of which yielded differences in colony colour phenotype. The location of the transposon was determined from 11 mutant strains, resulting in the identification of six potential regulators. This screen was performed in part by Despoina Sifouna under my supervision. Gene candidates of interest are summarised in Table 5-3. Transposon insertions within *cmpX*, *algB* and *fimS* were studied further. Due to time constraints transposon insertions within *p30/crcZ*, *PA1429* and *PA2696* were not investigated further.

Table 5-3: Transposon candidates for potential regulators of trehalose and  $\alpha$ -glucan biosynthesis in PAO1.

Gene Hit	Gene Product	Colony Phenotype
<b>PA1775</b>	CmpX	Dark Blue
<b>PA5483</b>	AlgB	Dark Blue
<b>PA4726.11/2</b>	P30/CrcZ	Light Blue
<b>PA5262</b>	FimS	Light Blue
<b>PA1429</b>	Probable cation-transporting P-type ATPase	Dark Blue
<b>PA2696</b>	Probable transcriptional Regulator	Light Blue

### 5.3.6 Deletion of *cmpX* resulted in increased trehalose production but sensitivity to osmotic stress.

The first mutant candidate harboured a transposon insertion within the gene encoding CmpX (*PA1775*). This gene target was only hit once during this screen. *tn::cmpX* yielded a dark blue colony phenotype when incubated with X-Gal suggesting increased activity of LacZ. This therefore would suggest that CmpX is a repressor of GlgA expression in PAO1 so transposon insertion within the *cmpX* gene would result in increased levels of trehalose and  $\alpha$ -glucan. To further validate this, the soluble metabolome of *tn::cmpX* was extracted and analysed using  $^1\text{H-NMR}$  spectroscopy. The levels of trehalose and maltose 1-phosphate (M1P) were compared to that of the PAO1  $P_{glgA}$ -LacZ reporter strain. The levels of trehalose were significantly increased whereas the concentration of M1P did not differ from the parental reporter strain (Table 5-4, Figure 5-7). Consistent with an increase in LacZ activity,

these results suggest that CmpX is a repressor of GlgA and therefore trehalose and  $\alpha$ -glucan biosynthesis in PAO1.

Table 5-4: Concentrations of trehalose and M1P produced by PAO1  $P_{glgA}$ -*lacZ* transposon mutants. Metabolites are presented as percentages of cellular dry weight  $\pm$  standard error ( $n \geq 2$ ). \* indicates significant differences ( $p \leq 0.05$ ) as compared to the parental strain as determined by a student's t-test.

Strain	Trehalose (%)	M1P (%)
<b>PAO1 <math>P_{glgA}</math>-<i>lacZ</i></b>	0.21 $\pm$ 0.03	0.12 $\pm$ 0.05
<b>tn::<i>cmpX</i></b>	0.36 $\pm$ 0.01 *	0.23 $\pm$ 0.03
<b>tn::<i>algB</i></b>	0.57 $\pm$ 0.00 *	0.25 $\pm$ 0.08
<b>tn::<i>fimS</i></b>	0.08 $\pm$ 0.02 *	0.07 $\pm$ 0.04

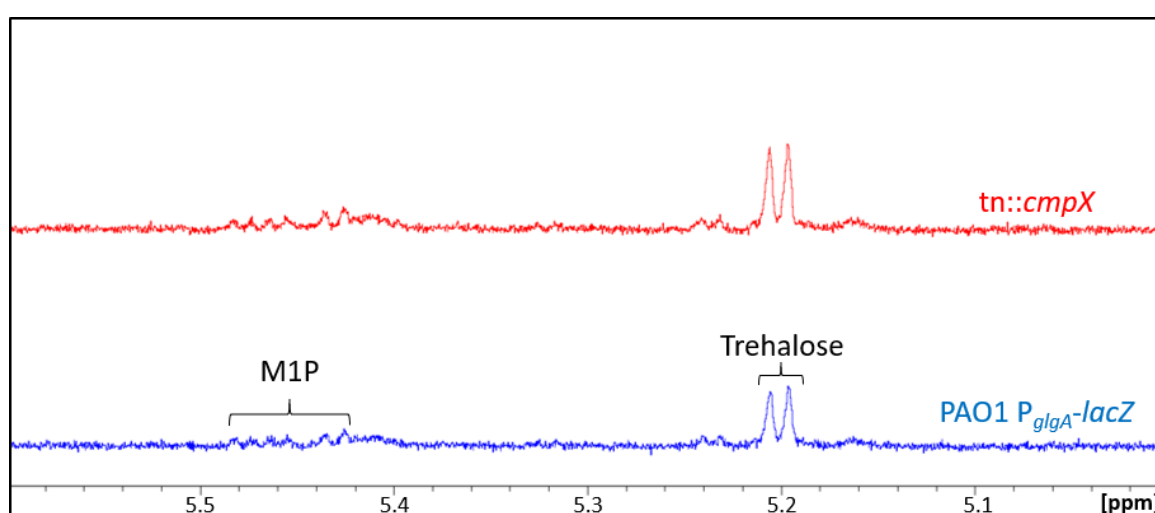


Figure 5-7:  $^1\text{H}$ -NMR spectroscopy of the soluble metabolome following transposon insertion within *cmpX* in the PAO1  $P_{glgA}$ -*lacZ* strain. Metabolomes were extracted from PAO1  $P_{glgA}$ -*lacZ* (blue) and tn::*cmpX* (red) cultured on M9 minimal medium. Peak assignments are as indicated based on previously established spectra. (M1P; maltose 1-phosphate). Resonances corresponding to trehalose increased within the metabolome of tn::*cmpX* as compared to the parental PAO1  $P_{glgA}$ -*lacZ*.

Since the transposon insertion within *cmpX* resulted in increased levels of intracellular trehalose, it would follow that tn::*cmpX* might exhibit increased tolerance to osmotic stress. To test this, tn::*cmpX* was cultured with and without osmotic stress as described previously (Section 2.7) and its growth characteristics were compared to that of the wild-type reporter strain PAO1  $P_{glgA}$ -*lacZ*. Under non-stressed conditions PAO1  $P_{glgA}$ -*lacZ* and tn::*cmpX* exhibited similar growth profiles. Following the addition of NaCl, PAO1  $P_{glgA}$ -*lacZ* exhibited a delayed growth phenotype, whereas tn::*cmpX* did not proliferate within the time-scale of the experiment despite increased trehalose production (Figure 5-8).

Owing to the nature of transposon mutagenesis, the decrease in viability of tn::*cmpX* during osmotic stress could be due to unknown polar effects. To account for this, a non-polar

deletion of *cmpX* was generated as described previously (Section 2.2.1). When grown under osmotic conditions,  $\Delta cmpX$  behaved similarly to the phenotypes exhibited by *tn::cmpX* (Figure 5-8). This suggests that the osmotic sensitivity is not due to polar effects and is a result of *cmpX* disruption. The observation of osmotic sensitivity in both *tn::cmpX* and  $\Delta cmpX$  strains indicates that the increase in trehalose levels could be an indirect consequence of *cmpX* disruption and that further investigation is required to validate CmpX as a regulator of trehalose and  $\alpha$ -glucan biosynthesis.

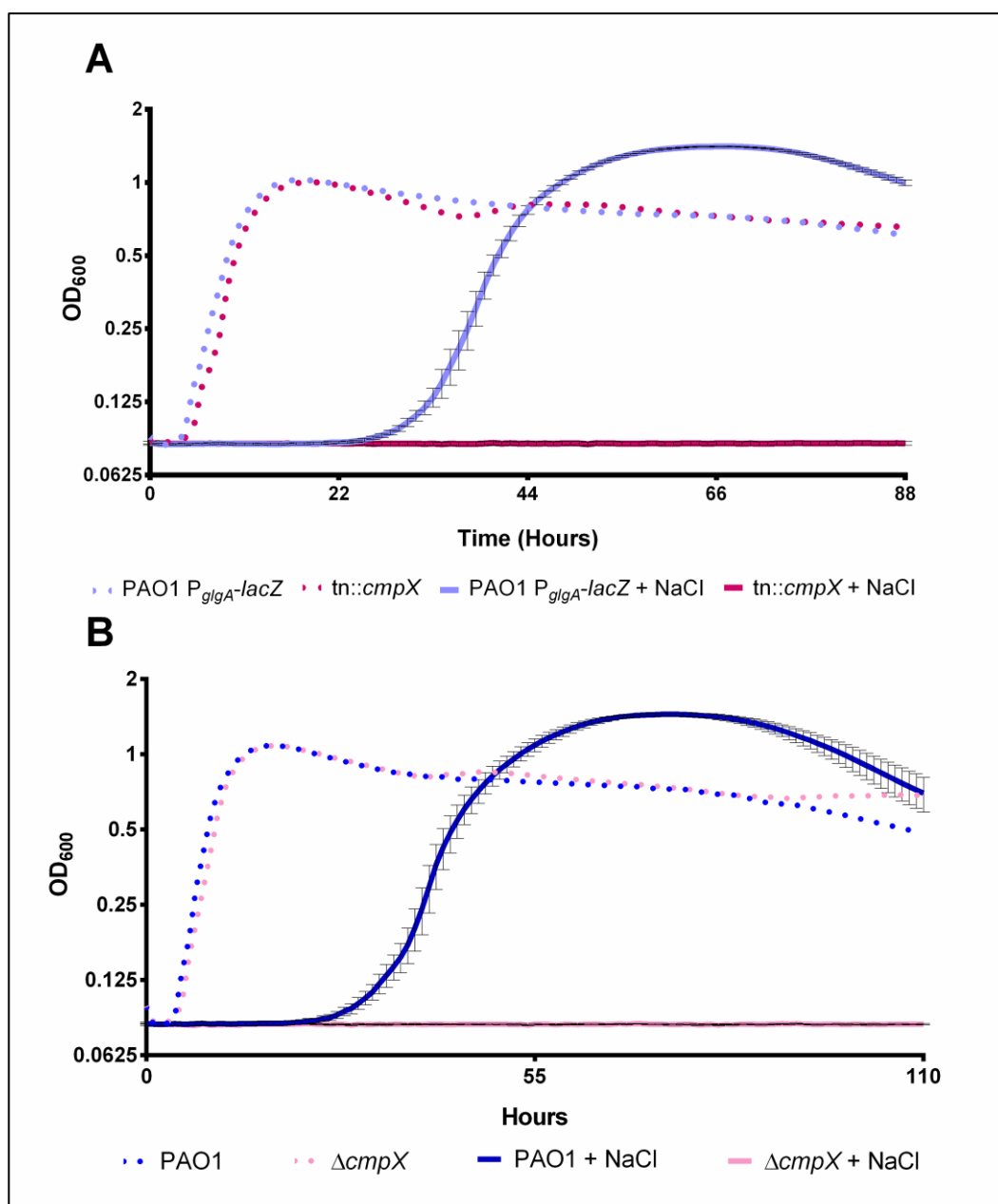


Figure 5-8: Growth of PAO1 and *cmpX* mutant strains in M9 minimal medium with and without addition of 0.85 M NaCl. (A) PAO1 P<sub>glgA</sub>-lacZ and *tn::cmpX*, (B) PAO1 and  $\Delta cmpX$ . Values represent the mean OD<sub>600</sub> of five replicates. Results are representative of two independent experiments. Error not shown for growth under non-stressed conditions. Both *tn::cmpX* and  $\Delta cmpX$  exhibited attenuated growth under osmotic conditions when compared to the parental strain.

### 5.3.7 Disruption of *algB* indicates a role as a repressor of trehalose and $\alpha$ -glucan biosynthesis in PAO1.

The second mutant candidate harboured a transposon insertion within the gene encoding AlgB (PA5483). This gene target was hit twice arising from two independent transformation events. *tn::algB* yielded a dark blue colony phenotype when incubated with X-Gal indicating increased LacZ activity and suggesting that trehalose and  $\alpha$ -glucan biosynthesis were increased. Because of this, I would predict that AlgB is a repressor of GlgA expression in PAO1 and that transposon insertion within *algB* would result in increased levels of trehalose and  $\alpha$ -glucan.

The soluble metabolome of *tn::algB* yielded a significant increase in the intracellular levels of trehalose when compared to the wild-type reporter strain ( $p \leq 0.01$ , Table 5-4, Figure 5-9). Although levels of M1P did not significantly differ, the peak corresponding to  $\alpha$ -1,4-glucan appears to increase in *tn::algB*.

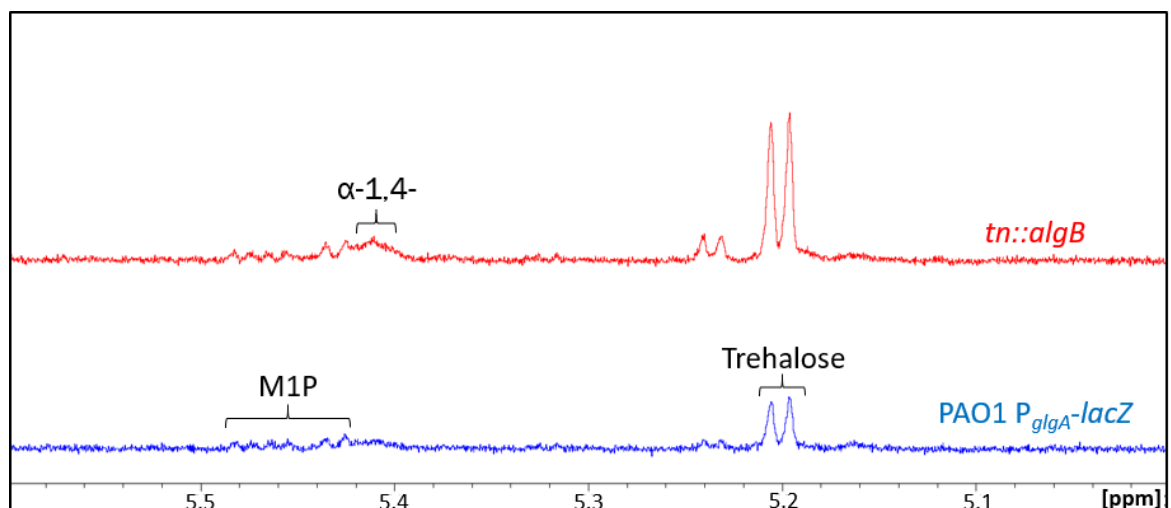


Figure 5-9:  $^1\text{H}$ -NMR spectroscopy of the soluble metabolome following insertion within *algB* of the PAO1  $P_{glgA}$ -*lacZ* strain. Metabolomes were extracted from PAO1  $P_{glgA}$ -*lacZ* (blue) and *tn::algB* (red) cultured on M9 minimal medium. Peak assignments are as indicated based on previously established spectra. (M1P; maltose 1-phosphate). Resonances corresponding to trehalose increased within the metabolome of *tn::algB* as compared to the parental PAO1  $P_{glgA}$ -*lacZ*.

Since transposon insertion within *algB* resulted in the increase of trehalose and  $\alpha$ -glucan production, it would follow that *tn::algB* would be enhanced in its ability to tolerate osmotic stress as compared to the wild-type reporter strain. Under non-stressed conditions PAO1  $P_{glgA}$ -*lacZ* and *tn::algB* exhibited similar growth profiles. When cultured in the presence of NaCl, *tn::algB* possessed a shorter lag phase than that of the PAO1  $P_{glgA}$ -*lacZ* strain, suggesting increased tolerance to osmotic stress (Figure 5-10). Taken together,

increased LacZ activity, intracellular trehalose concentration and osmotic tolerance suggests that AlgB is a repressor of trehalose and  $\alpha$ -glucan biosynthesis in PAO1.

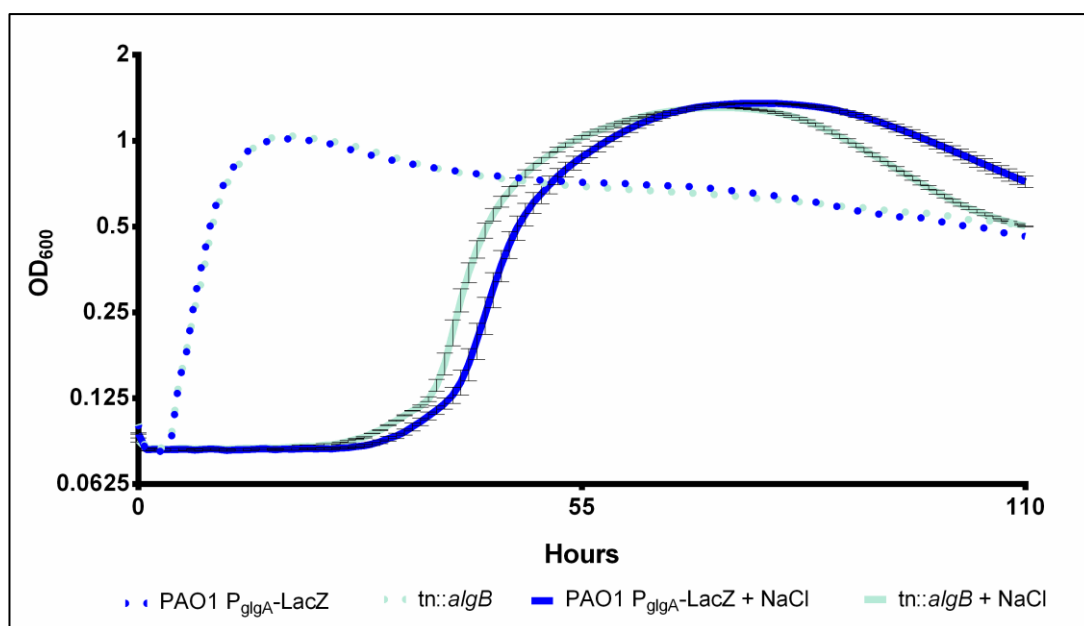


Figure 5-10: Growth of PAO1  $P_{glgA}$ -*lacZ* and  $tn::algB$  in M9 minimal medium with and without addition of 0.85 M NaCl. Values represent the mean OD<sub>600</sub> of five replicates. Results are representative of two independent experiments. Error not shown for growth under non-stressed conditions.  $tn::algB$  exhibited enhanced tolerance to osmotic conditions as compared to the parental PAO1  $P_{glgA}$ -*lacZ* strain.

5.3.8 Disruption of *fimS* implicates the AlgR/FimS two-component system as an activator of trehalose and  $\alpha$ -glucan biosynthesis in PAO1.

The third mutant candidate harboured a transposon insertion within the gene encoding FimS (PA5483). This gene target was only hit once during this mutagenesis screen.  $tn::fimS$  yielded a light blue colony phenotype when incubated with X-Gal indicating decreased LacZ activity and therefore a decrease in trehalose and  $\alpha$ -glucan biosynthesis. Therefore, I would predict that FimS plays a role in activating the expression of *glgA* in PAO1 and that disruption of *fimS* would result in decreased levels of trehalose and  $\alpha$ -glucan.

Consistent with LacZ activity, <sup>1</sup>H-NMR spectroscopy revealed that the soluble metabolome of  $tn::fimS$  yielded significantly less trehalose than that of the wild-type reporter strain PAO1  $P_{glgA}$ -*lacZ* (Table 5-4, Figure 5-11). Concordantly, when cultured under osmotic stress,  $tn::fimS$  exhibited increased sensitivity (Figure 5-12). There was no difference in growth between  $tn::fimS$  and PAO1  $P_{glgA}$ -*lacZ* when grown under non-stressed conditions.

Taken together, these results show that FimS disruption results in a decrease in *glgA* expression, trehalose accumulation and osmotic tolerance in PAO1. This indicates a role of FimS in the activation of trehalose and  $\alpha$ -glucan biosynthesis.

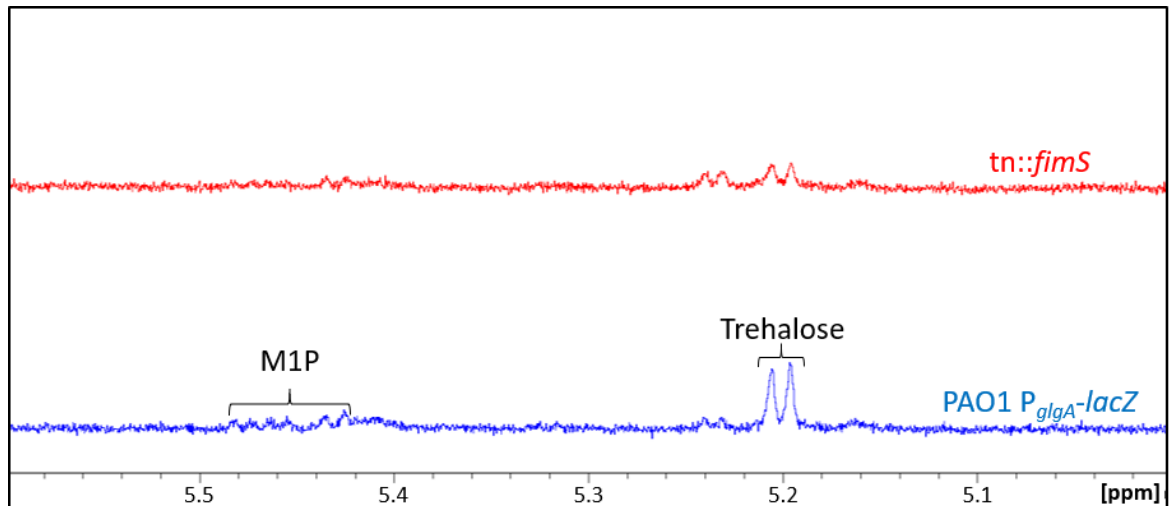


Figure 5-11:  $^1\text{H-NMR}$  spectroscopy of the soluble metabolome following transposon insertion within *fimS* in the PAO1  $P_{glgA-lacZ}$  strain. Metabolomes were extracted from PAO1  $P_{glgA-lacZ}$  (blue) and  $tn::fimS$  (red) cultured on M9 minimal medium. Peak assignments are as indicated based on previously established spectra. (M1P; maltose 1-phosphate). Resonances corresponding to trehalose decreased within the metabolome of  $tn::fimS$  as compared to the parental PAO1  $P_{glgA-lacZ}$ .

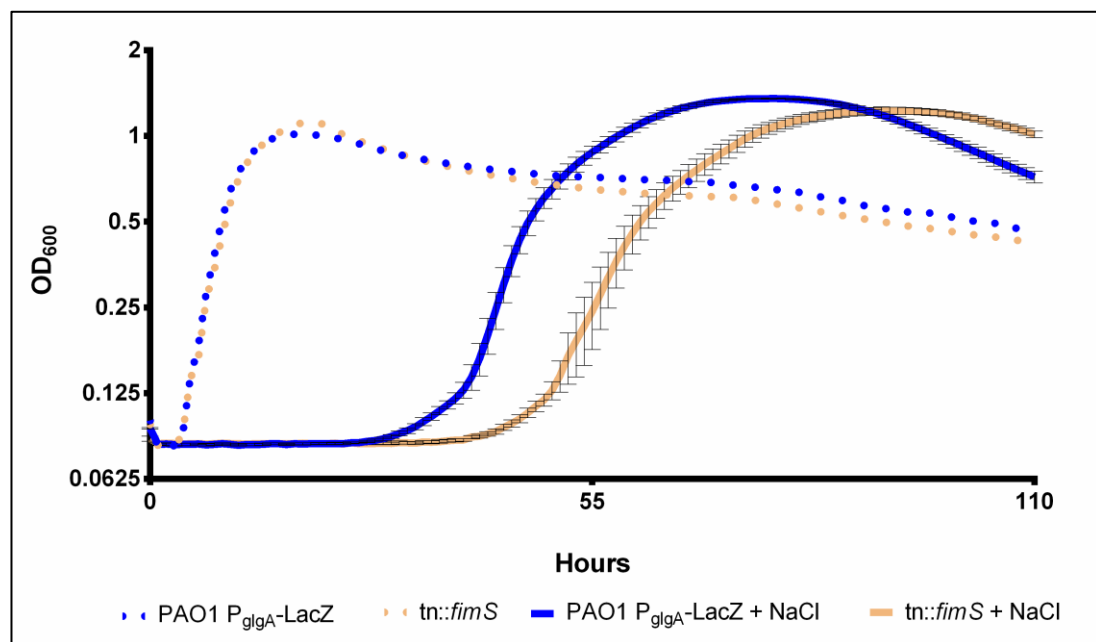


Figure 5-12: Growth of PAO1  $P_{glgA-lacZ}$  and  $tn::fimS$  in M9 minimal medium with and without addition of 0.85 M NaCl. Values represent the mean  $\text{OD}_{600}$  of five replicates. Results are representative of two independent experiments. Error not shown for growth under non-stressed conditions.  $tn::fimS$  exhibited attenuated growth under osmotic conditions when compared to the parental PAO1  $P_{glgA-lacZ}$  strain.

### 5.3.9 Gac/Rsm System

The transposon mutagenesis screens of both PAO1 and *Pto* yielded hits within *cmpX* and *ladS* respectively, both of which have been shown to interact with the Gac/Rsm signalling system, discussed in more depth earlier (Section 5.1.3). To investigate whether the Gac/Rsm system plays a role in the regulation of trehalose and  $\alpha$ -glucan biosynthesis, I

collaborated with Stephen Heeb (University of Nottingham) who kindly gifted a range of Gac/Rsm system mutants generated within *P. aeruginosa* sublines. Strains harbouring disruptions in the genes encoding GacA and GacS were generated in the Lausanne subline of PAO1 (PAO1-L). Deletion of the genes encoding RsmA, RsmN, both individually and in combination, were generated in the Nottingham subline of PAO1 (PAO1-N) (Stephen Heeb, personal communication). To investigate the impact of perturbations of the Gac/Rsm system on the levels of trehalose and  $\alpha$ -glucan, the small metabolome of these strains was extracted and analysed using  $^1\text{H-NMR}$  spectroscopy.

PAO1-L produced trehalose and M1P to approximately 0.29% and 0.28% of the total cellular dry weight, respectively. Following deletion of *gacA*, levels of trehalose were significantly reduced to approximately 0.07% of the cell dry weight (Table 5-5, Figure 5-13). Peaks corresponding to M1P were not detected from this strain's metabolome. Similarly, following deletion of *gacS*, trehalose levels may have been reduced, but this was not significant ( $p = 0.07$ ). M1P was not detected from the metabolome of this strain. This suggests that the Gac/Rsm system positively regulates trehalose and  $\alpha$ -glucan biosynthesis.

To further implicate the Gac/Rsm system in the regulation of trehalose and  $\alpha$ -glucan biosynthesis, it would follow that the negative regulators RsmA and RsmN would repress the production of trehalose and  $\alpha$ -glucan. This suggests that deletion of *rsmA* and *rsmN* would result in an increase in the levels of these metabolites.

The soluble metabolomes of PAO1-N,  $\Delta rsmA$  and  $\Delta rsmN$  strains were examined using  $^1\text{H-NMR}$  spectroscopy. PAO1-N accumulated trehalose and M1P to approximately 0.13% and 0.16% of the cellular dry weight, respectively (Table 5-6, Figure 5-13). There was no significant difference in the levels of trehalose or M1P following deletion of *rsmA* or *rsmN* individually. However, when RsmA and RsmN were both absent, the levels of trehalose reduced significantly and M1P was not detected. There was also an increase in the levels of maltose/glucose and the formation of two unknown broad sugar-like species labelled *a* and *b* (Figure 5-13). Although the levels of trehalose and M1P did not increase as predicted, absence of both Rsm proteins changes the metabolites produced which provides further evidence that the Gac/Rsm system plays a role in the regulation of trehalose and  $\alpha$ -glucan biosynthesis.

Table 5-5: Concentrations of trehalose and M1P produced by PAO1-L,  $\Delta gacA$  and  $\Delta gacS$  strains. Metabolites are presented as percentages of cellular dry weight  $\pm$  standard error ( $n \geq 2$ ). \* indicates significant differences ( $p \leq 0.05$ ) as compared to the parental strain as determined by a student's t-test. – indicates no detected metabolite.

Strain	Trehalose (%)	M1P (%)
<b>PAO1-L</b>	0.29 $\pm$ 0.04	0.28 $\pm$ 0.08
<b><math>\Delta gacA</math></b>	0.07 $\pm$ 0.01 *	-
<b><math>\Delta gacS</math></b>	0.14 $\pm$ 0.01	-

Table 5-6: Concentrations of trehalose and M1P produced by PAO1-N,  $\Delta rsmA$ ,  $\Delta rsmN$ , and  $\Delta rsmA \Delta rsmN$  strains. Metabolites are presented as percentages of cellular dry weight  $\pm$  standard error ( $n \geq 2$ ). \* indicates significant differences ( $p \leq 0.05$ ) as compared to the parental strain as determined by a student's t-test. – indicates no detected metabolite.

Strain	Trehalose (%)	M1P (%)
<b>PAO1-N</b>	0.13 $\pm$ 0.01	0.16 $\pm$ 0.03
<b><math>\Delta rsmA</math></b>	0.09 $\pm$ 0.01	0.07 $\pm$ 0.02
<b><math>\Delta rsmN</math></b>	0.13 $\pm$ 0.02	0.11 $\pm$ 0.02
<b><math>\Delta rsmA \Delta rsmN</math></b>	0.02 $\pm$ 0.02 *	-

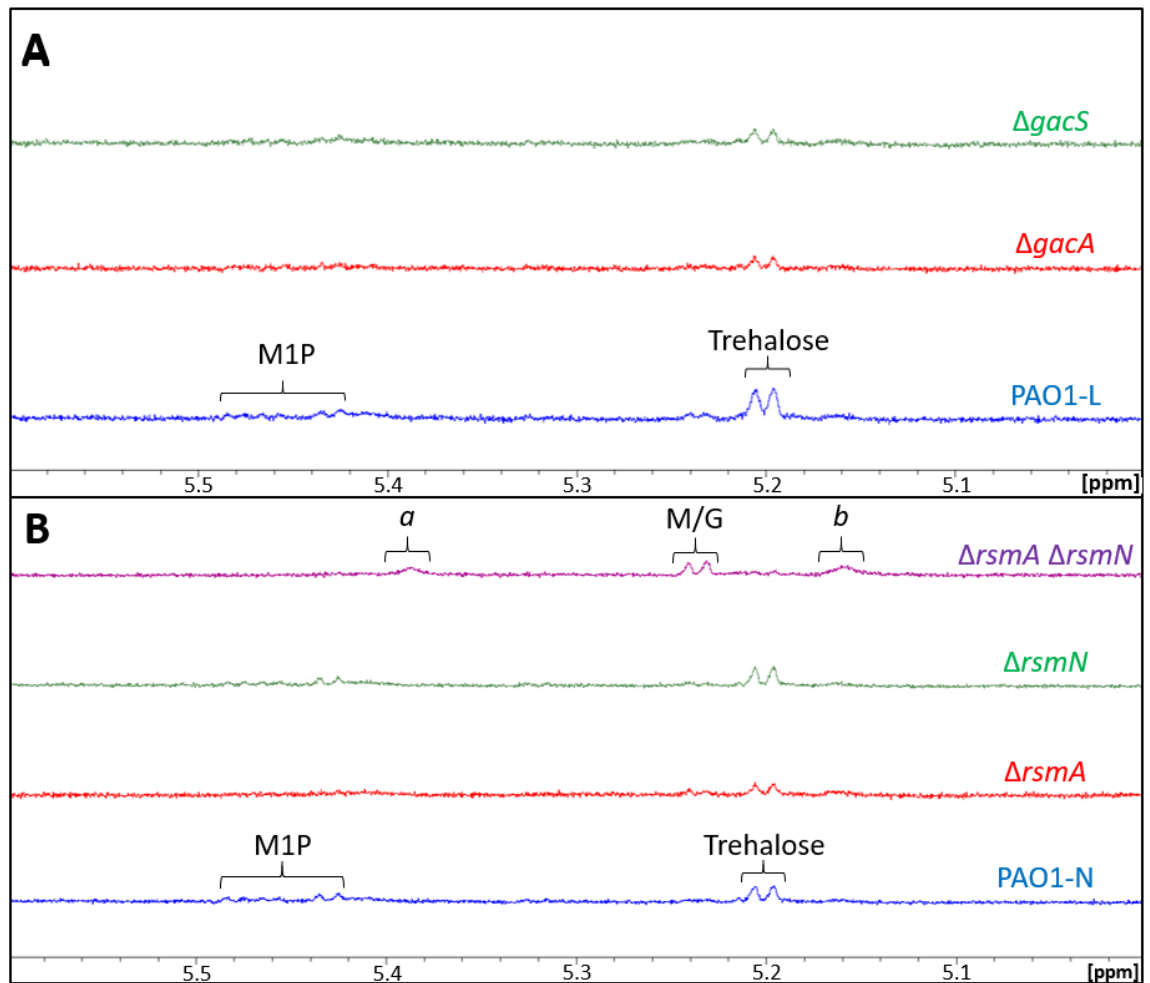


Figure 5-13: <sup>1</sup>H-NMR spectroscopy of the soluble metabolome following Gac/Rsm system mutations in *Pseudomonas aeruginosa* strains. Metabolomes were extracted from from the PAO1 Lausanne subline (PAO1-L) (blue) following disruption of *gacA* (red) and *gacS* (blue) (A) and from the PAO1 Nottingham subline (PAO1-N) (blue) following deletion of *rsmA* (red), *rsmN* (green) and *rsmA* and *rsmN* in combination (purple) (B) cultured on M9 minimal medium. Peak assignments are as indicated based on previously established spectra. (M/G; maltose and/or glucose, M1P; maltose 1-phosphate, *a* and *b* represent currently unknown species). Resonances corresponding to trehalose decreased following deletion of *gacA* and *gacS* when compared to PAO1-L. Furthermore, M1P was absent in the metabolomes of *ΔgacA* and *ΔgacS*. Deletion of either *rsmA* or *rsmN* did not affect the metabolome as compared to that of PAO1-N. When both *rsmA* and *rsmN* were absent, the peaks corresponding to unknown species were present.

### 5.3.10 DNA-affinity chromatography

To identify candidates that regulated trehalose and α-glucan biosynthesis directly, we used DNA-affinity chromatography to select for and identify any DNA-binding proteins. A biotinylated form of the PAO1 *glgA* promoter was used as bait to pull down *glgA* promoter-specific binding proteins. Non-specific biotinylated DNA was used as a control to exclude non-specific DNA binding proteins. To ensure optimal *glgA* regulation, cell lysates were extracted from PAO1 cultured under hyperosmotic conditions. Candidates were selected

based on predicted function with at least five unique peptide reads that did not bind to the non-specific DNA control. DNA-affinity chromatography was performed in collaboration with Richard Little. Peptide digestion, mass spectrometry and peptide analysis were performed by Gerhard Saalbach and Carlo de-Oliveira-Martins.

The sigma factor RpoN and five regulatory proteins FleQ, TrpI, BauR, OxyR and FleN were predicted as *glgA* promoter binding proteins through DNA-affinity chromatography (Table 5-7), the implications of each of these candidates is discussed below (Section 5.4).

Table 5-7: Putative regulators that were identified through specific binding to PAO1 *P<sub>glgA</sub>*.

<b>Protein Name</b>	<b>Unique peptide count</b>
<b>FleQ</b>	20
<b>RpoN</b>	5
<b>FleN</b>	5
<b>TrpI</b>	5
<b>BauR</b>	5
<b>OxyR</b>	7

## 5.4 Discussion

The regulation of bacterial trehalose biosynthesis is complex and surprisingly understudied. Conversely the regulation of classical  $\alpha$ -glucan biosynthesis has been extensively studied, but regulation of the GlgE pathway has only been studied in *M. tuberculosis* [260]. Nevertheless, as very little is known about the regulation of trehalose or  $\alpha$ -glucan biosynthesis in *Pseudomonas* spp., I aimed to identify potential regulators in both *P. aeruginosa* PAO1 and *Pto.*, I first generated reporter strains in both PAO1 and *Pto.*, I then employed random transposon mutagenesis to generate and identify global regulators of trehalose and  $\alpha$ -glucan biosynthesis. In order to identify direct regulators of trehalose and  $\alpha$ -glucan biosynthesis, I also utilised DNA-affinity chromatography to identify DNA binding proteins specific to *glgA* regulation.

I first identified evidence of transcriptional regulation of the trehalose and  $\alpha$ -glucan biosynthesis pathway in *Pto* during growth in liquid culture. In order to identify the regulatory network governing trehalose and  $\alpha$ -glucan biosynthesis in PAO1 and *Pto*, I performed two complementary screens. The first screening method employed transposon mutagenesis in an unbiased approach to identify global regulators directly or indirectly involved in the transcription of *glgA*. The second approach utilised DNA-affinity chromatography and was designed to identify regulators which directly interact with the

promoter of the *glgA* gene. The combination of these approaches has resulted in the identification or implication of several regulatory systems that control trehalose and  $\alpha$ -glucan biosynthesis in *Pseudomonas* spp.

Although a number of known regulators were identified, transposon mutagenesis also resulted in insertions within genes that were not predicted to have regulatory functions. Unlikely to regulate GlgA directly, transposon insertions in metabolic or transport genes generally resulted in reduced LacZ expression (light blue colony phenotypes) suggesting that trehalose and  $\alpha$ -glucan biosynthesis were down-regulated indirectly. For example, transposon insertions within the TauC taurine ABC transporter and ArgJ, a predicted glutamate N-acetyltransferase/amino acid acetyltransferase, most likely interfere with taurine and glutamate metabolism. Taurine has been shown to be a compatible solute in eukaryotic cells, but can also accumulate during osmotic conditions in *E. coli* [289]. ArgJ is a component of the bacterial arginine biosynthesis pathway and utilises the osmoprotectant glutamate as a substrate [290, 291]. Disruption of ArgJ may result in a build-up of glutamate and therefore solute concentration. The cell may respond in turn by decreasing the biosynthesis of other solutes such as trehalose. Similarly, SyrB, a syringafactin synthetase, is involved in the biosynthesis of syringafactin. Syringafactin is a hydroscopic surfactant that has been shown to have high water-holding potential and to protect *P. syringae* strain B728a from water stress [292]. Increases in the levels of syringafactin may increase the water potential of the cell, leading to a reduced requirement for compatible solutes and therefore decreased levels of trehalose biosynthesis. However, due to the unpredictable nature of this assay, transposon insertion in *syrB* may also have resulted in the decrease in the production of syringafactin, a possibility that is harder to rationalise. One explanation could be that disruption of syringafactin biosynthesis may result in a differential flux in carbon metabolism, reducing inputs into trehalose and  $\alpha$ -glucan biosynthesis. Although these candidates are not likely to be regulators, this illustrates a potential limitation of this methodology. Changes in osmotic potential or carbon metabolism caused by transposon insertion has the potential to result in altered levels of trehalose and  $\alpha$ -glucan biosynthesis, thereby resulting in the selection of less-relevant transposon mutant strains.

In PAO1, a transposon insertion was identified within the probable cation-transporting P-type ATPase (*PA1429*). Although unlikely to be directly related to the regulation of trehalose and  $\alpha$ -glucan biosynthesis, disruption of this gene resulted in an increase in LacZ

activity. Disruption of *PA1429* could lead to changes in the osmotic balance of the cell, and therefore an increase the biosynthesis of trehalose and  $\alpha$ -glucan. Although this protein has not been studied, P-type ATPases are responsible for the transport of charged substrates such as potassium ions [293]. The import of potassium ions is one strategy for resisting osmotic stress in *E. coli* [294]. Therefore, interruption of potassium import, such as with *PA1429* disruption, could lead to changes in the cellular osmotic potential. Compatible solutes, such as trehalose, would be synthesised in response accounting for the observed increase in LacZ activity.

The first regulatory pathway identified through the transposon mutagenesis screen was the Gac/Rsm system. The accessory sensor kinases CmpX and Lads were identified in screens in PAO1 and *Pto*, respectively. Disruption of *ladS* resulted in reduced LacZ activity and therefore suggested that LadS activated *glgA* expression. Subsequently, *ladS* disruption led to decreased levels of intracellular trehalose. Conversely, *cmpX* disruption resulted in increased LacZ activity and increased levels of intracellular trehalose, implicating LadS and CmpX as an activator and repressor of *glgA* expression, respectively.

Although the data suggested that CmpX is a repressor of trehalose and  $\alpha$ -glucan biosynthesis, *cmpX* disruption resulted in severe growth attenuation under osmotic conditions despite increased trehalose levels. Polar effects resulting from transposon insertion were not responsible for osmotic sensitivity, because a strain harbouring a non-polar deletion of *cmpX* also yielded a similar phenotype. This suggests that pleotropic effects arising from the deletion of *cmpX* may be responsible. Bhagirath *et al.* reported that a PAO1 strain lacking functional CmpX had altered levels of gene transcripts and molecules involved in signalling or regulation. For example, *cmpX* deletion resulted in increased levels of the signalling molecule cyclic di-guanosine monophosphate, and the cyclic di-guanosine monophosphate synthase *wspR*. Furthermore, the transcripts corresponding to the membrane porin *oprF* and the sigma factor *sigX* were both decreased following deletion of *cmpX*. PAO1  $\Delta$ *cmpX* exhibited sensitivity to membrane detergents and increased susceptibility to a range of antibiotics [258]. This demonstrates that deletion of *cmpX* influences other regulatory systems and causes increased sensitivity to toxic molecules, possibly due to membrane defects. These pleotropic effects could therefore be responsible for the observed osmotic attenuation. For example, the OprF porin has been shown to be required for growth in hypoosmotic conditions [295] and therefore could be required to maintain osmotic balance in hyperosmotic conditions. Taken together, it is uncertain

whether trehalose accumulation is due to de-repression of the Gac/Rsm system or that trehalose accumulation is in response to dysregulation of cellular osmotic potential due to pleiotropic effects arising from *cmpX* deletion.

As CmpX and LadS both play a role in modulating GacS activity as discussed earlier, I investigated the effect of disruption of other components of the Gac/Rsm system on trehalose and  $\alpha$ -glucan biosynthesis in PAO1 strains. I showed that GacA and GacS function as activators of trehalose and  $\alpha$ -glucan biosynthesis. Therefore, RsmA and RsmN would likely function as repressors and that deletion of the negative regulators *rsmA* and *rsmN* would result in an increase in trehalose and  $\alpha$ -glucan biosynthesis. Although PAO1-N  $\Delta$ *rsmA*  $\Delta$ *rsmN* yielded reduced levels of trehalose and M1P, this strain produced two unknown sugar-like species. Further analysis of the products following deletion of *rsmA* and *rsmN* is required. Nonetheless, this supports the hypothesis of Gac/Rsm regulation of the trehalose and  $\alpha$ -glucan biosynthesis pathway in *Pseudomonas* spp. Further work is also needed to characterise the osmotic and desiccation phenotypes of strains following Gac/Rsm system deletions.

Literature mining further supports the hypothesis of Gac/Rsm system mediated regulation of trehalose and  $\alpha$ -glucan biosynthesis in *Pseudomonas* spp. as UTP-glucose-1-phosphate uridylyltransferase (GalU) was shown to be a target of RsmN in PAO1 [282]. This suggests RsmN negatively regulates the translation of GalU and prevents trehalose and  $\alpha$ -glucan biosynthesis. This is reminiscent of CsrA repression of GlgC in *E. coli* [240] where the expression of the enzymes responsible for the metabolism of glucose 1-phosphate in both *E. coli* and PAO1 are translationally repressed by CsrA homologues. Moreover, PAO1 RsmA, but not RsmN, can functionally replace CsrA and repress  $\alpha$ -glucan biosynthesis in *E. coli* [241]. As my results suggest that both RsmA and RsmN are required to modulate levels of trehalose and  $\alpha$ -glucan in PAO1, it would be interesting to see if expression of *E. coli* CsrA in PAO1  $\Delta$ *rsmA*  $\Delta$ *rsmN* would result in a wild-type metabolome.

The CrbA/CrbB two-component system was implicated as an activator of trehalose and  $\alpha$ -glucan biosynthesis in *Pto* as CbrB disruption resulted in decreased LacZ activity and decreased levels of intracellular trehalose. I would therefore predict that transposon insertion within *cbrB* would result in an osmotically-sensitive strain. However, due to time constraints, this hypothesis could not be tested. These results implicate either the Crc protein in the repression of *glgA* or that GlgA belongs to the CbrB regulon. Although this could be determined using *in vitro* DNA-binding assays to assess protein binding to the *glgA*

promoter, other authors have reported that GlgA is under the direct control of CbrB in *P. putida*. Chromatin immunoprecipitation sequencing revealed the genome-wide binding sites of CbrB in *P. putida*, including both the promoters of *algD* and *glgA*. Furthermore, the mRNA transcripts of GlgA were reduced following a deletion of *cbrB* [280].

The *crcZ* RNA was also identified as a potential regulatory factor in the biosynthesis of trehalose and  $\alpha$ -glucan in PAO1. Disruption of *crcZ* would lead to de-repression of the negative regulator Crc. The *crcZ* RNA is a target of the regulatory protein RsmN [282], linking the Gac/Rsm and CbrA/B systems. Although trehalose and  $\alpha$ -glucan biosynthesis is under the control of both the Gac system and CbrB, there are no published data to suggest that GlgA is under the control of Crc. However, this remains to be tested experimentally.

Finally, the alginate regulatory network was implicated in the control of trehalose and  $\alpha$ -glucan biosynthesis in PAO1. Disruption of *FimS* resulted in decreased LacZ activity, decreased intracellular trehalose levels and yielded an osmotically-sensitive strain. This suggests *FimS* plays a role in activating trehalose and  $\alpha$ -glucan biosynthesis in PAO1, however, there is no data reported in the literature to suggest direct regulation of *glgA* by *FimS*.

In contrast, disruption of *AlgB* resulted in increased levels of LacZ activity, increased trehalose concentration and a strain exhibiting increased osmotic resistance as compared to the parental strain. This suggests that *AlgB* acts as a repressor of trehalose and  $\alpha$ -glucan biosynthesis.

There are contradictory reports as to the role the *AlgB/KinB* system plays in the regulation of trehalose and  $\alpha$ -glucan biosynthesis. For example, a PAO1 *kinB* mutant produced higher levels of trehalose compared to the wild-type strain [214]. Conversely, other groups reported *kinB* deletion resulted in decreased transcription of genes involved in trehalose and  $\alpha$ -glucan biosynthesis [218].

Thus far, all the regulatory networks that have been implicated in the regulation of trehalose and  $\alpha$ -glucan biosynthesis are also known to regulate the production of alginate in *Pseudomonas* spp. Furthermore, trehalose and  $\alpha$ -glucan biosynthesis genes are highly co-expressed with the alginate biosynthesis genes in transcriptomic data of clinically isolated strains of *P. aeruginosa* (Susanne Haeussler, personal communication). Given their apparent functional and regulatory relationship (Chapter 4), it seems unlikely that *AlgB* would activate alginate production, but repress the production of trehalose and  $\alpha$ -glucan.

As discussed earlier, the nature of transposon mutagenesis can result in unpredictable polar effects. To address this, non-polar deletions of *algB* and *kinB* should be made in *Pto* and PAO1 and their effects on the synthesis of trehalose and  $\alpha$ -glucan should be assessed.

AlgU regulates the expression of both AlgB and AlgR [265]. AlgU, AlgR, AlgB and KinB are all upregulated in response to hyperosmotic conditions in *Pseudomonas* species [129, 184]. Furthermore, deletion of AlgU results in a decrease in the transcription of *glgA* [296], the inability to produce trehalose in response to NaCl or ethanol [214], as well as yielding strains sensitive to both osmotic and desiccation stress [129]. This further supports the hypothesis that trehalose and  $\alpha$ -glucan biosynthesis are controlled by the alginate regulatory network, AlgU, AlgR and AlgB.

Potential regulators identified from DNA-affinity chromatography assays included RpoN, FleQ, FleN, TrpI, BauR and OxyR. These candidates were suggested to bind directly to the *glgA* promoter under osmotic conditions, indicating that they function to activate trehalose and  $\alpha$ -glucan biosynthesis. Additional *in vitro* DNA-binding assays should be performed to validate the binding of these candidate regulators to the *glgA* promoter DNA. Transcriptomic, metabolomic and phenotypic assays should also be performed to assess the effect of individual non-polar deletions of the genes encoding these regulators.

RpoN is required for alginate overexpression in mucoid strains because deletion results in decreased alginate production to non-mucoid levels [269]. Deletion of *rpoN* also resulted in the down-regulation of genes involved with trehalose and  $\alpha$ -glucan biosynthesis in a *P. aeruginosa*  $\Delta kinB$  strain [218]. However, the loss of RpoN in *P. putida* did not result in osmotic sensitivity [297]. This suggests that RpoN regulates the production of trehalose and  $\alpha$ -glucan biosynthesis in *Pseudomonas* spp., but likely plays a minor role.

The transcriptional regulator FleQ and putative ATPase FleN work in concert to regulate gene expression [298]. FleQ regulates genes involved in biofilm formation [299] and flagellar biosynthesis [300]. FleN does not bind DNA alone [298], so its identification in the DNA-affinity chromatography screen is likely due to interaction with FleQ. Recently the FleQ regulon had been investigated in *P. fluorescens* and *P. putida* through chromatin immunoprecipitation sequencing. It was found that FleQ is enriched at the promoter of *algD* thereby linking FleQ to the regulation of alginate [301]. Outside of this study, no evidence exists to suggest FleQ is involved in the regulation of trehalose and  $\alpha$ -glucan biosynthesis.

The possibility of *glgA* being part of the FleQ regulon is convincing for two reasons. Firstly, 20 unique peptide hits were recorded for the FleQ protein which was the highest recorded for any of the candidates. Secondly, the cognate binding protein FleN was also identified in the same screen suggesting a genuine interaction between FleQ, FleN and the *glgA* promoter.

Other candidates included TrpI and BauR. TrpI is a tryptophan biosynthesis regulator and activates the expression of the genes encoding the tryptophan synthases *trpB* and *trpA* [302]. There is no published evidence to suggest involvement in the regulation of *glgA*. BauR is a regulator of polyamine and  $\beta$ -alanine metabolism in PAO1 [303], however there is only one report currently published regarding this regulator.

OxyR is a positive regulator of genes involved in the oxidative stress response where mutants lacking OxyR were sensitive to hydrogen peroxide [304]. Chromatin immunoprecipitation sequencing integrated with transcriptomic analysis in *P. aeruginosa* identified *rsmZ* and *glgA* as targets of OxyR *in vivo* [305]. No link to alginate biosynthesis was reported. Furthermore, *E. coli* mutants lacking OxyR were attenuated during hyperosmotic conditions [306]. This strongly supports the hypothesis of OxyR acting as a positive regulator of trehalose and  $\alpha$ -glucan biosynthesis in *Pseudomonas* spp.

In order to probe the regulatory network governing trehalose and  $\alpha$ -glucan biosynthesis in *Pseudomonas* spp. I used multiple approaches to identify and experimentally characterise key candidates. I identified three distinct systems of regulation which control the expression of trehalose and  $\alpha$ -glucan at the level of transcription and translation. This regulatory network further solidifies the link between trehalose,  $\alpha$ -glucan and alginate, as nearly all regulatory elements control the expression of both biosynthetic systems.

This work combines experimental evidence resulting from both PAO1 and *Pto*. Although regulatory elements identified in this chapter overlapped in some cases between these organisms, further work should be conducted to identify the existence of species-specific regulation. Further characterisation of this network would include establishing experimental evidence of protein-DNA binding and protein-protein interactions *in vitro* to determine direct interaction with the *glgA* promoter and thereby establish a hierarchy of regulation.

The following diagram summarises the regulatory network controlling the biosynthesis of trehalose and  $\alpha$ -glucan in PAO1 and *Pto* based on experimental data presented within this chapter combined with data reported by other researchers (Figure 5-14).

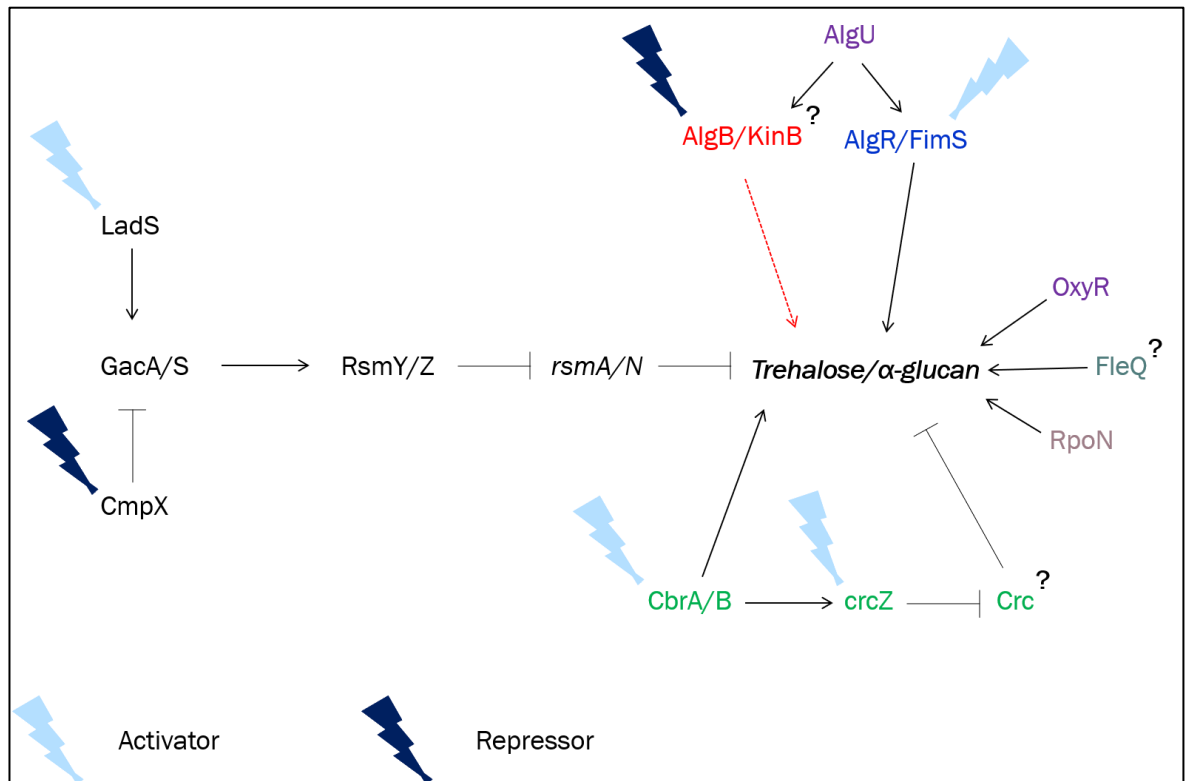


Figure 5-14: The current understanding of the regulatory network governing trehalose and  $\alpha$ -glucan in *Pseudomonas* spp. The three main systems identified are the Gac/Rsm system, the CbrA/B-CrcZ-Crc system and the alginate regulatory network. Other regulators included OxyR, FleQ and RpoN. Arrows indicate activation whereas blunted lines indicate repression. Lightning indicates identification through transposon mutagenesis, with light blue colour indicating decrease in LacZ activity and dark blue indicating an increase in LacZ activity. Question marks indicate there is either no direct evidence linking the regulator to the biosynthesis pathway in the case of Crc, or whether a regulator activates or represses activation is unknown as with AlgB/KinB.

# Chapter 6: General Discussion

## 6.1 Introduction

Bacterial disease and infection are ubiquitous and affect almost every aspect of life with significant social and economic costs. *Pseudomonas* spp. represent significant pathogens of humans, animals and plants. Soil, water, plants, animals and even hospital surfaces represent important reservoirs of pathogenic *Pseudomonas* bacteria [1-8]. During this environmental lifestyle these bacteria will be exposed to a variety of abiotic stresses. Bacteria employ various strategies to resist these stresses in order to survive and eventually establish infection [66]. Understanding these bacterial stress resistance mechanisms may offer new targets for the prevention of infection by eradicating environmental reservoirs of pathogens.

The main aim of this thesis was to investigate the existence of a novel  $\alpha$ -glucan biosynthesis pathway and its role in pathogenic *Pseudomonas* spp. To this end, I have utilised genetic and biochemical techniques to experimentally characterise the pathway and examined the function of  $\alpha$ -glucan in protecting *Pseudomonas* spp. against environmental stress both *in vitro* and during plant infection.

## 6.2 Does the GlgE pathway exist and function in *Pseudomonas* spp.?

Prior to the work described in this thesis, the biosynthesis of trehalose and  $\alpha$ -glucan was relatively understudied in *Pseudomonas* spp. The trehalose biosynthetic loci in *Pseudomonas* were discovered in 2010 but trehalose biosynthesis in these organisms has not been extensively investigated [74, 180]. Until now, previous studies into trehalose biosynthesis in *Pseudomonas* spp. consisted of the generation and analysis of trehalose-deficient strains arising from the deletion of whole operons or large regions of the genome [74, 180]. Although these strains did not produce trehalose, the function of individual gene products was not assessed. Furthermore, these operon deletions also included additional genes, including those involved with classical and GlgE-dependent  $\alpha$ -glucan biosynthesis. The existence of the GlgE pathway was not appreciated by previous researchers therefore the impact of the loss of  $\alpha$ -glucan biosynthesis was not considered.

The only work attempting to elucidate the specifics of *Pseudomonas* trehalose biosynthesis involved the characterisation of some of the enzymes involved. For example, the kinetics and activity of trehalose synthase (TreS) from *P. putida* was studied for its industrial application in the production of trehalose [145, 307]. Additionally, there was one report of

the characterisation of a trehalose 6-phosphate phosphatase from certain *P. aeruginosa* strains [195]. However, there is no evidence to suggest the existence of a trehalose 6-phosphate synthase in *P. aeruginosa* or *P. syringae* so one can conclude that the presence of trehalose 6-phosphate phosphatase is not representative of the species or the genus in general [181, 195].

To address this gap in our knowledge, I described the elucidation of the biochemical pathways linking trehalose and  $\alpha$ -glucan for the first time in *Pseudomonas* spp. in Chapter 3. *Pseudomonas* spp. synthesise trehalose through the TreY/TreZ pathway. Contrary to previous reports, the TreS pathway does not synthesise trehalose in *Pseudomonas* spp. Instead, like *Mycobacterium* spp., the TreS pathway forms part of the GlgE pathway and metabolises trehalose into  $\alpha$ -glucan. This work demonstrates for the first time that the GlgE pathway is functional and produces  $\alpha$ -glucan in *Pseudomonas* spp. Additionally, this is the first report of genetic and biochemical characterisation of trehalose into  $\alpha$ -glucan biosynthesis in an organism that contains both GlgA and GlgE mechanisms of synthesising  $\alpha$ -glucan. To the best of our knowledge, this is also the first report of a widely-conserved mechanism for *de novo* maltose biosynthesis within *Pseudomonas* spp.

As a result of this work, I have shown that *Pseudomonas* spp. possess one conserved mechanism of trehalose biosynthesis. However, certain species, including *Pto*, also possess additional TreS homologues. Although the activity of this enzyme is described in chapter 3, its physiological role remains unknown. The presence of TreS(2) within *Pseudomonas* is restricted to dedicated pathogenic and commensal plant-associated species. The presence of TreS(2) could therefore suggest a particular adaptation reflecting the lifestyle of these bacteria. Future work should include investigating the significance and relevance of TreS(2) carriage. For example, is TreS(2) under distinct regulation compared to the TreY/TreZ or TreS operons? Alternatively, transcript and protein abundance or activity could be measured in response to different environmental conditions to determine the biological relevance of TreS(2).

Another aspect of trehalose and  $\alpha$ -glucan biosynthesis that requires further investigation is the existence of additional input into the biosynthetic pathways in *Pto*. Deletion of *glgA* in *Pto* did not result in the abolition of the biosynthesis of trehalose and  $\alpha$ -glucan as expected. The identification of enzyme(s) responsible would further our understanding of this system in *Pto*.

### 6.3 How do trehalose and $\alpha$ -glucan function in *Pseudomonas* spp.?

Trehalose is thought to play an important role in a wide range of environmental stresses, notably protecting against osmotic and desiccation stress in *Pseudomonas* spp. [74, 107, 151]. However, conflicting reports exist that claim trehalose does not function as a stress protectant in *Pseudomonas* [180]. Furthermore, trehalose has also been implicated as a virulence factor during *Pseudomonas* plant infection [74, 180].

Classical  $\alpha$ -glucan functions as a form of carbon storage which is accumulated during nutrient limiting conditions [234, 236]. The GlgC-GlgA  $\alpha$ -glucan biosynthesis pathway is possessed by approximately 20% of sequenced bacterial genomes [183]. Recently, it was discovered that *Mycobacterium* spp. possesses the GlgE pathway, a novel pathway involved with the biosynthesis of  $\alpha$ -glucan which exists in 14% of sequenced bacterial genomes. However, until now, the function of GlgE-dependent  $\alpha$ -glucan had only been studied in *M. tuberculosis*. Mycobacterial  $\alpha$ -glucan interacts with the human immune system and plays a role in the outcome of human disease [208, 308]. The GlgE pathway is predicted to be largely possessed by plant-associated bacteria, suggesting that GlgE-dependent  $\alpha$ -glucan may play a role during plant infection or colonisation. The discovery of a new function for mycobacterial  $\alpha$ -glucan combined with the existence of a novel GlgE pathway has renewed interest regarding the function of this polysaccharide.

In Chapter 4, I describe an investigation into the roles of trehalose and  $\alpha$ -glucan in the human pathogen PAO1 and the plant pathogen *Pto*. I showed that trehalose was required for optimal growth during hyperosmotic conditions whereas  $\alpha$ -glucan was required for survival during low humidity or desiccation stress, two related but distinct environmental stresses. This study also demonstrated functional similarities between  $\alpha$ -glucan and the exopolysaccharide alginate, where  $\alpha$ -glucan and alginate exhibit functional redundancy in *Pto*. This is the first report of  $\alpha$ -glucan and alginate functioning to protect PAO1 and *Pto* against desiccation stress, a role previously attributed to trehalose. Although functionally distinct, the biosynthesis of trehalose and  $\alpha$ -glucan are intrinsically linked through the TreY/TreZ and GlgE pathways. This means that changes in trehalose biosynthesis would have impacted on the biosynthesis of GlgE-dependent  $\alpha$ -glucan, accounting for the observed changes in desiccation tolerance [74, 151]. Deletion of the genes required for both trehalose and  $\alpha$ -glucan biosynthesis did not result in deleterious effects during *Pto* plant infection in contrast to and contradicting published reports [74, 180].

However, when bacteria also lacked the ability to synthesise alginate, attenuation was observed. Infections were only attenuated when bacteria were exposed to dry conditions on the surface of the leaf. Infiltration into the stomata or increased RH resulted in wild-type like infections. This illustrated the effect of water stress on survival on the surface of leaves and its implication for subsequent infection.

The understanding of the stress tolerance mechanisms of *Pseudomonas* spp. could be exploited to try and prevent *Pseudomonas* infections. GlgE and GlgB have been validated as potential antibiotic targets in *Mycobacterium* spp. due to their essentiality [153]. Although these gene products are not essential in *Pseudomonas* spp., targeting these enzymes may result in decreased environmental viability and therefore reduce the incidence or severity of infection or the survival of bacteria in typically dry environmental reservoirs, such as hospital surfaces and plant leaves. However, as discussed below, the GlgE pathway is widespread and these enzymatic drug targets may not be specific solely to pathogenic bacteria.

#### **6.4 How are trehalose and $\alpha$ -glucan biosynthesis regulated in *Pseudomonas* spp.?**

The regulation of trehalose biosynthesis in bacteria is complex and surprisingly understudied. Although the regulation of classical  $\alpha$ -glucan biosynthesis in bacteria has been well studied (Section 5.1.3), there is only one report concerning the regulation of the GlgE pathway in bacteria. Mycobacterial GlgE activity is controlled at protein activity level by phosphorylation *via* the kinase PknB [260].

To address this gap in our knowledge, I described the identification of regulatory elements controlling trehalose and  $\alpha$ -glucan biosynthesis in *Pseudomonas* spp. in Chapter 5. By using a combination of transposon mutagenesis and DNA-affinity chromatography we identified several global regulators that play a role in regulating trehalose and  $\alpha$ -glucan biosynthesis in *Pseudomonas* spp. This includes the Gac-Rsm pathway and the CbrA/CbrA-Crc catabolite repression system. Furthermore, trehalose and  $\alpha$ -glucan biosynthesis were found to be regulated by two-component systems involved with alginate biosynthesis regulation, AlgR/FimS and AlgB/KinB, providing further evidence for a functional link between  $\alpha$ -glucan and alginate. Moreover, the abiotic stress regulator OxyR, the stress response sigma factor RpoN, and the motility regulator FleQ were implicated in the regulation of PAO1 *glgA*.

As discussed earlier (Section 5.1.3) the Gac-Rsm system is involved during *P. aeruginosa* colonization of the CF lung, regulating biofilm formation and the acute-chronic switch during infection. Furthermore, the functional and regulatory links between trehalose,  $\alpha$ -glucan and alginate suggest that both biosynthetic systems would be activated in response to similar environmental signals. Moreover, the trehalose and  $\alpha$ -glucan biosynthesis genes are highly co-expressed with the alginate biosynthesis genes in transcriptomic data of clinically-isolated strains of *P. aeruginosa* (Susanne Haeussler, Personal communication). Taken together, these results may reflect the abiotic stresses encountered in the CF lung and suggests that trehalose and  $\alpha$ -glucan may help promote *P. aeruginosa* survival and therefore promote chronic infection. Furthermore, the Gac-Rsm system and FleQ are involved with the switch between planktonic and biofilm lifestyles. This suggests that trehalose and  $\alpha$ -glucan biosynthesis are activated during the biofilm lifestyle. This may explain why this system is not active in *Pto* during non-stressed growth in liquid culture.

Future work in this area could include continuing the screening for potential regulators of trehalose and  $\alpha$ -glucan biosynthesis in *Pseudomonas* spp. Further downstream analysis, including *in vitro* biochemical experiments are required to further verify individual regulators and define the regulatory hierarchy for trehalose and  $\alpha$ -glucan biosynthesis. For example, the promoters controlling each of the operons/genes involved in trehalose and  $\alpha$ -glucan biosynthesis should be characterised, including regulator-promoter interactions.

Until now, the identification of regulators in *Pseudomonas* spp. has been focused on the regulation of the *glgA* promoter and therefore the *treY/treZ* operon. Although the *treS* operon appears to be similarly upregulated in response to osmotic stress as compared to the *treY/treZ* operon [107, 202], it is not known if there is independent regulation of the *treS* operon. This therefore raises the question: do we see differential regulation between the *treS* and *treY/treZ* operons? For example, regulation specific to the products of the *treS* operon could take the form of GlgE modulation by the kinase PpkA. *Pseudomonas* spp. possess genes encoding PpkA, a protein homologue of the mycobacterial kinase PknB, a negative regulator of mycobacterial GlgB ([309]). PAO1 PpkA shares 39% protein sequence similarity with PknB therefore PpkA interaction with *Pseudomonas* GlgE should be investigated to determine if any regulatory activity exists.

The  $P_{glgA}$ -LacZ reporter strains for this study could be utilised further to identify environments and conditions that favour trehalose and  $\alpha$ -glucan production. Furthermore,

techniques such as qRT-PCR or RNA sequencing could be used to identify the spatial and temporal expression pattern of trehalose and  $\alpha$ -glucan biosynthetic genes during infection scenarios.

One important aspect in the regulation of trehalose and  $\alpha$ -glucan biosynthesis that has not been addressed in this thesis is the implied switch between trehalose or  $\alpha$ -glucan accumulation in response to water stress. It is likely that environmental signals favouring the accumulation of trehalose also promote the recycling of  $\alpha$ -glucan, facilitated by the activation of the GlgX and GlgP recycling enzymes [310]. The degradation of trehalose would also likely be prevented *via* the inhibition of trehalases (TreA) and modulation of TreS/Pep2 to prevent the conversion of trehalose into M1P. This could be at the level of transcription or translation, but because the transcription of both *treS* and *treY/treZ* operons are upregulated in response to osmotic stress in *Pseudomonas* spp. [107], regulation of GlgX and TreS/Pep2 is likely to occur at the post-transcriptional level. This regulatory mechanism is currently unknown; identification of this would progress our understanding of the bacterial response to both osmotic and desiccation stresses.

## 6.5 What is the molecular basis for the function of $\alpha$ -glucan and alginate function in *Pseudomonas*?

The work described in this thesis has implicated both  $\alpha$ -glucan and alginate in the protection of *Pseudomonas* spp. against desiccation stress. However, the molecular basis of this protection is unknown. This prompts the following questions: how does  $\alpha$ -glucan function to protect the cell against desiccation stress? And how does this interplay with the role of alginate?

*Mycobacterium* spp. produce both intracellular and extracellular  $\alpha$ -glucan.  $\alpha$ -Glucan is exported to the capsule where it can function during infection. It is currently unknown whether *Pseudomonas* spp. can export  $\alpha$ -glucan outside of the cell or whether  $\alpha$ -glucan is retained within the cytosol. This could be investigated by the use of transmission electron microscopy.

The molecular mechanism of protection conferred by  $\alpha$ -glucan is currently unknown and should be investigated in future. Like alginate,  $\alpha$ -glucan might exhibit high water-binding capacity and form a hydrogel [311]. If this is the case, the two molecules may work together to protect the cell with  $\alpha$ -glucan preventing loss of water from the cytosol in desiccating

conditions whilst alginate retains water within the biofilm matrix, increasing the external water potential thereby reducing cellular water loss.

Alternatively,  $\alpha$ -glucan could function similarly to trehalose. Trehalose protects against osmotic stress by protecting intracellular macromolecules, notably proteins and membranes. For example, there are several non-mutually exclusive hypotheses which try to rationalise the molecular basis of this protection:

1. *The water replacement hypothesis*, where trehalose functions by forming hydrogen bonds with macromolecules instead of water. This prevents the denaturing of proteins [312]. and preserves the integrity of the membrane [313]. This hypothesis was further refined by proposing that membrane stability is achieved through the linking of multiple lipid headgroups forming a scaffold of hydrogen bonded trehalose molecules [314, 315].
2. *The vitrification hypothesis* suggests that upon dehydration trehalose forms a viscous material known as a glass. The glass-transition state of trehalose is thought to preserve the structural integrity of macromolecules and thereby prevent denaturation of proteins or disruption of the membrane [316, 317].
3. *The water entrapment hypothesis* suggests that during dehydration trehalose can preserve and concentrate water proximal to the macromolecule surface. This preserves the macromolecule in a relatively hydrated state, preserving the native conformation, and therefore function [318].

To determine the molecular function of  $\alpha$ -glucan in *Pseudomonas* spp. further phenotypic and biophysical analysis is required. For example, determining the exact location within the cell could aid efforts in elucidating its function. Alternatively, the function of  $\alpha$ -glucan could be elucidated by examining the effects of co-incubating pure  $\alpha$ -glucan with various macromolecules during desiccating conditions. Determining the functions of bacterial  $\alpha$ -glucan may also result in the industrial interest and production of this molecule. For example, if  $\alpha$ -glucan exhibits similar properties to hydrogels, it could be utilised for medical application [319].

## 6.6 Evolution of the GlgE Pathway

It is still unclear as to why *Pseudomonas* spp. have evolved two distinct biosynthetic pathways of  $\alpha$ -glucan biosynthesis. Genomic clustering suggests that GlgA-dependent  $\alpha$ -glucan is synthesised as a precursor to TreY/TreZ to produce trehalose whereas GlgE-

dependent  $\alpha$ -glucan is produced from trehalose. This therefore begs the question: why would *Pseudomonas* spp. evolve two distinct methods of synthesising  $\alpha$ -glucan rather than accumulating GlgA-dependent  $\alpha$ -glucan? The most plausible explanation is that there are differences between the lengths of GlgA- and GlgE-synthesised  $\alpha$ -glucan making them distinct molecules. In turn, this may determine substrate specificity. For example, are GlgA- and GlgE-dependent  $\alpha$ -glucan available as substrates to all  $\alpha$ -glucan metabolising enzymes? Is GlgB only able to branch GlgE synthesised  $\alpha$ -glucan? Can TreY metabolise both GlgA- and GlgE-dependent  $\alpha$ -glucan? Can GlgA polymerise GlgE-dependent  $\alpha$ -glucan? To try and address these questions, we first attempted to determine differences between the length of GlgA- and GlgE-synthesised linear  $\alpha$ -glucan, however we were unable to show any differences.

The length and substrate availability of  $\alpha$ -glucan produced by either GlgA and GlgE needs to be investigated further in *Pseudomonas* spp. For example, specific strains such as PAO1  $\Delta glgA :: otsA/otsB$  should produce GlgE-dependent  $\alpha$ -glucan, exclusively, whereas, PAO1  $\Delta glgE \Delta treY$  should produce only GlgA-dependent  $\alpha$ -glucan. These strains could therefore be used to answer the questions alluded to above. Firstly, the length of GlgA- and GlgE-dependent  $\alpha$ -glucan should be determined, secondly, the ability of each enzyme to use each purified  $\alpha$ -glucan as a substrate should be assessed biochemically.

The action of the branching enzyme GlgB determines the structure of  $\alpha$ -glucan in bacteria [196]. For example,  $\alpha$ -glucan extracted from *E. coli* possessed longer chains with a higher extent of branching than  $\alpha$ -glucan extracted from *M. tuberculosis* and *Streptomyces venezuelae*. The  $\beta$ -particles of these  $\alpha$ -glucans were also shown to be larger in diameter than those extracted from *E. coli*. Furthermore,  $\alpha$ -glucan chain length and branching frequency was shown to be modifiable by the modulation of the N-terminus of *E. coli* GlgB. Truncations of the N-terminus of GlgB result in longer  $\alpha$ -glucan chains whereas complete deletion of *glgB* resulted in a strain of *E. coli* which produced longer chains of  $\alpha$ -glucan without branch points. All mutants exhibited increased nutrient starvation sensitivity as compared to the wild-type strain. Moreover, GlgB N-terminal truncation strains exhibited increased desiccation resistance whereas *E. coli*  $\Delta glgB$  was more sensitive to desiccation stress [320]. This demonstrates that the differences in the structure of  $\alpha$ -glucan may alter its physiological role within the cell.

To investigate this further, a bacteria-wide structural-functional analysis of  $\alpha$ -glucan could be conducted. Structural differences of  $\alpha$ -glucan could be co-analysed with the associated

physiological traits exhibited by the bacteria thereby aiding determination of the molecular basis for the function of  $\alpha$ -glucan. The enzymes responsible for bacterial  $\alpha$ -glucan biosynthesis should also be investigated and compared. Variation in the protein sequence or structure could result in altered function and therefore the production of novel structures of  $\alpha$ -glucan. Based on this information, enzymes could be introduced or modified in target organisms, to induce the production of non-native  $\alpha$ -glucan. This could then confer novel or enhanced traits within the target bacterium, such as increased stress tolerance or increased survival during nutrient starvation.

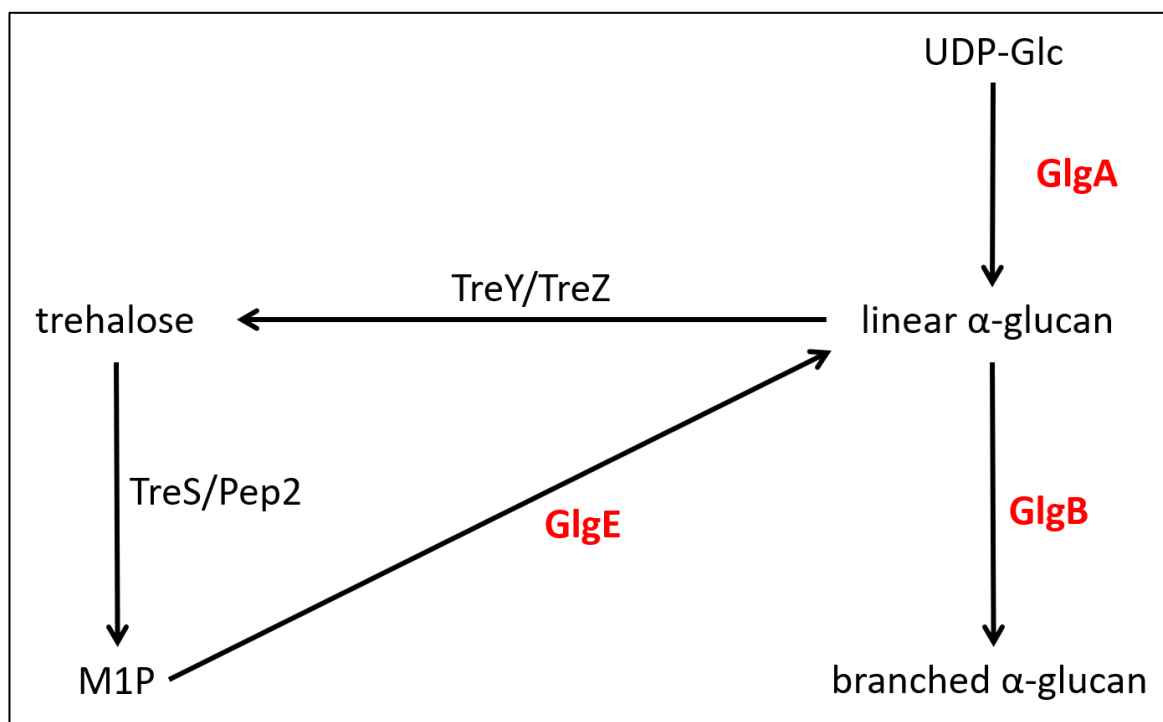


Figure 6-1: Illustration of futile cycling of  $\alpha$ -glucan biosynthesis and degradation in *Pseudomonas* spp. Linear  $\alpha$ -glucan is generated by GlgA using UDP-glucose (UDP-Glc) as a substrate, linear  $\alpha$ -glucan is then degraded into trehalose by TreY/TreZ. Trehalose is then converted into maltose 1-phosphate (M1P) by TreS/Pep2. Finally, linear  $\alpha$ -glucan is re-formed through the polymerisation of M1P by GlgE thus completing the cycle.

If there are no structural or functional differences between GlgA- and GlgE-dependent  $\alpha$ -glucan, an alternative hypothesis is that the GlgE pathway has evolved in bacteria as an efficient mechanism to degrade intracellular trehalose. In order to cope with environmental stress, bacteria must respond efficiently to rapidly changing environmental conditions. The existence of the GlgE pathway could represent an efficient method of degrading intracellular trehalose into  $\alpha$ -glucan in response to fluctuation in the levels of salt and RH. This may be especially true in bacteria lacking alternative trehalose degradative enzymes such as *Pto* [181].

If structural or functional differences did not exist between  $\alpha$ -glucan produced by either GlgA or GlgE in *Pseudomonas* spp., the existence of both pathways would lead to a futile cycling of  $\alpha$ -glucan biosynthesis and degradation through trehalose and M1P (Figure 6-1). Although unlikely, this could control the flux of carbon into glycolysis thereby ensuring optimal carbon utilisation [310].  $\alpha$ -Glucan recycling could also provide a source of metabolic intermediates for other processes, for example G1P and UDP-glucose can be used for Psl biosynthesis [321]. This means that  $\alpha$ -glucan recycling may serve as a regulatory mechanism of several important processes, including carbon metabolism, EPS and lipopolysaccharide biosynthesis. However, this form of regulation would be extremely costly in terms of ATP consumption, arguing against this model.

## 6.7 Widespread connections

The elucidation of the function of  $\alpha$ -glucan in *Pseudomonas* spp. has far reaching implications throughout the microbial world. For example, this work has established an additional biosynthetic link between trehalose and  $\alpha$ -glucan in *Pseudomonas* spp. with implications for other bacteria and microorganisms possessing gene homologues of the GlgE pathway.

As discussed above, the GlgE pathway is represented in 14% of sequenced bacterial genomes [171], largely in bacteria with soil or plant-associated lifestyles. The GlgE pathway is absent from most pathogenic bacteria, except for human and plant pathogens representing the *Pseudomonas*, *Mycobacterium*., *Burkholderia* and *Xanthomonas* genera. Although, mycobacterial  $\alpha$ -glucan plays a direct role in modulating virulence in human infections [322], *Pseudomonas*  $\alpha$ -glucan does not seem to play an active role in the infection process. Instead, it functions by determining susceptibility to environmental stresses (4.4.5).

The GlgE pathway is likely used as a widespread stress protection mechanism in environmental and commensal plant bacteria. Notable exceptions withstanding, where possessed by a pathogenic bacterium, this system may indirectly enhance infection phenotypes due to decreased susceptibility to abiotic stresses. I would predict that the GlgE pathway and the capacity to produce  $\alpha$ -glucan are likely to exist in bacteria whose lifestyles mean that they are likely to be exposed to extreme abiotic stresses like desiccation stress.

Similar to *Mycobacterium* spp. the existence of the GlgE pathway and therefore the function of  $\alpha$ -glucan in the *Burkholderia* genus may play a role in the outcome of infection

in humans. Interestingly *B. cepacia* is an important pathogen in the colonisation of the CF lung [323]. Like *P. aeruginosa*, the production of  $\alpha$ -glucan may decrease susceptibility to the dry environment of the CF lung. The function of  $\alpha$ -glucan should therefore be determined in these bacteria. To this end, the strategies/methodologies employed in this thesis provide a genetic framework for the decoupling and dissection of trehalose and  $\alpha$ -glucan biosynthesis, allowing the functions of these trehalose and  $\alpha$ -glucan to be elucidated individually in other bacteria possessing the GlgE pathway.

Furthermore, the existence of the GlgE pathway means that previous work investigating the function of bacterial trehalose must also be revisited because observations derived from altering the levels of trehalose production may also interfere with levels of  $\alpha$ -glucan, thereby implicating  $\alpha$ -glucan in roles typically attributed to trehalose. For example, high trehalose-producing organisms have been shown to possess high rates of desiccation resistance [150, 151]. Although I have shown that trehalose is not responsible for desiccation stress protection in *Pseudomonas* spp., the levels of trehalose could be indicative of  $\alpha$ -glucan levels and therefore the desiccation tolerance of an organism. Moreover, high trehalose-producing organisms have been shown to confer protection to plants against salt stress and drought when part of the rhizosphere [151, 324]. Further work must be conducted to determine whether this drought-protection ability is due to the production of trehalose or through the associated production of  $\alpha$ -glucan. It is predicted that environmental droughts will increase in frequency and severity in the future, resulting in loss of agricultural yield and the destruction of crops [325]. Desiccation-resistant bacteria could therefore be an attractive component of an engineered rhizosphere microbiome thereby becoming part of a strategy to promote drought tolerant plants [326]. If  $\alpha$ -glucan was the causal agent of this conferred drought protection, this in turn could be used as a formulation or product to enhance plant drought tolerance directly. However, this may also be utilised as a carbon source by commensal or pathogenic bacteria therefore the impact on the microbiome must be carefully considered.

## 6.8 Industrial application

Trehalose has multiple applications within the cosmetic, pharmaceutical and food industries [327], therefore, the optimisation of trehalose production has been a topic of recent research. *Pseudomonas* spp. have been shown to have industrial significance in the production of trehalose. Recombinant *P. putida* TreS was characterised and validated as a potential candidate for efficient trehalose production on an industrial scale [145, 307]. The

in-depth understanding of the trehalose metabolism and regulation in *Pseudomonas* spp. reported in this thesis may facilitate the bio-engineering of an enhanced trehalose-producing strain. For example, removing genes involved in trehalose degradation and the provision of conditions which optimise production of trehalose production. This establishes the potential of utilising *Pseudomonas* bacteria as whole-cell biocatalysts.

Alternatively, the understanding of trehalose and  $\alpha$ -glucan biosynthesis in *Pseudomonas* spp. may also play indirect roles in the industrial process itself. For example, during biotechnological applications, bacterial expression systems may be exposed to osmotic stress limiting cell density and yield. The understanding of trehalose and  $\alpha$ -glucan biosynthesis in *Pseudomonas* spp. may therefore aid in the bioengineering of improved stress-tolerant organisms for industrial applications [328].

Together, this work has shown the importance of  $\alpha$ -glucan biosynthesis in *Pseudomonas* spp. The existence of the novel GlgE pathway and the roles of trehalose,  $\alpha$ -glucan and alginate during water stress, as well as their complex global regulation, illustrates the environmental, industrial and clinical relevance of these systems. However, several questions remain unanswered. What is the molecular basis of  $\alpha$ -glucan function? Are there structural or functional differences between GlgA- and GlgE-synthesised  $\alpha$ -glucan? What are the regulatory elements which govern the switch between trehalose accumulation under osmotic stress or  $\alpha$ -glucan accumulation under desiccation stress? Finally, does  $\alpha$ -glucan function in the protection against any other stress in *Pseudomonas* spp.? Further work will answer these questions and further our understanding of the roles of  $\alpha$ -glucan biosynthesis in bacteria.

# Chapter 7: References

1. Green SK, Schroth MN, Cho JJ, Kominos SD, Vitanza-Jack VB: **Agricultural Plants and Soil as a Reservoir for *Pseudomonas aeruginosa***. *Applied Microbiology* 1974, **28**(6):987-991.
2. Berg G, Eberl L, Hartmann A: **The rhizosphere as a reservoir for opportunistic human pathogenic bacteria**. *Environmental Microbiology* 2005, **7**(11):1673-1685.
3. Khan NH, Ahsan M, Taylor WD, Kogure K: **Culturability and survival of marine, freshwater and clinical *Pseudomonas aeruginosa***. *Microbes and Environments* 2010, **25**(4):266-274.
4. Morris CE, Sands DC, Vinatzer BA, Glaux C, Guilbaud C, Buffiere A, Yan S, Dominguez H, Thompson BM: **The life history of the plant pathogen *Pseudomonas syringae* is linked to the water cycle**. *ISME Journal* 2008, **2**(3):321-334.
5. Kidd TJ, Gibson JS, Moss S, Greer RM, Cobbold RN, Wright JD, Ramsay KA, Grimwood K, Bell SC: **Clonal complex *Pseudomonas aeruginosa* in horses**. *Veterinary Microbiology* 2011, **149**(3-4):508-512.
6. Poonsuk K, Chuanchuen R: **Contribution of the MexXY multidrug efflux pump and other chromosomal mechanisms on aminoglycoside resistance in *Pseudomonas aeruginosa* isolates from canine and feline infections**. *The Journal of Veterinary Medical Science* 2012, **74**(12):1575-1582.
7. Vodovar N, Vinals M, Liehl P, Basset A, Degrouard J, Spellman P, Boccard F, Lemaitre B: ***Drosophila* host defense after oral infection by an entomopathogenic *Pseudomonas* species**. *Proceedings of the National Academy of Sciences of the United States of America* 2005, **102**(32):11414-11419.
8. Shigemura K, Arakawa S, Sakai Y, Kinoshita S, Tanaka K, Fujisawa M: **Complicated urinary tract infection caused by *Pseudomonas aeruginosa* in a single institution (1999–2003)**. *International Journal of Urology* 2006, **13**(5):538-542.
9. Gellatly SL, Hancock REW: ***Pseudomonas aeruginosa*: new insights into pathogenesis and host defenses**. *Pathogens and Disease* 2013, **67**(3):159-173.
10. Liu W-P, Tian Y-Q, Hai Y-T, Zheng Z-N, Cao Q-L: **Prevalence survey of nosocomial infections in the Inner Mongolia Autonomous Region of China [2012-2014]**. *Journal of Thoracic Disease* 2015, **7**(9):1650-1657.
11. Franzetti F, Cernuschi M, Esposito R, Moroni M: ***Pseudomonas* infections in patients with AIDS and AIDS-related complex**. *Journal of Internal Medicine* 1992, **231**(4):437-443.
12. Kielhofner M, Atmar RL, Hamill RJ, Musher DM: **Life-threatening *Pseudomonas aeruginosa* Infections in patients with human immunodeficiency virus infection**. *Clinical Infectious Diseases* 1992, **14**(2):403-411.
13. Chitkara YK, Feierabend TC: **Endogenous and exogenous infection with *Pseudomonas aeruginosa* in a burns unit**. *International Surgery* 1981, **66**(3):237-240.
14. Shirani KZ, Pruitt BA, Mason AD: **The influence of inhalation injury and pneumonia on burn mortality**. *Annals of Surgery* 1987, **205**(1):82-87.
15. Lange M, Hamahata A, Traber DL, Esechie A, Jonkam C, Bansal K, Nakano Y, Traber LD, Enkhbaatar P: **A murine model of sepsis following smoke inhalation injury**. *Biochemical and Biophysical Research Communications* 2010, **391**(3):1555-1560.
16. Williams BJ, Dehnbostel J, Blackwell TS: ***Pseudomonas aeruginosa*: host defence in lung diseases**. *Respirology* 2010, **15**(7):1037-1056.

17. Strateva T, Yordanov D: ***Pseudomonas aeruginosa* - a phenomenon of bacterial resistance.** *Journal of Medical Microbiology* 2009, **58**(Pt 9):1133-1148.
18. Pressler T, Bohmova C, Conway S, Dumcius S, Hjelte L, Høiby N, Kollberg H, Tümmler B, Vavrova V: **Chronic *Pseudomonas aeruginosa* infection definition: EuroCareCF Working Group report.** *Journal of Cystic Fibrosis* 2011, **10**:S75-S78.
19. Henry RL, Mellis CM, Petrovic L: **Mucoid *Pseudomonas aeruginosa* is a marker of poor survival in cystic fibrosis.** *Pediatric Pulmonology* 1992, **12**(3):158-161.
20. Lyczak JB, Cannon CL, Pier GB: **Establishment of *Pseudomonas aeruginosa* infection: lessons from a versatile opportunist.** *Microbes and Infection* 2000, **2**(9):1051-1060.
21. Costerton JW, Stewart PS, Greenberg EP: **Bacterial biofilms: a common cause of persistent infections.** *Science* 1999, **284**(5418):1318-1322.
22. Darouiche RO: **Treatment of infections associated with surgical implants.** *New England Journal of Medicine* 2004, **350**(14):1422-1429.
23. Govan JR, Deretic V: **Microbial pathogenesis in cystic fibrosis: mucoid *Pseudomonas aeruginosa* and *Burkholderia cepacia*.** *Microbiological Reviews* 1996, **60**(3):539-574.
24. Martin DW, Schurr MJ, Mudd MH, Govan JR, Holloway BW, Deretic V: **Mechanism of conversion to mucoidy in *Pseudomonas aeruginosa* infecting cystic fibrosis patients.** *Proceedings of the National Academy of Sciences* 1993, **90**(18):8377-8381.
25. Mathee K, McPherson CJ, Ohman DE: **Posttranslational control of the *algT* (*algU*)-encoded sigma22 for expression of the alginate regulon in *Pseudomonas aeruginosa* and localization of its antagonist proteins MucA and MucB (AlgN).** *Journal of Bacteriology* 1997, **179**(11):3711-3720.
26. Schurr MJ, Yu H, Martinez-Salazar JM, Boucher JC, Deretic V: **Control of AlgU, a member of the sigma E-like family of stress sigma factors, by the negative regulators MucA and MucB and *Pseudomonas aeruginosa* conversion to mucoidy in cystic fibrosis.** *Journal of Bacteriology* 1996, **178**(16):4997-5004.
27. Schaber JA, Triffo WJ, Suh SJ, Oliver JW, Hastert MC, Griswold JA, Auer M, Hamood AN, Rumbaugh KP: ***Pseudomonas aeruginosa* Forms Biofilms in Acute Infection Independent of Cell-to-Cell Signaling.** *Infection and Immunity* 2007, **75**(8):3715-3721.
28. Wolfgang MC, Jyot J, Goodman AL, Ramphal R, Lory S: ***Pseudomonas aeruginosa* regulates flagellin expression as part of a global response to airway fluid from cystic fibrosis patients.** *Proceedings of the National Academy of Sciences of the United States of America* 2004, **101**(17):6664-6668.
29. Hogardt M, Heesemann J: **Adaptation of *Pseudomonas aeruginosa* during persistence in the cystic fibrosis lung.** *International Journal of Medical Microbiology* 2010, **300**(8):557-562.
30. Angus BL, Carey AM, Caron DA, Kropinski AM, Hancock RE: **Outer membrane permeability in *Pseudomonas aeruginosa*: comparison of a wild-type with an antibiotic-supersusceptible mutant.** *Antimicrobial Agents and Chemotherapy* 1982, **21**(2):299-309.
31. Vahaboglu H, Oztürk R, Aygün G, Coşkun F, Yaman A, Kaygusuz A, Leblebicioglu H, Balik I, Aydın K, Otkun M: **Widespread detection of PER-1-type extended-spectrum beta-lactamases among nosocomial *Acinetobacter* and *Pseudomonas aeruginosa* isolates in**

- Turkey: a nationwide multicenter study.** *Antimicrobial Agents and Chemotherapy* 1997, **41**(10):2265-2269.
32. Jalal S, Wretling B: **Mechanisms of quinolone resistance in clinical strains of *Pseudomonas aeruginosa*.** *Microbial Drug Resistance* 1998, **4**(4):257-261.
  33. Nathwani D, Raman G, Sulham K, Gavaghan M, Menon V: **Clinical and economic consequences of hospital-acquired resistant and multidrug-resistant *Pseudomonas aeruginosa* infections: a systematic review and meta-analysis.** *Antimicrobial Resistance and Infection Control* 2014, **3**:32.
  34. Centres for Disease Control and Prevention: **Antibiotic Resistance Threats in the United States, 2013.** Atlanta: Centres for Disease Control and Prevention; 2013.
  35. Conway SP, Lee TW: **Prevention of chronic *Pseudomonas aeruginosa* infection in people with cystic fibrosis.** *Expert Review of Respiratory Medicine* 2009, **3**(4):349-361.
  36. Dwivedi M, Mishra A, Singh R, Azim A, Baronia A, Prasad K: **Nosocomial cross-transmission of *Pseudomonas aeruginosa* between patients in a tertiary intensive care unit.** *Indian Journal of Pathology and Microbiology* 2009, **52**(4):509-513.
  37. DiazGranados CA, Jones MY, Kongphet-Tran T, White N, Shapiro M, Wang YF, Ray SM, Blumberg HM: **Outbreak of *Pseudomonas aeruginosa* infection associated with contamination of a flexible bronchoscope.** *Infection Control and Hospital Epidemiology* 2009, **30**(6):550-555.
  38. Kominos SD, Copeland CE, Grosiak B: **Mode of transmission of *Pseudomonas aeruginosa* in a burn unit and an intensive care unit in a general hospital.** *Applied Microbiology* 1972, **23**(2):309-312.
  39. Clifton IJ, Peckham DG: **Defining routes of airborne transmission of *Pseudomonas aeruginosa* in people with cystic fibrosis.** *Expert Review of Respiratory Medicine* 2010, **4**(4):519-529.
  40. McCallum SJ, Gallagher MJ, Corkill JE, Hart CA, Ledson MJ, Walshaw MJ: **Spread of an epidemic *Pseudomonas aeruginosa* strain from a patient with cystic fibrosis (CF) to non-CF relatives.** *Thorax* 2002, **57**(6):559-560.
  41. Mohan K, Fothergill JL, Storrar J, Ledson MJ, Winstanley C, Walshaw MJ: **Transmission of *Pseudomonas aeruginosa* epidemic strain from a patient with cystic fibrosis to a pet cat.** *Thorax* 2008, **63**(9):839-840.
  42. Miriam RF, Fábio PS, Quézia M, Marcelo PNC, Paula NR, Louise C, Nilton L: **Zooanthroponotic transmission of drug-resistant *Pseudomonas aeruginosa*, Brazil.** *Emerging Infectious Disease journal* 2018, **24**(6):1160.
  43. Green SK, Schroth MN, Cho JJ, Kominos SK, Vitanza-jack VB: **Agricultural plants and soil as a reservoir for *Pseudomonas aeruginosa*.** *Applied Microbiology* 1974, **28**(6):987-991.
  44. Noura, Salih KM, Jusuf NH, Hamid AA, Yusoff WM: **High prevalence of *Pseudomonas* species in soil samples from Ternate island-Indonesia.** *Pakistan Journal of Biological Sciences* 2009, **12**(14):1036-1040.
  45. González AJ, Landeras E, Mendoza MC: **Pathovars of *Pseudomonas syringae* causing bacterial brown spot and halo blight in *Phaseolus vulgaris* L. are distinguishable by ribotyping.** *Applied and Environmental Microbiology* 2000, **66**(2):850-854.

46. Xin X-F, Kvitko B, He SY: ***Pseudomonas syringae*: what it takes to be a pathogen.** *Nature Reviews Microbiology* 2018, **16**:316.
47. Valencia-Botin AJ, Cisneros-Lopez ME: **A review of the studies and interactions of *Pseudomonas syringae* pathovars on wheat.** *International Journal of Agronomy* 2012, **2012**:5.
48. Preston GM: ***Pseudomonas syringae* pv. *tomato*: the right pathogen, of the right plant, at the right time.** *Molecular Plant Pathology* 2000, **1**(5):263-275.
49. Takikawa Y, Serizawa S, Ichikawa T, Tsuyumu S, Goto M: ***Pseudomonas syringae* pv. *actinidiae* pv. nov. The Causal Bacterium of Canker of Kiwifruit in Japan.** *Japanese Journal of Phytopathology* 1989, **55**(4):437-444.
50. Kiwifruit Vine Health: ***Psa* Statistics 29 September 2015.** In.: Available from: <http://www.kvh.org.nz/statistics>; 2015.
51. Vanneste JL: **The scientific, economic, and social impacts of the New Zealand outbreak of bacterial canker of kiwifruit (*Pseudomonas syringae* pv. *actinidiae*).** *Annual Review of Phytopathology* 2017, **55**(1):377-399.
52. Cameron A, Sarojini V: ***Pseudomonas syringae* pv. *actinidiae*: chemical control, resistance mechanisms and possible alternatives.** *Plant Pathology* 2014, **63**(1):1-11.
53. Morris CE, Monteil CL, Berge O: **The life history of *Pseudomonas syringae*: linking agriculture to earth system processes.** *Annual Review of Phytopathology* 2013, **51**:85-104.
54. Donati I, Cellini A, Buriani G, Mauri S, Kay C, Tacconi G, Spinelli F: **Pathways of flower infection and pollen-mediated dispersion of *Pseudomonas syringae* pv. *actinidiae*, the causal agent of kiwifruit bacterial canker.** *Horticulture Research* 2018, **5**(1):56.
55. Andrews JH, Harris RF: **The ecology and biogeography of microorganisms on plant surfaces.** *Annual Review of Phytopathology* 2000, **38**(1):145-180.
56. Lindow SE, Brandl MT: **Microbiology of the Phyllosphere.** *Applied and Environmental Microbiology* 2003, **69**(4):1875-1883.
57. Xin X-F, He SY: ***Pseudomonas syringae* pv. *tomato* DC3000: A model pathogen for probing disease susceptibility and hormone signaling in plants.** *Annual Review of Phytopathology* 2013, **51**(1):473-498.
58. Bender CL, Alarcon-Chaidez F, Gross DC: ***Pseudomonas syringae* phytotoxins: mode of action, regulation, and biosynthesis by peptide and polyketide synthetases.** *Microbiology and Molecular Biology Reviews* 1999, **63**(2):266-292.
59. Guo M, Block A, Bryan CD, Becker DF, Alfano JR: ***Pseudomonas syringae* catalases are collectively required for plant pathogenesis.** *Journal of Bacteriology* 2012, **194**(18):5054-5064.
60. Guo M, Tian F, Wamboldt Y, Alfano JR: **The majority of the type III effector inventory of *Pseudomonas syringae* pv. *tomato* DC3000 can suppress plant immunity.** *Molecular Plant-Microbe Interactions* 2009, **22**(9):1069-1080.
61. Zheng XY, Spivey NW, Zeng W, Liu PP, Fu ZQ, Klessig DF, He SY, Dong X: **Coronatine promotes *Pseudomonas syringae* virulence in plants by activating a signaling cascade that inhibits salicylic acid accumulation.** *Cell Host & Microbe* 2012, **11**(6):587-596.

62. Hirano SS, Upper CD: **Bacteria in the leaf ecosystem with emphasis on *Pseudomonas syringae*-a pathogen, ice nucleus, and epiphyte.** *Microbiology and Molecular Biology Reviews* 2000, **64**(3):624-653.
63. Pfeilmeier S, Caly DL, Malone JG: **Bacterial pathogenesis of plants: future challenges from a microbial perspective.** *Molecular Plant Pathology* 2016, **17**(8):1298-1313.
64. Beales N: **Adaptation of microorganisms to cold temperatures, weak acid preservatives, low pH, and osmotic stress: A review.** *Comprehensive Reviews in Food Science and Food Safety* 2004, **3**(1):1-20.
65. Pérez V, Hengst M, Kurte L, Dorador C, Jeffrey WH, Wattiez R, Molina V, Matallana-Surget S: **Bacterial survival under extreme UV radiation: A comparative proteomics study of *Rhodobacter* sp., isolated from high altitude wetlands in Chile.** *Frontiers in Microbiology* 2017, **8**:1173-1173.
66. Seshasayee ASN, Bertone P, Fraser GM, Luscombe NM: **Transcriptional regulatory networks in bacteria: from input signals to output responses.** *Current Opinion in Microbiology* 2006, **9**(5):511-519.
67. Majeed A, Muhammad Z, Ahmad H: **Plant growth promoting bacteria: Role in soil improvement, abiotic and biotic stress management of crops.** *Plant Cell Reports* 2018, **37**(12):1599-1609.
68. Bauer MA, Kainz K, Carmona-Gutierrez D, Madeo F: **Microbial wars: Competition in ecological niches and within the microbiome.** *Microbial Cell* 2018, **5**(5):215-219.
69. Leinweber A, Weigert M, Kümmerli R: **The bacterium *Pseudomonas aeruginosa* senses and gradually responds to interspecific competition for iron.** *Evolution; International Journal Of Organic Evolution* 2018, **72**(7):1515-1528.
70. Powers MJ, Sanabria-Valentín E, Bowers AA, Shank EA: **Inhibition of cell differentiation in *Bacillus subtilis* by *Pseudomonas protegens*.** *Journal of Bacteriology* 2015, **197**(13):2129-2138.
71. Murdoch SL, Trunk K, English G, Fritsch MJ, Pourkarimi E, Coulthurst SJ: **The opportunistic pathogen *Serratia marcescens* utilizes type VI secretion to target bacterial competitors.** *Journal of Bacteriology* 2011, **193**(21):6057-6069.
72. Stockwell VO, Loper JE: **The sigma factor RpoS is required for stress tolerance and environmental fitness of *Pseudomonas fluorescens* Pf-5.** *Microbiology* 2005, **151**(Pt 9):3001-3009.
73. Kurz M, Burch AY, Seip B, Lindow SE, Gross H: **Genome-driven investigation of compatible solute biosynthesis pathways of *Pseudomonas syringae* pv. *syringae* and their contribution to water stress tolerance.** *Applied and Environmental Microbiology* 2010, **76**(16):5452-5462.
74. Freeman BC, Chen C, Beattie GA: **Identification of the trehalose biosynthetic loci of *Pseudomonas syringae* and their contribution to fitness in the phyllosphere.** *Environmental Microbiology* 2010, **12**(6):1486-1497.
75. Bhagirath AY, Li Y, Somayajula D, Dadashi M, Badr S, Duan K: **Cystic fibrosis lung environment and *Pseudomonas aeruginosa* infection.** *BMC Pulmonary Medicine* 2016, **16**(1):174.

76. Imlay JA: **The molecular mechanisms and physiological consequences of oxidative stress: lessons from a model bacterium.** *Nature Reviews Microbiology* 2013, **11**:443.
77. Imlay JA: **Cellular defenses against superoxide and hydrogen peroxide.** *Annual Review of Biochemistry* 2008, **77**(1):755-776.
78. Liochev SI, Fridovich I: **Fumarase C, the stable fumarase of *Escherichia coli*, is controlled by the *soxRS* regulon.** *Proceedings of the National Academy of Sciences* 1992, **89**(13):5892-5896.
79. Poole K: **Bacterial stress responses as determinants of antimicrobial resistance.** *Journal of Antimicrobial Chemotherapy* 2012, **67**(9):2069-2089.
80. Kimmitt PT, Harwood CR, Barer MR: **Toxin gene expression by shiga toxin-producing *Escherichia coli*: the role of antibiotics and the bacterial SOS response.** *Emerging Infectious Diseases* 2000, **6**(5):458-465.
81. Lee AK, Detweiler CS, Falkow S: **OmpR Regulates the Two-Component System SsrA-SsrB in *Salmonella* Pathogenicity Island 2.** *Journal of Bacteriology* 2000, **182**(3):771-781.
82. Beaber JW, Hochhut B, Waldor MK: **SOS response promotes horizontal dissemination of antibiotic resistance genes.** *Nature* 2004, **427**(6969):72-74.
83. Miller C, Thomsen LE, Gaggero C, Mosseri R, Ingmer H, Cohen SN: **SOS response induction by beta-lactams and bacterial defense against antibiotic lethality.** *Science* 2004, **305**(5690):1629-1631.
84. Keren I, Shah D, Spoering A, Kaldalu N, Lewis K: **Specialized persister cells and the mechanism of multidrug tolerance in *Escherichia coli*.** *Journal of Bacteriology* 2004, **186**(24):8172-8180.
85. Cramer GR, Urano K, Delrot S, Pezzotti M, Shinozaki K: **Effects of abiotic stress on plants: a systems biology perspective.** *BMC Plant Biology* 2011, **11**(1):163.
86. Glick BR: **Modulation of plant ethylene levels by the bacterial enzyme ACC deaminase.** *FEMS Microbiology Letters* 2005, **251**(1):1-7.
87. Ulrich DEM, Sevanto S, Ryan M, Albright MBN, Johansen RB, Dunbar JM: **Plant-microbe interactions before drought influence plant physiological responses to subsequent severe drought.** *Scientific Reports* 2019, **9**(1):249.
88. Chandra D, Srivastava R, Glick BR, Sharma AK: **Drought-tolerant *Pseudomonas* spp. Improve the growth performance of finger millet (*Eleusine coracana* (L.) Gaertn.) under non-stressed and drought-stressed conditions.** *Pedosphere* 2018, **28**(2):227-240.
89. Niu X, Song L, Xiao Y, Ge W: **Drought-tolerant plant growth-promoting rhizobacteria associated with foxtail millet in a semi-arid agroecosystem and their potential in alleviating drought stress.** *Frontiers in Microbiology* 2018, **8**(2580).
90. Wood JM: **Bacterial responses to osmotic challenges.** *The Journal of General Physiology* 2015, **145**(5):381-388.
91. Potts M: **Desiccation tolerance of prokaryotes.** *Microbiological Reviews* 1994, **58**(4):755-805.
92. Holden PA: **Biofilms in unsaturated environments.** In: *Methods in Enzymology*. Edited by Doyle RJ, vol. 337: Academic Press; 2001: 125-143.

93. Vriezen JAC, de Bruijn FJ, Nüsslein K: **Responses of Rhizobia to Desiccation in Relation to Osmotic Stress, Oxygen, and Temperature.** *Applied and Environmental Microbiology* 2007, **73**(11):3451-3459.
94. Mary P, Ochin D, Tailliez R: **Rates of drying and survival of *Rhizobium meliloti* strains during storage at different relative humidities.** *Applied and Environmental Microbiology* 1985, **50**(2):207-211.
95. Asada S, Takano M, Shibasaki I: **Deoxyribonucleic acid strand breaks during drying of *Escherichia coli* on a hydrophobic filter membrane.** *Applied and Environmental Microbiology* 1979, **37**(2):266-273.
96. Kosanke JW, Osburn RM, Shuppe GI, Smith RS: **Slow Rehydration Improves the Recovery of Dried Bacterial Populations.** *Canadian Journal of Microbiology* 1992, **38**(6):520-525.
97. Van De Mortel M, Halverson LJ: **Cell envelope components contributing to biofilm growth and survival of *Pseudomonas putida* in low-water-content habitats.** *Molecular Microbiology* 2004, **52**(3):735-750.
98. Deng X, Li Z, Zhang W: **Transcriptome sequencing of *Salmonella enterica* serovar Enteritidis under desiccation and starvation stress in peanut oil.** *Food Microbiology* 2012, **30**(1):311-315.
99. Leggett MJ, McDonnell G, Denyer SP, Setlow P, Maillard J-Y: **Bacterial spore structures and their protective role in biocide resistance.** *Journal of Applied Microbiology* 2012, **113**(3):485-498.
100. Setlow P: **Spores of *Bacillus subtilis*: their resistance to and killing by radiation, heat and chemicals.** *Journal of Applied Microbiology* 2006, **101**(3):514-525.
101. McBride MJ, Ensign JC: **Effects of intracellular trehalose content on *Streptomyces griseus* spores.** *Journal of Bacteriology* 1987, **169**(11):4995-5001.
102. Thomas P: **Isolation of an ethanol-tolerant endospore-forming Gram-negative *Brevibacillus* sp. as a covert contaminant in grape tissue cultures.** *Journal of Applied Microbiology* 2006, **101**(4):764-774.
103. Battista JR, Park M-J, McLemore AE: **Inactivation of two homologues of proteins presumed to be involved in the desiccation tolerance of plants sensitizes *Deinococcus radiodurans* R1 to desiccation.** *Cryobiology* 2001, **43**(2):133-139.
104. Reyes JL, Rodrigo M-J, Colmenero-Flores JM, Gil J-V, Garay-Arroyo A, Campos F, Salamini F, Bartels D, Covarrubias AA: **Hydrophilins from distant organisms can protect enzymatic activities from water limitation effects *in vitro*.** *Plant, Cell & Environment* 2005, **28**(6):709-718.
105. Chakrabortee S, Boschetti C, Walton LJ, Sarkar S, Rubinsztein DC, Tunnacliffe A: **Hydrophilic protein associated with desiccation tolerance exhibits broad protein stabilization function.** *Proceedings of the National Academy of Sciences* 2007, **104**(46):18073-18078.
106. D'Souza-Ault MR, Smith LT, Smith GM: **Roles of N-acetylglutaminylglutamine amide and glycine betaine in adaptation of *Pseudomonas aeruginosa* to osmotic stress.** *Applied and Environmental Microbiology* 1993, **59**(2):473-478.

107. Freeman BC, Chen C, Yu X, Nielsen L, Peterson K, Beattie GA: **Physiological and transcriptional responses to osmotic stress of two *Pseudomonas syringae* strains that differ in their epiphytic fitness and osmotolerance.** *Journal of Bacteriology* 2013.
108. Roychoudhury A, Bieker A, Haussinger D, Oesterhelt F: **Membrane protein stability depends on the concentration of compatible solutes--a single molecule force spectroscopic study.** *Biological Chemistry* 2013, **394**(11):1465-1474.
109. Killian MS, Taylor AJ, Castner DG: **Stabilization of dry protein coatings with compatible solutes.** *Biointerphases* 2018, **13**(6):06e401.
110. Hinch DK, Hagemann M: **Stabilization of model membranes during drying by compatible solutes involved in the stress tolerance of plants and microorganisms.** *The Biochemical journal* 2004, **383**(Pt 2):277-283.
111. Zeidler S, Muller V: **The role of compatible solutes in desiccation resistance of *Acinetobacter baumannii*.** *MicrobiologyOpen* 2019, **8**(5):e00740.
112. Reina-Bueno M, Argandoña M, Salvador M, Rodríguez-Moya J, Iglesias-Guerra F, Csonka LN, Nieto JJ, Vargas C: **Role of Trehalose in Salinity and Temperature Tolerance in the Model Halophilic Bacterium *Chromohalobacter salexigens*.** *PLoS ONE* 2012, **7**(3):e33587.
113. Reina-Bueno M, Argandoña M, Nieto JJ, Hidalgo-García A, Iglesias-Guerra F, Delgado MJ, Vargas C: **Role of trehalose in heat and desiccation tolerance in the soil bacterium *Rhizobium etli*.** *BMC Microbiology* 2012, **12**(1):207.
114. Hoffmann T, Bremer E: **Protection of *Bacillus subtilis* against cold stress via compatible-solute acquisition.** *Journal of Bacteriology* 2011, **193**(7):1552-1562.
115. Tapia H, Young L, Fox D, Bertozzi CR, Koshland D: **Increasing intracellular trehalose is sufficient to confer desiccation tolerance to *Saccharomyces cerevisiae*.** *Proceedings of the National Academy of Sciences of the United States of America* 2015, **112**(19):6122-6127.
116. Lucht JM, Bremer E: **Adaptation of *Escherichia coli* to high osmolarity environments: osmoregulation of the high-affinity glycine betaine transport system proU.** *FEMS Microbiology Reviews* 1994, **14**(1):3-20.
117. Kang Y, Hwang I: **Glutamate uptake is important for osmoregulation and survival in the rice pathogen *Burkholderia glumae*.** *PLoS ONE* 2018, **13**(1):e0190431.
118. Botsford JL, Lewis TA: **Osmoregulation in *Rhizobium meliloti*: Production of glutamic acid in response to osmotic stress.** *Applied and Environmental Microbiology* 1990, **56**(2):488-494.
119. Bogino PC, Oliva MdM, Sorroche FG, Giordano W: **The role of bacterial biofilms and surface components in plant-bacterial associations.** *International Journal of Molecular Sciences* 2013, **14**(8):15838-15859.
120. Waite RD, Paccanaro A, Papakonstantinou A, Hurst JM, Saqi M, Littler E, Curtis MA: **Clustering of *Pseudomonas aeruginosa* transcriptomes from planktonic cultures, developing and mature biofilms reveals distinct expression profiles.** *BMC Genomics* 2006, **7**(1):1-14.
121. Waite RD, Papakonstantinou A, Littler E, Curtis MA: **Transcriptome analysis of *Pseudomonas aeruginosa* growth: comparison of gene expression in planktonic cultures and developing and mature biofilms.** *Journal of Bacteriology* 2005, **187**.

122. Mah TF, O'Toole GA: **Mechanisms of biofilm resistance to antimicrobial agents.** *Trends in Microbiology* 2001, **9**(1):34-39.
123. Batoni G, Maisetta G, Esin S: **Antimicrobial peptides and their interaction with biofilms of medically relevant bacteria.** *Biochimica et Biophysica Acta (BBA) - Biomembranes* 2016, **1858**(5):1044-1060.
124. Yang L, Hu Y, Liu Y, Zhang J, Ulstrup J, Molin S: **Distinct roles of extracellular polymeric substances in *Pseudomonas aeruginosa* biofilm development.** *Environmental Microbiology* 2011, **13**(7):1705-1717.
125. Laue H, Schenk A, Li H, Lambertsen L, Neu TR, Molin S, Ullrich MS: **Contribution of alginate and levan production to biofilm formation by *Pseudomonas syringae*.** *Microbiology* 2006, **152**(Pt 10):2909-2918.
126. Mann EE, Wozniak DJ: ***Pseudomonas* biofilm matrix composition and niche biology.** *FEMS Microbiology Reviews* 2012, **36**(4):893-916.
127. Wai SN, Mizunoe Y, Takade A, Kawabata SI, Yoshida SI: ***Vibrio cholerae* O1 strain TSI-4 produces the exopolysaccharide materials that determine colony morphology, stress resistance, and biofilm formation.** *Applied and Environmental Microbiology* 1998, **64**(10):3648-3655.
128. Roberson EB, Firestone MK: **Relationship between desiccation and exopolysaccharide production in a soil *Pseudomonas* sp.** *Applied and Environmental Microbiology* 1992, **58**(4):1284-1291.
129. Schnider-Keel U, Lejbølle KB, Baehler E, Haas D, Keel C: **The sigma factor AlgU (AlgT) controls exopolysaccharide production and tolerance towards desiccation and osmotic stress in the biocontrol agent *Pseudomonas fluorescens* CHA0.** *Applied and Environmental Microbiology* 2001, **67**(12):5683-5693.
130. Chang W-S, van de Mortel M, Nielsen L, Nino de Guzman G, Li X, Halverson LJ: **Alginate production by *Pseudomonas putida* creates a hydrated microenvironment and contributes to biofilm architecture and stress tolerance under water-limiting conditions.** *Journal of Bacteriology* 2007, **189**(22):8290-8299.
131. Li X, Nielsen L, Nolan C, Halverson LJ: **Transient alginate gene expression by *Pseudomonas putida* biofilm residents under water-limiting conditions reflects adaptation to the local environment.** *Environmental Microbiology* 2010, **12**(6):1578-1590.
132. Yu X, Lund SP, Scott RA, Greenwald JW, Records AH, Nettleton D, Lindow SE, Gross DC, Beattie GA: **Transcriptional responses of *Pseudomonas syringae* to growth in epiphytic versus apoplastic leaf sites.** *Proceedings of the National Academy of Sciences* 2013, **110**(5):E425-E434.
133. Pacheco-Leyva I, Guevara Pezoa F, Diaz-Barrera A: **Alginate biosynthesis in *Azotobacter vinelandii*: Overview of molecular mechanisms in connection with the oxygen availability.** *International Journal of Polymer Science* 2016, **2016**:12.
134. Franklin MJ, Nivens DE, Weadge JT, Howell PL: **Biosynthesis of the *Pseudomonas aeruginosa* extracellular polysaccharides, alginate, Pel, and Psl.** *Frontiers in microbiology* 2011, **2**:167-167.
135. Schmid J, Sieber V, Rehm B: **Bacterial exopolysaccharides: biosynthesis pathways and engineering strategies.** *Frontiers in Microbiology* 2015, **6**(496).

136. Yang J, Toyofuku M, Sakai R, Nomura N: **Influence of the alginate production on cell-to-cell communication in *Pseudomonas aeruginosa* PAO1.** *Environmental Microbiology Reports* 2017, **9**(3):239-249.
137. SkjÅk-Bræk G, Paoletti S, Gianferrara T: **Selective acetylation of mannuronic acid residues in calcium alginate gels.** *Carbohydrate Research* 1989, **185**(1):119-129.
138. Gacesa P: **Bacterial alginate biosynthesis - recent progress and future prospects.** *Microbiology* 1998, **144**(5):1133-1143.
139. Elbein AD, Pan YT, Pastuszak I, Carroll D: **New insights on trehalose: a multifunctional molecule.** *Glycobiology* 2003, **13**(4):17R-27R.
140. Leloir LF, Cabib E: **The enzymic synthesis of trehalose phosphate.** *Journal of the American Chemical Society* 1953, **75**(21):5445-5446.
141. Piazza A, Zimaro T, Garavaglia BS, Ficarra FA, Thomas L, Maronedze C, Feil R, Lunn JE, Gehring C, Ottado J *et al*: **The dual nature of trehalose in citrus canker disease: a virulence factor for *Xanthomonas citri* subsp. *citri* and a trigger for plant defence responses.** *Journal of Experimental Botany* 2015, **66**(9):2795-2811.
142. Patist A, Zoerb H: **Preservation mechanisms of trehalose in food and biosystems.** *Colloids and Surfaces B: Biointerfaces* 2005, **40**(2):107-113.
143. Ohtake S, Wang YJ: **Trehalose: current use and future applications.** *Journal of Pharmaceutical Sciences* 2011, **100**(6):2020-2053.
144. Wang L, Huang R, Gu G, Fang H: **Optimization of trehalose production by a novel strain *Brevibacterium* sp. SY361.** *Journal of Basic Microbiology* 2008, **48**(5):410-415.
145. Wang T, Jia S, Dai K, Liu H, Wang R: **Cloning and expression of a trehalose synthase from *Pseudomonas putida* KT2440 for the scale-up production of trehalose from maltose.** *Canadian Journal of Microbiology* 2014, **60**(9):599-604.
146. Iordachescu M, Imai R: **Trehalose biosynthesis in response to abiotic stresses.** *Journal of Integrative Plant Biology* 2008, **50**(10):1223-1229.
147. Ruhel R, Kataria R, Choudhury B: **Trends in bacterial trehalose metabolism and significant nodes of metabolic pathway in the direction of trehalose accumulation.** *Microbial Biotechnology* 2013, **6**(5):493-502.
148. Wiemken A: **Trehalose in yeast, stress protectant rather than reserve carbohydrate.** *Antonie van Leeuwenhoek* 1990, **58**(3):209-217.
149. Larsen PI, Sydnes LK, Landfald B, Strøm AR: **Osmoregulation in *Escherichia coli* by accumulation of organic osmolytes: betaines, glutamic acid, and trehalose.** *Archives of Microbiology* 1987, **147**(1):1-7.
150. Zhang Q, Yan T: **Correlation of intracellular trehalose concentration with desiccation resistance of soil *Escherichia coli* populations.** *Applied and Environmental Microbiology* 2012, **78**(20):7407-7413.
151. Vílchez JI, García-Fontana C, Román-Naranjo D, González-López J, Manzanera M: **Plant Drought Tolerance Enhancement by Trehalose Production of Desiccation-Tolerant Microorganisms.** *Frontiers in Microbiology* 2016, **7**:1577.

152. Murphy HN, Stewart GR, Mischenko VV, Apt AS, Harris R, McAlister MS, Driscoll PC, Young DB, Robertson BD: **The OtsAB pathway is essential for trehalose biosynthesis in *Mycobacterium tuberculosis***. *The Journal of Biological Chemistry* 2005, **280**(15):14524-14529.
153. Kalscheuer R, Syson K, Veeraraghavan U, Weinrick B, Biermann KE, Liu Z, Sacchettini JC, Besra G, Bornemann S, Jacobs WR: **Self-poisoning of *Mycobacterium tuberculosis* by targeting GlgE in an alpha-glucan pathway**. *Nature Chemical Biology* 2010, **6**(5):376-384.
154. De Smet KAL, Weston A, Brown IN, Young DB, Robertson BD: **Three pathways for trehalose biosynthesis in *mycobacteria***. *Microbiology* 2000, **146**(1):199-208.
155. Giaever HM, Styrvold OB, Kaasen I, Strom AR: **Biochemical and genetic characterization of osmoregulatory trehalose synthesis in *Escherichia coli***. *Journal of Bacteriology* 1988, **170**(6):2841-2849.
156. Nishimoto T, Nakano M, Ikegami S, Chaen H, Fukuda S, Sugimoto T, Kurimoto M, Tsujisaka Y: **Existence of a novel enzyme converting maltose into trehalose**. *Bioscience, Biotechnology, and Biochemistry* 1995, **59**(11):2189-2190.
157. Miah F, Koliwer-Brandl H, Rejzek M, Field Robert A, Kalscheuer R, Bornemann S: **Flux through trehalose synthase flows from trehalose to the alpha anomer of maltose in *Mycobacteria***. *Chemistry & Biology* 2013, **20**(4):487-493.
158. Maruta K, Nakada T, Kubota M, Chaen H, Sugimoto T, Kurimoto M, Tsujisaka Y: **Formation of trehalose from maltooligosaccharides by a novel enzymatic system**. *Bioscience, Biotechnology, and Biochemistry* 1995, **59**(10):1829-1834.
159. Avonce N, Mendoza-Vargas A, Morett E, Iturriaga G: **Insights on the evolution of trehalose biosynthesis**. *BMC Evolutionary Biology* 2006, **6**:109-109.
160. Edstrom RD: **Structure of a low molecular weight form of glycogen isolated from the liver in a case of glycogen storage disease**. *Journal of Biological Chemistry* 1972, **247**(5):1360-1367.
161. Syson K, Stevenson CEM, Miah F, Barclay JE, Tang M, Gorelik A, Rashid AM, Lawson DM, Bornemann S: **Ligand-bound structures and site-directed mutagenesis identify the acceptor and secondary binding sites of *Streptomyces coelicolor* maltosyltransferase GlgE**. *Journal of Biological Chemistry* 2016, **291**(41):21531-21540.
162. Preiss J: **Bacterial glycogen synthesis and its regulation**. *Annual Review of Microbiology* 1984, **38**:419-458.
163. Espada J: **Enzymic synthesis of adenosine diphosphate glucose from glucose 1-phosphate and adenosine triphosphate**. *Journal of Biological Chemistry* 1962, **237**(12):3577-3581.
164. Baecker PA, Furlong CE, Preiss J: **Biosynthesis of bacterial glycogen. Primary structure of *Escherichia coli* ADP-glucose synthetase as deduced from the nucleotide sequence of the *glgC* gene**. *Journal of Biological Chemistry* 1983, **258**(8):5084-5088.
165. Fox J, Kawaguchi K, Greenberg E, Preiss J: **Biosynthesis of bacterial glycogen. Purification and properties of the *Escherichia coli* B ADPglucose:1,4-alpha-D-glucan 4-alpha-glucosyltransferase**. *Biochemistry* 1976, **15**(4):849-857.
166. Kumar A, Larsen CE, Preiss J: **Biosynthesis of bacterial glycogen. Primary structure of *Escherichia coli* ADP-glucose:alpha-1,4-glucan, 4-glucosyltransferase as deduced from**

- the nucleotide sequence of the *glgA* gene.** *The Journal of Biological Chemistry* 1986, **261**(34):16256-16259.
167. Lerner J: **The action of branching enzymes on outer chains of glycogen.** *Journal of Biological Chemistry* 1953, **202**(2):491-503.
168. Abad MC, Binderup K, Rios-Steiner J, Arni RK, Preiss J, Geiger JH: **The X-ray crystallographic structure of *Escherichia coli* branching enzyme.** *The Journal of Biological Chemistry* 2002, **277**(44):42164-42170.
169. Dauvillee D, Kinderf IS, Li Z, Kosar-Hashemi B, Samuel MS, Rampling L, Ball S, Morell MK: **Role of the *Escherichia coli glgX* gene in glycogen metabolism.** *Journal of Bacteriology* 2005, **187**(4):1465-1473.
170. Alonso-Casajús N, Dauvillée D, Viale AM, Muñoz FJ, Baroja-Fernández E, Morán-Zorzano MT, Eydallin G, Ball S, Pozueta-Romero J: **Glycogen Phosphorylase, the Product of the *glgP* Gene, Catalyzes Glycogen Breakdown by Removing Glucose Units from the Nonreducing Ends in *Escherichia coli*.** *Journal of Bacteriology* 2006, **188**(14):5266-5272.
171. Chandra G, Chater KF, Bornemann S: **Unexpected and widespread connections between bacterial glycogen and trehalose metabolism.** *Microbiology* 2011, **157**(Pt 6):1565-1572.
172. Bornemann S:  **$\alpha$ -Glucan biosynthesis and the GlgE pathway in *Mycobacterium tuberculosis*.** *Biochemical Society Transactions* 2016, **44**(1):68-73.
173. Syson K, Stevenson CEM, Rejzek M, Fairhurst SA, Nair A, Bruton CJ, Field RA, Chater KF, Lawson DM, Bornemann S: **Structure of *Streptomyces maltosyltransferase GlgE*, a homologue of a genetically validated anti-tuberculosis target.** *Journal of Biological Chemistry* 2011, **286**(44):38298-38310.
174. Roy R, Usha V, Kermani A, Scott DJ, Hyde EI, Besra GS, Alderwick LJ, Fütterer K: **Synthesis of alpha-glucan in *mycobacteria* involves a hetero-octameric complex of trehalose synthase TreS and Maltokinase Pep2.** *ACS Chemical Biology* 2013, **8**(10):2245-2255.
175. Elbein AD, Pastuszak I, Tackett AJ, Wilson T, Pan YT: **Last step in the conversion of trehalose to glycogen: a mycobacterial enzyme that transfers maltose from maltose 1-phosphate to glycogen.** *Journal of Biological Chemistry* 2010, **285**(13):9803-9812.
176. Cywes C, Hoppe HC, Daffé M, Ehlers MR: **Nonopsonic binding of *Mycobacterium tuberculosis* to complement receptor type 3 is mediated by capsular polysaccharides and is strain dependent.** *Infection and Immunity* 1997, **65**(10):4258-4266.
177. Sambou T, Dinadayala P, Stadthagen G, Barilone N, Bordat Y, Constant P, Levillain F, Neyrolles O, Gicquel B, Lemassu A *et al*: **Capsular glucan and intracellular glycogen of *Mycobacterium tuberculosis*: biosynthesis and impact on the persistence in mice.** *Molecular Microbiology* 2008, **70**(3):762-774.
178. Stover CK, Pham XQ, Erwin AL, Mizoguchi SD, Warrenner P, Hickey MJ, Brinkman FS, Hufnagle WO, Kowalik DJ, Lagrou M *et al*: **Complete genome sequence of *Pseudomonas aeruginosa* PA01, an opportunistic pathogen.** *Nature* 2000, **406**.
179. Buell CR, Joardar V, Lindeberg M, Selengut J, Paulsen IT, Gwinn ML, Dodson RJ, Deboy RT, Durkin AS, Kolonay JF *et al*: **The complete genome sequence of the *Arabidopsis* and tomato pathogen *Pseudomonas syringae* pv. *tomato* DC3000.** *Proceedings of the National Academy of Sciences of the United States of America* 2003, **100**(18):10181-10186.

180. Djonović S, Urbach JM, Drenkard E, Bush J, Feinbaum R, Ausubel JL, Traficante D, Risec M, Kocks C, Fischbach MA *et al*: **Trehalose biosynthesis promotes *Pseudomonas aeruginosa* pathogenicity in plants.** *PLoS Pathogens* 2013, **9**(3):e1003217.
181. Winsor GL, Griffiths EJ, Lo R, Dhillon BK, Shay JA, Brinkman FS: **Enhanced annotations and features for comparing thousands of *Pseudomonas* genomes in the *Pseudomonas* genome database.** *Nucleic Acids Research* 2016, **44**(D1):D646-653.
182. Padilla L, Morbach S, Krämer R, Agosin E: **Impact of heterologous expression of *Escherichia coli* UDP-glucose pyrophosphorylase on trehalose and glycogen synthesis in *Corynebacterium glutamicum*.** *Applied and Environmental Microbiology* 2004, **70**(7):3845-3854.
183. Koliwer-Brandl H, Syson K, van de Weerd R, Chandra G, Appelmelk B, Alber M, Ioerger TR, Jacobs WR, Jr., Geurtsen J, Bornemann S *et al*: **Metabolic network for the biosynthesis of intra- and extracellular  $\alpha$ -glucans required for virulence of *Mycobacterium tuberculosis*.** *PLoS Pathogens* 2016, **12**(8):e1005768.
184. Aspedon A, Palmer K, Whiteley M: **Microarray analysis of the osmotic stress response in *Pseudomonas aeruginosa*.** *Journal of Bacteriology* 2006, **188**.
185. Miller JH: **Experiments in molecular genetics:** Cold Spring Harbor Laboratory; 1972.
186. Sambrook J, Fritsch EF, Maniatis T: **Molecular Cloning: A Laboratory Manual:** Cold Spring Harbor Laboratory; 1989.
187. Voisard C, Bull CT, Keel C, Laville J, Maurhofer M, Schnider U, D efago G, Haas D: **Biocontrol of Root Diseases by *Pseudomonas fluorescens* CHA0: Current Concepts and Experimental Approaches.** In: *Molecular Ecology of Rhizosphere Microorganisms.* Wiley-VCH Verlag GmbH; 1994: 67-89.
188. Manzanera M, Garc a-Fontana C, V lchez JI, Narv ez-Reinaldo JJ, Gonz alez-L pez J: **Genome sequence of *Microbacterium* sp. Strain 3J1, a highly desiccation-tolerant bacterium that promotes plant growth.** *Genome Announcements* 2015, **3**(4):e00713-00715.
189. Heeb S, Blumer C, Haas D: **Regulatory RNA as mediator in GacA/RsmA-dependent global control of exoproduct formation in *Pseudomonas fluorescens* CHA0.** *Journal of Bacteriology* 2002, **184**(4):1046-1056.
190. Choi K-H, Gaynor JB, White KG, Lopez C, Bosio CM, Karkhoff-Schweizer RR, Schweizer HP: **A Tn7-based broad-range bacterial cloning and expression system.** *Nature Methods* 2005, **2**:443.
191. Choi KH, Schweizer HP: **mini-Tn7 insertion in bacteria with single attTn7 sites: example *Pseudomonas aeruginosa*.** *Nature Protocols* 2006, **1**(1):153-161.
192. Choi KH, Kumar A, Schweizer HP: **A 10-min method for preparation of highly electrocompetent *Pseudomonas aeruginosa* cells: application for DNA fragment transfer between chromosomes and plasmid transformation.** *Journal of Microbiological Methods* 2006, **64**(3):391-397.
193. Choi K-H, Mima T, Casart Y, Rholl D, Kumar A, Beacham IR, Schweizer HP: **Genetic tools for select-agent-compliant manipulation of *Burkholderia pseudomallei*.** *Applied and Environmental Microbiology* 2008, **74**(4):1064-1075.

194. Usui T, Yokoyama M, Yamaoka N, Matsuda K, Tuzimura K, Sugiyama H, Seto S: **Proton magnetic resonance spectra of D-gluco-oligosaccharides and D-glucans.** *Carbohydrate Research* 1974, **33**(1):105-116.
195. Cross M, Biberacher S, Park S-Y, Rajan S, Korhonen P, Gasser RB, Kim J-S, Coster MJ, Hofmann A: **Trehalose 6-phosphate phosphatases of *Pseudomonas aeruginosa*.** *The FASEB Journal* 2018, **32**(10):5470-5482.
196. Rashid AM, Batey SFD, Syson K, Koliwer-Brandl H, Miah F, Barclay JE, Findlay KC, Nartowski KP, Khimyak YZ, Kalscheuer R *et al*: **Assembly of  $\alpha$ -Glucan by GlgE and GlgB in *Mycobacteria* and *Streptomyces*.** *Biochemistry* 2016, **55**(23):3270-3284.
197. Bailey JM, Whelan WJ: **Physical properties of starch. I. Relationship between iodine stain and chain length.** *Journal of Biological Chemistry* 1961, **236**:969-973.
198. Berbis MA, Sanchez-Puelles JM, Canada FJ, Jimenez-Barbero J: **Structure and function of prokaryotic UDP-glucose pyrophosphorylase, a drug target candidate.** *Current Medicinal Chemistry* 2015, **22**(14):1687-1697.
199. Korte J, Alber M, Trujillo CM, Syson K, Koliwer-Brandl H, Deenen R, Köhrer K, DeJesus MA, Hartman T, Jacobs WR, Jr. *et al*: **Trehalose-6-phosphate-mediated toxicity determines essentiality of OtsB2 in *Mycobacterium tuberculosis* in vitro and in mice.** *PLOS Pathogens* 2016, **12**(12):e1006043.
200. Roy R, Usha V, Kermani A, Scott DJ, Hyde EI, Besra GS, Alderwick LJ, Fütterer K: **Synthesis of  $\alpha$ -glucan in *mycobacteria* involves a hetero-octameric complex of trehalose synthase TreS and Maltokinase Pep2.** *ACS Chemical Biology* 2013, **8**(10):2245-2255.
201. De Goffau MC, Yang X, Van Dijl JM, Harmsen HJM: **Bacterial pleomorphism and competition in a relative humidity gradient.** *Environmental Microbiology* 2009, **11**(4):809-822.
202. Gulez G, Dechesne A, Workman CT, Smets BF: **Transcriptome dynamics of *Pseudomonas putida* KT2440 under water stress.** *Applied and Environmental Microbiology* 2012, **78**(3):676-683.
203. Robles-Price A, Wong TY, Sletta H, Valla S, Schiller NL: **AlgX is a periplasmic protein required for alginate biosynthesis in *Pseudomonas aeruginosa*.** *Journal of Bacteriology* 2004, **186**(21):7369-7377.
204. Jain S, Franklin MJ, Ertesvag H, Valla S, Ohman DE: **The dual roles of AlgG in C-5-epimerization and secretion of alginate polymers in *Pseudomonas aeruginosa*.** *Molecular Microbiology* 2003, **47**(4):1123-1133.
205. Klähn S, Hagemann M: **Compatible solute biosynthesis in cyanobacteria.** *Environmental Microbiology* 2011, **13**(3):551-562.
206. Yoshida T, Sakamoto T: **Water-stress induced trehalose accumulation and control of trehalase in the cyanobacterium *Nostoc punctiforme* IAM M-15.** *The Journal of General and Applied Microbiology* 2009, **55**(2):135-145.
207. Preiss J: **Biochemistry and Molecular Biology of Glycogen Synthesis in Bacteria and Mammals and Starch Synthesis in Plants.** In: *Comprehensive Natural Products II*. Edited by Liu H-W, Mander L. Oxford: Elsevier; 2010: 429-491.
208. Geurtsen J, Chedammi S, Mesters J, Cot M, Driessen NN, Sambou T, Kakutani R, Ummels R, Maaskant J, Takata H *et al*: **Identification of Mycobacterial  $\alpha$ -Glucan as a novel ligand**

- for DC-SIGN: involvement of mycobacterial capsular polysaccharides in host immune modulation. *The Journal of Immunology* 2009, **183**(8):5221-5231.
209. Xin X-F, Nomura K, Aung K, Velásquez AC, Yao J, Boutrot F, Chang JH, Zipfel C, He SY: **Bacteria establish an aqueous living space in plants crucial for virulence.** *Nature* 2016, **539**(7630):524-529.
210. Moradali MF, Ghods S, Rehm BHA: ***Pseudomonas aeruginosa* Lifestyle: A Paradigm for Adaptation, Survival, and Persistence.** *Frontiers in Cellular and Infection Microbiology* 2017, **7**(39).
211. Rumbaugh KP: **Genomic complexity and plasticity ensure *Pseudomonas* success.** *FEMS Microbiology Letters* 2014, **356**(2):141-143.
212. Galán-Vásquez E, Luna B, Martínez-Antonio A: **The Regulatory Network of *Pseudomonas aeruginosa*.** *Microbial Informatics and Experimentation* 2011, **1**(1):3-3.
213. Kandror O, DeLeon A, Goldberg AL: **Trehalose synthesis is induced upon exposure of *Escherichia coli* to cold and is essential for viability at low temperatures.** *Proceedings of the National Academy of Sciences* 2002, **99**(15):9727-9732.
214. Harty CE, Martins D, Doing G, Mould DL, Clay ME, Occhipinti P, Nguyen D, Hogan DA: **Ethanol stimulates trehalose production through a SpoT-DksA-AlgU-dependent pathway in *Pseudomonas aeruginosa*.** *Journal of Bacteriology* 2019, **201**(12).
215. Hengge-Aronis R, Klein W, Lange R, Rimmele M, Boos W: **Trehalose synthesis genes are controlled by the putative sigma factor encoded by *rpoS* and are involved in stationary-phase thermotolerance in *Escherichia coli*.** *Journal of Bacteriology* 1991, **173**(24):7918-7924.
216. Sarniguet A, Kraus J, Henkels MD, Muehlchen AM, Loper JE: **The sigma factor sigma S affects antibiotic production and biological control activity of *Pseudomonas fluorescens* Pf-5.** *Proceedings of the National Academy of Sciences of the United States of America* 1995, **92**(26):12255-12259.
217. Riordan JT, Tietjen JA, Walsh CW, Gustafson JE, Whittam TS: **Inactivation of alternative sigma factor 54 (RpoN) leads to increased acid resistance, and alters locus of enterocyte effacement (LEE) expression in *Escherichia coli* O157 : H7.** *Microbiology* 2010, **156**(Pt 3):719-730.
218. Damron FH, Owings JP, Okkotsu Y, Varga JJ, Schurr JR, Goldberg JB, Schurr MJ, Yu HD: **Analysis of the *Pseudomonas aeruginosa* regulon controlled by the sensor kinase KinB and sigma factor RpoN.** *Journal of Bacteriology* 2012, **194**(6):1317-1330.
219. Xiao H, Kalman M, Ikehara K, Zemel S, Glaser G, Cashel M: **Residual guanosine 3',5'-bispyrophosphate synthetic activity of *relA* null mutants can be eliminated by *spoT* null mutations.** *The Journal of Biological Chemistry* 1991, **266**(9):5980-5990.
220. Boes N, Schreiber K, Schobert M: **SpoT-triggered stringent response controls *usp* gene expression in *Pseudomonas aeruginosa*.** *Journal of Bacteriology* 2008, **190**(21):7189-7199.
221. An G, Justesen J, Watson RJ, Friesen JD: **Cloning the *spoT* gene of *Escherichia coli*: identification of the *spoT* gene product.** *Journal of Bacteriology* 1979, **137**(3):1100-1110.
222. Magnusson LU, Farewell A, Nyström T: **ppGpp: a global regulator in *Escherichia coli*.** *Trends in Microbiology* 2005, **13**(5):236-242.

223. Neijssel OM, Snoep JL, Teixeira de Mattos MJ: **Regulation of energy source metabolism in streptococci.** *Journal of Applied Microbiology* 1997, **83**(S1):12s-19s.
224. De la Fuente IM, Cortés JM, Valero E, Desroches M, Rodrigues S, Malaina I, Martínez L: **On the dynamics of the adenylate energy system: homeorhesis vs homeostasis.** *PloS One* 2014, **9**(10):e108676-e108676.
225. Ballicora MA, Iglesias AA, Preiss J: **ADP-glucose pyrophosphorylase, a regulatory enzyme for bacterial glycogen synthesis.** *Microbiology and Molecular Biology Reviews* 2003, **67**(2):213-225.
226. Preiss J, Shen L, Greenberg E, Gentner N: **Biosynthesis of bacterial glycogen. IV. Activation and inhibition of the adenosine diphosphate glucose pyrophosphorylase of *Escherichia coli* B\*.** *Biochemistry* 1966, **5**(6):1833-1845.
227. Seok YJ, Sondej M, Badawi P, Lewis MS, Briggs MC, Jaffe H, Peterkofsky A: **High affinity binding and allosteric regulation of *Escherichia coli* glycogen phosphorylase by the histidine phosphocarrier protein, HPr.** *The Journal of Biological chemistry* 1997, **272**(42):26511-26521.
228. Kotrba P, Inui M, Yukawa H: **Bacterial phosphotransferase system (PTS) in carbohydrate uptake and control of carbon metabolism.** *Journal of Bioscience and Bioengineering* 2001, **92**(6):502-517.
229. Deutscher J, Francke C, Postma PW: **How phosphotransferase system-related protein phosphorylation regulates carbohydrate metabolism in bacteria.** *Microbiology and Molecular Biology Reviews* 2006, **70**(4):939-1031.
230. Moreno-Bruna B, Baroja-Fernandez E, Munoz FJ, Bastarrica-Berasategui A, Zanduetta-Criado A, Rodriguez-Lopez M, Lasa I, Akazawa T, Pozueta-Romero J: **Adenosine diphosphate sugar pyrophosphatase prevents glycogen biosynthesis in *Escherichia coli*.** *Proceedings of the National Academy of Sciences of the United States of America* 2001, **98**(14):8128-8132.
231. Morán-Zorzano MT, Viale AM, Muñoz FJ, Alonso-Casajús N, Eydallín GG, Zugasti B, Baroja-Fernández E, Pozueta-Romero J: ***Escherichia coli* AspP activity is enhanced by macromolecular crowding and by both glucose-1,6-bisphosphate and nucleotide-sugars.** *FEBS Letters* 2007, **581**(5):1035-1040.
232. Leckie MP, Ng RH, Porter SE, Compton DR, Dietzler DN: **Regulation of bacterial glycogen synthesis. Stimulation of glycogen synthesis by endogenous and exogenous cyclic adenosine 3':5'-monophosphate in *Escherichia coli* and the requirement for a functional CRP gene.** *The Journal of Biological Chemistry* 1983, **258**(6):3813-3824.
233. Zheng D, Constantinidou C, Hobman JL, Minchin SD: **Identification of the CRP regulon using *in vitro* and *in vivo* transcriptional profiling.** *Nucleic Acids Research* 2004, **32**(19):5874-5893.
234. Wilson WA, Roach PJ, Montero M, Baroja-Fernandez E, Munoz FJ, Eydallin G, Viale AM, Pozueta-Romero J: **Regulation of glycogen metabolism in yeast and bacteria.** *FEMS Microbiology Reviews* 2010, **34**(6):952-985.
235. Taguchi M, Izui K, Katsuki H: **Augmentation of glycogen synthesis under stringent control in *Escherichia coli*.** *Journal of Biochemistry* 1980, **88**(2):379-387.
236. Montero M, Eydallin G, Viale Alejandro M, Almagro G, Muñoz Francisco J, Rahimpour M, Sesma María T, Baroja-Fernández E, Pozueta-Romero J: ***Escherichia coli* glycogen**

metabolism is controlled by the PhoP-PhoQ regulatory system at submillimolar environmental Mg<sub>2+</sub> concentrations, and is highly interconnected with a wide variety of cellular processes. *Biochemical Journal* 2009, **424**(1):129-141.

237. Eydallin G, Montero M, Almagro G, Sesma MT, Viale AM, Muñoz FJ, Rahimpour M, Baroja-Fernández E, Pozueta-Romero J: **Genome-wide screening of genes whose enhanced expression affects glycogen accumulation in *Escherichia coli***. *DNA Research* 2010, **17**(2):61-71.
238. Timmermans J, Van Melderen L: **Post-transcriptional global regulation by CsrA in bacteria**. *Cellular and Molecular Life Sciences* 2010, **67**(17):2897-2908.
239. Sabnis NA, Yang H, Romeo T: **Pleiotropic regulation of central carbohydrate metabolism in *Escherichia coli* via the gene *csrA***. *Journal of Biological Chemistry* 1995, **270**(49):29096-29104.
240. Baker CS, Morozov I, Suzuki K, Romeo T, Babitzke P: **CsrA regulates glycogen biosynthesis by preventing translation of *glgC* in *Escherichia coli***. *Molecular Microbiology* 2002, **44**(6):1599-1610.
241. Morris ER, Hall G, Li C, Heeb S, Kulkarni RV, Lovelock L, Silistre H, Messina M, Cámara M, Emsley J *et al*: **Structural rearrangement in an RsmA/CsrA ortholog of *Pseudomonas aeruginosa* creates a dimeric RNA-binding protein, RsmN**. *Structure* 2013, **21**(9):1659-1671.
242. Ge Y, Lee JH, Liu J, Yang HW, Tian Y, Hu B, Zhao Y: **Homologues of the RNA binding protein RsmA in *Pseudomonas syringae* pv. tomato DC3000 exhibit distinct binding affinities with non-coding small RNAs and have distinct roles in virulence**. *Molecular Plant Pathology* 2019.
243. Goodman AL, Kulasekara B, Rietsch A, Boyd D, Smith RS, Lory S: **A signaling network reciprocally regulates genes associated with acute infection and chronic persistence in *Pseudomonas aeruginosa***. *Developmental Cell* 2004, **7**(5):745-754.
244. Chambers JR, Sauer K: **Small RNAs and their role in biofilm formation**. *Trends in Microbiology* 2013, **21**(1):39-49.
245. Goodman AL, Merighi M, Hyodo M, Ventre I, Filloux A, Lory S: **Direct interaction between sensor kinase proteins mediates acute and chronic disease phenotypes in a bacterial pathogen**. *Genes & Development* 2009, **23**(2):249-259.
246. Brenic A, McFarland KA, McManus HR, Castang S, Mogno I, Dove SL, Lory S: **The GacS/GacA signal transduction system of *Pseudomonas aeruginosa* acts exclusively through its control over the transcription of the RsmY and RsmZ regulatory small RNAs**. *Molecular Microbiology* 2009, **73**(3):434-445.
247. Valverde C, Heeb S, Keel C, Haas D: **RsmY, a small regulatory RNA, is required in concert with RsmZ for GacA-dependent expression of biocontrol traits in *Pseudomonas fluorescens* CHA0**. *Molecular Microbiology* 2003, **50**(4):1361-1379.
248. Blumer C, Heeb S, Pessi G, Haas D: **Global GacA-steered control of cyanide and exoprotease production in *Pseudomonas fluorescens* involves specific ribosome binding sites**. *Proceedings of the National Academy of Sciences* 1999, **96**(24):14073-14078.
249. Pessi G, Williams F, Hindle Z, Heurlier K, Holden MTG, Cámara M, Haas D, Williams P: **The global posttranscriptional regulator RsmA modulates production of virulence**

- determinants and *N*-acylhomoserine lactones in *Pseudomonas aeruginosa*. *Journal of Bacteriology* 2001, **183**(22):6676-6683.
250. Reimann C, Valverde C, Kay E, Haas D: **Posttranscriptional repression of GacS/GacA-controlled genes by the RNA-binding protein RsmE acting together with RsmA in the biocontrol strain *Pseudomonas fluorescens* CHA0.** *Journal of Bacteriology* 2005, **187**(1):276-285.
251. Irie Y, Starkey M, Edwards AN, Wozniak DJ, Romeo T, Parsek MR: ***Pseudomonas aeruginosa* biofilm matrix polysaccharide Psl is regulated transcriptionally by RpoS and post-transcriptionally by RsmA.** *Molecular Microbiology* 2010, **78**(1):158-172.
252. Brencic A, Lory S: **Determination of the regulon and identification of novel mRNA targets of *Pseudomonas aeruginosa* RsmA.** *Molecular Microbiology* 2009, **72**(3):612-632.
253. Heurlier K, Williams F, Heeb S, Dormond C, Pessi G, Singer D, Cámara M, Williams P, Haas D: **Positive control of swarming, rhamnolipid synthesis, and lipase production by the posttranscriptional RsmA/RsmZ system in *Pseudomonas aeruginosa* PAO1.** *Journal of Bacteriology* 2004, **186**(10):2936-2945.
254. Parkins MD, Ceri H, Storey DG: ***Pseudomonas aeruginosa* GacA, a factor in multihost virulence, is also essential for biofilm formation.** *Molecular Microbiology* 2001, **40**(5):1215-1226.
255. Kong W, Chen L, Zhao J, Shen T, Surette MG, Shen L, Duan K: **Hybrid sensor kinase PA1611 in *Pseudomonas aeruginosa* regulates transitions between acute and chronic infection through direct interaction with RetS.** *Molecular Microbiology* 2013, **88**(4):784-797.
256. Ventre I, Goodman AL, Vallet-Gely I, Vasseur P, Soscia C, Molin S, Bleves S, Lazdunski A, Lory S, Filloux A: **Multiple sensors control reciprocal expression of *Pseudomonas aeruginosa* regulatory RNA and virulence genes.** *Proceedings of the National Academy of Sciences of the United States of America* 2006, **103**(1):171-176.
257. Chambonnier G, Roux L, Redelberger D, Fadel F, Filloux A, Sivaneson M, de Bentzmann S, Bordi C: **The hybrid histidine kinase LadS forms a multicomponent signal transduction system with the GacS/GacA two-component system in *Pseudomonas aeruginosa*.** *PLOS Genetics* 2016, **12**(5):e1006032.
258. Bhagirath AY, Somayajula D, Li Y, Duan K: **CmpX affects virulence in *Pseudomonas aeruginosa* through the Gac/Rsm signaling pathway and by modulating c-di-GMP levels.** *Journal of Membrane Biology* 2018, **251**(1):35-49.
259. Grenga L, Little RH, Malone JG: **Quick change: post-transcriptional regulation in *Pseudomonas*.** *FEMS Microbiology Letters* 2017, **364**(14).
260. Leiba J, Syson K, Baronian G, Zanella-Cleon I, Kalscheuer R, Kremer L, Bornemann S, Molle V: ***Mycobacterium tuberculosis* maltosyltransferase GlgE, a genetically validated antituberculosis target, is negatively regulated by Ser/Thr phosphorylation.** *The Journal of Biological Chemistry* 2013, **288**(23):16546-16556.
261. Hershberger CD, Ye RW, Parsek MR, Xie ZD, Chakrabarty AM: **The *algT* (*algU*) gene of *Pseudomonas aeruginosa*, a key regulator involved in alginate biosynthesis, encodes an alternative sigma factor (sigma E).** *Proceedings of the National Academy of Sciences* 1995, **92**(17):7941-7945.

262. DeVries CA, Ohman DE: **Mucoid-to-nonmucoid conversion in alginate-producing *Pseudomonas aeruginosa* often results from spontaneous mutations in *algT*, encoding a putative alternate sigma factor, and shows evidence for autoregulation.** *Journal of Bacteriology* 1994, **176**(21):6677-6687.
263. Martin DW, Holloway BW, Deretic V: **Characterization of a locus determining the mucoid status of *Pseudomonas aeruginosa*: AlgU shows sequence similarities with a Bacillus sigma factor.** *Journal of Bacteriology* 1993, **175**(4):1153-1164.
264. Damron FH, Goldberg JB: **Proteolytic regulation of alginate overproduction in *Pseudomonas aeruginosa*.** *Molecular Microbiology* 2012, **84**(4):595-607.
265. Wozniak DJ, Ohman DE: **Transcriptional analysis of the *Pseudomonas aeruginosa* genes *algR*, *algB*, and *algD* reveals a hierarchy of alginate gene expression which is modulated by *algT*.** *Journal of Bacteriology* 1994, **176**(19):6007-6014.
266. Goldberg JB, Ohman DE: **Construction and characterization of *Pseudomonas aeruginosa* *algB* mutants: role of *algB* in high-level production of alginate.** *Journal of Bacteriology* 1987, **169**(4):1593-1602.
267. Leech AJ, Sprinkle A, Wood L, Wozniak DJ, Ohman DE: **The NtrC family regulator AlgB, which controls alginate biosynthesis in mucoid *Pseudomonas aeruginosa*, binds directly to the *algD* promoter.** *Journal of Bacteriology* 2008, **190**(2):581-589.
268. Ma S, Selvaraj U, Ohman DE, Quarless R, Hassett DJ, Wozniak DJ: **Phosphorylation-independent activity of the response regulators AlgB and AlgR in promoting alginate biosynthesis in mucoid *Pseudomonas aeruginosa*.** *Journal of Bacteriology* 1998, **180**(4):956-968.
269. Damron FH, Qiu D, Yu HD: **The *Pseudomonas aeruginosa* sensor kinase KinB negatively controls alginate production through AlgW-dependent muca proteolysis.** *Journal of Bacteriology* 2009, **191**(7):2285-2295.
270. Mohr CD, Hibler NS, Deretic V: **AlgR, a response regulator controlling mucoidy in *Pseudomonas aeruginosa*, binds to the FUS sites of the *algD* promoter located unusually far upstream from the mRNA start site.** *Journal of Bacteriology* 1991, **173**(16):5136-5143.
271. Amador CI, Canosa I, Govantes F, Santero E: **Lack of CbrB in *Pseudomonas putida* affects not only amino acids metabolism but also different stress responses and biofilm development.** *Environmental Microbiology* 2010, **12**(6):1748-1761.
272. Nishijyo T, Haas D, Itoh Y: **The CbrA-CbrB two-component regulatory system controls the utilization of multiple carbon and nitrogen sources in *Pseudomonas aeruginosa*.** *Molecular Microbiology* 2001, **40**(4):917-931.
273. García-Mauriño SM, Pérez-Martínez I, Amador CI, Canosa I, Santero E: **Transcriptional activation of the CrcZ and CrcY regulatory RNAs by the CbrB response regulator in *Pseudomonas putida*.** *Molecular Microbiology* 2013, **89**(1):189-205.
274. Sonnleitner E, Abdou L, Haas D: **Small RNA as global regulator of carbon catabolite repression in *Pseudomonas aeruginosa*.** *Proceedings of the National Academy of Sciences* 2009, **106**(51):21866-21871.
275. Hester KL, Lehman J, Najjar F, Song L, Roe BA, MacGregor CH, Hager PW, Phibbs PV, Sokatch JR: **Crc is involved in catabolite repression control of the *bkd* operons of *Pseudomonas putida* and *Pseudomonas aeruginosa*.** *Journal of Bacteriology* 2000, **182**.

276. Linares JF, Moreno R, Fajardo A, Martínez-Solano L, Escalante R, Rojo F, Martínez JL: **The global regulator Crc modulates metabolism, susceptibility to antibiotics and virulence in *Pseudomonas aeruginosa***. *Environmental Microbiology* 2010, **12**(12):3196-3212.
277. Ruiz-Manzano A, Yuste L, Rojo F: **Levels and Activity of the *Pseudomonas putida* Global Regulatory Protein Crc Vary According to Growth Conditions**. *Journal of Bacteriology* 2005, **187**(11):3678-3686.
278. Moreno R, Marzi S, Romby P, Rojo F: **The Crc global regulator binds to an unpaired A-rich motif at the *Pseudomonas putida alkS* mRNA coding sequence and inhibits translation initiation**. *Nucleic Acids Research* 2009, **37**(22):7678-7690.
279. Ertesvåg H, Sletta H, Senneset M, Sun Y-Q, Klinkenberg G, Konradsen TA, Ellingsen TE, Valla S: **Identification of genes affecting alginate biosynthesis in *Pseudomonas fluorescens* by screening a transposon insertion library**. *BMC Genomics* 2017, **18**(1):11.
280. Barroso R, García-Mauriño SM, Tomás-Gallardo L, Andújar E, Pérez-Alegre M, Santero E, Canosa I: **The CbrB regulon: promoter dissection reveals novel insights into the CbrAB expression network in *Pseudomonas putida***. *PLoS ONE* 2018, **13**(12):e0209191.
281. Manzo J, Cocotl-Yañez M, Tzontecomani T, Martínez VM, Bustillos R, Velásquez C, Goiz Y, Solís Y, López L, Fuentes LE *et al*: **Post-transcriptional regulation of the alginate biosynthetic gene *algD* by the Gac/Rsm system in *Azotobacter vinelandii***. *Journal of Molecular Microbiology and Biotechnology* 2011, **21**(3-4):147-159.
282. Romero M, Silistre H, Lovelock L, Wright VJ, Chan K-G, Hong K-W, Williams P, Cámara M, Heeb S: **Genome-wide mapping of the RNA targets of the *Pseudomonas aeruginosa* riboregulatory protein RsmN**. *Nucleic Acids Research* 2018, **46**(13):6823-6840.
283. Koressaar T, Lepamets M, Kaplinski L, Raime K, Andreson R, Remm M: **Primer3\_masker: integrating masking of template sequence with primer design software**. *Bioinformatics* 2018, **34**(11):1937-1938.
284. Rocha DJ, Santos CS, Pacheco LG: **Bacterial reference genes for gene expression studies by RT-qPCR: survey and analysis**. *Antonie Van Leeuwenhoek* 2015, **108**(3):685-693.
285. O'Toole GA, Kolter R: **Initiation of biofilm formation in *Pseudomonas fluorescens* WCS365 proceeds via multiple, convergent signalling pathways: a genetic analysis**. *Molecular Microbiology* 1998, **28**(3):449-461.
286. Jutras BL, Verma A, Stevenson B: **Identification of novel DNA-binding proteins using DNA-affinity chromatography/pull down**. *Current Protocols in Microbiology* 2012, **Chapter 1**:1F.1.1-1F.1.13.
287. Shevchenko A, Tomas H, Havlis J, Olsen JV, Mann M: **In-gel digestion for mass spectrometric characterization of proteins and proteomes**. *Nature Protocols* 2006, **1**(6):2856-2860.
288. Tyanova S, Temu T, Cox J: **The MaxQuant computational platform for mass spectrometry-based shotgun proteomics**. *Nature Protocols* 2016, **11**(12):2301-2319.
289. McLaggan D, Epstein W: ***Escherichia coli* accumulates the eukaryotic osmolyte taurine at high osmolarity**. *FEMS Microbiology Letters* 1991, **65**(2):209-213.
290. Xu Y, Labedan B, Glansdorff N: **Surprising arginine biosynthesis: a reappraisal of the enzymology and evolution of the pathway in microorganisms**. *Microbiology and Molecular Biology Reviews* 2007, **71**(1):36-47.

291. Roberts MF: **Organic compatible solutes of halotolerant and halophilic microorganisms.** *Saline Systems* 2005, **1**:5.
292. Hernandez MN, Lindow SE: ***Pseudomonas syringae* increases water availability in leaf microenvironments via production of hygroscopic syringafactin.** *bioRxiv* 2019:626630.
293. Axelsen KB, Palmgren MG: **Evolution of substrate specificities in the P-type ATPase superfamily.** *Journal of Molecular Evolution* 1998, **46**(1):84-101.
294. Rojas E, Theriot JA, Huang KC: **Response of *Escherichia coli* growth rate to osmotic shock.** *Proceedings of the National Academy of Sciences* 2014, **111**(21):7807-7812.
295. Rawling EG, Brinkman FS, Hancock RE: **Roles of the carboxy-terminal half of *Pseudomonas aeruginosa* major outer membrane protein OprF in cell shape, growth in low-osmolarity medium, and peptidoglycan association.** *Journal of Bacteriology* 1998, **180**(14):3556-3562.
296. Tart AH, Wolfgang MC, Wozniak DJ: **The alternative sigma factor AlgT represses *Pseudomonas aeruginosa* flagellum biosynthesis by inhibiting expression of *fleQ*.** *Journal of Bacteriology* 2005, **187**(23):7955-7962.
297. Cases I, de Lorenzo V: **The limits to genomic predictions: role of  $\sigma$ N in environmental stress survival of *Pseudomonas putida*.** *FEMS Microbiology Ecology* 2001, **35**(2):217-221.
298. Hickman JW, Harwood CS: **Identification of FleQ from *Pseudomonas aeruginosa* as a c-di-GMP-responsive transcription factor.** *Molecular Microbiology* 2008, **69**(2):376-389.
299. Baraquet C, Murakami K, Parsek MR, Harwood CS: **The FleQ protein from *Pseudomonas aeruginosa* functions as both a repressor and an activator to control gene expression from the *pel* operon promoter in response to c-di-GMP.** *Nucleic Acids Research* 2012, **40**(15):7207-7218.
300. Arora SK, Ritchings BW, Almira EC, Lory S, Ramphal R: **A transcriptional activator, FleQ, regulates mucin adhesion and flagellar gene expression in *Pseudomonas aeruginosa* in a cascade manner.** *Journal of Bacteriology* 1997, **179**(17):5574-5581.
301. Blanco-Romero E, Redondo-Nieto M, Martínez-Granero F, Garrido-Sanz D, Ramos-González MI, Martín M, Rivilla R: **Genome-wide analysis of the FleQ direct regulon in *Pseudomonas fluorescens* F113 and *Pseudomonas putida* KT2440.** *Scientific Reports* 2018, **8**(1):13145.
302. Gao JG, Gussin GN: **Activation of the *trpBA* promoter of *Pseudomonas aeruginosa* by TrpI protein *in vitro*.** *Journal of Bacteriology* 1991, **173**(12):3763-3769.
303. Yao X, He W, Lu C-D: **Functional characterization of seven  $\gamma$ -glutamylpolyamine synthetase genes and the *bauRABCD* locus for polyamine and  $\beta$ -alanine utilization in *Pseudomonas aeruginosa*.** *Journal of Bacteriology* 2011, **193**(15):3923-3930.
304. Ochsner UA, Vasil ML, Alsabbagh E, Parvatiyar K, Hassett DJ: **Role of the *Pseudomonas aeruginosa oxyR-recG* operon in oxidative stress defense and DNA repair: OxyR-dependent regulation of *katB-ankB*, *ahpB*, and *ahpC-ahpF*.** *Journal of Bacteriology* 2000, **182**(16):4533-4544.
305. Wei Q, Minh PNL, Dötsch A, Hildebrand F, Panmanee W, Elfarash A, Schulz S, Plaisance S, Charlier D, Hassett D *et al*: **Global regulation of gene expression by OxyR in an important human opportunistic pathogen.** *Nucleic Acids Research* 2012, **40**(10):4320-4333.

306. Rothe M, Alpert C, Engst W, Musiol S, Loh G, Blaut M: **Impact of nutritional factors on the proteome of intestinal *Escherichia coli*: Induction of OxyR-dependent proteins AhpF and Dps by a lactose-rich diet.** *Applied and Environmental Microbiology* 2012, **78**(10):3580-3591.
307. Yang S, Lv X, Wang X, Wang J, Wang R, Wang T: **Cell-surface displayed expression of trehalose synthase from *Pseudomonas putida* ATCC 47054 in *Pichia pastoris* using Pir1p as an anchor protein.** *Frontiers in Microbiology* 2017, **8**(2583).
308. Gagliardi MC, Lemassu A, Teloni R, Mariotti S, Sargentini V, Pardini M, Daffe M, Nisini R: **Cell wall-associated alpha-glucan is instrumental for *Mycobacterium tuberculosis* to block CD1 molecule expression and disable the function of dendritic cell derived from infected monocyte.** *Cell Microbiol* 2007, **9**(8):2081-2092.
309. Lombana TN, Echols N, Good MC, Thomsen ND, Ng HL, Greenstein AE, Falick AM, King DS, Alber T: **Allosteric activation mechanism of the *Mycobacterium tuberculosis* receptor Ser/Thr protein kinase, PknB.** *Structure* 2010, **18**(12):1667-1677.
310. Belanger AE, Hatfull GF: **Exponential-phase glycogen recycling is essential for growth of *Mycobacterium smegmatis*.** *Journal of Bacteriology* 1999, **181**(21):6670-6678.
311. Lee KY, Mooney DJ: **Alginate: properties and biomedical applications.** *Progress in Polymer Science* 2012, **37**(1):106-126.
312. Allison SD, Chang B, Randolph TW, Carpenter JF: **Hydrogen bonding between sugar and protein is responsible for inhibition of dehydration-induced protein unfolding.** *Archives of Biochemistry and Biophysics* 1999, **365**(2):289-298.
313. Golovina EA, Golovin AV, Hoekstra FA, Faller R: **Water replacement hypothesis in atomic detail--factors determining the structure of dehydrated bilayer stacks.** *Biophysical Journal* 2009, **97**(2):490-499.
314. Pereira CS, Hünenberger PH: **Effect of trehalose on a phospholipid membrane under mechanical stress.** *Biophysical Journal* 2008, **95**(8):3525-3534.
315. Pereira CS, Hünenberger PH: **Interaction of the sugars trehalose, maltose and glucose with a phospholipid bilayer: a comparative molecular dynamics study.** *The Journal of Physical Chemistry B* 2006, **110**(31):15572-15581.
316. Sun WQ, Leopold AC, Crowe LM, Crowe JH: **Stability of dry liposomes in sugar glasses.** *Biophysical Journal* 1996, **70**(4):1769-1776.
317. Green JL, Angell CA: **Phase relations and vitrification in saccharide-water solutions and the trehalose anomaly.** *The Journal of Physical Chemistry* 1989, **93**(8):2880-2882.
318. Massari AM, Finkelstein IJ, McClain BL, Goj A, Wen X, Bren KL, Loring RF, Fayer MD: **The influence of aqueous versus glassy solvents on protein dynamics: Vibrational echo experiments and molecular dynamics simulations.** *Journal of the American Chemical Society* 2005, **127**(41):14279-14289.
319. Camponeschi F, Atrei A, Rocchigiani G, Mencuccini L, Uva M, Barbucci R: **New formulations of polysaccharide-based hydrogels for drug release and tissue engineering.** *Gels* 2015, **1**(1):3-23.
320. Wang L, Regina A, Butardo VM, Jr., Kosar-Hashemi B, Larroque O, Kahler CM, Wise MJ: **Influence of in situ progressive N-terminal is still controversial truncation of glycogen**

- branching enzyme in *Escherichia coli* DH5 $\alpha$  on glycogen structure, accumulation, and bacterial viability.** *BMC Microbiology* 2015, **15**:96.
321. Byrd MS, Sadovskaya I, Vinogradov E, Lu H, Sprinkle AB, Richardson SH, Ma L, Ralston B, Parsek MR, Anderson EM *et al*: **Genetic and biochemical analyses of the *Pseudomonas aeruginosa* Psl exopolysaccharide reveal overlapping roles for polysaccharide synthesis enzymes in Psl and LPS production.** *Molecular Microbiology* 2009, **73**(4):622-638.
322. Geurtsen J, Chedammi S, Mesters J, Cot M, Driessen NN, Sambou T, Kakutani R, Ummels R, Maaskant J, Takata H *et al*: **Identification of mycobacterial alpha-glucan as a novel ligand for DC-SIGN: involvement of mycobacterial capsular polysaccharides in host immune modulation.** *Journal of Immunology* 2009, **183**(8):5221-5231.
323. Scoffone VC, Chiarelli LR, Trespidi G, Mentasti M, Riccardi G, Buroni S: ***Burkholderia cenocepacia* infections in cystic fibrosis patients: Drug resistance and therapeutic approaches.** *Frontiers in Microbiology* 2017, **8**:1592-1592.
324. Orozco-Mosqueda MD, Duan J, DiBernardo M, Zetter E, Campos-Garcia J, Glick BR, Santoyo G: **The production of ACC deaminase and trehalose by the plant growth promoting bacterium *Pseudomonas* sp. UW4 synergistically protect tomato plants against salt stress.** *Frontiers in Microbiology* 2019, **10**:10.
325. Lesk C, Rowhani P, Ramankutty N: **Influence of extreme weather disasters on global crop production.** *Nature* 2016, **529**:84.
326. Quiza L, St-Arnaud M, Yergeau E: **Harnessing phytomicrobiome signaling for rhizosphere microbiome engineering.** *Frontiers in Plant Science* 2015, **6**(507).
327. Cai X, Seitzl I, Mu W, Zhang T, Stressler T, Fischer L, Jiang B: **Biotechnical production of trehalose through the trehalose synthase pathway: current status and future prospects.** *Applied Microbiology and Biotechnology* 2018, **102**(7):2965-2976.
328. Jia H, Fan Y, Feng X, Li C: **Enhancing stress-resistance for efficient microbial biotransformations by synthetic biology.** *Frontiers in Bioengineering and Biotechnology* 2014, **2**:44-44.
329. Cuppels DA: **Generation and characterization of Tn5 insertion mutations in *Pseudomonas syringae* pv. tomato.** *Applied and Environmental Microbiology* 1986, **51**(2):323-327.
330. Holloway BW: **Genetic recombination in *Pseudomonas aeruginosa*.** *Journal of General Microbiology* 1955, **13**(3):572-581.
331. Reimann C, Beyeler M, Latifi A, Winteler H, Foglino M, Lazdunski A, Haas D: **The global activator GacA of *Pseudomonas aeruginosa* PAO positively controls the production of the autoinducer N-butyryl-homoserine lactone and the formation of the virulence factors pyocyanin, cyanide, and lipase.** *Molecular Microbiology* 1997, **24**(2):309-319.
332. Pérez-Martínez I, Haas D: **Azithromycin Inhibits Expression of the GacA-Dependent Small RNAs RsmY and RsmZ in *Pseudomonas aeruginosa*.** *Antimicrobial Agents and Chemotherapy* 2011, **55**(7):3399-3405.

# Appendix

Table i: Primers used for genetic manipulations

Target	N°	Primer Name	Primer Sequence (5' – 3')	Restriction Site	Primer melting temperature (T <sub>m</sub> , °C)
PAO1 <i>glgE</i> (PA2151)	1	PA2151_UPFP	CGCGGGATCCTGGACGAAAGCGTCAC	<i>Bam</i> HI	78
	2	PA2151_UPRP	CGCGTCTAGAGACAATCGAACTCATCGAG	<i>Xba</i> I	72
	3	PA2151_DNFP	CGCGTCTAGAGTCGACGCATAAGGAGAAAC	<i>Xba</i> I	73
	4	PA2151_DNRP	CGCGAAGCTTAATAGAAGCGGTGCCAGTAG	<i>Hind</i> III	74
	5	PA2151_TestF	TGGTGCTGATCACCTG	None	65
	6	PA2151_TestR	GTTTCGATCAGGTAGGGAATC	None	62
PAO1 <i>treS/pep2</i> (PA2152)	7	PA2152_UPFP	CGGGATCCGACTGCTACCGGCCGAAC	<i>Bam</i> HI	80
	8	PA2152_UPRP	CGTCTAGACGGTTTCTCGCTCTGG	<i>Xba</i> I	73
	9	PA2152_DNFP	CGTCTAGACTCCACCGAACACCTCCTG	<i>Xba</i> I	74
	10	PA2152_DNRP	CGGAATTCCTCGTACTTGTACAGTTC	<i>Eco</i> RI	67
	11	PA2152_TestF	CCGAACTCAACCAGCCAC	None	66
	12	PA2152_TestR	CGGCAGGAGGCCGTCGTG	None	75
PAO1 <i>glgB</i> (PA2153)	13	PA2153_UPFP	CGCGGGATCCACGCTTCATCGACTTCGAG	<i>Bam</i> HI	78
	14	PA2153_UPRP	CGCGTCTAGAGAGGAAGGCGAATGGATC	<i>Xba</i> I	74
	15	PA2153_DNFP	CGCGTCTAGAGACGTGCTGCTCAATAGC	<i>Xba</i> I	75
	16	PA2153_DNRP	CGCGAAGCTTAGCAACTGGTCGCTGATG	<i>Hind</i> III	76
	17	PA2153_TestF	CTGCTGATCAGGGTTCAC	None	63
	18	PA2153_TestR	GCCCTGCAAGGCCTGCTC	None	73
PAO1 <i>glgA</i> (PA2165)	19	PA2165_UPFP	CGCGGGATCCATTACGCAAGGTCACCAG	<i>Bam</i> HI	77
	20	PA2165_UPRP	CGCGTCTAGAAACAGAATGTCCCATGTC	<i>Xba</i> I	71
	21	PA2165_DNFP	CGCGTCTAGACGCCTGTTGAGGAATAC	<i>Xba</i> I	73
	22	PA2165_DNRP	CGCGAAGCTTCAGATGCTTGAGTTGCTC	<i>Hind</i> III	74
	23	PA2165_TestF	AGCACCTGGTTCAGCAACAG	None	68
	24	PA2165_TestR	GAAGTGGTTGTAGATCACG	None	60

Table ii: Primers used for genetic manipulations

Target	N°	Primer Name	Primer Sequence (5' – 3')	Restriction Site	Primer melting temperature (T <sub>m</sub> , °C)
PAO1 <i>treZ</i> (PA2164)	25	PA2164_UPFP	CGCGGGATCCTGGAGATCAGCGATGC	<i>Bam</i> HI	78
	26	PA2164_UPRP	CGCGTCTAGATTGGAAGTGGGCGCCGAAG	<i>Xba</i> I	78
	27	PA2164_DNFP	CGCGTCTAGAATCGCGGTCAGCCTG	<i>Xba</i> I	76
	28	PA2164_DNRP	CGCGAAGCTTCAGCAGGTCCTCGAGG	<i>Hind</i> III	78
	29	PA2164_TestF	AACACGCGCTACGTGGAG	None	68
	30	PA2164_TestR	GCAGGACATTGAAGAACAGC	None	64
PAO1 <i>malQ</i> (PA2163)	31	PA2163_UPFP	CGCGGGATCCAACCGTTCCTGTATTTAC	<i>Bam</i> HI	75
	32	PA2163_UPRP	CGCGTCTAGACAGGCGTGCGTCACTCATG	<i>Xba</i> I	78
	33	PA2163_DNFP	CGCGTCTAGATGCATCGGCTATGTCGG	<i>Xba</i> I	75
	34	PA2163_DNRP	CGCGAAGCTTTCCTGCCACCAGGGATTG	<i>Hind</i> III	78
	35	PA2163_TestF	GATAGCGCTGCAACTGCTC	None	67
	36	PA2163_TestR	GGATTCCCACTGAATG	None	56
PAO1 <i>treY</i> (PA2162)	37	PA2162_UPFP	CGCGGGATCCTGCTGCTCTTCGAG	<i>Bam</i> HI	77
	38	PA2162_UPRP	CGCGTCTAGAGAAATAGTCCAGCCAG	<i>Xba</i> I	71
	39	PA2162_DNFP	CGCGTCTAGAGACTTCCCGTCAACCTG	<i>Xba</i> I	74
	40	PA2162_DNRP	CGCGAAGCTTAACAGGCACAGCTCGACCTTG	<i>Hind</i> III	78
	41	PA2162_TestF	AACGTCTCTGGCTGATCC	None	64
	42	PA2162_TestR	GTGTACTCGGGCAATTC	None	60
PAO1 <i>glgX</i> (PA2160)	43	PA2160_UPFP	CGCGGGATCCAGTCTCTCCGAATGCAC	<i>Bam</i> HI	77
	44	PA2160_UPRP	CGCGTCTAGATTCGCTGATCCGCGAAG	<i>Xba</i> I	75
	45	PA2160_DNFP	CGCGTCTAGAAGTTTCCTGCTGTTCG	<i>Xba</i> I	72
	46	PA2160_DNRP	CGCGAAGCTTAAGAAAGGCTCAGTAGTG	<i>Hind</i> III	71
	47	PA2160_TestF	CAGTCGTCACGGTTGCCTG	None	69
	48	PA2160_TestR	ACGGCTTTCATGGCGTTC	None	66

Table iii: Primers used for genetic manipulations

Target	N°	Primer Name	Primer Sequence (5' – 3')	Restriction Site	Primer melting temperature (T <sub>m</sub> , °C)
<b>PAO1 <i>glgP</i> (PA2144)</b>	49	PA2144_UPFP	CGCGGGATCCTTGGCAACGGCATT	<i>Bam</i> HI	77
	50	PA2144_UPRP	CGCGTCTAGAGAGGATGCTGGCTTTCAG	<i>Xba</i> I	74
	51	PA2144_DNFP	CGCGTCTAGAACGATCAGCGAATACG	<i>Xba</i> I	71
	52	PA2144_DNRP	CGCGAAGCTTGAATACCGAAGAATGC	<i>Hind</i> III	70
	53	PA2144_TestF	ATACGGGAAAGGTCCTG	None	61
	54	PA2144_TestR	CCATGAATGGAATTTTGAACC	None	61
<b><i>Pto glgE</i> (PSPTO_2760)</b>	55	PSPTO_2760_UPFP	CGCGAAGCTTGCACATTCATTGACCTGG	<i>Hind</i> III	74
	56	PSPTO_2760_UPRP	CGCGTCTAGACTGTTTCATTCATCGAGC	<i>Xba</i> I	71
	57	PSPTO_2760_DNFP	CGCGTCTAGAGGAATCTGGCGTATC	<i>Xba</i> I	71
	58	PSPTO_2760_DNRP	CGCGGGATCCGTTGGATGTCTCGGTGTC	<i>Bam</i> HI	79
	59	PSPTO_2760_TestF	TCAGACAACGCATCGTATGC	None	65
	60	PSPTO_2760_TestR	AACCGGTGCCAGAAATACTG	None	65
<b><i>Pto treS/pep2</i> (PSPTO_2761)</b>	61	PSPTO_2761_UPFP	CGGGATCCGACATCAATCCGCGCTTC	<i>Bam</i> HI	76
	62	PSPTO_2761_UPRP	CGTCTAGACGCGGCATCGGGCTTC	<i>Xba</i> I	77
	63	PSPTO_2761_DNFP	CGTCTAGAGGGTTGCTGCAACCGTC	<i>Xba</i> I	74
	64	PSPTO_2761_DNRP	CGGGTACCAGACGCGGAACAAAGATC	<i>Kpn</i> I	74
	65	PSPTO_2761_TestF	GAATTTCTTCGTC AACAC	None	55
	66	PSPTO_2761_TestR	CTCGTATTTGTAGACCTC	None	56
<b><i>Pto glgB</i> (PSPTO_2762)</b>	67	PSPTO_2762_UPFP	CGCGAAGCTTAGTTGGTCAGCGACCTG	<i>Hind</i> III	76
	68	PSPTO_2762_UPRP	CGCGTCTAGACGCATTCATATCGGTTC	<i>Xba</i> I	71
	69	PSPTO_2762_DNFP	CGCGTCTAGAGCTTCTCTGACTGAATC	<i>Xba</i> I	72
	70	PSPTO_2762_DNRP	CGCGGGATCCAAGGCCATGCGCTAAG	<i>Bam</i> HI	79
	71	PSPTO_2762_TestF	TCTGGACAAGGATGATCAG	None	61
	72	PSPTO_2762_TestR	TCGATGCGCTGGTGTATGAG	None	68

Table iv: Primers used for genetic manipulations

Target	Nº	Primer Name	Primer Sequence (5' – 3')	Restriction Site	Primer melting temperature (T <sub>m</sub> , °C)
<b><i>Pto glgA</i></b> <b>(PSPTO_3125)</b>	73	PSPTO_3125_UPFP	CGCGGGATCCGATGAGGCTCGTCAC	<i>Bam</i> HI	78
	74	PSPTO_3125_UPRP	CGCGTCTAGAGTTGACCTGAGACATG	<i>Xba</i> I	71
	75	PSPTO_3125_DNFP	CGCGTCTAGAGTGAGCATGACCAGCAA	<i>Xba</i> I	74
	76	PSPTO_3125_DNRP	CGCGAAGCTTTGTTTGAGCTGTTTCG	<i>Hind</i> III	71
	77	PSPTO_3125_TestF	CGGAGATTGAACATCAGG	None	60
	78	PSPTO_3125_TestR	AGAATCACCATCAGGCCAACG	None	68
<b><i>Pto treZ</i></b> <b>(PSPTO_3126)</b>	79	PSPTO_3126_UPFP	CGCGGGATCCACATCGTCAACAACGG	<i>Bam</i> HI	76
	80	PSPTO_3126_UPRP	CGCGTCTAGAATCGTCTGTACGCAGG	<i>Xba</i> I	73
	81	PSPTO_3126_DNFP	CGCGTCTAGAGCAAGTGATGTTCTGGAG	<i>Xba</i> I	73
	82	PSPTO_3126_DNRP	CGCGAAGCTTGCAGGCTGTAAAGCTG	<i>Hind</i> III	75
	83	PSPTO_3126_TestF	CACCTGATCTGTCACTTCG	None	62
	84	PSPTO_3126_TestR	AGCATTTCCAGTGCTCC	None	65
<b><i>Pto malQ</i></b> <b>(PSPTO_3127)</b>	85	PSPTO_3127_UPFP	CGCGGGATCCTTCATGGGCGATGAATG	<i>Bam</i> HI	76
	86	PSPTO_3127_UPRP	CGCGTCTAGAAAGCCTCTCCAATTGC	<i>Xba</i> I	72
	87	PSPTO_3127_DNFP	CGCGTCTAGACGACTGGAATTGCTGTC	<i>Xba</i> I	73
	88	PSPTO_3127_DNRP	CGCGAAGCTTCTGGTAGTGCTCGATG	<i>Hind</i> III	74
	89	PSPTO_3127_TestF	ACTGCGCTGTTGTTGCTCTC	None	68
	90	PSPTO_3127_TestR	GTTCCACTGTCTGCAATAAC	None	61
<b><i>Pto treY</i></b> <b>(PSPTO_3128)</b>	91	PSPTO_3128_UPFP	CGCGGGATCCATTGGTCCGATCAGGCAC	<i>Bam</i> HI	79
	92	PSPTO_3128_UPRP	CGCGTCTAGAGTCATCAAGGGTGAAG	<i>Xba</i> I	71
	93	PSPTO_3128_DNFP	CGCGTCTAGAATACCGCTCAGTGCAGC	<i>Xba</i> I	75
	94	PSPTO_3128_DNRP	CGCGAAGCTTCTGCTCTGGATCAGAG	<i>Hind</i> III	73
	95	PSPTO_3128_TestF	CTGTTGTTCGAACAGAAC	None	58
	96	PSPTO_3128_TestR	ATTCATGGTGCCTTCTGACG	None	68

Table v: Primers used for genetic manipulations

Target	Nº	Primer Name	Primer Sequence (5' – 3')	Restriction Site	Primer melting temperature (T <sub>m</sub> , °C)
<i>Pto glgX</i> (PSPTO_3130)	97	PSPTO_3130_UPFP	CGCGGGATCCGTCATGATGAGCGTCAC	<i>BamHI</i>	77
	98	PSPTO_3130_UPRP	CGCGTCTAGAAGAACTGTCGTGCGAAG	<i>XbaI</i>	73
	99	PSPTO_3130_DNFP	CGCGTCTAGAAGTCAAGCGTGAAG	<i>XbaI</i>	71
	100	PSPTO_3130_DNRP	CGCGAAGCTTTCGGCATTCTCGAACAC	<i>HindIII</i>	74
	101	PSPTO_3130_TestF	CCTATCAGATCTGGGAATC	None	58
	102	PSPTO_3130_TestR	TCTTCACGTTTGCCGATGTG	None	66
<i>Pto glgP</i> (PSPTO_5165)	103	PSPTO_5165_UPFP	CGCGGGATCCTGGCATGAGGTGTGGAG	<i>BamHI</i>	79
	104	PSPTO_5165_UPRP	CGCGTCTAGAATCAGCGTCACGAACAAG	<i>XbaI</i>	73
	105	PSPTO_5165_DNFP	CGCGTCTAGAACCATTTCGGAATACG	<i>XbaI</i>	72
	106	PSPTO_5165_DNRP	CGCGAAGCTTAGAATGACAGCATCCAC	<i>HindIII</i>	72
	107	PSPTO_5165_TestF	CCAGCTTCAGGTGGTATTG	None	66
	108	PSPTO_5165_TestR	GAAGTATCTGGGACCTGC	None	65
<i>Pto Putative treS</i> (PSPTO_2952)	109	PSPTO_2952_UPFP	CGCGGGATCCGATCATTACGTGCTTGC	<i>BamHI</i>	76
	110	PSPTO_2952_UPRP	CGCGTCTAGAGTCCACGTAAGTCTGTC	<i>XbaI</i>	74
	111	PSPTO_2952_DNFP	CGCGTCTAGAACCTTGCCGATCTGATC	<i>XbaI</i>	73
	112	PSPTO_2952_DNRP	CGCGAAGCTTCAATGCCTTTCTCCAGC	<i>HindIII</i>	74
	113	PSPTO_2952_TestF	TATCTGGAGCACCATCACTGG	None	66
	114	PSPTO_2952_TestR	TATCGCCTGAACGTCTACC	None	64
Promoter of <i>PA2165</i>	115	PA2165_UPR2	CGCGAAGCTTCTGCAACAGAATGTCCCATG	<i>HindIII</i>	75
Promoter of <i>PSPTO_3125</i>	116	PSPTO_3125_UPRP2	CGCGAAGCTTGCCTGTTGACCTGAGACATG	<i>HindIII</i>	77

Table vi: Primers used for genetic manipulations

Target	N°	Primer Name	Primer Sequence (5' – 3')	Restriction Site	Primer melting temperature (T <sub>m</sub> , °C)
<b><i>Pto glgA</i></b> <b>(PSPTO_3125)</b>	117	PSPTO_3125_UPFP2	CGCGGGATCCGTATAACTCGCTTGCAGTAC	<i>BamHI</i>	76
<b><i>Pto PSPTO_3131-3134</i></b>	118	PSPTO_3131-3134_UPFP	CGCGGGATCCCGTCCGTGAACTTCATC	<i>BamHI</i>	77
	119	PSPTO_3131-3134_UPRP	CGCGTCTAGAAGTCATTGCTGATCTTC	<i>XbaI</i>	69
	120	PSPTO_3131-3134_DNFP	CGCGTCTAGATCGCTGAACGCCTGAGC	<i>XbaI</i>	77
	121	PSPTO_3131-3134_DNRP	CGCGAAGCTTCACGATCTGGCAACGTC	<i>HindIII</i>	76
	122	PSPTO_3121-3134_TestF	GCAACATGTTCAACCAGC	None	62
	123	PSPTO_3121-3134_TestR	TCGAAGCCAGTGAAGATGC	None	65
<b><i>M. korensis 3J1</i></b> <b><i>otsA/otsB</i></b>	124	OtsA/B FP	CGCGGAATTCCACCCATGCCAGCCGCA	<i>EcoRI</i>	82
	125	OtsA/B RP	CGCGAGATCTGGACATGACGAGAGTCTATTCCCG	<i>BglII</i>	77
<b>pME6032 <i>tac</i></b> <b>cassette</b>	126	ptacFP	CGCGAAGCTTGACATCATAACGGTTCTG	<i>HindIII</i>	72
	127	ptacRP	CGCGACTAGTGTCCGAGGAGCTTTATGC	<i>SpeI</i>	75
<b>Promoter of</b> <b>PA2165</b>	128	[BIO]-PA2165p_UPFP	[BIO]-ATTACGCAAGGTCACCAG	None	62
	129	PA2165p_UPRP	CTGCAACAGAATGTCCCATG	None	64

Table vii: Primers used for arbitrary PCR and sequencing

<b>N°</b>	<b>Primer Name</b>	<b>Primer Sequence (5' – 3')</b>
<b>130</b>	Arb-PCR	CGCAAACCAACCCTTGGCAG
<b>131</b>	Arb1b	GGCCAGCGAGCTAACGAGACNNNGATAT
<b>132</b>	Arb1	GGCCAGCGAGCTAACGAGAC
<b>133</b>	Almar3-seq	ACATATCCATCGCGTCCGCC

Table viii: Primers used for qPCR

<b>N°</b>	<b>Primer Name</b>	<b>Primer Sequence (5' – 3')</b>
<b>134</b>	RpoD_FP	GAAGGCATCCGTGAAGTGAT
<b>135</b>	RpoD_RP	GAGAACGTCGGAGAGACGAC
<b>136</b>	Pto_GlgA_FP	AAATCAACGCCGATTACGTC
<b>137</b>	Pto_GlgA_RP	CAGGCCTTTCTGGTAAACGA
<b>138</b>	SecA_FP	CGACTTTGCCGTGAAAATGC
<b>139</b>	SecA_RP	GCAACTGCGCCATGATTTTC
<b>140</b>	GyrA_FP	AGGACTACATCGCTCACCTG
<b>141</b>	GyrA_RP	CTTCCGGGATCTCGTAGGTC

Table ix: List of *Pto* strains used in this study

Strain	Phenotype	Source
<i>Pseudomonas syringae</i> pv. tomato DC3000	Wild-type <i>Pseudomonas syringae</i> pv. tomato DC3000	[329]
<i>Pto</i> $\Delta$ glgE	Knockout of PSPTO_2760	This Study
<i>Pto</i> $\Delta$ treS/pep2	Knockout of PSPTO_2761	This Study
<i>Pto</i> $\Delta$ glgB	Knockout of PSPTO_2762	This Study
<i>Pto</i> $\Delta$ glgA	Knockout of PSPTO_3125	This Study
<i>Pto</i> $\Delta$ treZ	Knockout of PSPTO_3126	This Study
<i>Pto</i> $\Delta$ malQ	Knockout of PSPTO_3127	This Study
<i>Pto</i> $\Delta$ treY	Knockout of PSPTO_3128	This Study
<i>Pto</i> $\Delta$ glgX	Knockout of PSPTO_3130	This Study
<i>Pto</i> $\Delta$ glgP	Knockout of PSPTO_5165	This Study
<i>Pto</i> $\Delta$ treS(2)	Knockout of PSPTO_2952	This Study
<i>Pto</i> $\Delta$ PSPTO_2760-2762	Knockout of PSPTO_2760, PSPTO_2761 and PSPTO_2762	This Study
<i>Pto</i> $\Delta$ PSPTO_3125-3134	Knockout of PSPTO_3125 - PSPTO_3134	This Study
<i>Pto</i> $\Delta\Delta$	Knockout of PSPTO_2760-PSPTO_2762 and PSPTO_3125 - PSPTO_3134	This Study
<i>Pto</i> $\Delta$ alg	Knockout of PSPTO_1238 ( <i>algG</i> ) and PSPTO_1237 ( <i>algX</i> )	Sebastian Pfeilmeier (unpublished work)
<i>Pto</i> $\Delta$ alg $\Delta\Delta$	Knockout of PSPTO_1238 ( <i>algG</i> ), PSPTO_1237 ( <i>algX</i> ), PSPTO_2760-PSPTO_2762 and PSPTO_3125 - PSPTO_3134	This Study
<i>Pto</i> -P <sub>glgA</sub> -lacZ	<i>Pto</i> expressing lacZ under the control of the PSPTO_3125 promoter	This Study
<i>Pto</i> tn:: <i>cbrB</i>	Transposon insertion within the <i>cbrB</i> gene (PSPTO_0966) in the <i>Pto</i> -P <sub>glgA</sub> -lacZ reporter strain	This Study
<i>Pto</i> tn:: <i>ladS</i>	Transposon insertion within the <i>ladS</i> gene (PSPTO_4796) in the <i>Pto</i> -P <sub>glgA</sub> -lacZ reporter strain	This Study
<i>Pto</i> tn:: <i>PSPTO1866</i>	Transposon insertion within the <i>PSPTO_1866</i> gene in the <i>Pto</i> -P <sub>glgA</sub> -lacZ reporter strain	This Study
<i>Pto</i> tn:: <i>tauC</i>	Transposon insertion within the <i>tauC</i> gene (PSPTO_5321) in the <i>Pto</i> -P <sub>glgA</sub> -lacZ reporter strain	This Study
<i>Pto</i> tn:: <i>syrB</i>	Transposon insertion within the <i>syrB</i> gene (PSPTO_2830) in the <i>Pto</i> -P <sub>glgA</sub> -lacZ reporter strain	This Study
<i>Pto</i> tn:: <i>argJ</i>	Transposon insertion within the <i>argJ</i> gene (PSPTO_4399) in the <i>Pto</i> -P <sub>glgA</sub> -lacZ reporter strain	This Study

Table x: List of PAO1 strains used in this study

Strain	Phenotype	Source
<i>Pseudomonas aeruginosa</i> PAO1	Wildtype <i>Pseudomonas aeruginosa</i> PAO1	[330]
PAO1 $\Delta$ <i>glgE</i>	Knockout of <i>PA2151</i>	This Study
PAO1 $\Delta$ <i>treS/pep2</i>	Knockout of <i>PA2152</i>	This Study
PAO1 $\Delta$ <i>glgB</i>	Knockout of <i>PA2153</i>	This Study
PAO1 $\Delta$ <i>glgA</i>	Knockout of <i>PA2165</i>	This Study
PAO1 $\Delta$ <i>treZ</i>	Knockout of <i>PA2164</i>	This Study
PAO1 $\Delta$ <i>malQ</i>	Knockout of <i>PA2163</i>	This Study
PAO1 $\Delta$ <i>treY</i>	Knockout of <i>PA2162</i>	This Study
PAO1 $\Delta$ <i>glgX</i>	Knockout of <i>PA2160</i>	This Study
PAO1 $\Delta$ <i>glgP</i>	Knockout of <i>PA2144</i>	This Study
PAO1 $P_{glgA}$ - <i>lacZ</i>	PAO1 expressing <i>lacZ</i> under the control of the <i>PA2165</i> promoter	This Study
PAO1 $\Delta$ <i>glgE-glgB</i>	Knockout of <i>PA2151</i> , <i>PA2152</i> and <i>PA2153</i>	This Study
PAO1 :: <i>otsA/otsB</i>	PAO1 constitutively expressing <i>otsA/B</i>	This Study
PAO1 $\Delta$ <i>treS/pep2</i> :: <i>otsA/otsB</i>	PAO1 $\Delta$ <i>treS/pep2</i> constitutively expressing <i>otsA/B</i>	This Study
PAO1 $\Delta$ <i>glgA</i> :: <i>otsA/otsB</i>	PAO1 $\Delta$ <i>glgA</i> constitutively expressing <i>otsA/otsB</i>	This Study
PAO1- $P_{glgA}$ - <i>lacZ</i>	PAO1 expressing <i>lacZ</i> under the control of the <i>PA2165</i> promoter	This Study
PAO1 tn:: <i>cmpX</i>	Transposon insertion within the <i>cmpX</i> gene ( <i>PA1775</i> ) in the PAO1- $P_{glgA}$ - <i>lacZ</i> reporter strain	This Study
PAO1 tn:: <i>algB</i>	Transposon insertion within the <i>algB</i> gene ( <i>PA5483</i> ) in the PAO1- $P_{glgA}$ - <i>lacZ</i> reporter strain	This Study
PAO1 tn:: <i>fimS</i>	Transposon insertion within the <i>fimS</i> gene ( <i>PA5262</i> ) in the PAO1- $P_{glgA}$ - <i>lacZ</i> reporter strain	This Study
PAO1 tn:: <i>PA1429</i>	Transposon insertion within the <i>PA1429</i> gene in the PAO1- $P_{glgA}$ - <i>lacZ</i> reporter strain	This Study
PAO1 tn:: <i>PA2696</i>	Transposon insertion within the <i>PA2696</i> gene in the PAO1- $P_{glgA}$ - <i>lacZ</i> reporter strain	This Study
PAO1 tn:: <i>PA4726.11/2</i>	Transposon insertion within the <i>PA4726.11/2</i> gene in the PAO1- $P_{glgA}$ - <i>lacZ</i> reporter strain	This Study
PAO1 $\Delta$ <i>cmpX</i>	Knockout of <i>PA1775</i>	This Study
PAO1-L	PAO1 Lausanne subline	Stephen Heeb
PAO1-L $\Delta$ <i>gacA</i>	Deletion of <i>gacA</i> derived from PAO1-L	Stephen Heeb [331]
PAO1-L $\Delta$ <i>gacS</i>	Deletion of <i>gacS</i> derived from PAO1-L	Stephen Heeb [332]
PAO1-N	PAO1 Nottingham subline	Stephen Heeb
PAO1-N $\Delta$ <i>rsmA</i>	Deletion of <i>rsmA</i> derived from PAO1-N	Stephen Heeb [249]
PAO1-N $\Delta$ <i>rsmN</i>	Deletion of <i>rsmN</i> derived from PAO1-N	Stephen Heeb [241]
PAO1-N $\Delta$ <i>rsmA</i> $\Delta$ <i>rsmN</i>	Deletion of <i>rsmA</i> and <i>rsmN</i> derived from PAO1-N	Stephen Heeb (Dubern <i>et al.</i> unpublished)

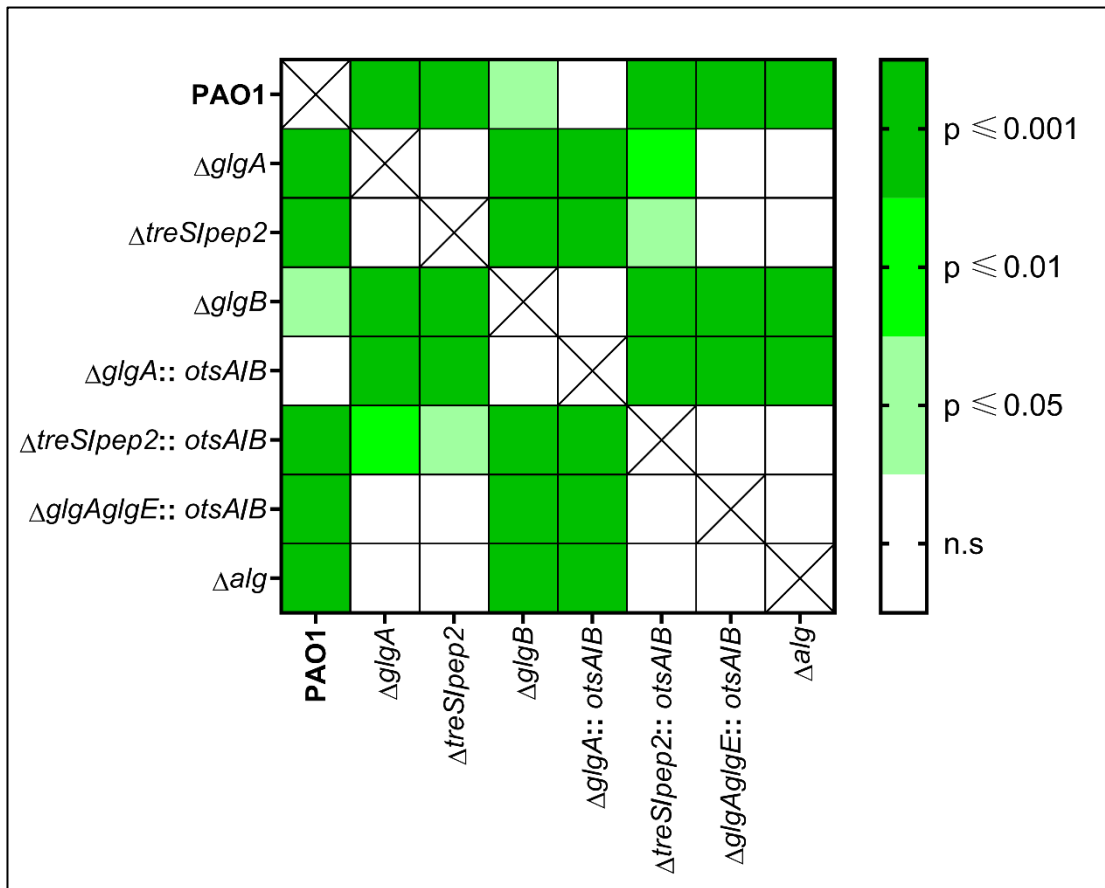


Figure i: Heat map representing the statistical significance of desiccation responses between PAO1 strains based on linear mixed modelling. Green colouring represents statistical significance of desiccation responses between individual strains.

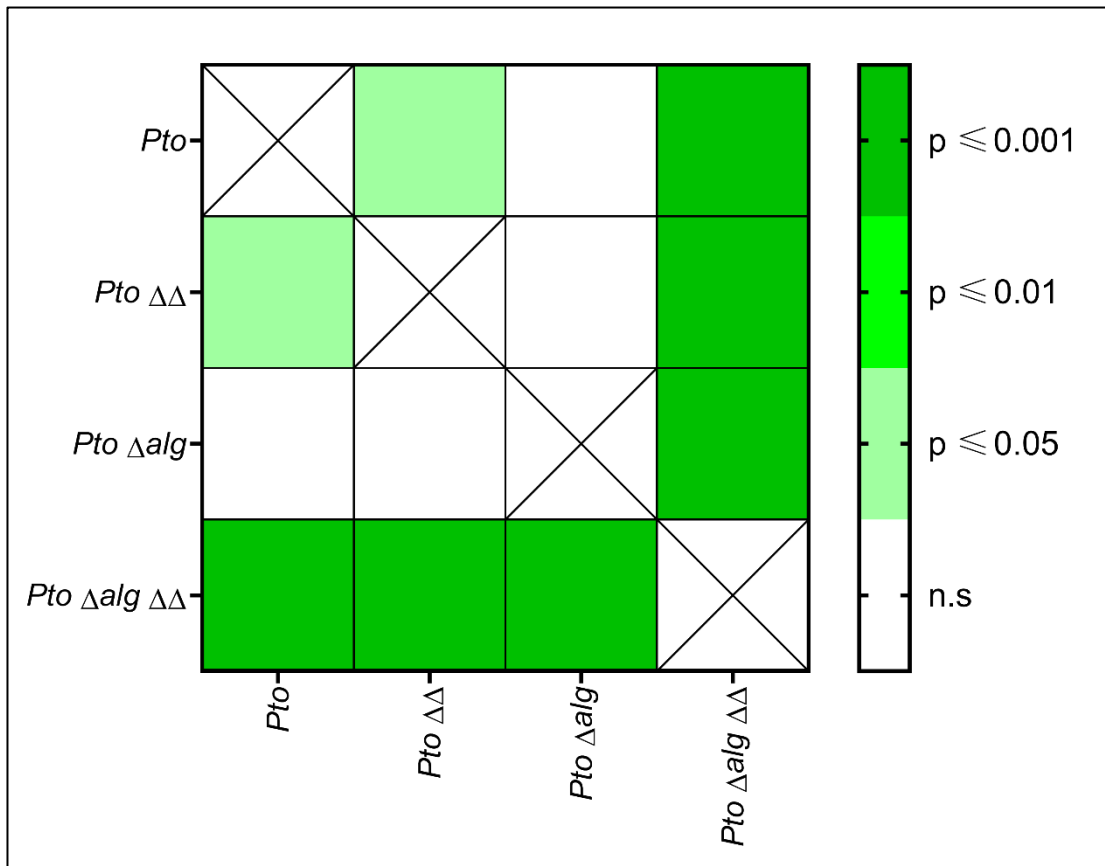


Figure ii: Heat map representing the statistical significance of desiccation responses between *Pto* strains based on linear mixed modelling. Green colouring represents statistical significance of desiccation responses between individual strains.